PAGES 1277–1396

ISSN 0003–2654

ROYAL SOCIETY
OF
CHEMISTRY

The Analyst

A monthly international journal dealing with all branches of the theory and practice of analytical chemistry, including instrumentation and sensors, and physical, biochemical, clinical, pharmaceutical, biological, environmental, automatic and computer-based methods

Vol.115 No.10 October 1990

The Analyst

The Analytical Journal of The Royal Society of Chemistry

Editorial Manager, Analytical Journals: Judith Egan

Editor, *The Analyst*
Harpal S. Minhas
The Royal Society of Chemistry,
Thomas Graham House, Science Park,
Milton Road, Cambridge CB4 4WF, UK
Telephone 0223 420066.
Fax 0223 423623. Telex No. 818293 ROYAL.

US Associate Editor, *The Analyst*
Dr J. F. Tyson
Department of Chemistry,
University of Massachusetts,
Amherst MA 01003, USA
Telephone 413 545 0195
Fax 413 545 4490

Senior Assistant Editor
Paul Delaney

Assistant Editors
Paula O'Riordan, Sheryl Whitewood

Editorial Secretary: Claire Harris

Advertisements: Advertisement Department, The Royal Society of Chemistry, Burlington House, Piccadilly, London, W1V 0BN. Telephone 071-437 8656. Telex No. 268001. Fax 071-437 8883.

The Analyst (ISSN 0003–2654) is published monthly by The Royal Society of Chemistry, Thomas Graham House, Science Park, Milton Road, Cambridge CB4 4WF, UK. All orders accompanied with payment should be sent directly to The Royal Society of Chemistry, The Distribution Centre, Blackhorse Road, Letchworth, Herts. SG6 1HN, England. 1990 Annual subscription rate UK £220.00, EEC £233.00, Rest of World £253.00, USA $493.00. Purchased with *Analytical Abstracts* UK £476.00, EEC £520.00, Rest of World £547.00, USA $995.00. Purchased with *Analytical Abstracts* plus *Analytical Proceedings* UK £561.00, EEC £611.00, Rest of World £645.00, USA $1187.00. Purchased with *Analytical Proceedings* UK £279.00, EEC £296.50, Rest of World £321.00, USA $626.00. Air freight and mailing in the USA by Publications Expediting Inc., 200 Meacham Avenue, Elmont, NY 11003.
USA Postmaster: Send address changes to: *The Analyst,* Publications Expediting Inc., 200 Meacham Avenue, Elmont, NY 11003. Second class postage paid at Jamaica, NY 11431. All other despatches outside the UK by Bulk Airmail within Europe, Accelerated Surface Post outside Europe. PRINTED IN THE UK.

Information for Authors

Full details of how to submit material for publication in *The Analyst* are given in the Instructions to Authors in the January issue. Separate copies are available on request.

The Analyst publishes papers on all aspects of the theory and practice of analytical chemistry, fundamental and applied, inorganic and organic, including chemical, physical, biochemical, clinical, pharmaceutical, biological, environmental, automatic and computer-based methods. Papers on new approaches to existing methods, new techniques and instrumentation, detectors and sensors, and new areas of application with due attention to overcoming limitations and to underlying principles are all equally welcome. There is no page charge.

The following types of papers will be considered:

Full papers, describing original work.

Short papers: the criteria for originality are the same as for full papers, but short papers generally report less extensive investigations or are of limited breadth of subject matter.

Communications, which must be on an urgent matter and be of obvious scientific importance. Rapidity of publication is enhanced if diagrams are omitted, but tables and formulae can be included. Communications receive priority and are usually published within 5–8 weeks of receipt. They are intended for brief descriptions of work that has progressed to a stage at which it is likely to be valuable to workers faced with similar problems. A fuller paper may be offered subsequently, if justified by later work.

Reviews, which must be a critical evaluation of the existing state of knowledge on a particular facet of analytical chemistry.

Every paper (except Communications) will be submitted to at least two referees, by whose advice the Editorial Board of *The Analyst* will be guided as to its acceptance or rejection. Papers that are accepted must not be published elsewhere except by permission. Submission of a manuscript will be regarded as an undertaking that the same material is not being considered for publication by another journal.

Regional Advisory Editors. For the benefit of potential contributors outside the United Kingdom, a Panel of Regional Advisory Editors exists. Requests for help or advice on any matter related to the preparation of papers and their submission for publication in *The Analyst* can be sent to the nearest member of the Panel. Currently serving Regional Advisory Editors are listed in each issue of *The Analyst.*

Manuscripts (four copies typed in double spacing) should be addressed to:
Harpal S. Minhas, Editor, *The Analyst,*
Royal Society of Chemistry,
Thomas Graham House,
Science Park, Milton Road,
CAMBRIDGE CB4 4WF, UK *or*:
Dr. J. F. Tyson
US Associate Editor, *The Analyst*
Department of Chemistry
University of Massachusetts
Amherst MA 01003, USA

Particular attention should be paid to the use of standard methods of literature citation, including the journal abbreviations defined in Chemical Abstracts Service Source Index. Wherever possible, the nomenclature employed should follow IUPAC recommendations, and units and symbols should be those associated with SI.

All queries relating to the presentation and submission of papers, and any correspondence regarding accepted papers and proofs, should be directed to the Editor, *The Analyst* (address as above). Members of the Analytical Editorial Board (who may be contacted directly or via the Editorial Office) would welcome comments, suggestions and advice on general policy matters concerning *The Analyst.*

Fifty reprints are supplied free of charge.

Adaptation of On-line Reactions Developed for Use With Flow Injection With Amperometric Detection for Use in Disposable Sensor Devices: Reductive Determination of Phosphate as Pre-formed 12-Molybdophosphate in a Capillary-fill Device

Arnold G. Fogg, S. Paul Scullion and Tony E. Edmonds
Chemistry Department, Loughborough University of Technology, Loughborough, Leicestershire LE11 3TU, UK

Brian J. Birch
Unilever Research, Colworth House, Sharnbrook, Bedfordshire MK44 1LQ, UK

Preliminary experiments have been carried out to show that on-line reactions developed for use with flow injection can be adapted for use in capillary-fill devices. The reversibility of the oxidation of a 1×10^{-3} M solution of potassium hexacyanoferrate(II) in 1 M HCl solution at a screen-printed carbon electrode in a capillary-fill device (CFD) incorporating a screen-printed silver reference electrode was found to be only slightly less than at a smoothly operating glassy carbon electrode (GCE) [$E_{pa} - E_{pc}$ = 95 mV (CFD), 65 mV (GCE)]. For the determination of phosphate as 12-molybdophosphate by reduction at a screen-printed carbon electrode in a CFD, a device with a screen-printed unchloridised silver reference/counter electrode was preferred to a chloridised silver electrode. A stable measurement potential was obtained when the measured solution was made 0.1 M in potassium chloride. The presence of potassium ion was found to affect markedly the linear sweep voltammograms obtained for the reduction of 12-molybdophosphate particularly at a GCE but also to a lesser extent at a screen-printed carbon electrode; this effect was controlled in further work with the CFD by the inclusion of potassium chloride in the measured solution. A rectilinear response was obtained for 5×10^{-6} M (the detection limit) -2×10^{-3} M pre-formed 12-molybdophosphate solutions at an applied potential of 0.16 V. The acidity required to carry out the reaction of phosphate can be provided by the addition of potassium hydrogen sulphate. It should be possible, therefore, to produce a satisfactory CFD for the determination of phosphate by screen-printing a mixture of sodium molybdate, potassium hydrogen sulphate and potassium chloride on to the glass face opposite to the screen-printed electrodes.

Keywords: *Flow injection; capillary-fill device; disposable sensor; phosphate determination; amperometric detection*

Previously in this laboratory, methods have been developed based on on-line derivatisation reactions for the determination of phosphate as 12-molybdophosphate[1,2] and nitrite as nitrosyl bromide[3] using flow injection (FI) with amperometric detection. In addition to the normal flow injection (nFI) methods, in which sample is injected into a reagent stream, methods were also developed in which reagent was injected into a carrier stream[4]; this technique was termed reverse flow injection (rFI) by Johnson and Petty.[5] Two advantages of rFI are that the sample is analysed with very little dilution and there is a saving in reagent costs. The use of the sample solution as the carrier stream has advantages for on-line monitoring as different reagents can be injected sequentially into the same sample stream, the stream can be switched to different detectors, and the detection parameters can be changed as required. Studies of the differences in the shapes of normal and reverse FI signals have been made.[6–8] Reverse FI peaks are broader and more prone to double-peaked character than are nFI peaks. Methods have also been developed in which a monitorand, which is not the determinand, is formed in the rFI manner[9–12]; this is brought about by the reagent, which limits the concentration of the monitorand formed, being included in the carrier stream. The injectate contains the determinand and a second reagent, which is needed to form the monitorand, and the determination is made by measuring the decrease which occurs in the size of the monitorand signal when the determinand is present. Such reactions have been developed for the determination of aromatic amines by on-line diazotisation,[9] the on-line bromination of phenol[10] and the iodimetric determination of sulphite.[11,12] Studies have also been carried out of the direct oxidation of sulphite,[13] ethylenediaminetetraacetic acid,[14] oxalate,[15] cyanide[16] and nitrite[17] by FI amperometry using an electrochemically pre-treated glassy carbon electrode.

Unilever have developed and patented a form of disposable sensor device that can be termed a capillary-fill device (CFD) using both optical and electrochemical detection regimes.[18,20] The device consists of two ceramic, plastic or glass plates fixed at the edges, possibly by means of a resin containing monodisperse ballotini (glass beads), so that there is a precise gap of, typically, 100 μm between the plates. Carbon and silver electrodes may be screen-printed on one plate whilst chemicals in a suitable matrix may be screen-printed on the other plate such that they are positioned directly above the electrodes in the completed device. Sample solution is taken up into the device by capillary action, the chemicals dissolve and may react with the determinand, and an electrochemical response is obtained at the electrodes. The screen-printed chemicals may simply be a buffer or other electrolyte or they could be reagents. The patents should be consulted for a full description of the invention. The main advantage of these devices is that a constant pre-determined volume is defined between the plates, and the devices therefore do not require individual standardisation. The electrochemical CFDs use potentiometry and/or thin-layer amperometry (coulometry) as measurement methods. Chemistries have been developed to determine, *e.g.*, pH, glucose, lactate and trace metals in this CFD configuration.[18–20]

Several of the methods that have been developed for use on-line in FI with amperometric detection appear to be ideally suited for use in these CFDs. For example, the development of an amperometric CFD for the determination of phosphate based on screen-printed sodium molybdate and potassium hydrogen sulphate (as a source of acidity) seems a possibility.

When the phosphate sample was taken up by capillary action the screen-printed reagents would dissolve and 12-molybdophosphate would be formed: this could then be determined reductively at the screen-printed electrodes. Sulphite (or ascorbic acid) might be determined iodimetrically in a CFD in which potassium iodate, potassium iodide and a small amount of potassium carbonate (the last to prevent premature formation of iodine) were screen-printed on the plate opposite (and above) the screen-printed electrodes. In this instance potassium hydrogen sulphate might be screen-printed separately on the other plate, *i.e.*, on the electrodes. When sulphite sample solution was taken up by capillary action, iodine would be formed owing to the acidification of the iodate - iodide mixture but some of the iodine would be consumed by the sulphite present. Individual standardisation of the CFDs would clearly be impossible, but, fortunately, owing to the nature of the device this is unnecessary: the size of the signal given by the unreacted iodine is an indirect measure of the sulphite present.

Preliminary results in the development of a CFD for the determination of phosphate are presented here.

Experimental

Screen-printed electrodes were provided by Unilever Research in the form of single ceramic plates and as complete CFDs consisting of a lower larger ceramic plate and an upper glass plate. The dimensions of the lower plate on which the electrodes were screen-printed were 5 × 2.5 cm. The upper glass plate of the CFD was 3.5 × 2.5 cm, and was positioned 0.2 cm from the end of the ceramic plate leaving a space for the application of the sample solution. The gap between the plates was 100 μm. The main area of the working electrode was rectangular, 1.5 × 0.8 cm, and the reference electrode was a screen-printed silver line 0.1 cm in width extending around the working electrode. Both two- and three-electrode CFDs were provided but they were used as two-electrode devices. Working electrodes were carbon electrodes made by screen-printing with carbon ink; in some, the carbon ink had been printed directly on to the ceramic plate but in others, the carbon ink was printed on top of screen-printed silver. The reference electrodes were screen-printed silver ink; some of these had been left as silver whilst others had been chloridised. The carbon electrodes overlaid on silver gave sharper voltammograms, presumably because of the increased electrical conductivity of the screen-printed electrode thin layer. For measuring the reductive signal of 12-molybdophosphate the unchloridised silver reference electrode was preferred. The electrodes had been screen-printed nearly to the end of the ceramic plate, away from where the sample was applied, to facilitate connecting them to a voltammetric instrument.

All electrochemical measurements were made with a PAR 174A polarographic analyser (Princeton Applied Research) in conjunction with either a Gould Advance 2000 *x* - *y* recorder or a Linseis *y* - *t* recorder. The glassy carbon electrode was constructed in the laboratory, polished carefully in the usual way and used without electrochemical pre-treatment. The potential of the glassy carbon electrode, and that of the screen-printed carbon electrode on the single-plate units, was applied using a three-electrode system incorporating conventional saturated calomel reference and platinum counter electrodes. The potential of the carbon electrode in the CFD was measured against the internal silver electrode. With the glassy carbon electrode and the uncovered screen-printed electrodes scan speeds of 10 mV s^{-1} were used for cyclic and linear sweep voltammetry, and 2 mV s^{-1} for differential-pulse voltammetry (pulse amplitude 50 mV, pulse interval 1 s). With the CFDs a scan speed of 2 mV s^{-1} was used. A simple form of coulometry in which the current decays at a constant applied potential was carried out with the CFD.

Reagent Solutions

Sodium molybdate dihydrate solution (2.7%). Sodium molybdate (6.85 g) was dissolved in 1.5 ml of concentrated sulphuric acid in 200 ml of water, and the resulting solution was diluted to 250 ml.

Potassium dihydrogen orthophosphate solution (0.10 M). Potassium dihydrogen orthophosphate (0.681 g) was dissolved in 30 ml of water and diluted to 50 ml.

Potassium hexacyanoferrate(II) solution (1×10^{-3} M). Potassium hexacyanoferrate(II) (0.0210 g) was dissolved in 30 ml of water containing the appropriate electrolyte and diluted to 50 ml with water.

Standard phosphate solutions. Phosphate solution (1–10 ml) of the appropriate concentration was added to 25 ml of the acidic molybdate solution and diluted to 50 ml with water.

Procedure for Using CFDs

The CFDs were filled by dipping the end of the devices away from the electrode connections into the appropriate solution such that the solution was taken up by capillary action. The CFDs were placed flat on the bench before a potential sweep or step was applied.

Results

Some preliminary tests and comparisons were made with the CFDs using cyclic voltammetry of potassium hexacyanoferrate(II) solutions. Anodic and cathodic peak potentials are given in Table 1. Increasing the electrolyte concentration improved the apparent reversibility probably by reducing the resistance of the thin layer of solution. The fact that the glassy carbon electrode had been well prepared was shown by the excellent reversibility of the hexacyanoferrate(II) couple with $E_{pa} - E_{pc} = 65$ mV. For the CFDs this behaviour was approached most closely by those in which the carbon

Table 1. Comparison of the cyclic voltammetric responses of a 1×10^{-3} M potassium hexacyanoferrate(II) solution in various electrolytes in the CFDs and at a glassy carbon electrode

Electrode system	Supporting electrolyte	Anodic peak potential (E_{pa})/mV	Cathodic peak potential (E_{pc})/mV	$E_{pa} - E_{pc}$/mV
Screen-printed carbon *versus* screen-printed Ag	0.1 M KCl	425	−40	465
	1.0 M KCl	375	185	190
	0.1 M HCl	395	265	130
	1.0 M HCl	550	455	95
Screen printed carbon *versus* screen-printed chloridised Ag (AgCl)	1.0 M KCl	425	125	300
	1.0 M HCl	590	415	185
Glassy carbon *versus* saturated calomel electrode	1.0 M KCl	275	210	65
	1.0 M HCl	500	435	65

electrode overlaid a silver coating and in which the silver reference electrode was unchloridised ($E_{pa} - E_{pc} = 95$ mV).

During these preliminary tests it was noticed that erratic responses were obtained if the devices were not kept flat and free from vibration whilst measurements were being made. This behaviour would not be expected in a thin-layer device and further study is required.

Initial linear sweep voltammetric studies were made with the phosphate system using the single-plate devices and measuring the potential of the working electrode against a conventional saturated calomel electrode (SCE). The responses were compared with voltammograms obtained at the glassy carbon electrode. The addition of potassium chloride to the electrolyte was found to have a marked effect on the voltammograms, particularly those at the glassy carbon electrode. This is shown in the linear sweep voltammograms obtained using the glassy carbon, screen-printed carbon, and screen-printed carbon on silver electrodes shown in Figs. 1–3. This effect of potassium was shown even more clearly for the glassy carbon electrode using differential-pulse voltammetry (DPV) (not shown but see Table 2). Change in the acidity (from 0.01 to 1 M sulphuric acid) of the 12-molybdophosphate solution also had a marked effect on the voltammograms obtained. The effect of added potassium was more pronounced at the lower acidities. This marked effect is seen in Table 2 in which the DPV peak heights are listed for 0.01 M sulphuric acid solution; the peak at 0.18 V increases in size markedly whilst those at 0.43 and 0.27 V are decreased. The addition of potassium salts has been shown to affect the polarograms of 12-molybdophosphate.[21] Moffat[22] has shown that potassium ions and ions of similar size greatly increase the surface area of 12-molybdophosphate; the effect of potassium ion on the voltammetry of 12-molybdophosphate may be associated with this. The effect at the screen-printed carbon electrodes is not as marked, but, clearly, it would seem advisable to control the potassium concentration in the measuring system. The voltammograms obtained with the single plate in which the carbon ink is screen-printed directly on to the ceramic plate are more drawn out (Fig. 3); this is probably owing to the higher resistance of the conducting layer in the absence of the underlying silver layer.

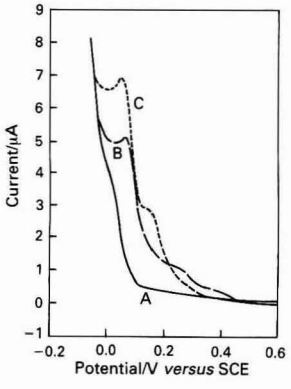

Fig. 1. Linear sweep voltammogram of 12-molybdophosphate at a glassy carbon electrode showing the effect of the addition of potassium ion. 12-Molybdophosphate concentration: A, 0; B and C, 1×10^{-3} M. Potassium chloride concentration: A and B, 0; C, 1×10^{-3} M

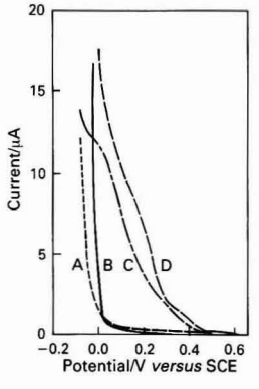

Fig. 2. Linear sweep voltammogram of 12-molybdophosphate at a screen-printed carbon electrode overlaid on silver showing the effect of the addition of potassium ion. 12-Molybdophosphate concentration: A and B, 0; C and D, 1×10^{-3} M. Potassium chloride concentration: A and C, 0; B and D, 1×10^{-3} M

The CFD is designed to be a disposable "one-shot" device, but in this work only a limited number were available, and so they were re-used as much as possible. After they had been used once they became increasingly difficult to fill and it became impossible to remove all the air bubbles that formed. Measurements were not taken if the bubbles were directly over the working electrode. The space over the electrodes filled more slowly than the remaining volume; this was probably due to the hydrophobicity of the electrode surfaces and the different thickness of the space. Also, with increased use, the devices began to leak owing to the plate fixative being attacked by the solution; when this happened erratic signals were obtained.

Linear sweep voltammograms are shown in Figs. 4 and 5 for solutions of various phosphate concentrations with and without the addition of potassium chloride. Clearly the addition of chloride (sodium chloride is also effective) stabilises the reference electrode and leads to a rectilinear

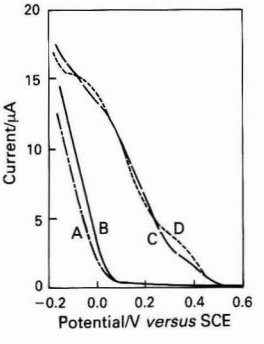

Fig. 3. Linear sweep voltammogram of 12-molybdophosphate at a screen-printed carbon electrode (directly on ceramic) showing the effect of addition of potassium ion. 12-Molybdophosphate concentration: A and B, 0; C and D, 1×10^{-3} M. Potassium chloride concentration: A and C, 0; B and D, 1×10^{-3} M

Table 2. Peak heights (μA) of differential-pulse voltammograms of 5×10^{-4} M 12-molybdophosphate in 0.01 M sulphuric acid solution and different concentrations of potassium chloride at a glassy carbon electrode *versus* SCE

Potassium chloride concentration/M	Peak currents (μA) at the peaks at			
	+0.43 V	+0.27 V	+0.18 V	+0.10 V
0	0.40	0.55	0.35	3.15
0.01	0.30	0.60	0.65	3.20
0.03	0.25	0.55	1.15	3.65
0.05	0.15	0.40	1.35	3.75
0.07	0.13	0.40	1.65	3.70
0.10	0.10	0.30	1.90	3.90

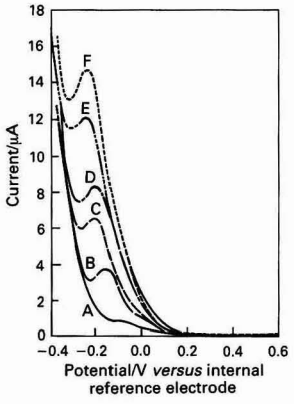

Fig. 4. Linear sweep voltammogram of 12-molybdophosphate in a CFD without the addition of chloride. 12-Molybdophosphate concentration: A, 0; B, 1×10^{-4}; C, 2.5×10^{-4}; D, 5×10^{-4}; E, 7.5×10^{-4}; and F, 10×10^{-4} M

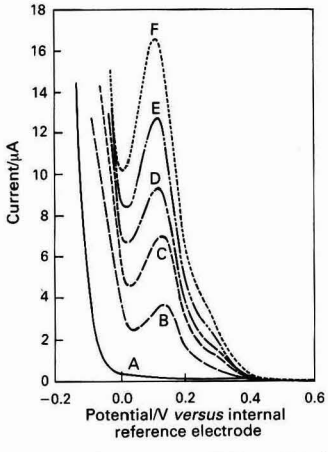

Fig. 5. Linear sweep voltammogram of 12-molybdophosphate in a CFD with the addition of chloride. 12-Molybdophosphate concentration: A, 0; B, 2×10^{-4}; C, 4×10^{-4}; D, 6×10^{-4}; E, 8×10^{-4}; and F, 10×10^{-4} M. Potassium chloride concentration, 0.1 M

response over the range 5×10^{-6} M (the detection limit)–2×10^{-3} M 12-molybdophosphate at a steady potential of 0.16 V *versus* the internal reference electrode. Owing to the different potential of the reference electrode in the absence of chloride the peak occurs at about −0.2 V. Clearly the addition of potassium chloride to the solution used in the device satisfies the requirement of maintaining a controlled level of potassium ion and of chloride.

The reproducibility of the response in different CFD units was studied in a limited way using three units. The peak potential and current were measured in each unit at two concentrations of 12-molybdophosphate. The results are shown in Table 3. A reasonably good level of reproducibility of potential and current is shown.

In use the CFDs might, with advantage, be used as coulometric devices producing exhaustive depletion at a fixed potential. A simple form of chronoamperometry was applied by monitoring the decay of current on an x - t recorder when the potential was stepped from open circuit to 0.1 V; the results are shown in Table 4 and again show reasonable reproducibility. At the higher determinand concentrations the current took 13 min to decay to within 2% of the baseline value which would be too long in a practical device.

Table 3. Reproducibility of peak potential (E_p) and peak current (i_p) at two levels of 12-molybdophosphate in CFDs

12-Molybdophosphate concentration/M	Device 1		Device 2		Device 3	
	E_p/V	i_p/μA	E_p/V	i_p/μA	E_p/V	i_p/μA
4×10^{-5}	0.16	0.75	0.15	0.73	0.15	0.80
4×10^{-4}	0.14	7.50	0.13	8.00	0.13	7.95

Table 4. Determination of 12-molybdophosphate by chronoamperometry in a CFD

12-Molybdophosphate concentration/10^{-4} M	Peak area, arbitrary units	Peak area to concentration, arbitrary units M^{-1}
0	0.5	—
2	12.8	6.40
4	25.5	6.38
6	43.0	7.20
8	57.0	7.13
10	69.6	6.96

Discussion

On-line and plant-side monitoring units and disposable sensor devices might be considered to be complementary; each has its advantages in particular situations. Much of our previous work has been concerned with the development of on-line reactions for use in FI monitoring devices.[1–4,6–17] In the later stages of this work it became obvious that much of the reaction chemistry developed for use in these monitors was directly applicable to use in disposable sensor devices such as the CFDs developed by Unilever Research. Preliminary studies of the adaptation of the method for the determination of phosphate based on the reductive amperometric determination of 12-molybdophosphate have been described here. It has been shown that the determination is best made at a screen-printed carbon electrode that is underlaid by a screen-printed silver layer, which increases the conductivity of the layer, and using a screen-printed unchloridised silver electrode as the counter/reference electrode. So far the reaction has only been studied with a limited number of CFDs, but the results are very promising. It is hoped that studies of the screen-printing of the appropriate chemicals for the device and the construction of devices specifically for the determination of phosphate will be carried out soon. It is also intended that a device for the determination of nitrite, based on its reaction with acidic bromide, and for other species for which FI methods have previously been described, will be developed. The details of a method of determining nitrate directly in a CFD will be reported shortly.

A. G. F., S. P. S. and T. E. E. thank the Agricultural and Food Research Council for financial support for this project.

References

1. Fogg, A. G., and Bsebsu, N. K., *Analyst*, 1981, **106**, 1288.
2. Fogg, A. G., and Bsebsu, N. K., *Analyst*, 1982, **107**, 566.
3. Fogg, A. G., Bsebsu, N. K., and Abdalla, M. A., *Analyst*, 1982, **107**, 1040.
4. Fogg, A. G., and Bsebsu, N. K., *Analyst*, 1984, **109**, 19.
5. Johnson, K. S., and Petty, R. L., *Anal. Chem.*, 1982, **54**, 1185.
6. Fogg, A. G., *Analyst*, 1986, **111**, 859.
7. Fogg, A. G., Wang, X., and Tyson, J. F., *Analyst*, 1989, **114**, 1119.
8. Fogg, A. G., Cipko, E., Farabella, L., and Tyson, J. F., *Analyst*, 1990, **115**, 593.

9. Fogg, A. G., Bsebsu, N. K., and Abdalla, M. A., *Analyst*, 1982, **107**, 1462.
10. Fogg, A. G., Ali, Md. A., and Abdalla, M. A., *Analyst*, 1983, **108**, 840.
11. Fogg, A. G., Guta, C., and Chamsi, A. Y., *Analyst*, 1987, **112**, 253.
12. Fogg, A. G., Wang, X., and Tyson, J. F., *Analyst*, 1990, **115**, 305.
13. Fogg, A. G., Fernandez-Arciniega, M. A., and Alonso, R. M., *Analyst*, 1985, **110**, 851.
14. Fogg, A. G., Fernandez-Arciniega, M. A., and Alonso, R. M., *Analyst*, 1985, **110**, 1201.
15. Fogg, A. G., Alonso, R. M., and Fernandez-Arciniega, M. A., *Analyst*, 1986, **111**, 249.
16. Fogg, A. G., and Alonso, R. M., *Analyst*, 1987, **112**, 1071.
17. Chamsi, A. Y., and Fogg, A. G., *Analyst*, 1988, **113**, 1723.
18. Shanks, I. A., Smith, A. M., and Nylander, C. I., *Int. Pat., Appl. Nos.*, PCT/GB85/00260, 1986.
19. Birch, B. J., and Burns, I. W., *Eur. Pat. Appl. No.* 87306513.0, 1987.
20. Birch, B. J., and Burns, I. W., *Eur. Pat. Appl.*, 87 310527.4, 1987.
21. Boltz, D. F., De Vries, T., and Mellon, M. G., *Anal. Chem.*, 1949, **5**, 563.
22. Moffat, J. B., *Polyhedron*, 1986, **5**, 261.

Paper 0/02299C
Received May 23rd, 1990
Accepted June 22nd, 1990

Glass pH Electrodes With Improved Temperature Characteristics: Use of a Low-impedance pH Sensor as the Inner Reference Electrode

Derek Midgley
National Power PLC, Technology and Environmental Centre, Kelvin Avenue, Leatherhead, Surrey KT22 7SE, UK

Glass electrodes are generally preferred to the various types of low-impedance pH electrodes, despite their greater susceptibility to electrical noise and need for a better grade of electronics. This preference arises from the reversibility of the glass electrode and its freedom from interference by redox and complexing agents, with the result that it has an ideal (Nernstian) response over a wide pH range. pH meters apply a linear correction for changes in temperature, but for most electrodes this is a good approximation only over a range of ±10 °C, because of the properties of the solution inside the glass electrode. By use of a low-impedance pH electrode in controlled (interference-free) conditions inside the glass electrode, it was hoped to eliminate the variation of the internal pH as a factor in temperature compensation. A preliminary assessment of various candidate electrodes indicated that the mercury - mercury(II) oxide electrode was the best choice. Glass electrodes with Hg - HgO inner electrodes had good general characteristics, *i.e.*, their slope factors and standard potentials agreed with theory, and their temperature characteristics were better than those of some commercial pH electrodes, being linear from 10 to 50 °C. Deviation from linearity was, however, observed at lower temperatures. Because of the limitations of many pH meters, it is desirable that electrodes have the characteristic that both the isopotential pH (pH_{iso}) and the pH at which the e.m.f. of the cell is zero (pH°) = 7, *i.e.*, the e.m.f. at pH 7 is 0 mV at all temperatures. With the Hg - HgO inner electrode, however, pH_{iso} = 3.8 and pH° = 11.3.

Keywords: *pH; glass electrode; temperature compensation; isopotential; metal oxide electrode*

Temperature compensation[1,2] is important in the application of potentiometry to industrial and environmental analysis, where monitoring over long periods of time may be required and control of temperature may be impractical. Recent work[3–5] has identified problems in temperature compensation of pH measurements with glass electrodes. The ideal temperature characteristics of a potentiometric pH cell (given that a non-zero temperature coefficient is inevitable) are listed below.

1. The slope factor (k) varies linearly with temperature, in accordance with the theoretical Nernst slope factor

$$\partial k/\partial T = \frac{R}{F}\ln(10) \quad .. \quad .. \quad .. \quad (1)$$

2. The standard potential (E°) varies linearly with temperature.

3. The e.m.f. is independent of temperature at pH 7, *i.e.*, the isopotential pH (pH_{iso}) has the value 7.0. This is not a theoretical requirement, but a practical one if the electrodes are to be used with the majority of existing pH meters.

4. The pH at which the cell e.m.f. is zero should be 7.0. This is another practical requirement for compatibility with most existing meters.

5. The cell should have a low thermal capacity, enabling temperature equilibrium to be reached quickly.

6. The response to changes in temperature should be monotonic, *i.e.*, if individual components of the cell have temperature coefficients of opposite sign, the design of the cell should not permit these components to change in temperature at such different rates that the over-all cell e.m.f. changes direction *en route* to its new equilibrium value.

7. The system should not exhibit thermal hysteresis.

In addition to these characteristics, a pH cell must also satisfy the specification usually required for measurement at constant temperature, *e.g.*, precision, accuracy, range and freedom from interferences.

Experience with real electrodes[4,5] shows that characteristic (1) presents no problems and characteristic (4), taken in isolation, presents relatively few problems. Realising characteristics (2)–(4) simultaneously, however, is much more difficult. Characteristic (2) is rarely achieved in practice, because of the chemistry of the internal filling solution of the glass electrode; in most instances E° varies approximately linearly over a range of *ca.* 20 °C. With one or two exceptions, characteristics (5) and (6) appear to receive a low priority in the design of electrodes. Hysteresis could arise from the physical design of the cell and be considered as part of characteristic (6), however, the choice of reference electrode may be critical in this regard, even if the heat transfer characteristics are excellent.

The greatest source of non-linearity is the pH-dependence of the solution inside the glass electrode. This paper describes a design of glass electrode in which the usual silver - silver chloride (or similar) inner reference electrode is replaced by a low-impedance metal - metal oxide pH electrode. This should provide inherent automatic compensation for any changes in the pH of the inner reference solution. Such a system should be tolerant of changes in the pH of the solution that may be non-linear, non-monotonic and irreversible; hysteresis should also be tolerable. Corresponding characteristics in the responses of the inner reference electrode or the glass membrane are not tolerable. The internal electrode should have an ideal Nernstian response to pH and be unaffected by other species present in the buffer. With such an arrangement it should be possible to achieve linear temperature characteristics for the whole cell.

Older work on metal - metal oxide electrodes has been reviewed by Ives.[6] The mercury - mercury(II) oxide electrode appears to behave ideally in alkaline solutions. The antimony - antimony oxide electrode, which is the only commercially used metal electrode for pH determination, has a sub-Nernstian response ($k \approx 56.5$ mV per pH unit at 25 °C) and its slope factor has an anomalous temperature coefficient ($\partial k/\partial T \approx$ 0.145 mV per pH unit per degree instead of the theoretical 0.198). Other metals were found to be less satisfactory, the best being bismuth and tungsten.

More recent work has been reviewed briefly by Midgley[7]; notably Fog and Buck[8] tested TiO_2, RuO_2, RhO_2, SnO_2, Ta_2O_5,OsO_2, IrO_2 and PtO_2 electrodes. The only one with a

Nernstian response was IrO_2; this, however, depends on the mode of preparation.

The other low-impedance system that has been widely used consists of a platinum electrode in a saturated solution of quinhydrone.[9] Such systems were not suitable for use as reference electrodes, because of the large changes in potential that occur as they age.[10] In the present context it was particularly significant that the aged electrodes had much larger temperature coefficients than the thermodynamic values for fresh solutions and after a rapid initial response to a change in temperature the potential peaked and slowly decayed. For these reasons the quinhydrone electrode was not considered suitable for use inside a glass electrode.

Before the work with glass electrodes was started, a few metal - metal oxide electrodes were tested, including antimony and tungsten from the "older" group, iridium and tantalum from the more recently studied metals and niobium, which has also been proposed.[11] The inner reference electrode finally selected was the mercury - mercury(II) oxide electrode.

Theory

The derivation of the following equations (2)–(7) has been given in a review of the effect of temperature on pH measurements.[3]

The e.m.f. of a potentiometric cell for measuring pH is given by a form of the Nernst equation

$$E = E^{\circ}_{cell} - k\mathrm{pH} \quad .. \quad .. \quad .. \quad (2)$$

where k is the slope factor, which is theoretically equal to $RT\ln(10)/F$, R being the gas constant, T the absolute temperature and F the Faraday constant. E°_{cell} is the standard potential of the cell, which is constant at constant temperature and pressure; in practice E°_{cell} is usually quasi-thermodynamic because it also includes terms that are constant only because of control of the experimental conditions (pressure, temperature, concentrations, etc.).

The e.m.f. may be represented in a way that allows for convenient temperature compensation by pH meters

$$E = E_s - k(\mathrm{pH} - \mathrm{pH_{iso}}) \quad .. \quad .. \quad (3)$$

where E_s contains all the temperature-independent components of E°_{cell} and $k\mathrm{pH_{iso}}$ the temperature-dependent ones. $\mathrm{pH_{iso}}$ is the isopotential pH, the notional pH at which the e.m.f. is the same at all temperatures. It follows that

$$\partial E^{\circ}_{cell}/\partial T = \mathrm{pH_{iso}}\partial k/\partial T \; .. \quad .. \quad .. \quad (4)$$

It is implicit in temperature compensation of this kind that E°_{cell} varies linearly with temperature, *i.e.*, $\mathrm{pH_{iso}}$ is a constant. This is rarely true in theory, but may be useful as an approximation valid over a range of *ca.* 20 °C.

Most practical pH cells contain a glass electrode and a detailed analysis of such cells[3] shows that

$$\frac{\partial E^{\circ}_{cell}}{\partial T} = \left(\frac{\partial E^{\circ\prime}}{\partial T} + \frac{k}{z_Y}\frac{\partial \log a'_Y}{\partial T} + \frac{1}{z_Y}\log a'_Y\frac{\partial k}{\partial T} + \frac{k\,\partial \mathrm{pH'}}{\partial T} + \mathrm{pH'}\frac{\partial k}{\partial T}\right) + \frac{\partial E_j}{\partial T} - \left(\frac{\partial E^{\circ}}{\partial T} + \frac{k}{z_X}\frac{\partial \log a_X}{\partial T} + \frac{1}{z_X}\log a_X\frac{\partial k}{\partial T}\right) \; .. \quad .. \quad (5)$$

$$\mathrm{pH_{iso}} = \mathrm{pH^{\circ}} - \frac{\Delta E^{\circ} + E_j}{k} + \frac{\dfrac{\partial \Delta E^{\circ}}{\partial T} + \dfrac{\partial E_j}{\partial T} + \dfrac{k\partial \mathrm{pH'}}{\partial T}}{\partial k/\partial T} + \frac{i}{z_X}\log a_X \quad (6)$$

where $i = 1$ for a non-isothermal cell and 0 for an isothermal cell.

$$\mathrm{pH^{\circ}} = \frac{\Delta E^{\circ} + E_j}{k} + \log\frac{(a'_Y)^{1/z_Y}}{(a_X)^{1/z_X}} + \mathrm{pH'} \quad .. \quad (7)$$

where $E^{\circ\prime}$ is the standard potential of the internal reference electrode, a'_Y is the activity of the ion (charge, with sign, z_Y) to which it responds and pH′ is the pH of the filling solution of the glass electrode; E° is the standard potential of the external reference electrode and a_X the activity of the ion (charge, with sign, z_X) to which it responds; E_j is the liquid junction potential, $\Delta E^{\circ} = E^{\circ\prime} - E^{\circ}$ and $\mathrm{pH^{\circ}}$ is the pH at which the cell e.m.f. is zero (at 25 °C). Non-linearity of the temperature response mainly arises from the term $k\partial\mathrm{pH'}/\partial T$ in equation (5).

In practice, X and Y in equation (5) are usually identical (although a'_Y and a_X need not be and rarely are). In the great majority of commercial pH cells, $X \equiv Y \equiv Cl^-$ and either Ag - AgCl or Hg - Hg_2Cl_2 reference electrodes are used. Inspection of equation (5), however, shows that it is theoretically possible to use a pH-sensitive inner reference electrode, so that $Y \equiv H^+$ and the $\partial\log a'_Y/\partial T$ and $\partial\mathrm{pH'}/\partial T$ terms cancel, giving equations (8)–(10).

$$\frac{\partial E^{\circ}_{cell}}{\partial T} = \frac{\partial E^{\circ\prime}}{\partial T} + \frac{\partial E_j}{\partial T} - \left(\frac{\partial E^{\circ}}{\partial T} + \frac{k}{z_X}\frac{\partial \log a_X}{\partial T} + \frac{1}{z_X}\log a_X\frac{\partial k}{\partial T}\right) \quad (8)$$

$$\mathrm{pH_{iso}} = \frac{\dfrac{\partial \Delta E^{\circ}}{\partial T} + \dfrac{\partial E_j}{\partial T}}{\partial k/\partial T} + j\left(\mathrm{pH^{\circ}} - \frac{\Delta E^{\circ} + E_j}{k}\right) \quad .. \quad (9)$$

where $j = 0$ for a non-isothermal cell and 1 for an isothermal cell.

$$\mathrm{pH^{\circ}} = \frac{\Delta E^{\circ} + E_j}{k} - \frac{1}{z_X}\log a_X \quad .. \quad (10)$$

Equations (8)–(10) contain no terms relating to the solution inside the glass electrode and the temperature characteristics of the pH of the buffer become irrelevant. The pH-sensitive inner reference electrode need not be a very satisfactory general pH sensor, *e.g.*, being susceptible to interference by complexing agents or redox-active reagents or having a restricted range of linear calibration; in the controlled conditions inside the glass electrode these sources of error may be avoidable.

Experimental

Apparatus

Potentials were measured with a digital pH meter reading to 0.1 mV and were simultaneously displayed on a chart recorder. Electrodes were fixed in B14 Quickfit sockets in the lids of water-jacketed glass cells connected to a Techne C-100 thermocirculator and Techne 1000 cooler.

Reference Electrode

A modified Kent 1352 calomel electrode with a remote ceramic frit junction was used. The main body of the electrode was fitted with a water jacket connected to a Techne C-100 circulator at 25.0 °C. The filling solution of the electrode was 3 M KCl.

Experimental Glass Electrodes

Bodies from Kent 1070-1 standard glass electrodes were filled with borax buffer solution formulated by the National Institute of Standards and Technology (NIST) and fitted with Hg - HgO reference electrodes.

Mercury - Mercury(II) Oxide Electrodes

Clear plastic tubing (Radiospares 399–899) was heat-shrunk on to platinum wire with a 1 mm diameter, leaving a 1-cm

overlap at one end and 1 cm of exposed wire at the other. The wire was driven through a silicone rubber bung and then clamped vertically with the overlapping end of the poly(vinyl chloride) tubing uppermost and a small drop of mercury injected into the cavity from a syringe with a fine stainless-steel needle. Mercury(II) oxide (BDH) was added on top of the mercury and the tube plugged with cotton-wool soaked in borax buffer solution. The mercury and the oxide stayed in place when the electrode was turned the right way up and contact with the platinum wire was maintained.

Antimony - Antimony Oxide Electrodes

A commercial EIL 33-1224-900 electrode was used.

Tungsten Electrodes

A commercial EIL EW 23 electrode was used, without special treatment. In addition, a tungsten rod was cleaned electrochemically and then oxidised in an oven at 780 °C for 2 h to produce a yellow-green surface coating of tungsten oxide, in contrast to the dull grey finish of the EIL electrode.

Iridium Electrodes

Iridium wire (99.9%), 0.5 mm in diameter, from Johnson-Matthey was used without treatment and also after being cycled between −0.25 V and +1.25 V *versus* a 3 M KCl calomel reference electrode for 210 min in 0.5 M H_2SO_4.

Tantalum and Niobium Electrodes

Wire (99.85%), 1 mm in diameter, obtained from Johnson-Matthey was used without treatment and also after being anodised at 2 V *versus* a 3 M KCl calomel reference electrode for 3 min in 0.1 M H_2SO_4.

Commercial Glass Electrodes

Commercial glass electrodes were included in the tests for comparison. Measurements were made in the same solutions at the same time (within 1 min) so that conditions were identical for all electrodes. The Orion 91-01 and Corning 311101J were conventional glass electrodes used with the same reference electrode as above. An example of a Ross combination electrode (Orion 81-02) was also included; the inner and external reference elements of this electrode use a platinum electrode in contact with the I_2 - I^- couple and this design is intended to have particularly good temperature characteristics.

Procedure

As the temperature of the cell was varied, the e.m.f.s were followed on a chart recorder and the steady values at each temperature were noted. Steps in temperature were usually 10 °C. The electrodes were first calibrated at 25 °C every day in pH 4 and pH 6.86 buffers.

Reagents

The NIST buffers were prepared from BDH AnalaR chemicals: 0.05 mol kg^{-1} of potassium hydrogen phthalate (pH 4.005 at 25 °C); 0.025 mol kg^{-1} each of potassium dihydrogen phosphate and disodium hydrogen phosphate (pH 6.865 at 25 °C); and 0.01 mol kg^{-1} of sodium tetraborate (pH 9.18 at 25 °C).

Results

Metal - Metal Oxide Electrodes

The results obtained are summarised in Table 1. The performance of the tantalum and niobium electrodes was most unsatisfactory, with grossly sub-Nernstian responses. The responses of these electrodes were so slow that no truly steady potentials were recorded, even after 50 min of immersion. The antimony oxide electrode exhibited a non-linear response that was sub-Nernstian in alkaline solution. The tungsten electrodes were reasonably consistent, but definitely sub-Nernstian; after 1 week the thermally produced oxide film sloughed away from the surface of the electrode. The untreated iridium electrode was rather slow and unstable in its response. The electrochemically cycled electrode was better, but electrodes treated in this way can exhibit super-Nernstian responses.[12]

In general, the performance of these electrodes was too poor to offer any hope of following internal pH changes so as to simplify the temperature characteristics of glass electrodes. The mercury - mercury(II) oxide electrode is established as being thermodynamically reversible,[6] but it was not practical to test the same electrode in different buffers, because its mode of construction means that very long wash-out times are required. Work with an HgS - HgO membrane electrode,[13] however, showed a rapid and linear response at pH values greater than 9, but a deterioration in both respects at lower values of pH. Mercury - mercury(II) oxide electrodes were, therefore, chosen as the inner reference elements of the glass

Table 1. Performance of metal electrodes in buffer solutions at 25 °C

Electrode	Slope factor (mV per pH unit) over buffer pH range: 4.00–6.86	4.00–9.12	6.86–9.12	Change in standard potential/ mV d^{-1}
Sb - Sb_2O_3	61	56	49	−3 to +8
W (untreated)	42–46	45–49	52	−11 to +26
W - WO_3	47	39–44	—	−19 to +8
Ta (untreated)	1.2	18–34	—	−15 to +6
Ta (anodised)	25	—	—	−11*
Nb (untreated)	14	17–43	—	5 ± 2
Nb (anodised	3	—	—	−110*
Ir (untreated)	48	20	—	17–28
Ir (cycled)	54–68	54	56	−4 ± 1

* Change with respect to untreated electrode.

Table 2. Performance characteristics of glass electrodes with Hg - HgO internal reference electrodes and commercial glass electrodes at 25 °C

		Experimental electrode (Hg - HgO) A	B	C	Theory	Commercial electrode Corning	Ross	Orion
Slope factor/mV per pH unit	Mean	−58.7	−59.2	−58.5	−59.16	−58.77	−58.31	−58.92
	SD*	0.4	—	—	—	0.66	0.17	0.20
	n	5	1	1	—	6	5	3
Zero-point pH	Mean	11.4	11.2	11.4	11.3	6.98	6.8	6.13
	SD	0.05	0.1	—	—	0.03	0.06	0.05
	n	4	3	1	—	7	5	3
pH_{iso}	Mean	3.5	4.3	3.8	3.1	7.9	6.6	6.3
	SD	0.1	0.5	—	—	0.20	0.20	0.98
	n	5	3	1	—	8	5	4

* SD = standard deviation.

electrodes, with an alkaline (borax) filling solution, and were tested *in situ*.

Glass Electrodes With Hg - HgO Inner Elements

The main performance characteristics are shown in Table 2.

Slope Factor

The slope factors for the three electrodes were close to the theoretical Nernstian value and within the same range as the commercial electrodes. When the slope factors were checked at 45 or 9.5 °C and at 25 °C, the ratio $(\partial k/\partial T)_{observed}/(\partial k/\partial T)_{theoretical}$ was 1.002 ± 0.006 (n = 3). These results indicate that slope factors were unlikely to be a major cause of uncertainty in the assessment of temperature effects.

Zero-point pH

The mean zero-point pH was 11.3 ± 0.1 (n = 8), which combines results for the three electrodes in Table 2 and agrees with the theoretical value predicted by equation (7) with literature values for the standard potentials of the inner and external reference electrodes and the known activity of KCl in the external reference solution. The Hg - HgO electrode thus appears to be behaving ideally in the internal buffer solution. On many older pH meters, such a high zero-point pH could not be accommodated, but with modern microprocessor-based meters there should be no difficulty.

Temperature Response

The variation of the slope factor with temperature has already been shown to agree with the theoretical value.

Time course of e.m.f. change with temperature

Fig. 1 shows the response to sharp changes in temperature. The response was fairly rapid, although a small overshoot was evident when the temperature was reduced rapidly. This overshoot, however, compared favourably with those observed with some commercially available combination electrodes.[5]

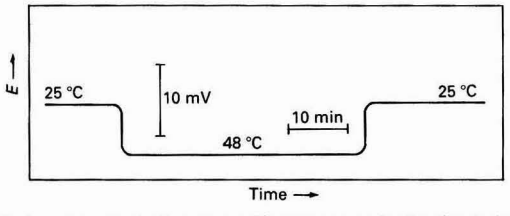

Fig. 1. Response to sharp changes in temperature in phthalate buffer for a glass electrode filled with borax buffer and having an Hg - HgO reference element

Table 3. Thermal hysteresis of electrodes in phthalate buffer

Electrode	Change in e.m.f.*/mV 1st cycle†	2nd cycle†
Experimental (Hg - HgO)	−1.2	+0.8
	+0.3	—
Corning	+0.7	+1.1
Orion 91-01	+0.1	—
Ross‡	+3.6	−0.8

* With respect to initial reading at 25 °C on first cycle.
† One cycle involves change from 25 to 49 ± 1 °C and back again.
‡ See reference 5.

Hysteresis

Electrodes were calibrated at 25 °C and then cycled between solutions at 25 and 49 °C. The changes from the first e.m.f. in phthalate buffer at 25 °C on the first cycle are shown in Table 3 and were similar to those obtained with commercial electrodes and better than for some commercial combination electrodes.[5]

Variation of E° *with temperature*

From equation (3), it follows that a plot of $E + k$pH *versus* k is linear (in the ideal situation) with a slope of pH_{iso}, which is related to $\partial E°/\partial T$ by equation (4). Plots for the borax - HgO electrode and two commercial electrodes are shown in Fig. 2. It has been shown that the dependence of the slope factor on temperature is ideal and it is therefore permissible to plot the slope factor against temperature if desired (on the upper scale); the slope would then be $(2.3R/F)pH_{iso} = 0.198\ pH_{iso}$.

Fig. 2 shows that the plot was linear from 10 to 50 °C, but curved at lower temperatures. The linearity was better than for many commercial glass electrodes (also shown in Fig. 2 and tested previously[4,5]). pH_{iso} was calculated from the linear parts of the plot and the values obtained for the three electrodes (Table 2) were higher than that expected from thermodynamic calculations of the properties of reference electrodes.[14] With such a low value of pH_{iso}, only a few pH meters would be able to apply temperature compensation accurately, even over the linear region of the plot.

Discussion

Glass electrodes with mercury - mercury(II) oxide inner reference electrodes satisfied the most basic performance tests, *i.e.*, their slope factors and standard potentials agreed closely with theory. Their temperature characteristics were better than those of some commercial pH electrodes[4,5] in that only small overshoots of potential occurred after large and rapid changes in temperature and the change in standard

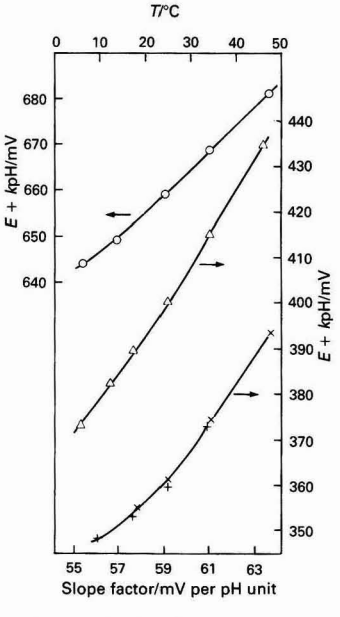

Fig. 2. Determination of pH_{iso} from measurements in phthalate buffer for glass electrode with ○, an Hg - HgO inner element; and two proprietary glass electrodes: + and ×, an Orion 91-01 (2 runs); and △, a Corning 311101J.

potential with temperature was almost linear (but curvature was evident below *ca.* 10 °C). The buffer inside the glass electrode had a fairly large and non-linear temperature coefficient ($\partial pH/\partial T = 5.4 \times 10^{-3}$ at 50 °C and 1.3×10^{-2} at 5 °C), so the principle of using a pH-sensitive inner electrode to simplify the temperature dependence worked well.

The zero-point and isopotential pH values of the glass electrodes with Hg - HgO inner reference electrodes could not be accommodated on many pH meters, preventing calibration and accurate temperature compensation, respectively. Modern microprocessor-based pH meters, however, are increasingly able to cope with such values of $E°pH$ and pH_{iso}. When the sample temperature varies widely from the calibration temperature, the linearity of the temperature response of the pH electrode becomes increasingly important, especially for process work in which frequent calibration is uneconomic. In such circumstances, *e.g.*, in a flue-gas desulphurisation plant, it would be advantageous to use the proposed electrode rather than commercial electrodes with less linear temperature characteristics, if a suitable microprocessor-based meter is available.

The work was carried out at the National Power, Technology and Environmental Centre and is published by permission of National Power PLC.

References

1. Mattock, G., "pH Measurement and Titration," Heywood, London, 1961.
2. Covington, A. K., *CRC Crit. Rev. Anal. Chem.*, 1974, **3**, 355.
3. Midgley, D., *Analyst*, 1987, **112**, 573.
4. Midgley, D., *Analyst*, 1987, **112**, 581.
5. Midgley, D., *Talanta*, 1988, **35**, 447.
6. Ives, D. J. G., *in* Ives, D. J. G., and Janz, G. J., *Editors*, "Reference Electrodes, Theory and Practice," Academic Press, New York, 1961, p. 322.
7. Midgley, D., *Talanta*, 1990, **37**, 767.
8. Fog, A., and Buck, R. P., *Sens. Actuators*, 1984, **5**, 137.
9. Janz, G. J., and Ives, D. J. G., *in* Ives, D. J. G., and Janz, G. J., *Editors*, "Reference Electrodes, Theory and Practice," Academic Press, New York, 1961, p. 270.
10. Midgley, D., *Analyst*, 1984, **109**, 445.
11. Biason Gomes, M. A., and Bulhoes, L. O. de S., *J. Electroanal. Chem.*, 1984, **165**, 289.
12. Hitchman, M. L., and Ramanathan, S., *Analyst*, 1988, **113**, 35.
13. Midgley, D., CERL Report TPRD/L/2451/R83, National Power, Leatherhead, 1983.
14. de Bethune, A. J., and Loud, N. S., *in* Hampel, C. A., *Editor*, "The Encyclopedia of Electrochemistry," Reinhold, New York, 1964, p. 414.

Paper 0/01919D
Received May 1st, 1990
Accepted June 14th, 1990

Multi-enzyme Electrodes for the Determination of Starch by Flow Injection

Junainah Abdul Hamid, G. J. Moody and J. D. R. Thomas*
School of Chemistry and Applied Chemistry, University of Wales College of Cardiff, P.O. Box 912, Cardiff CF1 3TB, UK

A tri-enzyme electrode has been developed for determining starch in a flowing stream based on amperometric monitoring of hydrogen peroxide at a potential of +600 mV *versus* a silver - silver chloride reference electrode. The nylon-based starch-sensing membranes (over a platinum electrode) were prepared from an enzyme cocktail containing various ratios of amyloglucosidase (AMG), mutarotase (MUT) and glucose oxidase (GO). The best starch-sensing membrane (to give the type A electrode) was made from an enzyme cocktail of AMG - MUT - GO (2000 + 100 + 100 U; where 1 U = 16.67 nanokatals), *i.e.*, containing a high level of AMG. In this system, starch samples were first incubated with soluble α-amylase (α-AMY) (1000 U) for 1 h at room temperature prior to analysis with the tri-enzyme electrode. Attempts were also made to immobilise α-AMY on to nylon net, either alone or as a component of a four-membrane starch - enzyme electrode but starch signals were weak compared with those generated by starch pre-treated with soluble α-AMY. This system, associated with the type A starch electrode, not only exhibited a calibration of wide linear range (1×10^{-4}–0.1% m/v starch) but also showed promising operational properties. It has excellent thermal stability over the range 30–70 °C.

Keywords: *Starch determination; amperometric starch sensor; multi-enzyme electrode; flow injection; thermal and γ-radiation stability*

Starch is normally determined after its enzymic hydrolysis with α-amylase (α-AMY) and amyloglucosidase (AMG) to glucose which reacts with nicotinamide adenine dinucleotide (NAD^+) or adenosine triphosphate (ATP) in the presence of glucose dehydrogenase (GDH) and hexokinase (HK), respectively, to give species which can be monitored spectrophotometrically. Another variation is by electrochemical detection of either the oxygen depletion or hydrogen peroxide production in the glucose oxidase (GO) reaction.

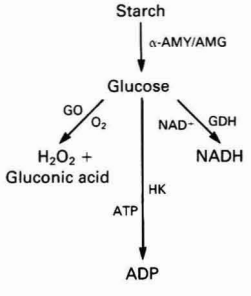

Enzyme-based electrochemical sensors developed for the amperometric detection of starch[1–6] either incorporate enzyme reactors, enzyme membranes or both. Starch has been determined electrochemically by passing the sample through an AMG reactor[1] for hydrolysis to glucose before passing through a GDH reactor in the presence of NAD^+. Amperometric detection was by the mediated oxidation of reduced NAD (NADH) at a modified electrode set to 0 mV *versus* a silver - silver chloride reference electrode. Starch showed a linear response from 0.1 to 1000 μg cm^{-3} (1×10^{-4}–1% m/v).

In another system, a reactor of immobilised α- and β-amylases (α- and β-AMY) plus AMG was used in conjunction with a GO - mutarotase (MUT) reactor.[3,4] Hydrogen peroxide production, a consequence of the ultimate enzymic reactions with glucose, was monitored amperometrically using a graphite palladium - gold coated electrode at +400 mV *versus* a silver - silver chloride reference electrode. A GO electrode has also been employed[3] with a previous AMG reactor for determining starch, the linear range being from 5×10^{-4} to 2×10^{-1}% m/v.

Pfeiffer *et al.*[5] developed a bi-enzyme membrane electrode for starch by co-immobilising GO and AMG on silk cross-linked with glutaraldehyde and bovine serum albumin. The enzyme membrane was then fitted to a platinum electrode and further protected with a cellulose acetate membrane. The resultant electrode when placed in a measuring cell (a Glucometer) and filled with sample solution, permitted the determination of starch by the amperometric detection of hydrogen peroxide at +600 mV *versus* a silver - silver chloride reference electrode. Steady-state measurements were achieved within 2–3 min with a linear range of up to 0.5% m/v starch.

An interesting enzyme membrane electrode for starch[6] includes inner GO and AMG membranes covered with an outer membrane of other enzymes, namely, co-immobilised GO and catalase acting as an anti-interference agent. Thus, any glucose admixed with the starch samples when passed through the anti-interference layer will be converted into hydrogen peroxide and decomposed into oxygen and water in the presence of catalase. Up to 2 mM glucose present in the sample could be eliminated in this way. Unfortunately, the glucose eliminating function of the anti-interference layer lasted for only 6 d.

The studies undertaken here on multi-enzyme membranes for starch were aimed at extending the lifetime of the electrode and defining the operational properties. Thus, the determination of starch was set up in a flow system with monitoring of hydrogen peroxide.

Experimental

Reagents

Amyloglucosidase (E.C. 3.2.1.3, 75 U mg^{-1}, isolated from *Aspergillus niger*), mutarotase (E.C. 5.1.3.3, 5800 U mg^{-1}, isolated from porcine kidney), glucose oxidase (E.C. 1.1.3.4, 150 U mg^{-1}, isolated from *Aspergillus niger*), α-amylase (E.C. 3.2.1.1, 680 U mg^{-1}, isolated from sweet potato), glutar-

* To whom correspondence should be addressed.

aldehyde (25% aqueous solution), lysine monohydrochloride, α-glucose, β-glucose, maltose, α-lactose, β-lactose, sucrose, fructose, mannose, raffinose, galactose, gluconic acid, citric acid, lactic acid, ascorbic acid, benzoic acid (sodium salt), arginine, ornithine, glycine and bovine serum albumin were purchased from Sigma (Poole, Dorset, UK) (1 U = 16.67 nkat). The α- and β-cyclodextrins were obtained from Technical (Stockport, Cheshire, UK). Dimethyl sulphate (99+%, Gold Label) was purchased from Aldrich (Gillingham, Dorset, UK). Glucose oxidase was stored desiccated in a freezer (−5 °C), the other enzymes were stored in a refrigerator at +4 °C. All other reagents used were of the best analytical-reagent grade available.

Sodium dihydrogen orthophosphate (0.1 M) and sodium acetate (0.1 M) buffers were adjusted to appropriate pH values with sodium hydroxide solution (4 M) and hydrochloric acid (4 M).

Nylon net with a 95-μm mesh size was kindly donated by Henry Simon (Stockport, Cheshire, UK).

Apparatus

The flow injection apparatus assembly employed was similar to that described previously for glucose sensors.[7]

Analysis of Flour Samples

All the starch-containing samples (*ca.* 1 g) were solubilised prior to analysis by incubation with 20 cm^3 of dimethyl sulphoxide and 5 cm^3 of hydrochloric acid at 60 °C for 30 min, with continuous stirring. After cooling, the pH of the solution was adjusted to between 4 and 5 with sodium hydroxide (4 M) and diluted to 100 cm^3 with water.

Starch Electrode Fabrication

Some starch-sensing membranes were prepared by immobilising AMG and GO on to methylated nylon net (mesh size 95 μm, N95 and surface area 1 × 1 cm^2) in a similar manner to that described previously for a lactose-sensing membrane.[8] A tri-enzyme system was also fabricated by including MUT. The enzymes were dissolved in appropriate volumes of 0.1 M phosphate buffer (pH 7) keeping the total protein concentration at ≈3 mg cm^{-3}.

Once prepared, the enzyme membrane was washed with buffer and fitted to the end of a platinum disc electrode. The resultant electrodes were evaluated with the flow injection apparatus for hydrogen peroxide[7] at a potential of +600 mV *versus* a silver - silver chloride reference electrode. When not in use, the enzyme membranes were stored in 0.1 M phosphate buffer (pH 7) at 4 °C, initially, which was subsequently replaced by 0.1 M acetate (pH 6) following the pH optimisation study.

Results and Discussion

Optimisation of Enzyme Composition

Attempts were made to improve the performance of the AMG - GO bi-enzyme starch electrode by including MUT and varying the proportion of AMG in the resultant tri-enzyme system.

Electrode responses were measured as peak heights and compared with those from a 0.1% m/v starch standard, dissolved in 0.1 M phosphate buffer (pH 7). The flow-rate of the buffer stream was kept at 1.7 cm^3 min^{-1} for injections of 0.5 cm^3 of starch.

Effect of MUT

Mutarotase (100 U) was introduced into the enzyme solution containing AMG - GO (1000 + 100 U) in order to fabricate a tri-enzyme membrane for a starch electrode. Its response towards starch was then compared with that of the bi-enzyme system based on AMG and GO (Fig. 1). The considerable signal enhancement, attributed to MUT, arose from increasing the rate of conversion of α-glucose into the β-anomer.

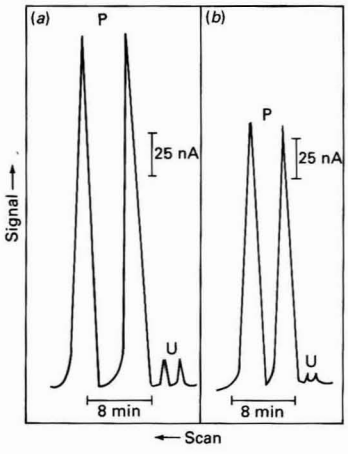

Fig. 1. Responses of bi- and tri-enzyme electrodes to starch (0.1% m/v). (*a*) AMG - GO - MUT (1000 + 100 + 100 U); (*b*) AMG - GO (1000 + 100 U). P, Starch pre-heated to 90 °C for 5 min; U, unheated (at room temperature)

The signals for unheated starch samples were very small compared with the pre-heated samples emphasising the ease with which starch is hydrolysed when it is already gelatinised or when the granules are broken up.[9] Hence, for most subsequent work the starch was first dissolved in buffer and heated to 90 °C until clear (*ca.* 5 min) before making up to the desired concentration. In both instances, the response peaks for starch were broad, suggesting slow diffusion of the bulky starch molecules and the hydrolytic fragments into, and out of, the enzyme membrane.

Effect of AMG

For this purpose, two different tri-enzyme membranes were prepared. Type A consisted of membranes prepared from a three-enzyme cocktail AMG - MUT - GO (2000 + 100 + 100 U) while type B membranes had less AMG (1000 U).

Starch signals for type A membrane electrodes [471 nA; standard deviation (SD) = 34 for n = 9] were about double those of type B (239 nA; SD = 45 for n = 9) (0.1 M phosphate buffer of pH 5; flow-rate, 1.7 cm^3 min^{-1}; and sample volume, 0.5 cm^3). Hydrolysis of starch by the AMG could well be the limiting step for the over-all enzymic reactions. Membranes containing even more AMG were not investigated owing to the cost. The type A starch electrode was chosen for further study.

Hydrolysis of Starch

The extent of starch hydrolysis with its three classical hydrolases, *i.e.*, α-AMY, β-AMY and AMG, was examined by electrochemical and chemical techniques. Starch (50 cm^3, 0.1% m/v) was allowed to react with the different hydrolases (1000 U each) in separate beakers at room temperature. At 5-min intervals, samples were spotted on to Whatman filter-paper pre-loaded with iodine - iodide solution for the classical starch blue colour test and also tested at reaction time intervals of 5, 15, 30, 45, 55 and 60 min with flow injection using the GO - MUT electrode (Table 1).

The iodine - iodide paper indicates the amylose content in starch. This simple test showed that α-AMY hydrolyses amylose almost immediately, according to the non-appearance of blue spots. Negative tests for amylose were observed

Table 1. Extent of starch hydrolysis using three different enzymes

	Peak height for electrode response $\Delta I_{glucose}$/nA (mean of three readings)			Iodine - iodide paper test* ($n = 3$)		
Time/min	AMG	α-AMY	β-AMY	AMG	α-AMY	β-AMY
5	500	75	10	+	+	+
10				+	−	+
15	850	100	10	+	−	+
20				+	−	+
25				+	−	+
30	980	120	10	−	−	+
35				−	−	+
40				−	−	+
45	1150	140	10	−	−	+
50				−	−	+
55	1220	160	13	−	−	+
60	1220	160	13	−	−	+

* + = Blue spot, *i.e.*, positive test for amylose component. − = No blue spot.

Table 2. Efficiency of conversion of starch into glucose after pre-treatment with two hydrolases

	Peak height ΔI_{starch}/nA (mean of three readings)		Iodine - iodide paper test* ($n = 3$)	
Incubation period/min	α-AMY	β-AMY	α-AMY	β-AMY
Initial (no pre-hydrolysis)	325	320	+	+
5	2150	875	−	+
10	2175	975	−	+
15	2200	1275	−	+
20	2200	1275	−	+
25	2200	1275	−	+
30	2200	1275	−	+

* + = Blue spot, *i.e.*, positive test for amylose component. − = No blue spot.

for AMG only after 25 min of enzymolysis, while β-AMY initiated the least starch hydrolysis.

The high glucose signals (detected amperometrically) from starch hydrolysis with AMG indicate an ability to attack both α-1,4 and α-1,6 bonds. Smaller signals were observed with the α-AMY starch for a given time as the α-AMY action stops at the branching points, *i.e.*, the α-1,6 glucosidic bonds primarily found in amylopectin. Even smaller glucose signals resulted from the hydrolytic action of β-AMY, suggesting a slow rate of partial starch hydrolysis by the enzyme. However, in all three instances, the glucose signals became stable after a 55-min reaction time.

In another set of experiments, starch (50 cm³, 0.1% m/v) was first pre-hydrolysed with α-AMY (1000 U) or β-AMY (1000 U) in order to investigate their efficiency prior to analysis with the starch electrode (type A) and the iodine - iodide paper technique (Table 2). No blue spots were observed on the iodine - iodide paper after incubation of starch with the α-AMY enzyme for 5 min, while the flow injection (FI) signal size was about seven times that for the untreated α-AMY starch solution. Further, addition of 500 U of β-AMY to the initial α-AMY starch solution resulted in weaker starch signals with the GO - MUT electrode (*ca.* 20%) suggesting the inhibition of either α-AMY, AMG, MUT or GO by β-AMY.

The variation in the response of the starch electrode type A to starch (0.1% m/v) after different incubation periods with α-AMY was also investigated by flow injection. Calibrations of starch samples, untreated and treated with α-AMY only, after incubation with the hydrolase for 30 min and 2 h, were compared at a flow-rate of 1.7 cm³ min⁻¹, phosphate buffer (pH 5) and a sample volume of 0.5 cm³ (Fig. 2). The graphs

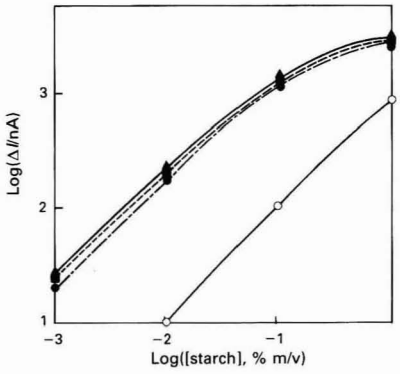

Fig. 2. Response of the type A starch electrode to starch standards for various treatments with α-AMY (each at room temperature). ●, Zero time; ■, after 30 min; ▲, after 2 h; and ○, with no α-AMY pre-treatment

were similar, however, the untreated α-AMY samples displayed signals even lower than for "zero time" as, in the latter instance, some hydrolysis occurs between the mixing with α-AMY, and the actual electrode response in the flow stream.

Pre-treatment of starch with β-AMY alone assists the conversion of starch into glucose, but not to the same extent as α-AMY. This was confirmed with the iodine - iodide paper where blue spots were still observed after incubation of starch with the enzyme for 30 min (Table 2). Hence, in all subsequent studies, starch solutions were incubated with α-AMY (1000 U) for about 1 h prior to their analysis, unless stated otherwise. This time was chosen to ensure complete hydrolysis, although clearly (Fig. 2) 15–30 min seems adequate.

Optimisation of Operational Conditions

These include parameters such as pH, flow-rate and sample volume.

Optimisation of pH

Two buffers, phosphate and acetate (each 0.1 M), were investigated. Starch (0.1% m/v) was prepared in phosphate buffers between pH 3.3 and 8.1 and in acetate buffers at pH values between 4 and 7.8. The starch samples (0.5 cm³) were then injected into the carrier stream (of the appropriate buffer, set at the pH of the samples), flow-rate 1.7 cm³ min⁻¹, of the corresponding pH and the peak signals were measured. Steady-state measurements were also performed by continuous pumping of the starch samples.

The pH profiles of peak signals and steady-state measurements for both buffers were unusual, with "humps" at pH values of ≈4.5 and ≈6, respectively, and reflected a combination of the pH optima of the three enzymes (Fig. 3). Higher signals were observed with phosphate buffer at pH 4.5 than at pH 6 but the reverse situation was found for the acetate buffer. At pH 6, starch in acetate buffer produced larger signals than phosphate, but the reverse was true at lower pH. Acetate buffer (0.1 M) at pH 6 was chosen as immobilised GO has an optimum pH of 7. An extended sensor lifetime could also be expected at this pH, rather than by working at pH 4.7.

Optimisation of flow-rate and sample volume

The effect of flow-rate (1.7–3.5 cm³ min⁻¹) for 0.5-cm³ samples was studied for starch, at pH 5 with 0.1 M phosphate buffer, by peak-height and steady-state measurements. The plateau type for both measurements (with a maximum at ≈2.5 cm³ min⁻¹) differed from the exponential-type flow profiles reported earlier for glucose,[7] sucrose[10] and lactose[8] elec-

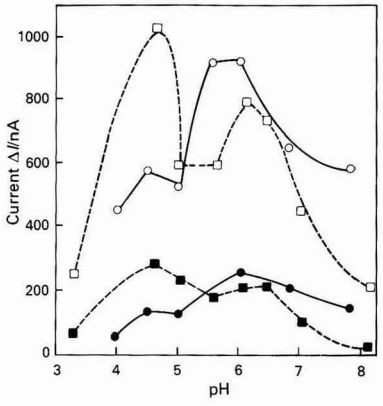

Fig. 3. Responses at various pH values of type A starch electrode. ■ and □, measurements for phosphate buffer samples; ● and ○, measurements for acetate buffer samples; ○ and □ for maximum response by continuous pumping of sample; and ● and □ peak signals for 0.5-cm³ samples

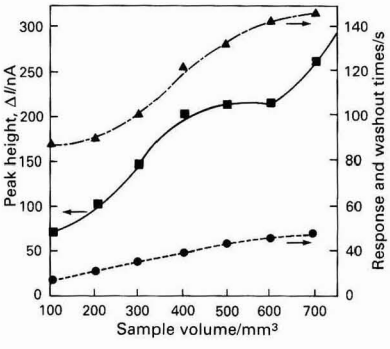

Fig. 4. Effect of sample volume on response of type A starch electrode. ▲, Washout times; ■, peak heights; and ●, response times

trodes. A flow-rate of 1.7 cm^3 min^{-1} was chosen as a compromise between reagent consumption and signal size.

The sample loop volume was optimised at a flow-rate of 1.7 cm^3 min^{-1} in a background of phosphate buffer (0.1 M, pH 6). Peak heights for various volumes of starch increased with increasing volume of sample, as did the response and washout times (Fig. 4). An optimum sample volume of 0.5 cm^3 was chosen for subsequent work.

Electrode Calibration

The type A starch electrode was calibrated with a starch stock solution, pre-treated with 1000 U of α-AMY for 1 h and then serially diluted with acetate buffer (0.1 M) at pH 6. Signal reproducibility was good for each sample concentration (*ca.* <1%). The signals consisted of peaks with broad bases which increased with starch concentration, but the average response times were 15–20 s and the linear range was from 1×10^{-4} to 1×10^{-1}% m/v starch (Fig. 5) with a regression equation of $\log(\Delta I/A) = 0.866 \log([\text{starch}], \%\ \text{m/v}) - 13.8$ ($r = 1.000$). The calibration for untreated starch was relatively poor (Fig. 6).

Properties of the Starch Electrode

Thermal stability, γ-radiation stability, electrode selectivity and lifetime stability are important parameters.

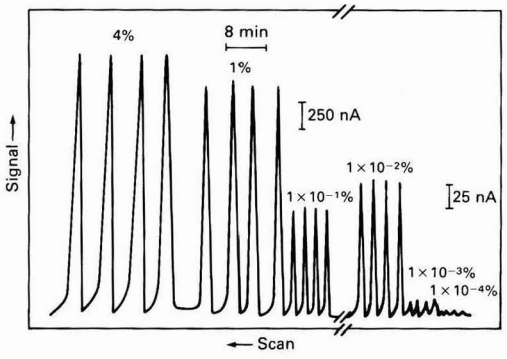

Fig. 5. FI profiles of type A starch electrode for starch standards (1×10^{-4}–4% m/v) pre-treated with α-AMY for 1 h at room temperature

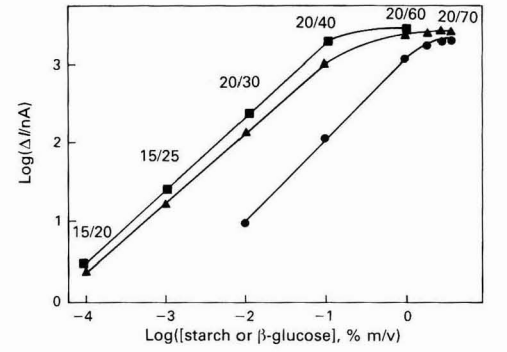

Fig. 6. Calibration of type A starch electrode under various conditions. ●, Untreated starch; ▲, starch treated with α-AMY for 1 h; and ■, β-glucose. Numerators and denominators are response and wash times, respectively, for the α-AMY hydrolyses studies

Thermal stability

Two different experiments were performed. In the first, the complete starch electrode assembly was exposed to temperatures ranging between 5 and 70 °C, achieved by keeping the temperature of the pre-treated starch solution (0.1% m/v) and the phosphate buffer stream constant in each run, using an ice - water-bath to obtain the lower temperatures. The temperatures of the sample and the buffer stream were then raised gradually, prior to the injection of each sample into the flow system. The temperature profile (Fig. 7) indicates a maximum response at about 50 °C for both the initial and repeat runs, illustrating the good stability of the enzyme electrode.

The second approach was a more stringent test of robustness wherein the enzyme membrane was exposed to the given temperatures for periods of 10 min. Thus, the starch-sensing membrane was removed from the base working electrode and dipped in acetate buffer (0.1 M at pH 6) which was set at various temperatures from 20 to 100 °C. The membrane was exposed to the selected temperature for 10 min and re-fitted as a working electrode for re-calibration with starch standards. For 0.1% m/v starch the signal strength fell dramatically, *e.g.*, from 1850 to 545 nA as the temperature increased from 60 to 70 °C, but the relative effect was far less noticeable at the low starch levels (Fig. 8).

γ-Radiation stability

The recommended dose of γ-radiation to sterilise food is 24 kGy.[11] Thus, it was pertinent to consider γ-radiation as a

means of sterilising the type A starch enzyme electrode. For this purpose, resistance of the starch electrode to ^{60}Co γ-radiation was tested after exposure of fresh enzyme membranes in 0.1 M acetate buffer to set doses of 12, 24 and 48 kGy. Starch calibration graphs (using the working electrode carrying the same irradiated membrane) showed a drop in the electrode response after exposure to 12 kGy and, as might be expected, a larger drop after irradiation with 24 and 48 kGy. Nevertheless, useful working ranges were still achievable (Fig. 9).

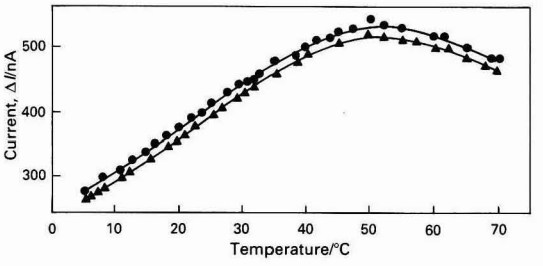

Fig. 7. Thermal stability of type A starch electrode. Concentration of starch, 1×10^{-1}% m/v; ●, first run; and ▲, repeat run

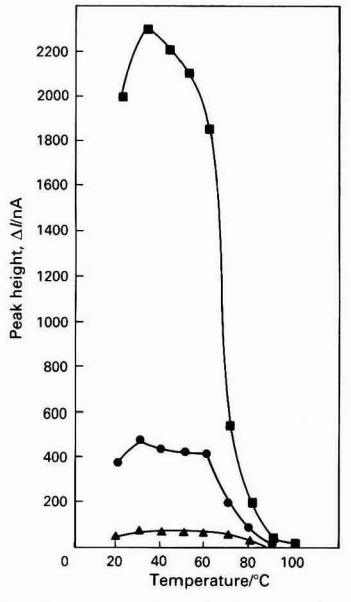

Fig. 8. Effect of heat on type A starch electrode. Concentration of starch: ■, 1×10^{-1}; ●, 1×10^{-2}; and ▲, 1×10^{-3}% m/v

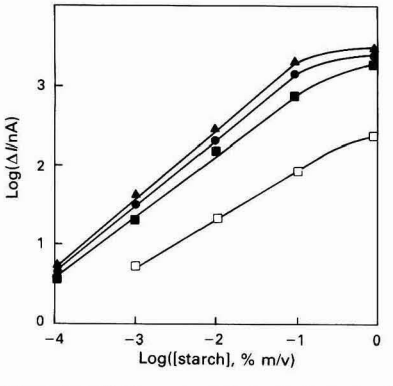

Fig. 9. Effect of γ-radiation on type A starch electrode. ▲, Initial; ●, 12; ■, 24; and □, 48 kGy

Electrode selectivity

Response of the starch electrode to ten sugars (α-glucose, β-glucose, maltose, α-lactose, β-lactose, sucrose, fructose, mannose, raffinose and galactose), five organic acids (gluconic, citric, lactic, benzoic and ascorbic) and five amino acids/proteins (lysine, arginine, ornithine, glycine and serum albumin) was studied as described previously.[9] Readings were normalised with respect to those for 1 mM starch (calculated on the basis of its glucose residues). As expected, α-glucose, β-glucose, maltose and ascorbic acid interfered significantly with starch sensing, whilst the remainder displayed negligible interference (Table 3).

Lifetime stability

The storage stability of the tri-enzyme starch electrode was tested using freshly prepared enzyme membranes stored at 4 °C at pH 6 in 0.1 M acetate buffer. The response to 0.1% m/v starch was then checked daily for 1 week and then at 7-d intervals over a period of 4 months. The response was stable for *ca.* 3 months before enzyme denaturation occurred and the percentage of the initial activity remaining, fell to 50% by day 119.

The operational stability of the electrode was also tested by continuously pumping 1×10^{-1}% m/v starch over a freshly prepared starch electrode when its response remained steady for a period of 60 h but fell to ≈40% after 96 h of this treatment.

Effect of Glucose Units in Various Carbohydrates

The effect of six carbohydrates containing various numbers of glucose units on the type A starch electrode was also investigated (Table 4). Substrates (1 mM concentration in starch solution, prepared on content of glucose units, *i.e.*, with

Table 3. Effect of sugars, organic acids and proteins on the type A starch electrode

Interferent	Signal normalised against the response of 1 mM starch: Separate injection*	Mixture technique†
Sugars—		
β-Glucose	0.66	1.13
α-Glucose	0.43	1.13
Maltose	0.48	1.05
β-Lactose	0	1.01
α-Lactose	0	1.01
Sucrose	0	1.01
Fructose	0	0.98
Mannose	0	0.98
Raffinose	0	1.01
Galactose	0	0.98
Organic acids—		
Gluconic acid	0	0.97
Citric acid	0	1.01
Lactic acid	0	0.97
Benzoate	0	0.98
Ascorbic acid	1.27	1.68
Proteins—		
Lysine	0	0.98
Arginine	0	0.93
Ornithine	0	0.95
Glycine	0	1.00
Bovine serum albumin,% m/v	Negligible	1.04

* Interferent, 1mM.
† Interferent, 1mM plus starch, 1mM.

Table 4. Effect of carbohydrates with various glucose units on the flow response of the type A starch electrode

Number of glucose residues	Substrate*	Response ΔI/nA ($n = 3$)
1	β-Glucose	800
2	Maltose	475
3	Maltotriose	900
4	Maltotetraose	1350
5	Maltopentose	1500
	Starch (without α-AMY pre-treatment)	210
	Starch (with α-AMY pre-treatment)	1900
6	α-Cyclodextrin	12.5
7	β-Cyclodextrin	10.0

* All substrates were 1 mM in concentration.

Table 5. Two-electrode analysis of synthetic samples of 1% starch (equivalent to 61.7 mM glucose) and added glucose

		Analysis by flow injection	
Glucose added/mM	Total glucose/ mM equivalent	Glucose content/mM ($n = 3$)	Starch content/mM ($n = 3$)
1.1	62.8	1.2	61.8
2.5	64.2	2.4	61.5
3.7	65.4	3.7	63.3
4.9	66.6	5.0	63.0
0	62.0	0	62.0

relative molecular mass = 162) were incubated with α-AMY (1000 U) for *ca.* 1 h, before analysis by the normal flow injection method.

Maltose produced about half the peak response observed with glucose at the starch electrode, but the peaks were broader. Increasing glucose units from maltose to maltotetraose showed a proportionate increase in signals, but not with maltopentose (Table 4). The rate of hydrolysis of each substrate decreases with an increase in the number of glucose units and the components containing α-1,6 branching linkages, as in starch, are hydrolysed more slowly.[10] Further, the rate of diffusion of the substrate into the enzyme membrane decreases when the molecules become more bulky, thus lowering their responses at the electrode.

The cyclic compounds (α- and β-cyclodextrin) produced very small signals and were not sufficiently degraded by the hydrolase enzymes before analysis.

Analysis of Synthetic Glucose - Starch Mixtures

This flow injection study examined the efficiency of a starch electrode (type A) in determining starch in glucose mixed with 1% m/v starch (equivalent to 61.7 mM glucose). Four standards containing starch (equivalent to 61.7 mM glucose) plus four different amounts of glucose (without α-AMY pre-treatment) were first analysed for glucose using a pre-calibrated GO - MUT electrode. Total glucose was then determined with a pre-calibrated starch electrode after incubation for 1 h with 1000 U of α-AMY (Table 5). This two-electrode technique showed good reproducibility (coefficient of variation, <2%).

Analysis of Real Starch Samples

Starch samples (potato, wheat, rice, tapioca and corn flour) were analysed amperometrically and spectrophotometrically using the Boehringer Mannheim Starch Test Combination Kit (Cat. No. 207748) (Table 6). Samples were solubilised prior to their analysis according to the method described earlier. Results obtained with the two techniques were in close agreement.

Table 6. Analysis of flour samples with the type A starch electrode and Boehringer Mannheim starch kit. Data in parentheses have been corrected for glucose content

	Starch content/g per 100 g	
Flour sample	Starch enzyme electrode ($n = 3$)	Spectrophotometric kit
Potato . .	120 (97)	120 (97)
Corn	140 (98)	130 (95)
Wheat . .	90	88
Rice	80	79
Tapioca . .	100	98

Table 7. Response of various starch electrodes to 0.1% m/v starch. In all instances, the amounts of AMG, α-AMY, MUT and GO in the enzyme cocktail are 2000, 1000, 100 and 100 U, respectively

Number of membranes	Enzyme membrane arrangement	Peak height ΔI/nA ($n = 3$)
1	AMG - MUT - GO (type A) with and without pre-treatment with soluble α-AMY	1225 275
1	AMG - MUT - GO - α-AMY	500
2	α-AMY and AMG - MUT - GO	975
	α-AMY - AMG and MUT - GO	1125
4	α-AMY - AMG - MUT - GO	785

Misleadingly high starch contents in both potato and corn flour samples were attributed to their high endogenous glucose content (not found in the other samples) as verified by the determination of glucose with the MUT - GO electrode.

Starch Electrodes Based on Immobilised α-AMY

The above studies involved pre-incubation of starch samples with soluble α-AMY (1000 U) for ≈1 h at room temperature before determining starch content. This is, of course, time consuming and attempts were made to develop a starch electrode with immobilised α-AMY using one, two or four enzyme membranes in order to eliminate the time consuming starch pre-hydrolysis stage.

Single membrane electrode

For this purpose, a tetra-enzyme system was prepared by co-immobilising AMG, MUT and GO plus α-AMY (2000 + 100 + 100 + 1000 U) on to activated nylon net, N95 (1 × 1 cm^2).

The response of the tetra-enzyme electrode to starch (0.1% m/v) was compared with the tri-enzyme electrode (type A) without α-AMY treatment of the starch samples (Table 7). The tetra-enzyme electrode gave approximately twice the response to starch relative to that of the tri-enzyme electrode when the starch solution was pre-hydrolysed with soluble α-AMY.

Multi-membrane electrodes

Two types of double-membrane electrode were fabricated (Table 7), the first with a piece of immobilised α-AMY and a piece of randomly co-immobilised tri-enzyme membrane (AMG - MUT - GO, *i.e.*, the type A electrode mentioned above) and the second, with a sandwich of a bi-enzyme membrane of AMG - α-AMY and a bi-enzyme membrane of GO - MUT. In both instances, the membrane with the α-AMY was placed outermost from the platinum of the base working electrode.

For the four-membrane enzyme electrode, α-AMY, AMG, MUT and GO were each immobilised separately on a piece of nylon net, sandwiched together and placed next to the base

electrode in the order of electrode GO, MUT, AMG and α-AMY.

Responses of these electrodes to a 1×10^{-1}% m/v starch solution (Table 7) were no better than those using the sample pre-treatment with soluble α-AMY. However, the two-membrane (AMG - α-AMY plus GO - MUT) system approximated to that which included soluble α-AMY pre-treatment (Table 7), but the longer response times (40 s for 1×10^{-3}% m/v starch compared with 15 s for the type A electrode) of the multi-membrane electrodes is disadvantageous in analysis times because of restricted substrate/product diffusion through the membranes.

Conclusion

The determination of starch with a flow-through tri-enzyme electrode (type A) exhibited a linear range over three decades with excellent analytical properties. However, starch solutions had to be incubated with soluble α-AMY prior to analysis. Unfortunately, immobilising the α-AMY on to nylon net to give a single- or multi-enzyme membrane electrode did not enhance the electrode signals. In view of the electrode response to glucose and many other polysaccharides degradable by α-AMY or AMG in the electrode system, a practical starch electrode in the form of micro-electrode arrays consisting of appropriate enzyme electrodes for the other sample components, and linked to a micro-computer is worthy of investigation.

The authors thank the Malaysian Public Service Department for financial support to J. A. H.

References

1. Emneus, J., Appelqvist, R., Marko-Varga, G., Gorton, L., and Johansson, G., *Anal. Chim. Acta*, 1986, **180**, 3.
2. Appelqvist, R., Marko-Varga, G., Gorton, L., and Johansson, G., Second International Meeting on Chemical Sensors, Bordeaux, France, 1986, p. 603.
3. Appelqvist, R., *PhD Thesis*, University of Lund, Sweden, 1987.
4. Emneus, J., and Gorton, L., *Anal. Chem.*, 1990, **62**, 263.
5. Pfeiffer, D., Scheller, F., Janchen, M., and Bertermann, K., *Biochimie*, 1980, **62**, 587.
6. Renneberg, R., Scheller, F., Riedel, K., Litschko, E., and Richter, M., *Anal. Lett.*, 1983, **16**, 877.
7. Moody, G. J., Sanghera, G. S., and Thomas, J. D. R., *Analyst*, 1986, **111**, 605.
8. Abdul Hamid, J., Moody, G. J., and Thomas, J. D. R., *Analyst*, 1989, **114**, 1587.
9. Kusunoki, K., Kawakani, K., Shiraishi, F., Kator, K., and Kai, M., *Biotechnol. Bioeng.*, 1982, **24**, 347.
10. Abdul Hamid, J., Moody, G. J., and Thomas, J. D. R., *Analyst*, 1988, **113**, 81.
11. Choppin, G. R., and Rydberg, J., "Nuclear Chemistry: Theory and Application," Pergamon Press, Oxford, 1980, p. 239.

Paper 0/01828G
Received April 25th, 1990
Accepted June 19th, 1990

Determination of L-Ascorbic Acid in Fruit and Vegetable Juices by Flow Injection With Immobilised Ascorbate Oxidase

Gillian M. Greenway and Peter Ongomo
School of Chemistry, University of Hull, Hull HU6 7RX, UK

Ascorbate oxidase was immobilised on cyanogen bromide activated-Sepharose 4B and incorporated in a flow-injection system with amperometric detection at a glassy carbon electrode at +0.6 V. On passage through the immobilised ascorbate oxidase a fraction of the L-ascorbic acid was converted into dehydroascorbic acid and the decrease in signal was measured. This could be directly related to the amount of L-ascorbic acid present. The calibration graph was linear over the range 0–400 ng ml^{-1} with a correlation coefficient of 0.9994. The detection limit (2σ) in phosphate buffer (0.08 M, pH 5.5) was 4.0 ng ml^{-1}. The relative standard deviation for a 200 ng ml^{-1} standard was 1.0% (n = 10) and the sampling throughput was 30 samples h^{-1}. The method was used for the simple and rapid determination of L-ascorbic acid in fruit and vegetable juice.

Keywords. *L-Ascorbic acid determination; flow injection; immobilised ascorbate oxidase; fruit juice*

Many methods have been developed for the determination of vitamin C (L-ascorbic acid), however, most of them have been based on its reducing properties.[1–5] These methods lack specificity and are prone to interferences by other reducing agents present in the sample. The alternative method for analysis in complex matrices such as food samples is to use high-performance liquid chromatography, however, this is a time-consuming technique.[6]

Ascorbate oxidase is an enzyme that catalyses the oxidation of ascorbic acid as follows:

$$\text{L-Ascorbic acid} + \tfrac{1}{2}O_2 \xrightarrow{\text{ascorbate oxidase}} \text{dehydroascorbic acid} + H_2O$$

This enzyme can be used to devise more specific methods for the determination of ascorbic acid. Esaka *et al.*[7] detected ascorbic acid using ascorbate oxidase physically trapped in calcium alginate and treated with 1% m/v glutaraldehyde. The system was static and the ascorbic acid concentration was monitored by measuring spectrophotometrically the change in enzyme activity. Stevanato *et al.*[8] immobilised ascorbic oxidase on to 6-aminohexanoic acid-Sepharose 4B using carbodiimide. The immobilised enzyme was utilised in a flow-through system equipped with a polarographic detector which monitored the oxygen depletion during the reaction.

In this paper immobilised ascorbate oxidase is incorporated in a flow-injection system with an amperometric detector using a glassy carbon electrode. The detector monitors the decrease in the concentration of ascorbic acid after it passes through the enzyme column.

Experimental

Reagents

Ascorbate oxidase (E.C. 1.10.3.3 250 U mg^{-1} from *Cucurbita* species) and cyanogen bromide activated-Sepharose 4B were obtained from Sigma (Poole, Dorset, UK). L-Ascorbic acid, disodium hydrogen orthophosphate, sodium dihydrogen orthophosphate, glycine, ethylenediaminetetraacetic acid (EDTA) and all other chemical reagents were obtained from BDH (Poole, Dorset, UK). All reagents used were of analytical-reagent grade and solutions were made up in doubly distilled, de-ionised water. Great care had to be taken in the preparation of samples and standards as ascorbic acid can degrade rapidly, especially above pH 4. Fresh stock solutions (1.0 mg ml^{-1}) were prepared daily in ice-cold 0.05 M $HClO_4$. This was then used to prepare a working solution in phosphate buffer (pH 5.5, 0.08 M).

Immobilisation of Enzyme

Ascorbate oxidase (1 mg) was dissolved in 2.5 ml of 0.1 M sodium hydrogen carbonate. Enzyme solution (1 ml) was mixed with 0.200 g of the activated Sepharose. The mixture was shaken gently for 24 h at 4 °C. Glycine (0.05 g) was then added to the slurry and shaken gently for a further 9 h. The Sepharose-bound enzyme was filtered off and washed with distilled water followed by 0.1 M sodium hydrogen carbonate and sodium chloride (0.5 M) in order to remove any residues. The immobilised enzyme was then packed into a glass mini-column (25 × 2.5 mm i.d.) which was stored overnight at 4 °C in sodium pyrophosphate (0.1 M) containing 0.1% NaN_3.

Instrumentation and Measurement Procedure

The three-electrode amperometric detector was based on the wall-jet flow cell design with a glassy carbon working electrode (Model LCA15, EDT, London, UK). The electrode was electrochemically pre-treated every 2 d to maintain electrode stability and reproducibility.[9] This was carried out by exposing the electrode to a high oxidation potential (+2.00 V) for 5 min and then −1.0 V for 1 min. It was then left to stabilise for 15 min before setting it to the potential used for analysis (+0.6 V). Results were recorded using a chart recorder (Model SE120, BBC Goerz Metrawatt, Labdata, Carshalton, Surrey, UK). The flow-injection manifold shown in Fig. 1 consisted of a peristaltic pump (Model SA8031, Ismatec, Zurich, Switzerland), an injection valve (with a 50-μl loop) and two switching valves (Omnifit, Anachem, Luton, Bedfordshire, UK). All connections were made with polytetrafluoroethylene tubing (0.5 mm i.d.) and polypropylene flangeless connections (Omnifit).

Two Sepharose columns were incorporated in the system; a reactive column with the immobilised enzyme and a blank column. Two measurements were made for each determination, one using the enzyme column and one using the blank

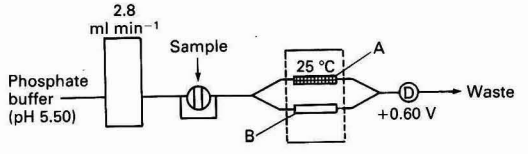

Fig. 1. Manifold for L-ascorbic acid determination. A, Ascorbate oxidase immobilised with cyanogen bromide activated-Sepharose 4B; and B, blank column with no enzyme. D is the detector

column. On passage through the immobilised ascorbate oxidase column a fraction of the ascorbic acid was converted into dehydroascorbic acid (which is not electroactive) and the decrease in signal compared with the blank was measured. This could be directly related to the amount of ascorbic acid present. All measurements were made in triplicate.

Preparation of Samples

Lemon and orange juice were prepared by squeezing cut pieces of fruit between two clean glass beakers. A 5.0-ml aliquot of the juice was then treated with 10.0 ml of 0.05 M $HClO_4$ and centrifuged at 4000 rev min^{-1} for 15 min. The supernatant was filtered off through a Whatman No. 4 filter-paper, transferred into a 100.0-ml flask and diluted with 0.05 M $HClO_4$. Further dilutions were made as necessary. The blackcurrant juice only required dilution with $HClO_4$.

Results and Discussion

The activity of the immobilised enzyme was very high and initially resulted in total conversion of the ascorbic acid into dehydroascorbic acid; this did not allow the measurement of the difference in ascorbic acid before and after it passed through the immobilised enzyme. As the aim was to develop a technique with high sensitivity and low detection limits the activity of the column was reduced by dilution of the immobilised enzyme with inactive Sepharose (1 + 100). This dilution was chosen so that only a fraction of the ascorbic acid was converted, even for very low ascorbic acid concentrations, so that quantitative measurements could be made.

The effect of pH on the activity of the immobilised enzyme was then investigated by using phosphate buffer (0.1 M) in the range pH 4.5–7.5 (Fig. 2). The maximum activity occurred at pH 5.0, however, a pH of 5.5 was found to provide a more stable baseline and greater reproducibility. The concentration of the buffer was also studied, the response decreasing slightly with increased concentration. A relatively high concentration of phosphate buffer (0.08 M) was chosen to buffer against the injection of acidic samples such as orange and lemon juice.

Temperature effects on the enzyme activity in the range 20–40 °C (Fig. 3) were studied by circulating water around the packed reactor column. The activity of the enzyme increased with temperature up to 35 °C before falling off, but further experiments were carried out at 25 °C to prolong the lifetime of the enzyme.[7]

Fig. 4 shows the effect of flow-rate on the enzyme activity. The peak height increases as the flow-rate increases. At low flow-rates the L-ascorbic acid in the sample is in contact with the enzyme for longer and, therefore, the peak height will be low as more of the ascorbic acid is converted into dehydroascorbic acid. In order to obtain a high sensitivity a large decrease in the signal is required for a particular starting concentration of ascorbic acid.

The flow-rate of the system (2.8 ml min^{-1}) was selected as a compromise, slow enough to give reasonable sensitivity but rapid enough to give sharp peaks and a good sampling rate. Experiments were also carried out using different injection volumes. The signals increased with increasing volume. Sample volumes of 50 µl were employed as a compromise between speed and sensitivity.

The immobilised enzyme was used continuously each day for a period of 3 weeks without any significant loss in activity. Over a period of 3 months the activity of the enzyme decreased by approximately 30% when stored at 4 °C. This agreed with the work by Stevanato *et al.*[8]

Analytical Results and Interference Study

A calibration graph was obtained by injecting L-ascorbic acid standard solutions into the manifold under the optimum conditions. All measurements were made in triplicate. The calibration graph was linear over the range 0–400 ng ml^{-1} and the linear regression equation of best fit was $y = 0.33x - 1.37$ (where x is the concentration of ascorbic acid in ng ml^{-1}, and y is the difference in current for ascorbic acid before and after it passed through the ascorbate oxidase in nA). The correlation coefficient for this line was 0.9994 and the detection limit (2 σ) in phosphate buffer was 4.0 ng ml^{-1}. The relative standard deviation for a 200 ng ml^{-1} standard was 1.0% (n = 10) and the sampling throughput was 30 samples h^{-1}.

Interferences

The design of this system was aimed at eliminating interferences caused by reducing agents other than ascorbic acid,

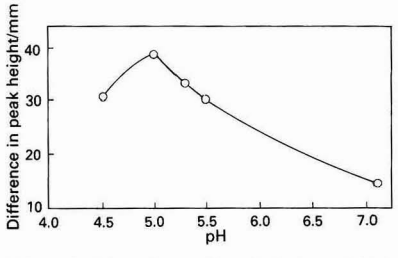

Fig. 2. Effect of pH on the activity of the immobilised ascorbic oxidase (0.1 M phosphate buffer, 160 ng ml^{-1} L-ascorbic acid)

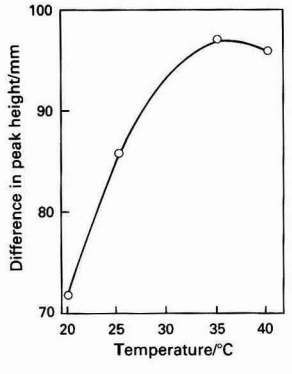

Fig. 3. Effect of temperature on the activity of ascorbate oxidase (200 ng ml^{-1} L-ascorbic acid)

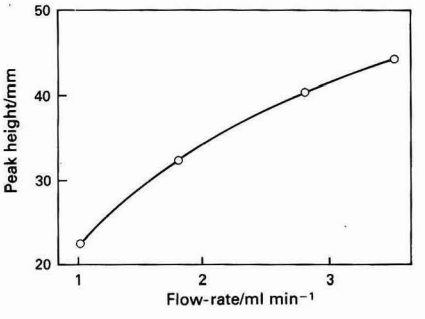

Fig. 4. Effect of flow-rate on the activity of ascorbate oxidase (160 ng ml^{-1} L-ascorbic acid)

Table 1. Interference study for ascorbic acid (100 ng ml^{-1}) in phosphate buffer (0.1 M, pH 5.5)

Interferent	Concentration found/μg ml^{-1}	Response, %
Oxalic acid	50	100
Tartaric acid	60	111
Citric acid	250	91
Glucose	200	81
Copper(II)*	2.4	97

* L-Ascorbic acid, 200 ng ml^{-1}

Table 2. L-Ascorbic acid content of various fruit and vegetable juices

Sample	L-Ascorbic acid concentration/ mg per 100 ml
Lemon juice	52
Orange juice	65
Ribena*	31
Cucumber juice	0.007

* Blackcurrant drink.

Table 3. Recovery tests for blackcurrant and fresh orange juice

Sample	L-Ascorbic acid added/ng ml^{-1}	Recovery, %
Ribena	100	100
Lemon juice	50	91

because although the detector was not selective the ascorbate oxidase should be highly selective. The design could not, however, eliminate interferences that affected the activity of the enzyme.

Fresh fruits contain a number of organic acids and sugars such as citric acid, tartaric acid, malic acid, fructose and sucrose.[4] Gerwin *et al.*[10] reported that citrate competitively inhibits with respect to ascorbate oxidase at low substrate concentrations and its anion also inhibited the enzyme. Studies were carried out to determine the interference effects of Cu^{2+}, glucose, citric acid, tartaric acid and oxalic acid on the determination of ascorbic acid. The interferents were added in increasing amounts to 100 ng ml^{-1} of L-ascorbic acid (Table 1). Glucose, oxalic acid, citric acid and tartaric acid did not seriously interfere even in great excess. Copper has a catalytic effect on the decomposition of ascorbic acid and was shown to interfere at lower levels (2.4 μg ml^{-1}). This effect was successfully eliminated by the addition of EDTA (250 μg ml^{-1}).

Sample Analysis

The content of L-ascorbic acid was then determined in samples of orange, lemon, cucumber and blackcurrant drink (Table 2). These were in agreement with results reported by other workers.[8] Recovery tests were performed for the blackcurrant drink and lemon juice (Table 3) and found to be satisfactory. The 2,6-dichloroindophenol titration method[11] was carried out in order to compare the two methods. For blackcurrant juice there was a difference of 7% between the results obtained by the different methods. This difference was not considered to invalidate the enzyme method as the titration end-point was difficult to determine and also the method was prone to interferences.[12]

Conclusion

The method described is very simple and rapid (2 min per sample), but also has high sensitivity (4 ng ml^{-1}) and selectivity. Only small sample sizes are required (2 × 50 μl) and the reproducibility is good (1% at 100 ng ml^{-1}). The accuracy of the method has been illustrated for various juice samples but with the good sensitivity achieved it would also be suitable for clinical analysis. An automated system that included dialysis for sample clean-up and computerised data treatment could be of real value, allowing the rapid determination of ascorbic acid before degradation.

References

1. Pachla, L. A., Reynolds, D. C., and Kissenger, P. T., *J. Assoc. Off. Anal. Chem.*, 1985, **68**, 1.
2. Dabrowski, K., and Hinterleitner, S., *Analyst*, 1989, **114**, 83.
3. Salinas, F., and Galeano Díaz, T., *Analyst*, 1988, **113**, 1657.
4. Lau, O.-W., Luk, S.-F., and Wong, K. S., *Analyst*, 1986, **111**, 665.
5. Abdalla, M. A., and Al-Swaidan, H. M., *Analyst*, 1989, **114**, 583.
6. Macrae, R., "HPLC in Food Analysis," Academic Press, London, 1988, pp. 172–179.
7. Esaka, M., Suzuki, K., and Kubota, K., *Agric. Biol. Chem.*, 1985, **49**, 2955.
8. Stevanato, R., Avigliano, L., Finazzi-Agro, A., and Rigo, A., *Anal. Biochem.*, 1985, **149**, 537.
9. Fogg, A. G., and Sulman, A. M., *Analyst*, 1984, **109**, 1029.
10. Gerwin, B., Burstein, S. R., and Westerley, J., *J. Biol. Chem.*, 1974, **249**, 2005.
11. "Official Methods of Analysis of the Association of Official Analytical Chemists," Fourteenth Edition, Association of Official Analytical Chemists, Arlington, VA, 1984, 43.064-43.081.
12. Pacha, A. L., and Kissenger, P. T., *Anal. Chem.*, 1976, **48**, 364.

Paper 0/01673J
Received April 17th, 1990
Accepted June 6th, 1990

Influence of the Redox Potential of the Medium on Stripping Voltammetric Measurement Results

Khiena Z. Brainina, Elena A. Vilchinskaya and Rosa M. Khanina
Sverdlovsk Institute of National Economy, 8th March St. 62, 620219 Sverdlovsk GSP-985, USSR

It is shown that raising the redox potential of the medium leads to a substantial decrease in the lifetime of a graphite electrode plated, before use, with mercury. Electrochemical reduction of dissolved oxidants by applying pulses of potentials equal to −0.8 and 0 V extends the electrode service life by up to 2 d. No loss of the analyte elements [copper(II), and cadmium(II)] is detected. The lifetime of an electrode plated with mercury *in situ* was partly dependent on the redox potential of the medium. When the potential is increased, only the sensitivity of the determination of ions in solution, decreases.

Keywords: *Stripping voltammetry; natural waters; graphite electrode; mercury coating; redox potential*

All currently available versions of stripping voltammetric analysis, as a rule, exploit solutions that do not contain oxidants. Oxygen is removed before the analysis and solutions with a sufficiently low redox potential are analysed. The electrode surface is frequently renewed; the mercury drop is replaced by a new one, while the mercury coating is dissolved[1] or removed mechanically.[2] The above procedure, on the one hand, renders this usual discrete analysis more time consuming and, on the other hand, highly complicates the application of the stripping voltammetric method to flow systems.

At the same time, particular interest is attached to flow systems in the context of monitoring the environment, *e.g.*, natural and sewage waters. Here, preparing a sample for analysis must involve the destruction of organic substances,[3] because the adsorption of surfactants and the binding of the analyte elements, which are liable to form strong complexes, give rise to a systematic error in determination.[4] The adverse effect of organic substances can be eliminated in several ways. The most common method is ultraviolet irradiation.[5] However, irradiation is a lengthy procedure and requires the introduction of a sensitiser; ions of electropositive elements may be lost through reduction. An electrochemical method of oxidising organic substances in natural waters is proposed.[6] This includes a simultaneous electrochemical and chemical oxidation of organic substances by the oxidant produced in the anode space according to the reaction

$$2Cl^- \rightarrow Cl_2 + 2e^- \quad \ldots\ldots (1)$$

$$Cl_2 + H_2O \leftrightarrows HCl + HClO \quad \ldots\ldots (2)$$

$$2H_2O \rightarrow O_2 + 4H^+ + 4e^- \quad \ldots\ldots (3)$$

Taking into account the efficiency of the electrochemical oxidation of organic substances in overcoming their adverse effect on stripping voltammetric analysis[6] and allowing for the simultaneous acidification of the solution (specifically, acidification eliminates possible contamination of the test solution by impurities in acids which are used to acidify the medium), the electrochemical method[6] of preparing samples for analysis was used in this work.

The aims of the work described in the present paper were: (*i*) to study the effect of the redox potential of the medium on the lifetime of an indicator graphite electrode (sensitivity and validity of the findings) for the two most common versions, namely, electrodes plated with mercury prior to use and electrodes plated with mercury *in situ* and (*ii*) to search for conditions ensuring sufficiently long and adequate operation of the electrodes.

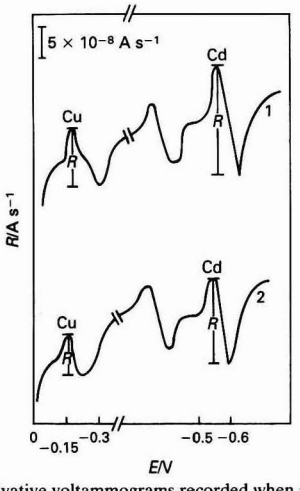

Fig. 1. Derivative voltammograms recorded when analysing a 0.5 M NaCl solution acidified to pH 2.7 using hydrochloric acid (1) and subjected to preliminary electrochemical oxidation at a potential of +1.5 V for 10 min (2). Metal ion concentration: Cu^{2+}, 5.0; Pb^{2+}, 2.0; and Cd^{2+}, 3.0 μg l^{-1}

Experimental

For stripping voltammetric measurements, a closed electrochemical cell incorporating a quartz electrolyser and additional vessels for auxiliary and reference electrodes was used. The auxiliary electrode was a graphite rod made of spectroscopically pure carbon (100 mm long and 15 mm in diameter), while the reference electrode was a saturated silver - silver chloride electrode. The indicator electrode was a graphite electrode impregnated with epoxy resin[7] and plated with mercury prior to use (electrode type I) or *in situ* (electrode type II). To improve the quality of the pre-deposited mercury coating (electrode type I), the electrode surface was modified with zinc adatoms[8,9] which were formed by under-voltage deposition.[10]

Voltammograms were obtained using an oscillographic polarograph, an IVA-1 semi-automatic stripping analyser (laboratory built) and a II-5827M potentiostat (Izmeritel). A 0.5 M NaCl solution and samples of river and sea-water were investigated. High-purity reagents and water, distilled with the addition of an alkaline solution of $KMnO_4$ to destroy organic impurities, were used. The distillate was re-distilled twice in glass apparatus free from rubber connections.

Information about electrode processes was obtained by recording derivative direct current (d.c.) voltammograms of

electrochemical transformations of the concentrate produced at the accumulation stage. The method of measuring the analytical signal (response) is shown in Fig. 1. Between analyses, the mercury-plated electrode was kept in the test solution at a potential of −0.2 V. The "introduced - found" results and the electrode sensitivity, determined as the derivative of the concentration that produced a response, were used as the criteria for electrode serviceability.

The organic substances present in the samples were subjected to preliminary electrochemical treatment by anodic oxidation in the presence of 0.5 M Cl^- at a potential of +1.5 V for 10–12 min (model solutions) and for 15–25 min (natural waters).[6]

During anodic oxidation the samples were acidified to pH 2.7. The surplus oxidant liberated during anodic oxidation was removed either by passing electrolytically produced hydrogen through the solution or by electrochemical reduction. An electrolyser with the anode and cathode spaces separated by a membrane was used. A glassy-carbon crucible served as both the electrolyser and the working electrode. This electrode was subject to anodic polarisation at the electrochemical oxidation stage and to cathodic polarisation at the electrochemical reduction stage. The reference electrode was a silver - silver chloride electrode and another glassy-carbon crucible served as the auxiliary electrode.

The concentration of oxidant in the solution and the efficiency of oxidant reduction were determined by the steady-state value of the limiting current observed in the d.c. voltammograms recorded using a graphite electrode. Alternatively, the above parameters can be evaluated from the redox potential of the medium, which was measured using platinum and silver - silver chloride electrodes and a high-resistance voltmeter. Changes of the electrode surface were observed with an MPP-20 bright-field microscope (×400) (Lomo). All chemicals were supplied by the Soviet Production Association Khimreactiv.

Results and Discussion

Electrode Plated Prior to Use With Mercury (Type I)

Fig. 1 presents an anodic-current time derivative (derivative voltammogram) recorded during the first 3 min of the electrode operation when analysing a 0.5 M NaCl solution acidified with hydrochloric acid. In this instance the redox potential of the system was 0.309 V. Curve 2 in the same figure was also registered during the first 3 min of the electrode operation when examining a 0.5 M NaCl solution subjected to electrochemical oxidation. The redox potential of the system was 1.129 V. Curves 1 and 2 are almost identical in shape; however, the responses diminish.

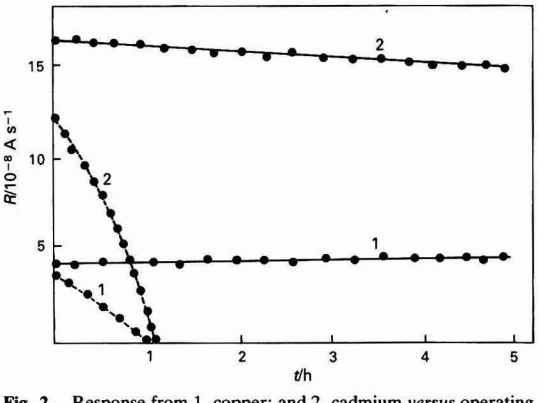

Fig. 2. Response from 1, copper; and 2, cadmium *versus* operating time of the type I electrode when registering curve 1 in Fig. 1 (solid lines) and curve 2 in Fig. 1 (broken lines)

The shape of the voltammograms changes with time: responses decrease (Fig. 2) as does sensitivity (Figs. 3 and 4; curves 1 and 2). The results are worse when a solution containing an oxidant is being analysed. In spite of pronounced changes in the electrode sensitivity when analysing solutions that were not subjected to the electrochemical treatment, the results of determining the concentration of metals remain at a satisfactory level over a period of 2 d [$s_r(Cu^{2+}) = 0.13$ and $s_r(Cd^{2+}) = 0.11$, where s_r is the relative standard deviation]. After the electrochemical treatment the electrode remains operable for less than 30 min. During this period a sharp decrease in cadmium response is observed, the response of copper disappearing almost completely (Fig. 2, broken lines).

A microscopic investigation shows that a freshly deposited film consists of small mercury droplets that measure about 2.5×10^{-4} cm in size and are distributed uniformly over the electrode surface. An "ageing" with time of the electrode surface is observed. This ageing manifests itself in the larger size of the mercury droplets, hence a decrease in the total working mercury surface and deterioration of the uniformity of the coating. Ageing of the electrode proceeds much faster in a solution that is subjected to electrochemical oxidation (*i.e.*, in a medium with a high redox potential). After 1 h of operation in the above solution, the mercury droplets increased 2–3 fold in size, whereas in an acidified solution the appearance of the electrode surface changes little, if at all (see Fig. 5). In addition, the rapid process of ageing that takes place in an electrochemically oxidised solution may be due to

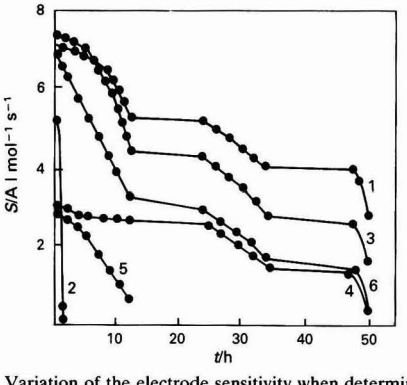

Fig. 3. Variation of the electrode sensitivity when determining the concentration of Cd^{2+} in a 0.5 M NaCl solution subjected to: 1, acidification to pH 2.7 with hydrochloric acid; 2, electrochemical oxidation at a potential of +1.5 V for 10 min; 3, electrochemical oxidation for 10 min at a potential of +1.5 V and reduction at potentials of −0.8 and 0 V alternating in steps every 30 s over a period of 20 min; 4, electrochemical oxidation for 10 min at a potential of +1.5 V with subsequent bubbling using electrolytically produced hydrogen; 5, electrolytic oxidation for 10 min and reduction at a potential of −0.2 V for 10 min; and 6, electrochemical oxidation for 10 min at a potential of +1.5 V and reduction at a potential of −0.3 V for 10 min

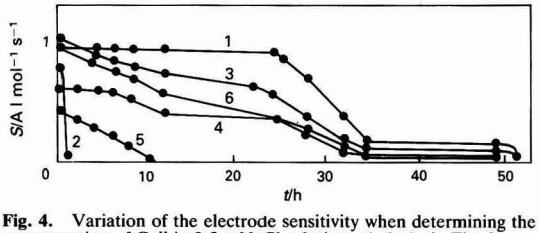

Fig. 4. Variation of the electrode sensitivity when determining the concentration of Cu^{II} in 0.5 M NaCl solutions. 1–6, As in Fig. 3

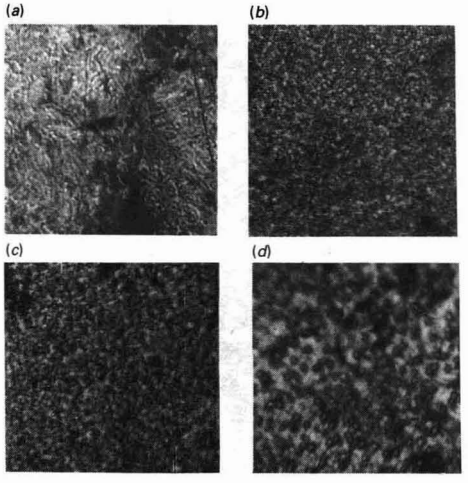

Fig. 5. Photographs of the type I electrode surface: (*a*) without mercury coating; (*b*) with mercury coating; (*c*) after operating for 1 h in a solution acidified with HCl; and (*d*) after electrolysis

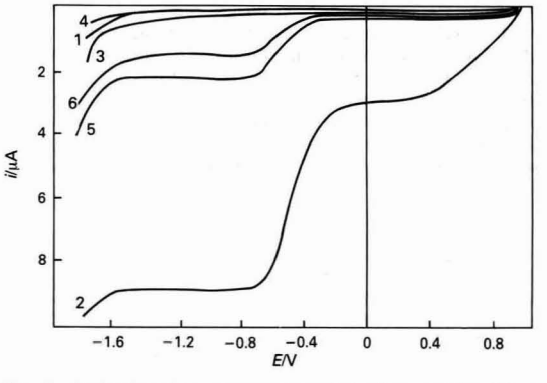

Fig. 6. Cathodic voltammograms recorded when studying 0.5 M NaCl solutions treated as described in Fig. 3 for curves 1–6

mercury compounds forming on the electrode surface. Evidence for this comes from a loss of lustre of the mercury coating. The direct current voltammograms of Fig. 6 show the reduction of the oxidants present in the solutions studied. The two waves that are observed over the potential intervals +1.0 to +0.4 V and −0.2 to −0.7 V are due to the reduction of the oxidants present in the solution. It can be seen that the oxidant content of the solution subjected to electrochemical oxidation is considerably higher than that of the solution acidified with hydrochloric acid. In the latter instance, only dissolved oxygen can serve as the oxidant. A correlation is observed between the wave height and the redox potential of the medium.

These experimental data show that the ageing of the electrode surface is due to the presence of oxidants in the solution. Therefore, reducing or removing the oxidant (lowering the redox potential of the medium) should improve the performance of the electrode.

The following, alternative, methods are proposed for the removal of oxidant: substitution of an inert gas for chlorine which shifts the equilibrium of reaction (2) to the left or reduction of the dissolved oxidant. Passing an inert gas through the solution is a rather time consuming procedure, therefore, it was used subsequently only for the sake of comparison with the method of electrochemical reduction of the dissolved oxidant.

Table 1. Results for the determination of copper(II), lead(II) and cadmium(II) ion concentrations in 0.5 M NaCl treated using different methods: I, acidified with hydrochloric acid up to pH 2.7; II, oxidation at a potential of +1.5 V for 10 min and subsequent reduction at potentials of −0.8 and 0 V, alternating in steps every 30 s for 20 min; and III, oxidation at a potential of +1.5 V for 10 min and subsequent reduction at a potential of −0.8 V for 10 min. Number of measurements (n) = 3

Element determined	Metal ion concentration ± Δ*/μg l^{-1}		
	I	II	III
Copper(II) ..	5.71 ± 0.30	5.64 ± 0.35	2.12 ± 0.40
Lead(II)	2.50 ± 0.23	2.65 ± 0.25	1.63 ± 0.30
Cadmium(II) ..	1.5 ± 0.08	1.5 ± 0.10	1.0 ± 0.12

* Δ = the confidence interval for the mean.

Table 2. Results of analysis of natural waters oxidised for 15 min at a potential of 1.5 V and then reduced at potentials of −0.8 and 0 V, alternating in steps every 30 s for 30 min (n = 5)

		Type I electrode operating for 30 h from the moment of coating deposition		Type II electrode. The electrode was cleaned mechanically before registering each calibration graph	
Sample	Determined element	Found $c \pm \Delta$*/ μg l^{-1}	s_r	Found $c \pm \Delta$/ μg l^{-1}	s_r
Sea-water	Copper(II)	1.03 ± 0.08	0.07	1.1 ± 0.06	0.05
	Lead(II)	1.30 ± 0.21	0.14	1.2 ± 0.14	0.1
	Cadmium(II)	0.97 ± 0.14	0.13	0.9 ± 0.10	0.1
River water ..	Copper(II)	3.7 ± 0.38	0.09	3.6 ± 0.21	0.05
	Lead(II)	1.45 ± 0.22	0.13	1.5 ± 0.17	0.1
	Cadmium(II)	0.87 ± 0.20	0.2	0.8 ± 0.12	0.12

* $c \pm \Delta$ = metal ion concentration ± the confidence interval for the mean.

Fig. 6 shows that the maximum diffusion current of dissolved oxidants is reached at potentials of 0.3–0.4 V (first wave) and −0.7 to −0.8 V (second wave). An efficient reduction of dissolved oxidants is realised at potentials lower than −0.7 V. Thus, curves 1, 3 and 4 depicted in Fig. 6 differ little. The redox potentials of the medium in these instances are 0.344 V after reduction at −0.8 V and 0.287 V after H_2 has been passed through the solution. However, the above conditions lead inevitably to the ions of the analytes being lost owing to their reduction and deposition at the cathode (Table 1).

Reducing the oxidant is inefficient at higher potentials. In this situation, the sensitivity (Figs. 3 and 4, curve 6) and lifetime (Figs. 3 and 4, curve 5) of the electrode decrease. Subsequently, the reduction process was performed with the potential varied asymmetrically with time: E = −0.8 V for 30 s and then E = 0 V for 30 s to dissolve the metals deposited at the first stage. The entire reduction cycle was completed in 20 min. It can be seen from Table 1 that no loss of the elements being determined occurs under these conditions.

An electrode operating in a medium "reduced" in this way retains its serviceability for a sufficiently long time (Figs. 3 and 4, curve 3); a one-to-one correspondence between the concentration introduced and the concentration found is preserved for 2 d [$s_r(Cu^{2+}) = 0.15$, $s_r(Cd^{2+}) = 0.14$].

Microscopic studies show that an electrode that has operated for a long time in "reduced" solution has a mercury coating identical with that produced on an electrode that has operated for the same time in a chemically acidified solution. In spite of the apparent enlargement of the mercury droplets, by a factor of 3–5 (see Fig. 7), the electrode maintains serviceability for 2 d.

Table 3. Electrode sensitivity for the determination of Cu^{2+} and Cd^{2+} content in a 0.5 M NaCl solution with different amounts of dissolved oxidants (electrode with mercury plated *in situ*)

Solution treatment	Solution redox potential	Electrode sensitivity/ A l mol^{-1} s^{-1}	
		$s_r(Cu^{2+})$	$s_r(Cd^{2+})$
Oxidised at E = +1.5 V for 10 min	1.129	3.3	1.4
Oxidised at E = +1.5 V for 10 min and reduced at −0.3 V for 10 min	0.546	3.5	3.7
Oxidised at E = +1.5 V during 10 min and reduced at −0.8 V (a.c.) for 20 min	0.344	3.7	4.5
Acidified using hydrochloric acid	0.309	4	4.8

Table 4. Results of analysis of sea- and river water (electrode plated with mercury *in situ*) treated using different methods: I, oxidised at E = +1.5 V (15 min); and II, oxidised at E = +1.5 V (15 min) and reduced at potentials of −0.8 and 0 V, alternating in steps every 30 s for 30 min (n = 5; p = 0.95)

Sample	Element determined	Found			
		I		II	
		$c \pm \Delta$*/μg l^{-1}	s_r	$c \pm \Delta$/μg l^{-1}	s_r
River water	Copper(II)	1.45 ± 0.17	0.10	1.5 ± 0.14	0.08
	Cadmium(II)	0.12 ± 0.02	0.12	0.17 ± 0.02	0.10
Sea-water	Copper(II)	2.71 ± 0.37	0.12	2.60 ± 0.30	0.10
	Cadmium(II)	0.54 ± 0.09	0.14	0.44 ± 0.05	0.10

* $c \pm \Delta$ = metal ion concentration ± the confidence interval for the mean.

Table 2 presents the results of an analysis of natural waters that were oxidised and then reduced. The results were obtained within 30 h from the moment the mercury coating was deposited, without renewal of the electrode surface. It can readily be seen that the discrepancy is not significant (s_r < 0.20).

Electrode Plated *in situ* (Type II)

An electrode plated with mercury *in situ* can operate for a long time (2 d or more) even in solutions with a high redox potential. With a solution oxidised at a potential of +1.5 V for 10 min, recording responses of copper(II) and cadmium(II) ions yielded s_r = 0.10 and s_r = 0.08, respectively.

However, the electrode sensitivity for the determination of Cu^{2+} and Cd^{2+} content of solutions with a high redox potential was found to be less (especially for Cd^{2+}) than that of solutions with a lower redox potential (Table 3).

The results obtained for the analysis of natural waters with the use of a type II electrode are given in Table 4.

Conclusions

The life of the electrode and its sensitivity in stripping voltammetric analysis depend on the redox potential of the medium. To prolong the lifetime of mercury-plated graphite electrodes and to improve the sensitivity of measurements for the analysis of natural waters by stripping voltammetric methods, the sample preparation process must include, not only the electrochemical oxidation of organic substances but also the electrochemical reduction of the surplus oxidant in solution, with the potential being varied asymmetrically.

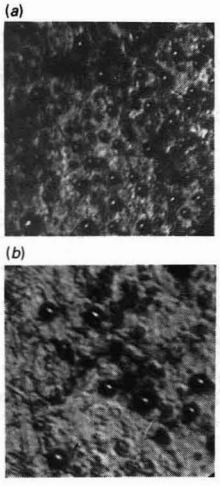

Fig. 7. Photographs of the surface of the type I electrode after operating for (*a*) 25; and (*b*) 50 h in a solution oxidised at a potential of +1.5 V for 10 min and then reduced at a potential of −0.8 and 0 V

References

1. Brainina, Kh. Z., Gruzkova, N. A., and Roitman, L. I., *Zavod. Lab.*, 1983, **49**, 11.
2. Thornton, D. C., Corby, T., Spendel, V. A., Jordan, J., Robbat, A., Jr., Rutstrom, D. J., Gross, M., and Ritzler, G., *Anal. Chem.*, 1985, **57**, 150.
3. Brezonik, P. L., Brauner, P. A., and Stumm, W., *Water Res.*, 1976, **10**, 605.
4. Brainina, Kh. Z., Khanina, R. M., and Roitman, L. I., *Anal. Lett.*, 1985, **18**, 117.
5. Laxen, D. H., and Harrison, R. M., *Sci. Total Environ.*, 1981, **19**, 59.
6. Brainina, Kh. Z., Khanina, R. M., Stozhko, N. Yu., and Chernysheva, A. V., *Zh. Anal. Khim.*, 1984, **39**, 2068.
7. Brainina, Kh. Z., and Neiman, E. Ya., "Solid Phase Reactions in Electroanalytical Chemistry," Khimiya, Moscow, 1982, p. 225.
8. Brainina, Kh. Z., Neiman, E. Ya., and Slepushkin, V. V., "Stripping Electroanalytical Methods," Khimiya, Moscow, 1988, p. 38.
9. Brainina, Kh. Z., and Kalnishevskaya, L. N., *Elektrokhimiya*, 1987, **23**, 222.
10. Schmidt, E., and Gygax, H. R., *J. Electroanal. Chem.*, 1966, **12**, 300.

Paper 9/02765C
Received June 29th, 1989
Accepted May 9th, 1990

Determination of Nitrite Ion by Differential-pulse Polarography Using *N*-(1-Naphthyl)ethylenediamine

Sunil Sabharwal
Bhabha Atomic Research Centre, Nuclear Research Laboratory, Srinagar, Kashmir-190 006, India

A highly sensitive differential-pulse polarographic method has been developed for the determination of sub-micromolar concentrations of nitrite ion after diazotisation with sulphanilic acid at low pH and coupling with *N*-(1-naphthyl)ethylenediamine dihydrochloride. At pH 2.0 and with 0.01 M potassium dihydrogen phosphate as the base electrolyte, the peak current at +0.020 V *versus* a saturated calomel electrode increases linearly in the concentration range 5×10^{-8}–2.12×10^{-6} M in simple aqueous solutions. The relative standard deviation is 3.3% for the determination of 1×10^{-7} M nitrite.

Keywords: *Nitrite determination; differential-pulse polarography;* N-*(1-naphthyl)ethylenediamine*

The occurrence of nitrite salts in the environment[1] and their use as food preservatives[2] is widespread. However, in recent years there has been increasing concern about the role of the nitrite ion in the formation of *N*-nitrosoamines, many of which have been shown to be carcinogenic.[1–3] It is, therefore, important that sensitive analytical methods be available for the determination of nitrite ion at very low concentrations. Spectrophotometric methods for the determination of nitrites are well known and general reviews dealing with procedures are available.[4] Many spectrophotometric methods for the determination of nitrite have been proposed[5–8] but in general these methods do not offer any improvement in sensitivity over the well established spectrophotometric method utilising the diazo coupling reaction with *N*-(1-naphthyl)ethylenediamine.[9]

Differential-pulse polarography has been used to determine nitrite ion both directly and indirectly.[10–13] The direct measurement involves its determination as nitrous acid but the method has limited sensitivity, *viz.*, 0.5 p.p.m.[10] A detection limit of 14 p.p.b. of nitrate or nitrite nitrogen has been reported by O'Laughlin and co-workers[11] using the enhancement of the ytterbium peak current. Utilising the reaction of nitrite ion and diphenylamine, Harrington and co-workers[12] reported a practical working limit of 4.6 p.p.b. The major disadvantage of the method is the toxicity of diphenylnitrosoamine (DPN), which may, under certain conditions, act as a nitrosating agent via transnitrosation.[12] Sulaiman[13] studied the differential-pulse polarographic behaviour of diazonium salts of sulphanilic acid and reported a detection limit of 8.6×10^{-8} M nitrite.

The purpose of the present study was to develop a differential-pulse polarographic method for the determination of nitrite ion at concentrations lower than can usually be determined by spectrophotometry. For this purpose, the differential-pulse polarogaphic behaviour of the azo dye product formed by the reaction of the diazonium salt of sulphanilic acid with *N*-(1-naphthyl)ethylenediamine was investigated.

Experimental

Apparatus

Polarograms were recorded with a Taccussel PRG-5 pulse polarographic analyser operating in the differential-pulse mode using an Ecoscript recorder. Unless stated otherwise all measurements were carried out at room temperature (*ca.* 25 °C), using a drop time of 2 s, a pulse amplitude of 100 mV and a scan rate of 2 mV s^{-1}. A three-electrode system was used with a Pt wire serving as the counter electrode and a saturated calomel electrode (SCE) as the reference electrode. The capillary used had the following characteristics: in 0.01 M dihydrogen phosphate at an open circuit, the natural drop time was 5.2 s with a mercury flow-rate of 0.92 mg s^{-1} at an uncorrected mercury column height [*h*(uncorr)] of 70 cm. De-oxygenation was carried out by flushing the solution with oxygen-free argon for 10 min.

Reagents

All chemicals used were of analytical-reagent grade and were used without further purification. *N*-(1-Naphthyl)ethylenediamine dihydrochloride was obtained from Fluka (purum grade). Sodium nitrite was dried at 110 °C for 4 h. A 1×10^{-3} M nitrite stock solution was prepared with triply distilled water. This stock solution was diluted as required.

Procedure

The standard colorimetric procedure for the determination of nitrite using *N*-(1-naphthyl)ethylenediamine as described in reference 10 was followed with slight modifications. The concentrations of the diazotising and coupling reagents were sufficiently reduced so as to minimise the base-line current while maintaining a complete chemical reaction. The completeness of the reaction was confirmed by spectrophotometry for higher concentrations.

Aliquots of standard nitrite solutions were transferred into a 100-ml calibrated flask containing 0.5 ml of 2 M sulphuric acid. To this solution were added 2 ml of sulphanilic acid (0.1% m/v) and, after 3 min, 0.2 ml of *N*-(1-naphthyl)ethylenediamine dihydrochloride (0.1% m/v). After adding 5 ml of 0.2 M potassium dihydrogen phosphate, the solutions were made up to volume with water and polarographed after being allowed to stand for 15 min. A blank solution without addition of nitrite was used to obtain the base current.

Results and Discussion

Fogg and Ahmed[14] studied the differential-pulse polarographic behaviour of the diazotised sulphanilamide coupled with *N*-(1-naphthyl)ethylenediamine, in order to determine sulphonamides at low concentrations, and reported that a pH of 4.1 was optimum for obtaining the polarographic peak of the azo dye product. However, the main peak at −0.2 V *versus* SCE was preceded by a steep baseline at about 0.0 V which limited its usefulness as an analytical peak. Also, these workers did not report the base electrolyte in which the polarograms were recorded.

The differential-pulse polarographic behaviour of the azo dye product of sulphanilic acid with *N*-(1-naphthyl)ethylenediamine under various conditions using 0.01 M potassium dihydrogen phosphate as the base electrolyte was studied. At pH 2, a single well defined peak at +0.020 V was

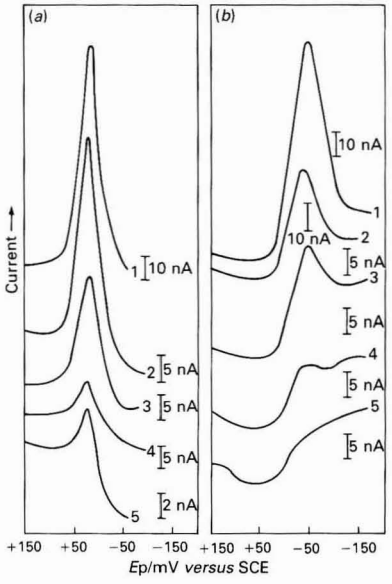

Fig. 1. Differential-pulse polarograms of the azo dye product formed with various nitrite concentrations. (*a*) 1, 1.1×10^{-6}; 2, 5.2×10^{-7}; 3, 2.6×10^{-7}; 4, 1×10^{-7}; and 5×10^{-8} M (pH 2). (*b*) 1, 1×10^{-6}; 2, 5×10^{-7}; 3, 2.5×10^{-7}; 4, 1×10^{-7}; and 5, 5×10^{-8} M (pH 3.5)

Table 1. Effect of pH on E_p and i_p of the azo dye product. Nitrite concentration, 1×10^{-6} M

pH	E_p/V *versus* SCE	i_p (corrected)/nA
1.6	+0.075	75
2.0	+0.020	75
2.5	−0.060	86
3.5	−0.150	89
4.0	−0.210	73
5.2	−0.290	58
6.1	−0.340	34

obtained [Fig. 1(*a*)]. The peak current (i_p) and the peak potential (E_p) of this peak were found to vary with pH, drop time and pulse amplitude.

Effect of pH

The differential-pulse polarograms of the azo dye product were investigated at various pH values. The results, shown in Table 1, indicate that the peak potential is pH dependent and the peak shifts towards negative potentials with an increase in pH. Table 1 also shows the effect of pH on peak current. Although at pH 3.5 the peak appeared at a sufficiently negative potential and the peak current was maximum, the peak obtained was broad and unsymmetrical and not suitable for determining very low concentrations [Fig. 1(*b*)]. On the other hand, the peak at pH 2, although at a more positive potential +0.020 V, was found to be sharp and symmetrical and could be used to determine low concentrations of nitrite [Fig. 1(*a*)]. Hence, a pH of 2 was chosen for this study.

Variation of Peak Current With Drop Time and Pulse Amplitude

Differential-pulse polarograms recorded at various drop times [Fig. 2(*a*)] and with various pulse amplitudes [Fig. 2(*b*)] illustrate that the peak current increased as the drop time and

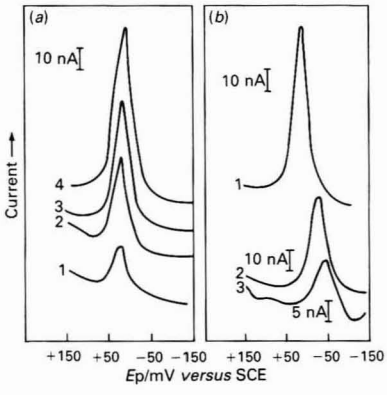

Fig. 2. Differential-pulse polarograms of the azo dye formed with 1×10^{-6} M nitrite at pH 2: (*a*) pulse amplitude, 100 mV; drop time: 1, 0.6; 2, 1.0; 3, 1.5; and 4, 2.0 s; and (*b*) drop time, 2 s; and pulse amplitude: 1, 100; 2, 50; and 3, 20 mV

pulse amplitude increased. Optimum conditions were found to be a pulse amplitude of 100 mV and a drop time of 2 s.

Stability of the Azo Dye Product

The differential-pulse polarograms of the azo dye product formed were recorded at different times over a period of 24 h. The results indicate that the dye product formed is stable for 24 h at pH 2 under the conditions of the analysis. The coefficient of variation was 2.1% for the dye formed with a 1×10^{-6} M nitrite concentration and analysed at different times over a period of 24 h.

Effect of Concentration

The peak current at +0.020 V was found to increase linearly in the concentration range 5×10^{-8}–2.12×10^{-6} M. The characteristics of the calibration graph of peak current *versus* concentration obtained by linear regression were: slope, 76.2 nA μM^{-1}; current intercept, 0.28 nA; and correlation coefficient, 0.999. The determination limit of nitrite was found to be 5×10^{-8} M. The relative standard deviation for the analysis of six nitrite samples at a 1×10^{-7} M concentration was 3.3%.

Interference Studies

In order to investigate the analytical applications of this method, the effect of several foreign ions that are usually present with nitrite was examined by carrying out the determination of 1×10^{-6} M nitrite in the presence of 1×10^{-5} and 1×10^{-4} M concentrations of each of these ions. A deviation of more than 5% from the peak current of the solution containing no interfering ion was taken as a sign of interference. The results indicate that the following ions, present in a 100-fold excess over the concentration of nitrite, do not interfere: Ca^{2+}, Mg^{2+}, Fe^{2+}, Fe^{3+}, Zn^{2+}, Cd^{2+}, Al^{3+}, Cl^-, SO_4^{2-} and NO_3^-. Only Cu^{2+} and Br^- interfered seriously enough to cause a positive and a negative error, respectively, even when present at a 1×10^{-5} M concentration. These results indicate that there are no serious interferences from most of the ions examined including Fe^{2+}, Fe^{3+} and NO_3^-, to which methods for the determination of nitrite are usually intolerant.

Comparison of the Proposed Method With Previous Methods

For concentrations of nitrite $>1 \times 10^{-6}$ M, the proposed method has no particular advantage over the existing spectrophotometric method using *N*-(1-naphthyl)ethylenediamine. However, concentrations lower than 1×10^{-6} M can be determined, with ease and accuracy, down to 5×10^{-8} M. This

lower limit of determination is better than most of the reported spectrophotometric[5–9] and polarographic methods.[13] The only exception is the method developed by Harrington and co-workers[12] which has a determination limit of 2×10^{-8} M with a standard deviation of 12%. However, as mentioned earlier, the main drawback of that procedure is the formation of toxic DPN.

Another advantage of the proposed method is that it follows a procedure which is similar to the commonly used Association of Official Analytical Chemists (AOAC) method.[15] Hence, if in routine analysis it is observed that the nitrite concentration is lower than 1×10^{-6} M, the same solution, after the addition of base electrolyte, can be analysed by differential-pulse polarography.

References

1. Lijinsky, W., and Epstein, S. S., *Nature (London)*, 1970, **225**, 21.
2. Wolft, I. A., and Wasserman, A. E., *Science*, 1972, **177**, 15.
3. Choi, K. K., and Fung, K. W., *Analyst*, 1980, **105**, 241.
4. Szekely, E., *Talanta*, 1968, **15**, 795.
5. Flamerz, S., and Bashir, W. A., *Analyst*, 1985, **110**, 1513.
6. Nakamura, M., Mazuka, T., and Yamashita, M., *Anal. Chem.*, 1984, **56**, 2242.
7. Balasubramanian, N., and Vijayanthimala, R., *Curr. Sci.*, 1986, **55**, 566.
8. MacCarthy, P., Klusman, R. W., and Rice, J. A., *Anal. Chem.*, 1987, **59**, 308R, and references cited therein.
9. Furman, H. N., *Editor*, "Standard Methods of Chemical Analysis," Sixth Edition, Robert E. Krieger, New York, 1975, pp. 745 and 746.
10. Princeton Applied Research Application Brief N-1, Princeton Applied Research, Princeton, NJ, 1974.
11. Boese, S. B., Archer, V. S., and O'Laughlin, J. W., *Anal. Chem.*, 1977, **49**, 479.
12. Chang, S. K., Kozeniauskas, R., and Harrington, G. W., *Anal. Chem.*, 1977, **49**, 2272.
13. Sulaiman, S. T., *Anal. Chem.*, 1984, **56**, 2405.
14. Fogg, A. G., and Ahmed, Y. Z., *Anal. Chim. Acta*, 1974, **70**, 241.
15. Horwitz, W., *Editor*, "Official Methods of Analysis of the Association of Official Analytical Chemists," Thirteenth Edition, Association of Official Analytical Chemists, Washington, 1980, pp. 381.

Paper 9/05486C
Received December 22nd, 1989
Accepted June 11th, 1990

Method for the Determination of Radioactivity in the C-2 Carbon of Glycine

Harinder Paul S. Makkar,* and Peter J. Buttery
University of Nottingham, School of Agriculture, Sutton Bonington, Loughborough LE12 5RD, UK

A method for the determination of the radioactivity of the C-2 carbon of glycine has been developed. The method is based on the degradation of glycine (135–137 °C for 50 s) to carbon dioxide and formaldehyde using chloramine T. The formaldehyde originated from the C-2 carbon of glycine was trapped with dimedone (5,5-dimethyl-1,3-cyclohexanedione) and the formaldehyde - dimedone complex extracted with toluene. The radioactivity of the toluene was a measure of the radioactivity in the C-2 carbon of glycine. Using (2-^{14}C)glycine, the percentage recoveries ranged from 88 to 105%, whereas with (1-^{14}C)glycine, these were <0.5%, suggesting that the label of the C-1 carbon did not interfere with the determination of radioactivity in the C-2 carbon of glycine. The method is simple, less time consuming than existing methods and a large number of samples can be handled at a time.

Keywords: *Carbon-14; radioactivity; glycine; chloramine T*

The method currently used for the determination of radioactivity in the C-2 carbon of glycine[1,2] is based on the degradation of glycine, by ninhydrin, to formaldehyde and CO_2.[3] The formaldehyde is trapped with dimedone (5,5-dimethyl-1,3-cyclohexanedione) following distillation. The distillation of samples makes this method time consuming, tedious and laborious, in addition, a slight leakage can cause a large error. Moreover, it requires special apparatus.

On treatment of amino acids with an alkali hypohalogenite such as chloramine T, CO_2 is evolved from the carboxyl group and aldehydes are formed with one carbon atom less than the original amino acids.[3,4] Degradation of glycine leads to the formation of CO_2 and formaldehyde which originate from the C-1 and C-2 carbons of glycine, respectively. Sardesai and Provido[4] determined glycine by its degradation with chloramine T to formaldehyde which was then measured by acetyl acetone reagent. In the proposed method for determining the radioactivity of the C-2 carbon of glycine, the formaldehyde was trapped with dimedone and the formaldehyde - dimedone complex was extracted with toluene. The radioactivity in the toluene was a measure of the radioactivity of the C-2 carbon of glycine.

Materials and Methods

Chemicals

Radiochemicals were purchased from Amersham International (Amersham, Buckinghamshire, UK) and the scintillant as "Fiso Fluor 1" was obtained from Fisons (Loughborough, Leicestershire, UK). All other chemicals were of analytical-reagent grade.

Procedure

An aliquot (0.1 ml) of authentic (2-^{14}C)glycine was placed in a 10-ml centrifuge tube, to which were added: 0.1 ml of glycine (10–80 μg); 0.1 ml of 76 mM chloramine T (Sigma, Poole, Dorset, UK); and 0.5 ml of sulphuric acid (0.1 M). These were mixed and kept in an oil-bath at 135–137 °C for exactly 50 s. The tubes were then transferred into an ice-bath. After about 5 min the pH of the solution was adjusted to 4.5 by the addition of 0.5 ml of 3 M sodium acetate (pH 4.5), then 0.2 ml of formaldehyde (0.1 M) and finally 0.4 ml of dimedone (0.4 M in 50% v/v ethanol). The tubes were covered using marbles and heated in a boiling water-bath for 10 min. The tubes were then cooled in an ice-bath. After warming the tubes to room temperature, 5 ml of toluene was added to extract the formaldehyde - dimedone complex, effected by shaking the tubes in a multi-tube vortex mixer for approximately 10 min. The tubes were centrifuged at *ca.* 1000*g* for 5 min at room temperature to separate the aqueous and toluene layers. An aliquot (3 ml) of the toluene layer was removed and added to 10 ml of scintillant for radioactivity counting.

An aliquot (0.1 ml) of the authentic (2-^{14}C)glycine was counted directly (3 ml of toluene plus 10 ml of scintillant) for calculation of percentage recovery.

The degradation conditions used were the same as those employed by Sardesai and Provido[4] except that 76 mM chloramine T was used and the samples were kept in an oil-bath for 50 s (see below).

Results and Discussion

Effect of Heating Time at Different Concentrations of Chloramine T

Table 1 shows the effect of keeping the tubes at 135–137 °C for different lengths of time, on the recoveries of the radioactive C-2 carbon of glycine (glycine concentration, 20 μg per sample). Chloramine T at two concentrations was used, 0.1 ml of each of 38 mM and 76 mM per sample. Using 0.1 ml of 38 mM chloramine T a time of 45–90 s was found to be optimum,

Table 1. Effect of keeping the tubes at 135–137 °C, for different lengths of time, on the recoveries of the radioactivity of the C-2 carbon of glycine. The concentration of glycine in the sample was 20 μg

	Recovery,* %	
Time/s	38 mM	76 mM
30	53.7	66
45	100.4	94.3
60	100.2	93.5
75	—	89.7
90	101.1	87
120	94.7	77.9
180	87.3	67.9
240	78.3	—
300	69.8	—

* Recovery on addition of 0.1 ml of chloramine T at the given concentrations.

* Present address: Indian Veterinary Research Institute, Regional Station, Palampur 176 061, H.P., India.

Table 2. Effect of different concentrations of glycine on the recoveries of the radioactivity of the C-2 carbon of glycine at two different concentrations of chloramine T. Time for which the samples were kept at 135–137 °C was 60 s when 0.1 ml of 38 mM chloramine T was used and 50 s when 0.1 ml of 76 mM chloramine T was used

Glycine in the sample/μg	Recovery,* %	
	38 mM	76 mM
20	99.8	101
40	96	101
60	84	102
80	—	98.8
100	62.7	99

* Recovery on addition of 0.1 ml of chloramine T at the given concentrations.

Table 3. Effect of different amounts of authentic (2-^{14}C) glycine on the recoveries of the C-2 carbon. Chloramine T used: 0.1 ml of 76 mM. Time for which samples kept in oil-bath (135–137 °C), 50 s

Amount of (2-^{14}C)glycine used/disintegrations min^{-1}	Recovery, %
2161	95–101
4293	98.4
8402	100.7
19001	87.5
39597	104.9

whereas for 0.1 ml of 76 mM chloramine T the optimum time was 45–60 s. Subsequently, times of 60 and 50 s, respectively were chosen for the determination of the radioactivity of the C-2 carbon of glycine when 0.1 ml of 38 mM and 76 mM chloramine T was used.

Effect of Glycine Concentration at Two Different Concentrations of Chloramine T

Table 2 shows the effect of two different concentrations of chloramine T on the recoveries of radioactivity of the C-2 carbon of glycine when the glycine concentration was changed. When using 0.1 ml of 38 mM chloramine T the percentage recoveries were satisfactory up to a glycine concentration of 40 μg per sample. However, at higher concentrations the recoveries decreased. With 0.1 ml of 76 mM chloramine T the percentage recoveries were satisfactory at glycine concentrations as high as 100 μg per sample. Chloramine T (0.1 ml of 76 mM) appeared to completely degrade up to 100 μg of glycine in the sample. Therefore, this concentration of chloramine T was used for subsequent experiments.

Effect of Different Concentrations of (2-^{14}C)Glycine Radioactivity

Using 0.1 ml of 76 mM chloramine T and 40 μg of glycine per sample, the method was tested using different amounts of authentic (2-^{14}C)glycine (Table 3). At all concentrations of (2-^{14}C)glycine tested, the recoveries were satisfactory, suggesting the applicability of the method for a wide range of (2-^{14}C)glycine radioactivities.

Effect of addition of (1-^{14}C)Glycine Instead of (2-^{14}C)Glycine

(1-^{14}C)Glycine was used in place of (2-^{14}C)glycine in order to study the specificity of the method. (1-^{14}C)glycine (about 40 000 disintegrations min^{-1}) was added. Virtually no (<0.5% of the added) radioactivity was obtained as (2-^{14}C)glycine, suggesting that (1-^{14}C)glycine did not interfere with the determination of the radioactivity of the C-2 carbon of glycine.

Degradation of Glycine at Room Temperature

Van Slyke *et al.*[3] reported that chloramine T caused the evolution of CO_2 from amino acids at a temperature as low as 20 °C. The degradation of glycine with chloramine T was carried out at room temperature (≈22 °C) for 10 min (other degradation conditions were as given earlier). The percentage recoveries of the radioactivity of the C-2 carbon was only 15% suggesting that degradation of glycine was not complete at this temperature, and lower temperatures (about 22 °C) can not be used for the determination of the radioactivity of the C-2 carbon of glycine.

The above results suggest that optimum conditions for the determination of the radioactivity of the C-2 carbon of glycine by its degradation are: 0.1 ml of 76 mM chloramine T at a temperature of 135–137 °C for 50 s.

Optimum Conditions for Trapping Formaldehyde

The pH of the degraded sample was adjusted to 4.5 to ensure optimum conditions for the formation of the formaldehyde - dimedone complex.[5,6] In preliminary trials, 0.5 ml of 1 or 2 M sodium acetate (pH 4.5) were added to adjust the pH of the degraded sample to 4.5, however, a pH of below 4.5 was obtained. A 3 M solution (0.5 ml) of sodium acetate (pH 4.5) brought the pH of the degraded sample to 4.5.

Dimedone, in excess, was added to form the formaldehyde - dimedone complex. Two moles of dimedone are required for every mole of formaldehyde for the formation of the complex. However, a molar excess of dimedone as large as 50 : 1 over formaldehyde does not interfere with the quantitative formation of the complex.[6]

The proposed method originated during our study of the pathways of glycine synthesis from serine in isolated perfused rat hind-limbs. Radioactive glycine was isolated from the perfusion medium using split-stream ion-exchange amino acid analysis. It was, therefore, present in lithium amino acid buffer (pH 2.58). The recoveries obtained for the radioactivity of the C-2 carbon of authentic (2-^{14}C)glycine in lithium buffer (pH 2.58) were determined by the proposed method. The recoveries were <5%, which suggested that the addition of lithium amino acid analyser buffer interferes either with the degradation of glycine by the chloramine T method or with the formation of the formaldehyde - dimedone complex, probably due to the change in pH of the sample.[3,5,6] The interference from the buffer was eliminated by removing the radioactive glycine from the lithium buffer. The radioactive glycine isolated from the split-stream amino acid analyser was passed through a previously prepared column of Dowex 50 × 8 cation resin (H), 100–200 mesh (Sigma) (bed size: 100 × 10 mm). The resin bed was washed with *ca.* 200 ml of distilled water and the effluent discarded. Glycine was retained on the column whereas other moieties of the sample passed through with the water. The glycine was then eluted from the column with about 150 ml of 4 M ammonium hydroxide, which was removed by evaporation of the eluted sample on a rotary evaporator. The dried sample was washed with distilled water and dried again. The dried glycine sample was dissolved in distilled water. An aliquot of this sample was taken for the determination of the radioactivity of the C-2 carbon of glycine. Recovery of (2-^{14}C)glycine after passing through the column was 95%. These observations suggest that the medium/buffer containing the glycine can interfere in the determination of the radioactivity of the C-2 carbon of glycine and the above approach can be employed to remove the interference.

The proposed method is simple, less time consuming than existing methods and a large number of samples can be handled at a time, in addition, it does not involve a distillation step. The described procedure should be valuable in the study of glycine, serine and other "one carbon" metabolisms. The method can also be extended to the determination of radioactivity in the beta carbon of serine after treatment with periodate which leads to the formation of glyoxylate and formaldehyde.[6]

H. P. S. M. thanks the Association of Commonwealth Universities and the British Council for financial help.

References

1. Kawasaki, H., Sato, T., and Kikuchi, G., *Biochem. Biophys. Res.*, 1966, **23**, 227.
2. Sato, T., Kochi, H., Motokawa, Y., Kawasaki, H., and Kikuchi, G., *J. Biochem.*, 1969, **65**, 63.
3. Van Slyke, D. D., Dillon, R. T., Macfadyen, D. A., and Hamilton, P., *J. Biol. Chem.*, 1941, **141**, 627.
4. Sardesai, V. M., and Provido, H. S., *Clin. Chim. Acta*, 1970, **29**, 67.
5. Yoe, J. H., and Reid, L. C., *Ind. Eng. Chem.*, 1941, **13**, 238.
6. Frisell, W. R., and Mackenzie, C. G., *in* Glick, D., *Editor*, "Methods of Biochemical Analysis," Volume 6, Wiley-Interscience, New York, 1956, p. 63.

Paper 0/01812K
Received April 24th, 1990
Accepted June 19th, 1990

Fourier Transform Raman Spectroscopy in the Analysis of Polypeptides

David Gani, Patrick J. Hendra,* William F. Maddams, Catherine Passingham, Isabelle A. M. Royaud, Harry A. Willis and Veronica Zichy
Department of Chemistry, University of Southampton, Southampton SO9 5NH, UK
Michael E. A. Cudby
School of Chemical Sciences, The University of East Anglia, Norwich NR4 7SS, UK

The use of near-infrared Fourier transform Raman spectroscopy in the analysis of polypeptides is critically reviewed. A range of peptides and polypeptides are discussed and show promising results in the pure crystalline form. However, in aqueous solution analogous to *in vitro* conditions the results are disappointing and further developments in Fourier transform Raman techniques are required before the technique, applicable to these compounds, can be successful.

Keywords: *Fourier transform Raman spectroscopy; peptide; polypeptide*

The analysis of complex polymeric biochemicals such as polypeptides has not benefited as much from the application of spectroscopic techniques as have synthetic polymeric systems. The reasons for the lack of interest are complex and fundamental but are worthy of consideration in order to provide a background to the work described in this paper.

Infrared (IR) vibrational spectroscopy although by no means valueless tends to be ignored in biochemical articles because water is a strong absorber and hydrogen bonding broadens the spectral detail. As a consequence, IR spectra of the polypeptides are far from specific to the species present but rather emphasise the presence of the amide groupings.

The complementary method to IR spectroscopy, *i.e.*, Raman scattering, appears promising in the analysis of "wet" systems because water is a very poor scatterer and hydrogen bonding causes very little feature broadening. As a result the Raman spectra of many biochemical species are detailed and very characteristic of the materials present. Unfortunately, however, Raman scattering is extremely weak and in biosystems is almost invariably overwhelmed by fluorescence.

Recently, reports have appeared demonstrating most convincingly that the newly developed near IR excited Fourier transform (FT) Raman method removes or drastically reduces the nuisance of fluorescence,[1] and, hence, the present workers have been approached on many occasions to explore the value of newer Raman methods to biochemistry in general and to the analysis of polypeptides in particular. The subject has been surveyed recently and it is clear that in some areas FT Raman methods are in the process of making major contributions in biochemistry. In this paper experiences in studying the polypeptides are reported and a considered view is given in the conclusion, on the current situation and immediate prospects.

In addition to vibrational spectroscopic techniques, effort has been expended in the area of nuclear magnetic resonance (NMR) studies. The complexity of the structure of polypeptides requires a very sophisticated approach to assign the large number of observed resonances to the various amino acid residues present.[2] However, it is possible to assign these resonances particularly with the use of ^{2}H NMR techniques given that sufficient time and effort are available. The determination of the conformation of poly-γ-benzyl L-glutamate is described by Tonelli[3] where ^{2}H techniques are used in conjunction with very high field spectrometers to provide the quality of resolution and dispersion of resonances necessary.

Some NMR studies have been carried out in the solid state using magic angle rotation and cross-polarisation experiments,[4] but these have required ^{13}C enrichment of particular amino acid residues in order to clarify conformational effects on the observed chemical shifts. Nevertheless, such studies are adding to the understanding of the complex nature of polypeptides.

Thus, although NMR techniques are being applied with some success to the determination of structure in polypeptides, it is necessary to have access to sophisticated, high-cost equipment over a considerable period of time.

Experimental

The spectra were measured on a spectrometer developed as the result of collaborative effort between staff of the Department of Chemistry, the University of Southampton, and Perkin-Elmer. This instrument has been described fully elsewhere,[5] therefore, only brief details are provided here.

The two major components are a Perkin-Elmer 1710 FT-IR spectrometer and a Spectron c/w Nd:YAG laser operating in the TEM_{00} mode, and coupled with a narrow bandpass filter to reject plasma lines. The 1.064-μm (9393 cm^{-1}) line from this laser was used for excitation. The laser beam is directed on to the sample via a small prism and its diameter at the sample position is approximately 0.5 mm. A 180° back-scattering geometry is used and the scattered radiation is focused to fill the 8-mm diameter Jacquinot stop of the interferometer. Three multi-layer dielectric transmission filters, one situated immediately before the Jacquinot stop and the other two prior to the detector, reject Rayleigh scattered radiation. An additional filter is used to eliminate the laser line at 632.8 nm. This filter combination limits observations to shifts of 300 cm^{-1} and greater. The detector is a 2-mm diameter semiconductor photodiode made from indium arsenide doped with gallium. It operates at ambient temperature and is sensitive to shifts as large as 3500 cm^{-1}. All spectra are corrected for the variation in detector sensitivity and filter profile as a function of wavelength. The various spectra were run at a resolution of 6 cm^{-1}, with approximately 400 mW of power in the excitation line, and 100 or 200 repetitive scans.

For purposes of comparison with conventional-type Raman spectra a limited number of measurements on aromatic amino acids were run on a Coderg T800 triple monochromator spectrometer, with 90° viewing of the scattered radiation. The 514.5-nm line from an argon ion laser was used for excitation. The slit width was 4 cm^{-1} and the scanning speed 50 cm^{-1} per minute.

The samples examined, all in the form of crystalline powders, were supplied by Sigma. The approximate relative molecular mass values for the homopolypeptides are: poly-

* To whom correspondence should be addressed.

glycine, 10 000; polyalanine, 25 000; poly-D-tyrosine, 95 000; poly-L-tryptophan, 9000; poly-L-phenylalanine, 5000; and polymethionine, 12 000.

Infrared spectra were recorded on a Model 1725 FT-IR instrument manufactured by Perkin-Elmer. A suite of software was available to print IR and Raman spectra against common frequency scales to permit their direct comparison. Where appropriate this has been included in the paper. In one or two instances it was found to be very difficult to acquire adequate IR spectra using conventional transmission methods such as KBr discs or mulls, thus other methods such as diffuse reflectance or photoacoustic resonance were attempted. These experiments were carried out at the Perkin-Elmer laboratories using a variety of accessories defined as appropriate later in the paper.

Results

As our intention was to define the limits of usefulness of FT Raman methods in the analysis of polypeptides, a dry specimen of the basic protein clupein (Fig. 1) was used as the first sample, followed by monomeric alanine in a solution of water (Fig. 2). Clearly the outcome, particularly where aqueous solutions are concerned, is not promising. Therefore, IR and Raman spectra of those monomeric amino acids and homopolymeric polypeptides that had not been successfully studied previously were examined.

Amino Acids

Several of these materials have been examined previously and the results reported in the literature.[1] As the pure materials do not fluoresce it is convenient to record Raman spectra with visible sources. To demonstrate both this point and the comparison in spectral quality available with FT instruments spectra of solid polyphenylalanine are shown in Figs. 3 and 4.

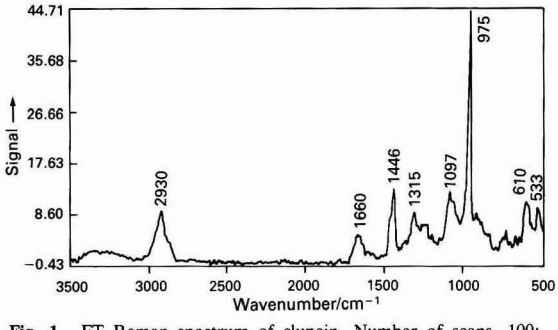

Fig. 1. FT Raman spectrum of clupein. Number of scans, 100; resolution, 6 cm^{-1}; and laser power, 400 mW

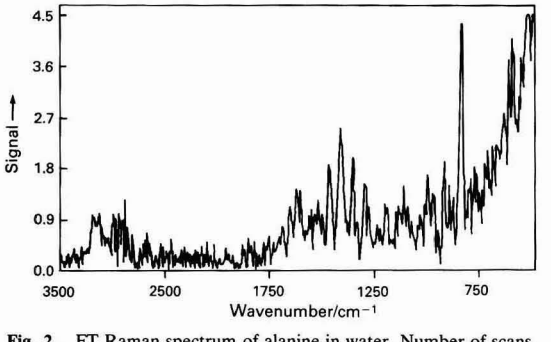

Fig. 2. FT Raman spectrum of alanine in water. Number of scans, 100; resolution, 6 cm^{-1}; and laser power, 800 mW. Concentration of alanine, 1 M

Spectral quality is similar in both instances but it is worth emphasising that to load the sample, align it in the spectrometer and record the spectrum took more than 1 h and required considerable skill using the visibly excited Coderg spectrometer (wavelength 514 nm); recording the spectrum on the FT instrument took less than 10 min and required little expertise.

The features of the L-phenylalanine spectrum (Fig. 3) are in good agreement with those reported by Simons *et al.*[6] In order to facilitate the subsequent discussion of the spectrum of poly-L-phenylalanine a brief comment on the strong peaks present in Fig. 3(*a*) is warranted. The major peaks, those at 620, 1001, 1035, 1215, 1583 and 1603 cm^{-1} arise from vibrational modes involving the benzene ring that is present,[6] and this, rather than the aliphatic portion of the molecule, including the amino acid group, determines the general form of the spectrum. This is also true for L-tyrosine (Fig. 5), the results for which are in good agreement with those of Inomata *et al.*[7] The aromatic ring peaks appear at 639, 829, 847, 1200, 1247, 1264, 1580 and 1613 cm^{-1}.[7] It is of some interest that the intensity ratio 829 : 847 cm^{-1} is 3 : 1, a value particularly noted by Inomata *et al.*

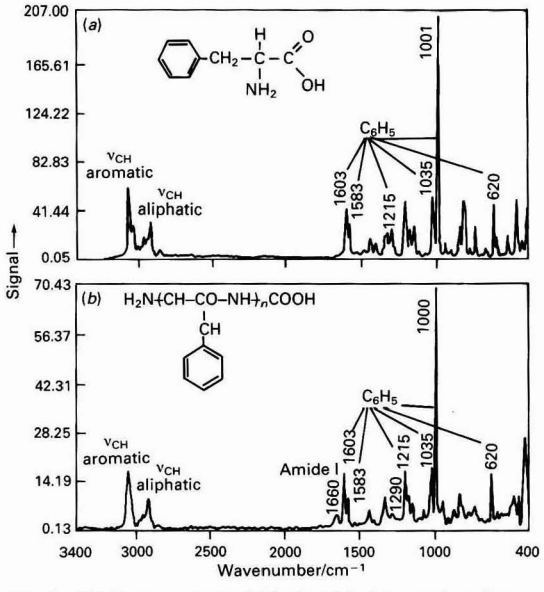

Fig. 3. FT Raman spectra of (*a*) phenylalanine; number of scans, 100; resolution, 6 cm^{-1}; and laser power, 270 mW; and (*b*) polyphenylalanine; number of scans, 200; resolution, 6 cm^{-1}; and laser power, 370 mW

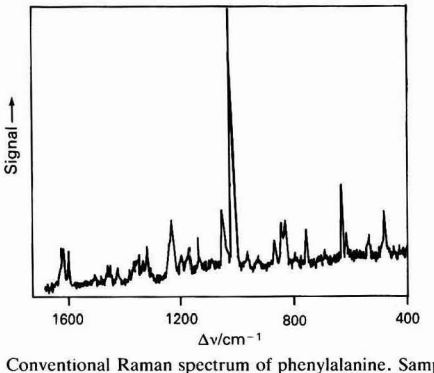

Fig. 4. Conventional Raman spectrum of phenylalanine. Sampling time, 30 min; resolution, 4 cm^{-1}; and laser power, 100 mW

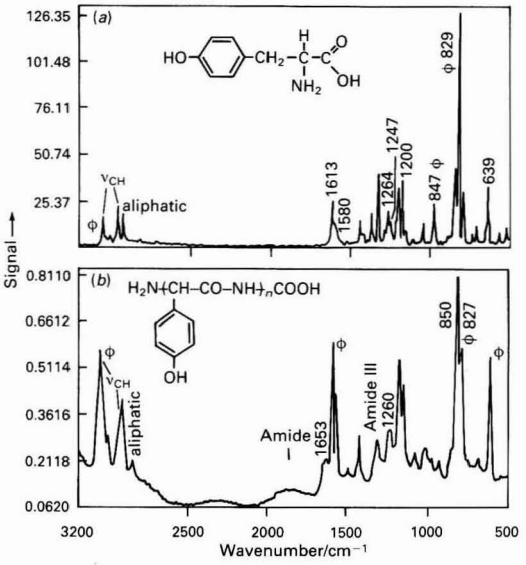

Fig. 5. FT Raman spectra of (*a*) L-tyrosine; number of scans, 100; resolution, 6 cm^{-1}; and laser power, 270 mW; and (*b*) polytyrosine; number of scans, 200; resolution, 6 cm^{-1}; and laser power, 400 mW

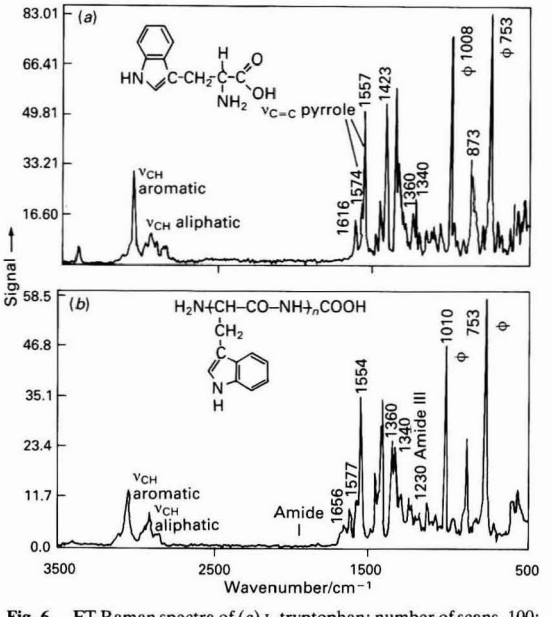

Fig. 6. FT Raman spectra of (*a*) L-tryptophan; number of scans, 100; resolution, 6 cm^{-1}; and laser power, 270 mW; and (*b*) polytryptophan; number of scans, 200; resolution, 6 cm^{-1}; and laser power, 300 mW

L-Tryptophan contains an indole group, and thus both an aromatic and a pyrrole ring. Bands characteristic for both appear in the spectrum [Fig. 6(*a*)]. In the former category there are peaks at 753, 873, 1423 and 1616 cm^{-1} whereas the pyrrole ring is responsible for those at 1008, 1557 and 1574 cm^{-1},[6] the second and the third of these arising from ν(C=C). The two relatively weak peaks at 1340 and 1360 cm^{-1} are of some interest, as they may be assigned to Fermi resonance between a fundamental and one or two combination bands of the out of plane bending vibration.[8] The spectrum as a whole

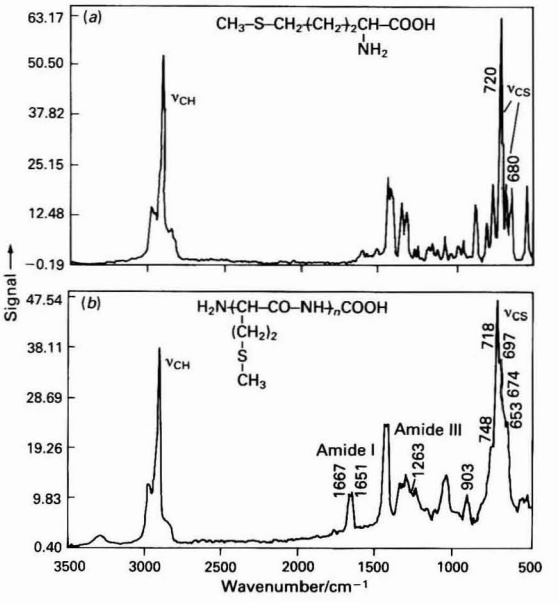

Fig. 7. FT Raman spectra of (*a*) methionine; number of scans, 100; resolution, 6 cm^{-1}; and laser power, 400 mW; and (*b*) polymethionine; number of scans, 200; resolution, 6 cm^{-1}; and laser power, 400 mW

is in agreement with that given by Hirakawa *et al.*[9] The spectrum of methionine is given in Fig. 7.

Homopolypeptides

The FT Raman and conventional Raman spectra of phenylalanine are included in Figs. 3 and 4. Comparison shows the considerable degree of similarity between these and the spectrum of phenylalanine, with vibrational modes characteristic of the aromatic ring again providing the strong peaks. However, two weak peaks should be noted at 1660 and 1290 cm^{-1}; they are the amide I and amide III vibrations, and their significance in the conformational context is considered below.

The spectrum of polytyrosine [Fig. 5(*b*)] also shows many features present in the spectrum of tyrosine, although the degree of correspondence is not as marked as for phenylalanine and polyphenylalanine. In particular, the intensity ratio of the doublet at 827 and 850 cm^{-1}, mentioned above, is now reversed, with the latter being the stronger. The peak at 1613 cm^{-1} has also intensified on a relative basis. Although weak, the amide I and amide III bands are readily discernible at 1653 and 1260 cm^{-1}, respectively.

For polytryptophan the spectrum [Fig. 6(*b*)] has many points of similarity to that obtained for tryptophan [Fig 6(*a*)]. The only substantial difference is that the Fermi resonance doublet at 1340 and 1360 cm^{-1} is now stronger, relatively, by a factor of three or four and the 1360 cm^{-1} component is now the stronger, contrary to what is found for tryptophan. Weak amide I and amide III bands appear at 1656 and 1230 cm^{-1}, respectively.

The spectra of methionine and polymethionine [Fig. 7(*a*) and (*b*)] have also been measured, as examples of a system having a non-aromatic functional group giving strong characteristic Raman peaks. However, in this instance the C–S moiety shows strongly only in the vicinity of 700 cm^{-1}. Elsewhere the spectra are reminiscent of those of glycine, polyglycine [Fig. 8(*a*) and (*b*)], alanine and polyalanine [Fig. 9(*a*) and (*b*)], with amide I and amide III bands standing out very clearly.

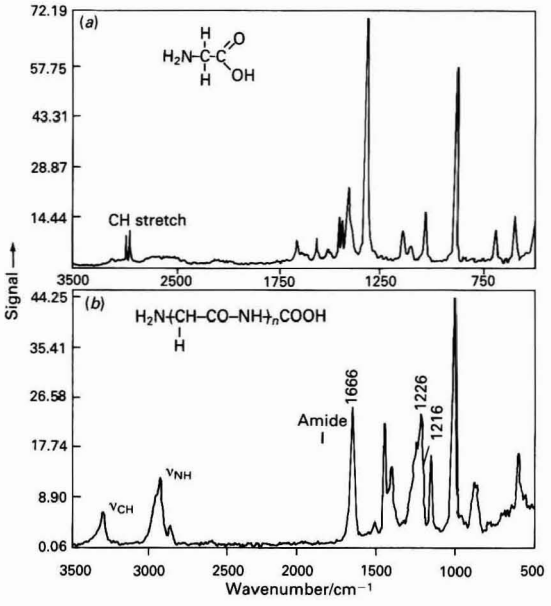

Fig. 8. FT Raman spectra of (*a*) glycine; number of scans, 100; resolution, 6 cm^{-1}; and laser power, 300 mW; and (*b*) polyglycine; number of scans, 200; resolution, 6 cm^{-1}; and laser power, 370 mW

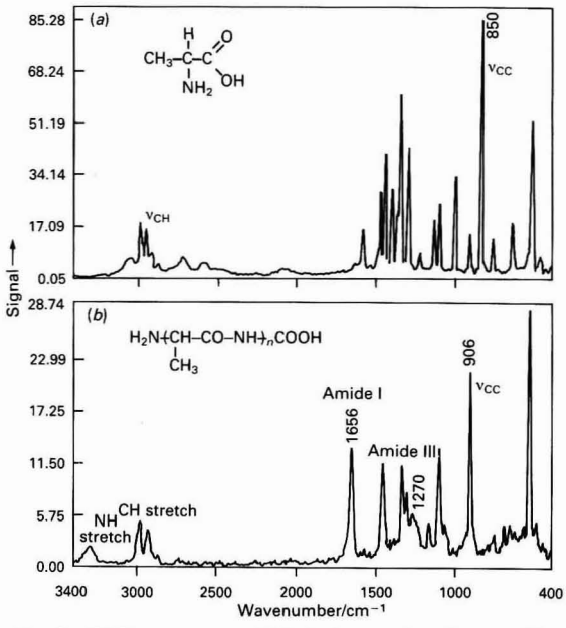

Fig. 9. FT Raman spectra of (*a*) alanine; number of scans, 100; resolution, 6 cm^{-1}; and laser power, 300 mW; and (*b*) polyalanine; number of scans, 200; resolution, 6 cm^{-1}; and laser power, 370 mW

Discussion

The above results merit comment in three contexts; the value of the spectra for purposes of identification, the relative intensities of the spectra of a given aromatic amino acid and the corresponding homopolypeptide, and the information that may be obtained about the conformation of the homopolypeptides. In each instance, the ability to obtain good quality spectra, readily and rapidly, by the FT technique, has opened the way to a new area for study.

The spectra of the three aromatic homopolypeptides are dominated by peaks characteristic for the aromatic moiety, and are therefore effectively the spectra of the particular side groups present, and not of the backbone structure, hence they are very characteristic of their particular structure. The value of Raman spectroscopy for structural diagnosis is worthwhile on aromatic compounds and is well established,[10] and the present results are no exception. This considerable degree of specificity, coupled with the ease with which spectra may be obtained from samples as small as a few micrograms is attractive and with this type of compound small amounts of water cause no difficulty in the Raman effect although they can cause difficulties in IR absorption. Further, the Raman bands are very sharp.

The measured intensities of Raman peaks obtained from conventional dispersive instruments are very markedly dependent upon the precise positioning of the sample, a consequence of the fact that very narrow slits form an integral part of the optical system. The comparison of intensities among a series of spectra has therefore been regarded, rightly, as wholly impractical. This limitation does not occur with FT instruments because of the large diameter of the Jacquinot stop, and the reproducibility of intensity measurements is determined largely by the stability of the Nd^{3+} : YAG laser. Recent measurements in this laboratory have shown that intensities are readily reproducible to about ±2%, and with this knowledge it is possible to discern another interesting feature relating to the spectra of the amino acids and the corresponding homopolypeptides, as follows.

A comparison of the spectra of methionine and polymethionine which have been run using comparable conditions, except that 100 scans were used for the former and 200 for the latter, is shown in Fig. 7(*a*) and (*b*). The average of the ratio of the intensities of equivalent bands in the former and the latter is 3:1 (as polymers are always weaker scatterers than their monomers), and this is typical of many, but not all, of the amino acids and their corresponding homopolypeptides examined here. This behaviour is not confined to biopolymers. A comparison of the spectra of styrene and polystyrene reveals a comparable effect, one for which, as yet, no explanation can be given.

That certain bands in the spectra of polypeptides are capable of yielding information on the conformations of these molecules is well established.[11–14] Hitherto, such studies have largely involved IR spectra and mathematical resolution enhancement techniques have been used to increase the specificity of the method.[15] The vibrational modes that have proved most useful in this context are[16] amide I, amide III and the skeletal ν(C–C). The amide I band is found, fairly intensely, at 1655 cm^{-1} for the random coil structure, and for the β-sheet conformations it is strong and is at 1670 cm^{-1}. The amide III band is weaker in all three instances, and it is found at 1275, 1245 and 1235 cm^{-1}, respectively. The skeletal mode gives strong peaks at 930 and 950 cm^{-1} for the α-helix and random coil structures, but it is not observed with the β-sheet systems. The peaks are sharper in the Raman effect than in their IR spectra, but this advantage is offset by the fact that they are weaker.

The conformation-sensitive bands are found at the anticipated positions for polyglycine and polyalanine, whose structures are well established. Amide I appears at 1666 cm^{-1}, amide III at 1216 cm^{-1} and no peak is detectable in the internal 900–930 cm^{-1} region. This is indicative of the antiparallel β-sheet conformation as already noted by Krimm.[14] Some bands may appear slightly shifted in comparison with the spectra observed by Krimm. However, the frequency reliability in FT Raman is excellent and some

re-assignment of bands may be forthcoming particularly with regard to amide III. Likewise, for polyalanine, amide I at 1656 cm^{-1} and amide III at 1270 cm^{-1} are consistent with the known α-helix structure.[14] Although the amide I and amide III bands are of value for conformational analytical studies, in polyglycine and polyalanine, which contain no side groups, they are valueless in the other homopolypeptides because frequently the amide III cannot be identified. This characteristic of the Raman spectra arises because of the relative intensities of bands due to the side group.

In the aromatic homopolypeptides, the situation is less clear cut. A weak broad amide I band is located at 1660 cm^{-1}, a position intermediate between those characteristic of the α-helix and random coil structures. A band at 1290 cm^{-1} is the only one that is available for assignment as amide III, but this value is higher than those associated with any of the three types of structure. Hence, no firm conclusions can be drawn. It is interesting to note that amide I is also located at 1660 cm^{-1} in the IR spectrum, and its assignment has been left in abeyance.[17] Polytyrosine has an amide I band near 1653 cm^{-1}, suggesting the α-helix conformation, as does the corresponding IR band at 1651 cm^{-1}. Amide III appears as a sharp band, whose position can therefore be readily measured at 1260 cm^{-1}, which is intermediate between the conventional values for the α-helix and random coil structures. There must be a strong suspicion that the value of 1275 cm^{-1} reported[16] as characteristic for the α-helix is capable of some variation, particularly for molecules, such as those now under consideration, with bulky side groups attached to the backbone chain.

The evidence is contradictory for polytryptophan. Amide I is found at 1656 cm^{-1}, suggesting an α-helix structure, whereas amide III at 1230 cm^{-1} suggests a β-sheet. Further, the value for amide I in the IR is 1660 cm^{-1}, which could be interpreted as evidence for a random coil or an α-helix. In contrast, polymethionine presents only minor assignment problems. There are peaks at 1667 and 1651 cm^{-1}, and the latter may be assigned confidently to the α-helix structure. Confirmatory evidence is provided by amide III at 1263 cm^{-1} and ν(C–C) at 903 cm^{-1}. The presence of the second peak at 1667 cm^{-1} may be indicative of some material having either the random coil or the β-sheet structure, unless it arises from an impurity in the sample.

Naturally Occurring Polypeptides

Over the last 2 years many of these materials, including specially prepared ones where one monomer predominates in the composition, have been investigated. In all instances, the Raman spectral quality has been so disappointing as to be of no value analytically and Fig. 1 is not in any way atypical. This is considered to have several causes. Real polypeptides are complex co-polymers, hence the side group vibrations from all of the monomers overlap. Further, the strong hydrogen bond interactions between the amide groups tighten the structure and encourage the vibrations of adjacent side groups to interact, broadening the Raman and IR bands. Add to this complication the inevitable broadening typical of materials of low crystallinity and the disappointing spectra recorded are to be anticipated.

Considerable effort has been expended over the last 2–3 years to record high quality solution spectra. Unfortunately, water absorbs in the near IR and this has been identified as the reason why dilute aqueous solutions are inaccessible. To give a guideline, pyridine in water gives a good spectrum but pyridine is a superb Raman scatterer. Unfortunately, the polypeptides are not.

Conclusion

Although some very adequate Raman spectra can be recorded with consummate ease using FT methods in the near IR, useful results are not available from complex polypeptides in the solid phase whilst aqueous solutions at low concentrations are most disappointing. These comments are, however, relevant only to early 1990. Advances in sensitivity are already in train[17] whilst sophisticated data analysis will certainly improve the value of the results obtained. Both developments will be needed before the method contributes to polypeptide analysis. Thus our advice to intending users is to be patiently hopeful!

Clearly the question must arise—why FT Raman spectroscopy—why not use the conventional method? Considerable advances have been made in the last few years in laser Raman spectrometry particularly the use of red sources and sensitive position-sensitive detectors such as the charge coupled devices. As a result, the conventional technique offers speed and/or sensitivity and it is clear that the best instruments perform better than the FT interferometer based systems available today. The FT technique is considered to be superior in that firstly, it is easy to use, which enables the instruments to be operated in complete safety by relatively untrained staff working in a routine laboratory. Secondly, the equipment is based on FT-IR machines and hence IR and Raman spectra can be recorded on the same instrument and the two spectra presented directly on to the data processing equipment. Thirdly, it is cheap; at least one manufacturer offers an IR machine plus a Raman accessory complete and including laser for about £60 000 and the laser costs almost nothing to run. All these features contrast markedly with a sophisticated modern Raman system based on a scanning/multiplex spectrometer/spectrograph and powered by an argon ion plus TiSapphire tuneable laser system.

The authors thank the office of Naval Research, Washington, DC, The Royal Society of Chemistry and CNRS for providing financial assistance.

References

1. Spiro, T. G., "Biological Applications of Raman Spectroscopy," Volume 1, Wiley, New York, 1987.
2. Wider, G., Lee, K. H., and Wüthrich, K. J., *J. Mol. Biol.*, 1982, **155**, 367.
3. Tonelli, A. E., "NMR Spectroscopy and Polymer Microstructure: the Conformational Connection," VCH, Weinheim, 1989.
4. Shinzi, A., Takeshi, Y., Isuo, A., Akira, S., Takuo, O., Ryoko, T., and Haziwe, S., *J. Am. Chem. Soc.*, 1985, **107**, 7648.
5. Ellis, G., Hendra, P. J., Hodges, C. M., Jawhari, T., Jones, C. H., Le Barazer, P., Passingham, C., Royaud, I. A. M., Sánchez-Blázquez, A., and Warnes, G. M., *Analyst*, 1989, **114**, 1061.
6. Simons, L., Bergström, G., Blomfelt, G., Forss, S., Stenbäack, H., and Wansen, G., *Commentat. Phys. Math.*, 1972, **42**, 314.
7. Inomata, Y., Inomata, T., and Moriwaki, T., *Bull. Chem. Soc. Jpn.*, 1974, **47**, 818.
8. Harada, I., Miura, T., and Takeuchi, H., *Spectrochim. Acta, Part A*, 1986, **42**, 307.
9. Hirakawa, A. Y., Nicshimura, M., Matsumoto, T., Nakarushi, M., and Tsuboi, M., *J. Raman Spectrosc.*, 1978, **7**, 282.
10. Dollish, F. R., Fateley, W. G., and Bentley, F. F., "Characteristic Raman Frequencies of Organic Compounds," Wiley-Interscience, New York, 1974.
11. Ambrose, E. J., and Elliott, A., *Proc. R. Soc. London, A*, 1951, **47**, 205.
12. Miyazawa, T., Shimanouchi, T., and Mizushima, S., *J. Chem. Phys.*, 1956, **24**, 408.
13. Krimm, S., and Abey, Y., *Proc. Natl. Acad. Sci. USA*, 1972, **69**, 2788.
14. Krimm, S., *in* Durig, J. R., *Editor*, "Vibrational Spectra and Structure," Volume 16, Elsevier, Amsterdam, 1987.

15. Yang, W.-J., Griffiths, P. R., Bylder, D. M., and Susi, H., *Appl. Spectrosc.*, 1985, **39**, 282.
16. Miyazawa, T., *in* Fasman, G. D., *Editor*, "Polypeptides and Amino-acids," Volume 1, Edward Arnold, London, 1967, Chapter 2.
17. Petty, C., and Bennett, R., *Spectrochim Acta, Part A*, 1990, **46**, 331.

Paper 0/01104E
Received March 13th, 1990
Accepted June 11th, 1990

Fourier Transform Infrared Spectrometric Determination of Stearic Acid in Styrenic Polymers

T. Kumar
Mobil Chemical Company, Edison Research Laboratory, P.O. Box 3029, Edison, NJ 08818, USA

The conventional polymer dissolution/re-precipitation method, in which stearic acid is extracted from the bulk and from the surface of styrenic polymers, fails to establish whether stearic acid is used as an external or internal lubricant, whereas an ethanol wash of the resin selectively removes external stearic acid. These simple additive isolation procedures, followed by infrared spectrometry, were used to show whether stearic acid was applied on the surface of the pellets or blended throughout the polymer. A rapid, precise and accurate method to determine both external and internal stearic acid by using Fourier transform infrared spectrometry is described. The accuracy of the method was determined to be within 6%. The detection limit was *ca.* 0.01% m/m in the resin.

Keywords: *External and internal lubricants; stearic acid; styrenic polymer; Fourier transform infrared spectrometry*

Processing aids or lubricants are widely used in a variety of polymers to improve resin processability. These additives can alter resin surface characteristics and internal lubricity by reducing the friction coefficient on the mould and extruder walls. The basic chemical classes of compounds used as lubricants[1] include: hydrocarbons, fatty amides, fatty acids, fatty acid alcohols, fatty acid esters, metallic soaps, silicones, fluoroplastics, orthophosphoric acid esters and certain proprietary classes of compounds.[2,3] These lubricants can be applied externally or internally, depending on the process or the application. The choice of lubricant depends on the polymer type and its interaction with other additives present in the formulation. Fatty acids, which contain a long hydrocarbon chain with a polar carboxylic acid functionality, are commonly used in styrenic polymers. They can function both externally and internally. Chain length and polarity of fatty acids determine their compatibility with the polymer system and the effectiveness of lubrication. Stearic acid, which has a chain length of 18 carbons, is widely used.

Determination of lubricants is, therefore, very important in evaluating resin processing characteristics such as polymer melt - flow effects on the equipment surfaces and end-use performance, and in analysing the resin needs of the customer. Conventional polymer dissolution followed by the re-precipitation method is widely used for isolating low levels of additive from the polymer matrix. This procedure effectively removes stearic acid from the bulk and the surface of styrenic resin pellets. However, it cannot distinguish whether or not stearic acid was used externally or internally. An analytical approach is needed to establish the method of stearic acid application and to determine it quantitatively.

A literature search indicated no references to the analysis of stearic acid in styrenic resins. In general, several techniques have been employed for analysing fatty acid mixtures. Gas - liquid chromatography[4,5] is commonly used for the analysis of fatty acids as their volatile methyl esters. A pre-chromatographic derivatisation of free fatty acids is required, which can cause problems owing to incomplete derivatisation. High-performance liquid chromatography (HPLC) has also been used for analysing fatty acid mixtures[6,7] and for the characterisation of fatty acids and their derivatives.[8,9]

In addition, HPLC has been used for analysing underivatised fatty acids in natural oils, alkyd resins,[10] margarines[11] and lubricating greases.[12] Al Sammerrai[13] has demonstrated the use of differential thermal analysis for determining free stearic acid in aluminium stearates.

In this paper, the application of additive isolation procedures and Fourier transform infrared (FT-IR) spectrometry will be described for quantifying external and internal stearic acid in styrenic resins.

Experimental

FT-IR Spectrometer

Fourier transform infrared transmission spectra were recorded by use of a fixed-path length alkali halide liquid cell and a Nicolet 7199 FT-IR spectrometer equipped with a Model 1280 data acquisition system, a liquid nitrogen cooled broad-band mercury - cadmium - telluride detector with a potassium bromide window, a water-cooled globar source and a Ge/KBr beam splitter. The interferograms were obtained with a four wavenumber resolution (number of data points = 4096) and a medium inter-scan correlation. A Happ - Genzel apodisation was used to transform interferometric data into single-beam spectra over the spectrometer range (4000–600 cm^{-1}). The corresponding single-beam spectra were ratioed against the single-beam instrumental background recorded without the liquid cell in the IR beam path. Sixty-four co-added scans yielded an adequate signal to noise ratio in the spectra.

Reagents and Materials

All reagents used were of analytical-reagent grade. Carbon tetrachloride (Baker Analysed Reagent); ethanol (a Reagent Alcohol Absolute, Mallinckrodt); stearic acid; and crystal polystyrene (clear, glass-like and non-crystalline) resins, referred to in the text as PS-1 (internal), PS-2 (internal) and PS-3 (external) containing *ca.* 1100, 800 and 300 μg g^{-1} of stearic acid, respectively, were used.

Isolation of Stearic Acid

External lubricant

Approximately 20 g of the resin were accurately weighed and washed twice with 50-ml portions of ethanol. The washings were collected in a beaker and evaporated to dryness on a steam-bath under a slow stream of nitrogen; the resulting residue was dissolved in a few millilitres of CCl_4 and transferred into a 10-ml calibrated flask. The beaker was subsequently washed several times with CCl_4 to ensure quantitative recovery of the residue, and the final solution of the residue was made up to 10 ml. A portion of this solution was used to obtain an IR spectrum.

Internal lubricant

Approximately 20 g of the resin were accurately weighed and dissolved in 150 ml of CH_2Cl_2. A 100-ml portion of ethanol

was added dropwise, while stirring, to precipitate the polymer. The polymer was filtered off and the filtrate was evaporated to dryness. The resulting residue was dissolved in CCl_4 and the solution was made up to 10 ml, following the steps described in the previous section.

Preparation of Standard Solutions

Stock solution I (25 mg ml^{-1} *of stearic acid in* CCl_4). Prepared by accurately weighing *ca.* 0.25 g of stearic acid into a 10-ml calibrated flask and making up to the mark with CCl_4.

Stock solution II. This was prepared by pipetting 5.0 ml of stock solution I into a 50-ml calibrated flask and adding CCl_4 to the mark. This corresponds to a 2.5×10^3 μg ml^{-1} solution.

From stock solution II, a series of standard solutions containing 250, 500, 750, 1000, 1250, 1500 and 2000 μg ml^{-1} of stearic acid was prepared to obtain IR absorbance spectra and subsequently establish a calibration graph.

Alternatively, a series of standard solutions, ranging from 0 to 2.2×10^3 μg ml^{-1} of stearic acid, was independently prepared by accurately weighing corresponding amounts of stearic acid into 50-ml calibrated flasks and making up to the mark with CCl_4. The IR absorbance spectra of these standard solutions were obtained to establish a linear calibration graph.

Quantitative Analysis

The Nicolet quantitative analysis software SETUP was used to obtain calibration data and to analyse the unknown spectral data. Table 1 gives the relevant quantitative analysis parameters. A linear baseline adjustment was performed and the integrated absorbance of the analytical band (1665–1730 cm^{-1}) was measured to determine the stearic acid content. A calibration graph was established in the range 0–2.2×10^3 μg ml^{-1}. The complete method was stored in the computer. The macro-programming capability of the Nicolet operating software allowed the operator to access the method, print out the calibration data and calculate the stearic acid content rapidly and automatically from a specified number of samples.

Results and Discussion

Commercial crystal polystyrene resins are analysed by IR spectrometry to detect the presence of stearic acid. Stearic acid is isolated by precipitating the resin, from solution in CH_2Cl_2, with ethanol, followed by IR examination of the residue. This is a satisfactory approach to determining the qualitative presence of stearic acid in the resin; however, it fails to establish whether this additive was used externally or internally. A simple approach would be to remove selectively the external stearic acid from the polymer matrix and to analyse the washings. Its presence in the washings would then establish whether stearic acid has been applied externally. Ethanol, which does not dissolve polystyrene, but is a suitable solvent for stearic acid, was chosen. The pellets were washed with ethanol, and the residue obtained after evaporating the solvent was examined by IR spectrometry.

Table 1. Quantitative analysis parameters for stearic acid determination

Analytical band	1708 cm^{-1} (C=O stretch)
Baseline adjustment:	
Start	1665–1670 cm^{-1}
End	1730–1735 cm^{-1}
Fixed path length	0.10 mm
Band measurement	Integrated absorbance (1665–1730 cm^{-1})
Calibration concentration range	0–2.2×10^3 μg ml^{-1}

To check the procedure two commercial polystyrene resins were first analysed; one containing external and the other internal stearic acid. Fig. 1 shows the corresponding IR spectra for ethanol wash residues from the two resins. Spectrum A indicates the carboxylic acid functionality absorption band at 1708 cm^{-1}, attributable to stearic acid. Spectrum B shows weak styrene oligomer bands, but no stearic acid absorption bands, suggesting that stearic acid was not applied externally.

Fig. 2 shows the corresponding IR spectrum (4000–600 cm^{-1}) of the second resin and a scale-expanded spectrum (1780–1650 cm^{-1}), indicating intense bands due to styrene oligomers, and a medium-intensity carboxylic acid carbonyl stretch band at 1708 cm^{-1} due to stearic acid. These two examples clearly show that an ethanol wash of styrenic resins can be used to establish external application of stearic acid, whereas the polymer dissolution/re-precipitation method can be used to determine internal stearic acid.

Another commercial polystyrene resin containing internal stearic acid and external substituted fatty amide was analysed to determine further the validity of this approach. Fig. 3 shows the IR spectra of residues obtained from this resin by the two additive isolation procedures described. The ethanol-wash residue spectrum showed peaks of weak intensity, due to styrene oligomers or polystyrene fines; no evidence for either stearic acid or a substituted fatty amide was observed. This suggests that an ethanol wash selectively removes stearic acid, but not a substituted fatty amide.

Bands due to styrene oligomers and stearic acid were found in the spectrum of the residue resulting from the polymer dissolution/re-precipitation method, indicating that stearic acid was used internally and not externally. A weak band in the N–H stretching region suggests the presence of a fatty amide-type external lubricant. In Fig. 4 this spectrum is compared with the residue spectrum obtained from a resin

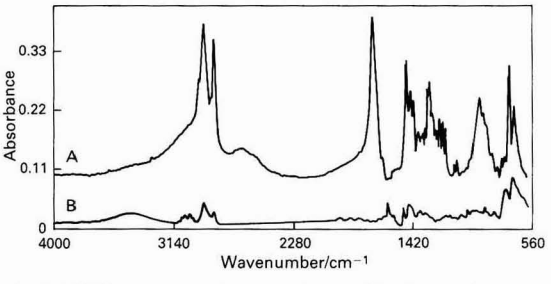

Fig. 1. FT-IR spectra of ethanol-washing residue from polystyrene resins containing stearic acid: A, on the pellet surface (external); and B, bulk (internal)

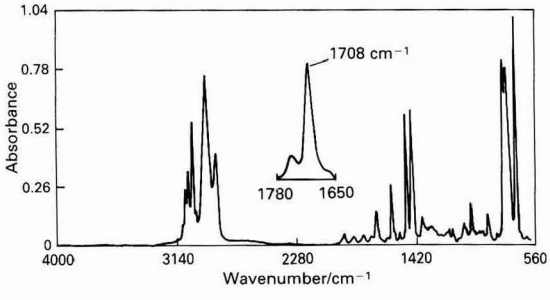

Fig. 2. FT-IR spectrum of the residue obtained from the polymer dissolution/re-precipitation procedure

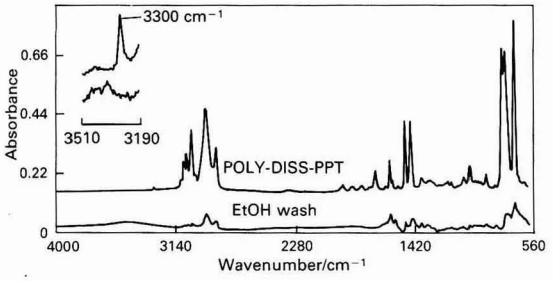

Fig. 3. FT-IR spectra of the residues obtained from a resin containing internal stearic acid and external substituted fatty amide by different additive isolation procedures

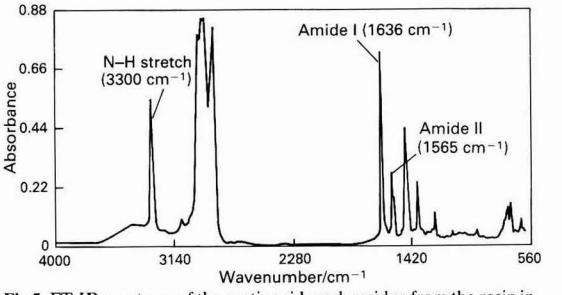

Fig 5. FT-IR spectrum of the acetic acid-wash residue from the resin in Fig. 3 (internal stearic acid - external substituted fatty amide)

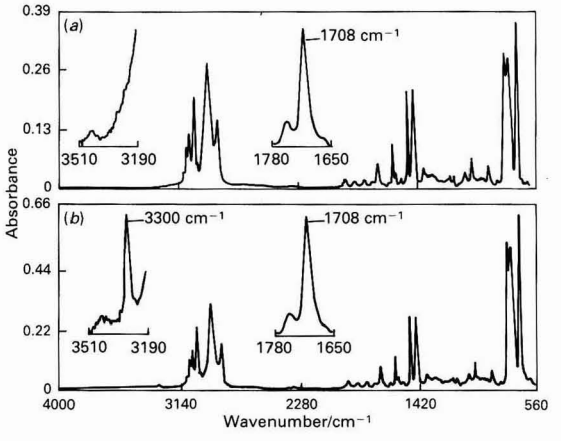

Fig. 4. Spectral comparison of residues obtained from the polymer dissolution/re-precipitation method. (*a*) Resin containing only internal stearic acid; and (*b*) resin containing internal stearic acid and external substituted fatty amide

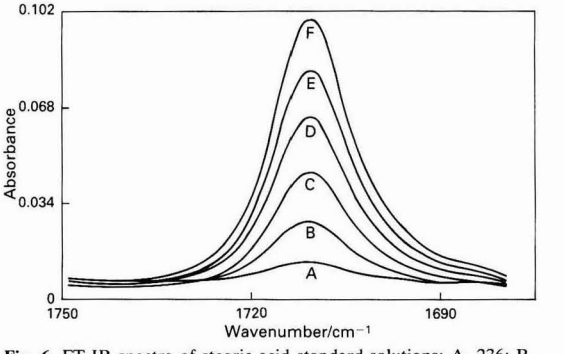

Fig. 6. FT-IR spectra of stearic acid standard solutions: A, 236; B, 616; C, 990; D, 1390; E, 1770; and F, 2190 μg g^{-1}

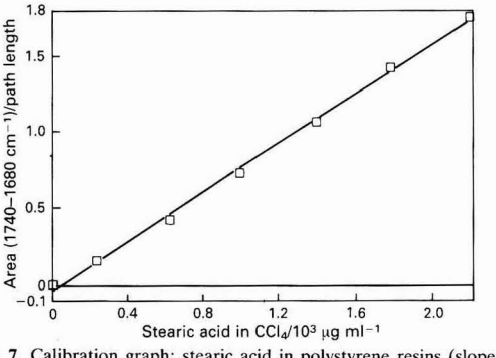

Fig. 7. Calibration graph: stearic acid in polystyrene resins (slope; 8×10^{-4}; intercept, 3.86×10^{-2}; and r^2, 0.998)

containing only internal stearic acid and no external substituted fatty amide. The respective spectral regions are scale expanded. These data suggest that the polymer dissolution/re-precipitation method can be used to detect external fatty amide. The success of this approach, however, is dependent on the amount of amide on the pellet surface. To confirm the presence of fatty amide, the resin was washed with hot glacial acetic acid; Fig. 5 shows the IR spectrum of the resulting residue, indicating all the bands attributable to a suspected amide component. This example illustrates that an external substituted fatty amide does not interfere in the determination of stearic acid.

Having established the specificity of additive isolation methods, quantitative analysis of stearic acid was attempted by measuring the integrated absorbance of the analytical band (1665–1730 cm^{-1}). Fig. 6 shows IR spectra of a series of independently prepared stearic acid standard solutions. Notice an increase in the analytical band intensity with an increase in the concentration of stearic acid. A calibration graph was established in the 0–2.2 $\times$ 10^3 μg ml^{-1} range, and the complete method was stored in the computer for future retrieval or modification. Nicolet software provided a calibration data table from which a calibration graph was plotted, as shown in Fig. 7.

A set of five stearic acid standard solutions was freshly, prepared with CCl_4 and analysed by use of the calibration data previously obtained (by serial dilution and with independently prepared standards) to test the validity of the method. The data in Table 2 demonstrate the reliability of the method, indicating that the accuracy of the method was within 5% for the first four samples, but slightly higher for the fifth sample. A resin standard containing 270 μg g^{-1} of stearic acid was prepared by incorporating stearic acid in the polymer by solvent blending, with CH_2Cl_2 as the solvent. Five determinations on this sample yielded an average of 260 μg g^{-1} with a relative standard deviation of 3.9–5.0%; Table 3 summarises the results.

Three commercial resin samples were analysed (see Table 4); PS-1 (internal), PS-2 (internal) and PS-3 (external) for stearic acid content. The anticipated levels were 1000–1100 μg g^{-1} for PS-1, *ca.* 800 μg g^{-1} for PS-2 and 300–400 μg g^{-1} for

Table 2. Analysis of stearic acid standard solutions by using the calibration data obtained by serial dilution and independently prepared standards

	Stearic acid in CCl_4/μg ml^{-1}				
	Serial dilution			Independent standards	
Sample	Estimated	Measured	Error, %	Measured	Error, %
Std. 1 ..	1670	1688	1.07	1696	1.56
Std. 2 ..	1340	1389	3.65	1375	2.65
Std. 3 ..	835	845	1.19	847	1.18
Std. 4 ..	668	680	1.79	690	3.29
Std. 5 ..	335	335	5.99	350	4.50

Table 3. Analysis of a resin containing 270 μg g^{-1} of stearic acid

	Stearic acid measured/μg g^{-1}	
Run No. 1	Serial dilution	Independent standards
1	277	280
2	253	255
3	256	249
4	260	250
5	254	263
$\bar{X}$* ..	260	259
S† ..	9.87	12.77
RSD‡ ..	3.9%	5.0%

* $\bar{X}$ = average value.
† S = standard deviation.
‡ RSD = relative standard deviation.

Table 4. Analysis of commercial resins

	Stearic acid/μg g^{-1}			
		Measured		
Sample identification	Expected	I	II	Average
PS-1 (internal)	1000–1100	1130	1000	1065
PS-2 (internal)	800	830	910	870
PS-3 (external)	300–400	280	374	327

PS-3. Based on duplicate determinations, 1065, 870 and 327 μg g^{-1} of stearic acid were found in PS-1, PS-2 and PS-3, respectively. These results indicate that the amount of internal and external stearic acid in polystyrene resins can be determined reliably and accurately by using IR spectrometry.

Conclusion

Simple sampling procedures are described to determine whether the stearic acid processing aid is applied externally or internally in styrenic resins. The polymer dissolution/re-precipitation method removes stearic acid from the resin, whereas an ethanol wash selectively removes the external stearic acid. A rapid, precise and accurate method to determine both external and internal stearic acid in polystyrene resins by using FT-IR spectrometry is described. The accuracy of the method is within 6%. The detection limit is *ca.* 0.01% m/m in the resin.

The author thanks K. Sivak and S. Demegillo for obtaining the spectral data, Dr. H. A. Spannuth for encouragement and helpful hints and Mobil Chemical Company for permission to publish this work.

References

1. Scholl, F., "Atlas of Polymer and Plastic Analysis," Volume 3, Carl Hanser Verlag, Munchen and Verlag Chemie, Weinheim, 1981, p. 139.
2. Breuer, T. E., "Modern Plastics Encyclopedia," McGraw-Hill, New York, 1989, p. 173.
3. Radian Corporation, "Chemical Additives for the Plastic Industry," Noyes Data, Park Ridge, NJ, 1987, p. 99.
4. Scholfield, C. R., *in*, Emken, E. A., and Dutton, J. J., *Editors*, "Analysis and Physical Properties of Isomeric Fatty Acids," American Oil Chemists' Society, Champaign, IL, 1979, pp. 17–43.
5. Carpenter, D. L., and Silver, H. T., *J. Chromatogr. Sci.*, 1976, **14**, 405.
6. Lingeman, H., *PhD Thesis*, State University of Utrecht, The Netherlands, 1986.
7. Kukis, A., *J. Chromatogr.*, 1977, **143**, 3.
8. Cooper, M. J., and Anders, M. W. J., *J. Chromatogr. Sci.*, 1975, **13**, 407.
9. Lie Ken Jie, M. S. F., *in* Giddings, J. C., Grusshka, E., Cazes, J., and Brown, P. R., *Editors*, "Advances in Chromatography," Volume 18, Marcel Dekker, New York, 1977, p. 1.
10. King, J. W., Adams, E. C., and Biddingmeyer, B. A., *J. Liq. Chromatogr.*, 1982, **5**, 275.
11. Bailie, A. G., Wilson, T. D., O'Brien, R. K., Beebe, J. M., Stewart, J. D., McCosh-Lilie, E. J., and Hill, D. W., *J. Chromatogr. Sci.*, 1982, **20**, 466.
12. Calabrese, K. L., *J. Chromatogr.*, 1987, **386**, 199.
13. Al Sammerrai, D., *Analyst*, 1985, **110**, 219.

Paper 0/00630K
Received February 12th, 1990
Accepted May 30th, 1990

Determination of Trace Amounts of Cobalt in Feed Grains and Forages by Solvent Extraction and Graphite Furnace Atomic Absorption Spectrometry

W. John Blanchflower, Andrew Cannavan and D. Glenn Kennedy
Department of Agriculture, Veterinary Research Laboratory, Stormont, Belfast BT4 3SD, UK

A method is described for the determination of trace amounts of cobalt in feed grains and forages with a detection limit of 1 ng g^{-1}. Samples are ashed in a muffle furnace and complexed with 2-nitroso-1-naphthol. Following solvent extraction, cobalt is determined using graphite furnace atomic absorption spectrometry. The assay can be carried out in a normal analytical laboratory without the need for special "clean" rooms. Reagents have been selected to keep reagent blank values at low levels, and heptan-2-one is used as extracting solvent to avoid problems with evaporation. The assay has been used for diagnostic purposes and to formulate special low cobalt diets for sheep for experimental purposes.

Keywords: *Cobalt determination; feed; graphite furnace; atomic absorption spectrometry*

Cobalt is an important element in animal nutrition, particularly for sheep, where it is utilised for the synthesis of vitamin B_{12} by rumen bacteria.[1] This vitamin is important as a co-factor for the enzyme methylmalonyl-CoA mutase which is required for the production of succinate from propionate, the main energy source for ruminants.[2] A deficiency of cobalt in the diet of sheep can, therefore, lead to impaired energy utilisation and decreased weight gain,[3] with subsequent economic loss to the farmer.

Direct diagnosis of cobalt deficiency in sheep is difficult because of the low concentrations of cobalt normally found in blood; diagnosis is usually made indirectly by determination of vitamin B_{12}[4] or methylmalonic acid[5] levels. It is also important, however, to determine the levels of cobalt present in animal feeds both for diagnostic and experimental purposes. Cobalt-adequate diets for sheep contain more than 70 μg kg^{-1},[6] levels of 4 μg kg^{-1} in barley have been used experimentally to produce cobalt deficiency in lambs.[7] Methods must therefore be capable of accurately measuring the relatively low amounts of cobalt present in cobalt-deficient feeds.

Methods have been published[8,9] for the determination of trace amounts of cobalt using graphite furnace atomic absorption spectrometry (GFAAS) following complexation with various ligands. Of these ligands, 2-nitroso-1-naphthol was shown to be the most suitable and free of interference from other metals.[10] A method was subsequently described,[11] using this ligand, to determine the levels of cobalt in various feeds. While this method was capable of achieving the sensitivity required for the assay, problems were experienced owing to high blank values, the wet-ashing procedure and to the extraction solvent used in the assay. A method is described in this paper which overcomes these problems and permits the accurate measurement of the trace levels of cobalt found in severely deficient diets.

Experimental

Apparatus

A Model 272 atomic absorption spectrometer equipped with an HGA-500 furnace, AS40 autosampler and a Model 56 pen recorder (all from Perkin-Elmer, Beaconsfield, Buckinghamshire, UK) were used to obtain readings. The spectrometer was fitted with a single-element hollow-cathode lamp (Perkin-Elmer). Pyrolytic graphite coated graphite tubes were used. A Model 9/68 muffle furnace (Carbolite, Bamford, Sheffield, UK) was used to ash samples.

Reagents

Nitric acid (concentrated, 70% m/m), glacial acetic acid, hydrogen peroxide (30 volumes) and potassium hydroxide (600 g l^{-1} in water) were all of AnalaR grade and heptan-2-one was of SpectrosoL grade. The indicator solution contained 2 g l^{-1} of Bromocresol Green and 0.5 g l^{-1} of Methyl Orange, in water. The complexing solution contained 20 g l^{-1} of 2-nitroso-1-naphthol in glacial acetic acid and was freshly prepared as required. All chemicals were obtained from BDH, Poole, Dorset, UK. Stock standard solutions (BDH, SpectrosoL grade) each contained 1 mg ml^{-1} of cobalt, iron, manganese, zinc or copper. A working cobalt standard (1 μg ml^{-1}) was freshly prepared as required by suitable dilution of the stock standard. De-ionised water was used throughout.

Feed Samples

Samples of forages and feed grains were obtained from local farms and were dried at 110 °C prior to analysis. All samples were ground using a Wiley Intermediate Mill fitted with stainless-steel cutters and 1-mm screen (Thomas Scientific, Swedesboro, NJ, USA). A National Institute of Standards and Technology (NIST) Standard Reference Material (SRM) 1568 Rice Flour with a certified cobalt content of 20 ng g^{-1} was obtained from the United States Department of Commerce, Gaithersburg, MD, USA.

Glassware

All glassware and silica crucibles were soaked for 1 h in 50% v/v nitric acid and then rinsed with water before use.

Method

Weigh duplicate aliquots of milled feed samples (10 g of cereals or 5 g of grass) into 50-ml silica crucibles. Also set up two empty crucibles as sample blanks. Place in a muffle furnace, raise the temperature to 600 °C and leave overnight. After cooling, wash the walls of the crucibles with 1 ml of concentrated nitric acid and gently heat on a hot-plate in a fume cupboard in order to dissolve any soluble residue. Wash the walls of the crucibles with 5 ml of water and again gently heat for a few minutes. Transfer the solutions into 110 × 30 mm tubes with ground-glass necks. Wash the crucibles with two 5-ml portions of water and add the washings to the ash solutions. Also set up duplicate reagent blanks and standards of 0, 62.5, 125 and 250 μl of the 1 μg ml^{-1} cobalt working standard. To these, add 0.5 ml of concentrated nitric acid and 15 ml of water. To all tubes, add 1 ml of glacial acetic acid and

Table 1. Atomiser conditions

Parameter	Assay step					
	Drying		Charring		Atomisation	
Temperature/°C	140	160	1000	1000	2400	2400
Ramp time/s	2	2	10	0	0	0
Hold time/s	10	10	10	5	6	5
Internal gas flow	ON	ON	ON	OFF	OFF	ON

5 drops of indicator solution. Adjust the pH to 4.5 ± 0.2 by the dropwise addition of potassium hydroxide solution (600 g l^{-1}). The indicator should change colour from yellow - green to blue - green when the correct pH is obtained (check, using a pH meter until confident of the colour change). Add 1 ml of hydrogen peroxide followed by 0.5 ml of complexing solution. Mix the contents of the tubes after each addition. Allow the tubes to stand for 30 min at room temperature and extract the cobalt complex into 2.5 ml of heptan-2-one by shaking each tube vigorously for 30 s. Allow the two layers to separate, and transfer the upper heptan-2-one extracts into glass autosampler vials for GFAAS.

Atomic Absorption Measurements

The wavelength and slit-width of the atomic absorption spectrometer are set according to the instructions of the manufacturer. Aliquots of extracts (50 µl) are injected into the graphite furnace by means of the autosampler, using ethanol as the wash solution. The atomiser conditions are shown in Table 1. The charring and atomisation temperatures are similar to those previously described.[11] Maximum power heating, with the internal argon gas flow off, is used for atomisation in order to achieve maximum sensitivity. Readings on the spectrometer are taken using the peak-height mode. The instrument is calibrated to give an 80% deflection on the pen recorder when the highest standard is injected. A calibration graph is constructed and the cobalt levels of unknown samples are calculated from it. Any samples outside the range of the standards are again carried through the assay using a smaller aliquot of sample.

Results

A calibration graph was constructed by using standards of 0, 50, 100, 150, 200 and 250 µl of the 1 µg ml^{-1} cobalt standard in the assay. The data were best fitted by the polynomial equation $y = a + bx + cx^2$, where y was the peak height in mm, and x was the concentration of cobalt in ng g^{-1} using a 10-g portion of sample. The results are shown in Fig. 1. The values for a, b and c were 9.32, 9.38 and −0.09, respectively. The correlation coefficient (r) was 1.000. For routine use, a blank and three standards in duplicate are sufficient to construct the graph.

The method was checked for possible interference from four other metals commonly found in plant material, *i.e.* Cu, Fe, Mn and Zn, by adding 1000 µg of each of these metals to 100 ng of cobalt standard and carrying out the extraction procedure. These levels are greatly in excess of those normally found in 10 g of cereal or 5 g of grass. The results are shown in Table 2. No interference was caused by any of the metals added.

The precision of the assay was determined by replicate analyses of barley, grass, and straw samples. The results are shown in Table 3. The coefficients of variation (CV) ranged from 4.3 to 8.5% for the samples tested.

Recovery values for the assay were determined by spiking barley, grass and straw samples which had been weighed into the silica crucibles, with aliquots of the 1 µg ml^{-1} standard.

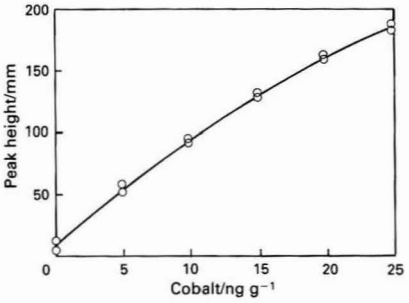

Fig. 1. Calibration graph for the determination of cobalt in feeds

Table 2. Test of interference from other metals. Results are the means of duplicate analyses; 1000 µg of each metal was added to 100 ng of cobalt

Metal added	Cobalt recovered/ng
Copper	102
Iron	102
Manganese	99
Zinc	95

Table 3. Precision of the assay

Parameter	Sample type			
	Barley 1	Barley 2	Grass	Straw
Mean/ng g^{-1}	8.4	16.7	32.1	39.1
SD/ng g^{-1}	0.36	1.30	2.73	2.45
CV, %	4.3	7.8	8.5	6.3
n	6	6	6	5

Table 4. Recovery of cobalt added to samples. Results are the means of duplicate analyses; 10-g portions were used for barley samples 1 and 4, and 5-g portions for the remainder

Sample	Cobalt in sample/ ng g^{-1}	Cobalt added/ ng g^{-1}	Cobalt found/ ng g^{-1}	Recovery, %
Barley 1	8.4	10	18.0	96
Barley 2	10.2	25	32.0	87
Barley 3	10.2	50	56.4	93
Barley 4	5.0	25	29.6	98
Straw	39.1	25	59.4	81
Grass	32.1	25	53.3	85
NIST SRM 1568 Rice Flour	20.0*	—	18.6	93

* Certified value.

The NIST SRM 1568 Rice Flour was also analysed. The results are shown in Table 4. Recoveries of added cobalt ranged from 81 to 98% ($\bar{x}$ = 90.4 ± 6.2), and the NIST SRM gave a cobalt level which was 93% of the certified value.

Sample blank values for five separate sets of analyses carried out over a period of several weeks ranged from the equivalent of 0.8 to 1.1 ng g^{-1} ($\bar{x}$ = 0.98 ± 0.13) for 10-g portions of sample.

Discussion

The assay described has been developed for use in a busy diagnostic/research laboratory without the necessity for special "clean" areas. By using large portions of samples (5 or 10 g), the small background levels of cobalt found in the sample blank became relatively insignificant and could be subtracted from the sample values. The use of acetic acid - potassium hydroxide to buffer the ash solutions gave blank values

approximately five times lower than the sodium citrate used in a previous paper.[11] High blank values were also obtained using citric acid - sodium hydroxide; the sodium hydroxide was found to be the main source of contamination. Supplies from different manufacturers did not improve the problem significantly. The heptan-2-one used was of SpectrosoL grade, which is stated to contain a maximum level of 0.02 μg ml $^{-1}$ cobalt. In theory, this could have contributed, by up to the equivalent of 5 ng g^{-1} of cobalt, to the blank value. In practice the blank values averaged 0.98 ng g^{-1} and it would seem more likely that this contribution came from the inorganic rather than the organic reagents used in the assay.

Muffle furnace ashing of samples was used instead of the wet-ashing procedure previously described.[11] This enabled larger portions of samples to be taken (10 g as opposed to 2 g) and was also less labour intensive and safer. The wet-ashing procedure involved an initial digestion using nitric acid, followed by three boiling steps of 2 h each using hydrogen peroxide. In contrast, the muffle-furnace procedure consisted of an unattended overnight heating step.

Various solvents such as chloroform or xylene have been used in previous work to extract the cobalt complex. These are relatively volatile, however, and precautions had to be taken to avoid evaporation of the solvents and concentration of the extracts. The use of heptan-2-one as the extraction solvent eliminated the need for any special precautions, and the sample cups could be left open for several hours without any significant loss.

The method described has been used in this laboratory for the last 2 years and provided moderate precautions are taken to avoid contamination of glassware and reagents with cobalt, reproducible results can be easily obtained. Eight samples, in duplicate, with standards and blanks can be assayed in one working day, and this number could be increased with increased muffle furnace capacity.

The detection limit for the assay is *ca.* 1 ng g^{-1} of cobalt in feed and in practice no samples containing less than 4 ng g^{-1} were found. If necessary, however, the sensitivity could be increased further by using a smaller volume of heptan-2-one for extraction. The method has been used to analyse grass, straw and cereal samples from farms in Northern Ireland, and has enabled areas of cobalt deficiency to be identified and diets, to experimentally produce cobalt/vitamin B_{12} deficiency in sheep, to be formulated.

References

1. Porter, J. W. G., *in* Lewis, D., *Editor*, "Digestive Physiology and Nutrition of the Ruminant," Butterworth, London, 1961, p. 226.
2. Bergman, E. N., Roe, W. E., and Kon, K., *Am. J. Physiol.*, 1966, **211**, 793.
3. Rice, D. A., McLoughlin, M., Blanchflower, W. J., McMurray, C. H., and Goodall, E. A., *Biol. Trace Element Res.*, 1989, **22**, 153.
4. Kennedy, D. G., O'Harte, F. P. M., Blanchflower, W. J., and Rice, D. A., *Vet. Res. Commun.*, 1990, **14**, 255.
5. McMurray, C. H., Blanchflower, W. J., Rice, D. A., and McLoughlin, M. J., *J. Chromatogr. Biomed. Appl.*, 1986, **378**, 201.
6. Mertz, W., "Trace Elements in Human and Animal Nutrition," Fifth Edition, Academic Press, New York, 1987, p. 156.
7. O'Harte, F. P. M., Kennedy, D. G., Blanchflower, W. J., and Rice, D. A., *Br. J. Nutr.*, 1989, **62**, 729.
8. Hageman, L., Torma, L., and Ginther, B. E., *J. Assoc. Off. Anal. Chem.*, 1975, **58**, 990.
9. Pedersen, B., Willems, M., and Jørgensen, S. S., *Analyst*, 1980, **105**, 119.
10. Borggaard, O. K., Christensen, H. E. M., Nielsen, T. K., and Willems, M., *Analyst*, 1982, **107**, 1479.
11. Borggaard, O. K., Christensen, H. E. M., and Lund, S. P., *Analyst*, 1984, **109**, 1179.

Paper 0/01183E
Received March 19th, 1990
Accepted June 5th, 1990

Assessment of Frozen Storage of Tributyltin in Sea-water Samples Using Hydride Derivatisation

Aldis O. Valkirs, Martha O. Stallard, Peter M. Stang and Steven Frank
Computer Sciences Corporation, San Diego, CA 92109, USA
Peter F. Seligman
Marine Environment Branch Code 522, Naval Ocean Systems Center, San Diego, CA 92152, USA

Frozen storage of unfiltered natural sea-water samples fortified with tributyltin (TBT) leachate from antifouling paint was evaluated by the analysis of replicate samples selected randomly over a 678-d period using a hydride derivatisation purge and trap method. A previous study indicated that the precision of the analytical method is typically 15% and hence a greater than 15% loss of TBT is considered significant. Depending on whether a linear or exponential regression analysis of the data is carried out, a 15% loss apparently occurred after 170 or 90 d. After approximately 2 years of storage, the TBT concentration of samples had fallen by about 50%.

Keywords: *Tributyltin in sea-water; frozen storage; hydride derivatisation; atomic absorption spectrometry*

The widespread distribution of tributyltin (TBT) in marine and freshwater environments and its high degree of toxicity to aquatic species has been well documented.[1–3] Thus, concern has been raised about its widespread detrimental ecological effects in several countries including the United Kingdom, France and the United States. This has resulted in restrictive legislation to ban the use of some antifouling paints containing TBT and restrict the use of others to large vessels.[4–6]

The low water quality criteria adopted by the United States (10 ng l^{-1} TBT in marine waters[7]) will necessitate extremely sensitive and accurate analytical methods for monitoring purposes. Additionally, it will be necessary to store collected samples in an appropriate manner and complete the analysis in a suitable time period. In a previous study Valkirs *et al.*[8] reported that frozen storage of sea-water samples containing TBT at sub-p.p.b. levels was possible in polycarbonate containers for a period of 2–3 months without any significant loss of analyte. After 41 weeks the TBT concentration was less than 50% of the initial concentration. To verify the results of this study further and to provide additional data on extended storage of sea-water samples containing TBT, results of a 678-d frozen storage period at −20 °C have been obtained.

Experimental

All polycarbonate plastic containers were cleaned with RBS-35 detergent prior to use. Polycarbonate plastic has previously been shown to be non-adsorptive to TBT.[9,10] A large 20 l polycarbonate carboy was filled with unfiltered offshore coastal sea-water circulated over panels painted with antifouling paint containing TBT. This TBT solution was dispensed into individual 500 ml polycarbonate plastic bottles which were then frozen and stored for subsequent analysis. Each bottle was analysed once. Three bottles were removed prior to freezing for initial TBT meaurements. Generally three or more replicate bottles were removed for analysis in a given time period. In two of the ten time periods only two bottles were withdrawn for measurements. On the 194th day of storage nine bottles were removed and analysed by three different individuals. Each person selected three bottles and prepared a separate TBT calibration standard to ascertain whether measurements were influenced by variability in calibration standards prepared by different individuals. Each bottle was analysed once. A one-way analysis of variance test indicated that the mean values were not significantly different ($p = 0.53$) at the 95% confidence level. After 678 d of storage, six previously analysed and re-frozen bottles were again analysed to determine whether the TBT concentration would be consistent with previous data and fit one or the other of the regression relationships calculated.

The hydride derivatisation method used is a purge and trap procedure using atomic absorption spectrometric detection and has been described previously.[8,11,12] Recent refinements involving modification of the quartz burner design to a single open end and silanising the glass cryotrap have permitted detection of butyltins at sub-ng l^{-1} concentrations.[13] Calibration was performed by external calibration graphs linear over the analyte concentration measured. Butyltins were quantified as the respective chlorides. As the method employs a direct sample derivatisation, the amount of analyte measured may be adjusted simply by altering the amount of sample used. Butyltin standards were used as received without further purification. Regression analysis of the data was performed using the Statistical Analysis System (SAS) software.[14]

Results and Discussion

Frozen storage of sea-water samples containing TBT at an initial concentration representative of values reported from a wide spectrum of geographical areas[12,15–17] has demonstrated that a significant loss of TBT occurs after several months (Fig. 1). If a previously reported[1] relative standard deviation of 15% is considered to be a representative value for estimating the precision of the hydride method, then a detectable loss of TBT occurs after a 3–5.7 month period, depending on the regression equation fitted to the data. In Fig. 1(*a*) the regression equation, using an exponential term over time indicates that a 15% loss of TBT would occur after 3 months of frozen storage. The lower and upper 95% confidence limits in terms of storage time were 2.3 and 3.7 months, respectively. If a straight-line regression equation is applied to the data, a 15% loss of TBT is seen after 5.7 months of storage with lower and upper 95% confidence limits of 4.1 and 7.2 months, respectively [Fig. 1(*b*)]. The differences in loss of TBT over time are mostly due to the different intercepts calculated for the initial TBT concentration by the regression equations used.

The degree of TBT loss considered significant over time is subjective. In a recent inter-agency workshop, issues associated with aquatic sampling and analysis of organotin samples were discussed by several research groups.[18] A relative standard deviation of 15% was considered representative among the analytical methods identified as having the requisite specificity and sensitivity for TBT monitoring. The

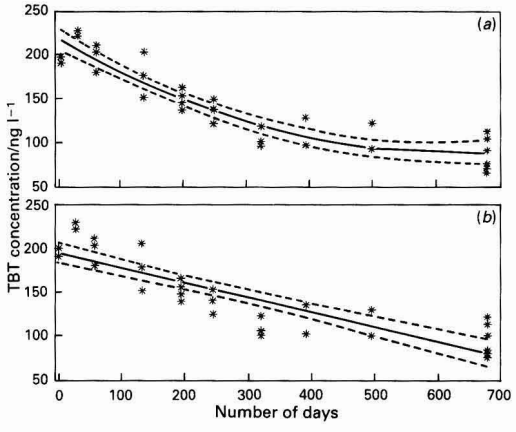

Fig. 1. Loss of TBT during frozen storage: (*a*) $y = 216 - 0.39x + 0.0003x^2$, coefficient of determination (R^2) = 0.86; (*b*) $y = 194 - 0.17x$, $R^2 = 0.75$. Individual identical values are superimposed

hydride derivatisation method used in the present study was among the methods considered acceptable. In 9 of the 12 measurement intervals examined during the study, relative standard deviations of less than 15% were calculated for single TBT measurements from each bottle. It therefore appears that a 15% relative standard deviation can be considered representative of the hydride derivatisation purge and trap method and that loss of TBT in stored samples can be considered significant at percentages greater than this value.

The data presented in this study are consistent with previous storage evaluations of TBT in sea-water indicating that a 3-month storage period would not result in a significant loss of TBT.[8,19] Previously, after a 10-month storage period, approximately half the initial TBT concentration was measurable.[8] Prolonged storage for a 10-month period and approximately 2-year period indicates that TBT loss is not linear and fits an exponential regression equation [Fig. 1(*a*)]. Previously, analysis of frozen samples showed no increase in TBT degradation products such as dibutyltin (DBT) or monobutyltin(MBT).[8] The appearance of DBT as a degradation product was not confirmed in the current work. Dibutyltin was measured at 14 intervals during the present storage study. The initial concentration was 0.016 μg l^{-1} with a final concentration of 0.018 μg l^{-1}. The slope of a straight-line regression equation fitted to the data was not significant [$y = -0.2\ (-7)x + 0.018$; the standard error of the slope was 3.6 (−6); $R^2 = -0.0086$]. Initial and final MBT values of 0.023 μg l^{-1} and 0.030 μg l^{-1} were also recorded over a 496-d period with nine measurement intervals. A straight-line regression equation fitted to the MBT values measured was significant over a 496-d period [$y = 4.35\ (-5)x + 0.008$; the standard error of the slope was 1.0 (−5); $R^2 = 0.64$].

It is not clear why TBT degradation products were not found in this study and in a previous study[1] at lower concentrations. The slight amount of MBT found in samples analysed after 496 d does not account for the approximate 50% loss of TBT at 496 d [Fig. 1(*a*)]. The loss of TBT during frozen storage may not involve de-alkylation[8] as no significant DBT and very little significant MBT was detected over time. During the course of this study, however, the appearance of white crystals on the bottom of bottles stored for at least 2–3 months or more was noticed. These crystals appeared to be of a carbonate nature as addition of hydrochloric acid resulted in the liberation of gas. X-ray diffraction analysis (Diano XRD-8000 diffractometer) produced a major peak at 33.8 (a scattering angle of 2θ degrees), suggesting that the majority of the material was $CaCO_3$. It is possible that, on freezing, differential formation of brine occurs which is saturated with respect to $CaCO_3$. Months of storage at −20 °C could create an environment where $CaCO_3$ crystallisation can occur and possibly remove some of the TBT in solution.

This work was sponsored by the Office of the Chief of Naval Research under the Navy Energy Research and Development Program.

References

1. Thompson, J. A. J., Sheffer, M. G., Pierce, R. C., Chau, Y. K., Cooney, J. J., Cullen, W. R., and Maguire, R. J., "Organotin Compounds in the Aquatic Environment: Scientific Criteria for Assessing Their Effects on Environmental Quality," (Publication No. 22494) National Research Council of Canada, Ottawa, 1985.
2. Maguire, R. J., *Appl. Organomet. Chem.*, 1987, **1**, 475.
3. Hall, L. W., and Pinkney, A. E., *CRC Crit. Rev. Toxicol.*, 1985, **14**, 159.
4. "Control of Pollution (Antifouling paints and treatments) Regulations. Statutory Instrument 1987 No. 783." HM Stationery Office, London, 1987.
5. *Decree* 82–782, 14th September 1982, France.
6. United States Congress. Organotin Antifouling Paint Control Act of 1988. Public Law 100–333, 1988.
7. United States Environmental Protection Agency. "Ambient Water Quality Criteria for Tributyltin." Office of Research and Development, Environmental Research Laboratories, Duluth, Minnesota and Narragansett, Rhode Island, 1988.
8. Valkirs, A. O., Seligman, P. F., Olson, G. J., Brinckman, F. E., Matthias, C. L., and Bellama, J. M., *Analyst*, 1987, **112**, 17.
9. Dooley, C. A., and Homer, V., *Technical Report No. 918*, Naval Ocean Systems Center, San Diego, CA, 1983.
10. Valkirs, A. O., Seligman, P. F., and Lee, R. F., "Proceedings of the Oceans 86 Symposium," September 23–25, 1986, Washington, DC, Volume 4, p. 1165.
11. Valkirs, A. O., Seligman, P. F., Vafa, G., Stang, P. M., Homer, V., and Lieberman, S. H., *Technical Report No. 1037*, Naval Ocean Systems Center, San Diego, CA, 1985.
12. Valkirs, A. O., Seligman, P. F., Stang, P. M., Homer, V., Lieberman, S. H., Vafa, G., and Dooley, C. A., *Mar. Pollut. Bull.*, 1986, **17**, 319.
13. Stallard, M. O., Cola, S. Y., and Dooley, C. A., *Appl. Organomet. Chem.*, 1989, **3**, 105.
14. SAS Institute Statistical Analysis System. SAS Institute Inc. Box 8000, Cary, NC 27511, 1982.
15. Seligman, P. F., Grovhoug, J. G., Valkirs, A. O., Stang, P. M., Fransham, R., Stallard, M. O., Davidson, B., and Lee, R. F., *Appl. Organomet. Chem.*, 1989, **3**, 31.
16. Waldock, M. J., Thain, J. E., and Waite, M. E., *Appl. Organomet. Chem.*, 1987, **1**, 287.
17. Maguire, R. J., Tkacz, R. J., Chau, Y. K., Bengert, G. A., and Wong, P. T. S., *Chemosphere*, 1986, **15**, 253.
18. Young, D. R., Schatzberg, P., Brinckman, F. E., Champ, M. A., Stewart, E. H., and Landy, R. B., "Proceedings of the Oceans 86 Symposium," September 23–25, 1986, Washington, DC, Volume 4, p. 1135.
19. Huggett, R. J., Unger, M. A., and Westbrook, D. J., "Proceedings of the Oceans 86 Symposium," September 23–25, 1986, Washington, DC, Volume 4, p. 1262.

Paper 9/05284D
Received December 12th, 1989
Accepted June 1st, 1990

Direct Introduction of Powdered Samples into an Inductively Coupled Plasma Mass Spectrometer Using a Spark Dispersion - Merging Sample Introduction Technique

Takafumi Hirata, Tasuku Akagi and Akimasa Masuda*
Department of Chemistry, Faculty of Science, The University of Tokyo, Hongo 113, Tokyo, Japan

By using a spark dispersion - merging sample introduction technique, the direct multi-element analysis of over 40 elements including the rare earth elements (REE) were performed on four geological standard rocks (JB-1, -2 and -3 and JG-1) by inductively coupled plasma mass spectrometry (ICP-MS). About 1 mg of powdered sample was loaded on to a discharge cell placed in a merging chamber and the dispersed sample was led to the ICP with a blank aerosol sprayed from the nebuliser. The relative sensitivity factors (RSFs) of the REE were all found to be similar. This indicates that the internal standardisation method is effective for the determination of REE. For other elements, however, the RSFs were significantly different from those for the REE; the values of volatile elements such as I, Tl and Bi were high, and those of refractory elements such as Ti and Zr were low. By using a standard rock sample as a calibration standard, the semi-quantitative determination of over 40 elements could be performed on one sample in a few minutes. In these analyses, the differences from reported values were better than ±30% for most of the elements, including the REE. The detection limit was better than 100 ng g^{-1} and an absolute detection limit of 100 pg could be obtained for most elements.

Keywords: *Inductively coupled plasma mass spectrometry; powdered sample; merging sample introduction; standard rock*

Inductively coupled plasma mass spectrometry (ICP-MS) is regarded as a very sensitive technique for elemental and isotopic analysis.[1–5] However, the nebulisation method of sample introduction usually employed has drawbacks. The method demands the dissolution of solid samples which consequently requires large amounts of the solvent medium. Furthermore, most of the nebulised solution goes to waste without being analysed. Several techniques have been developed for the direct introduction of solid samples into the ICP mass spectrometer, *e.g.*, laser ablation,[6–9] arc nebulisation[10,11] and slurry nebulisation.[12]

As reported earlier,[13] a merging chamber sample introduction method has been developed. Analytes are merged with an aerosol on their way to the ICP torch. The proposed introduction method was applied to the measurement of Os isotopic composition using a micro-heater in the merging chamber. The analytes were introduced effectively into the ICP without loss. Another important merit of this method is that the optimisation of the operational settings can be carried out using a standard solution, in the same way as conventional nebulisation sample introduction. In order to apply the merging sample introduction method to solid sample analysis, a spark dispersion apparatus has been devised.

This paper demonstrates the analytical merits of the spark dispersion - merging sample introduction technique for powdered solid samples.

Experimental

Apparatus

The ICP mass spectrometer used in this study was a VG Elemental PlasmaQuad (Type I). The operational settings are listed in Table 1.

A schematic diagram of the merging chamber is shown in Fig. 1 with an enlarged diagram of the discharge cell. In this study, a stainless-steel rod (diameter, 1.5 mm) was employed as the electrode, based on the following results. At the beginning of this study, both titanium and stainless-steel were examined as suitable materials for the electrode. Unexpectedly, with an electrode made of stainless-steel, there was no significant change in the background counts for Fe, Ni and Cr. This indicated that the region affected by the sputtering effect of the spark discharge was too small to cause a substantial contamination of those elements from the electrode. However, in the analysis using the titanium rod as the electrode, a significant amount of Ti contamination was observed which clearly originated from the electrode. This difference may have been due to the difference in the surface

Table 1. Instrumental operating conditions

ICP settings—	
Incident power	1.35 kW
Reflected power	<5 W
Argon gas flow-rates	
Cooling	13 l min^{-1}
Auxiliary	1.1 l min^{-1}
Nebuliser	0.75 l min^{-1}
Nebuliser—	
Nebuliser type, cross flow	
Solution uptake rate (pumped)	0.6 ml min^{-1}
Interface—	
Aperture diameter	0.9 mm
Skimmer diameter	1.0 mm
Load coil aperture spacing	10 mm
Measurement parameters—	
(*i*) Multi-element analysis	
Dwell time	80 μs
Number of channels (total 2048 channels)	10 channels per u
Number of scans	300 scans
Integration time	50 s per run
(*ii*) Isotopic analysis	
Dwell time	80 μs
Number of channels (total 512 channels)	50 channels per u
Number of scans	500 scans
Integration time	20 s per run

* To whom correspondence should be addressed.

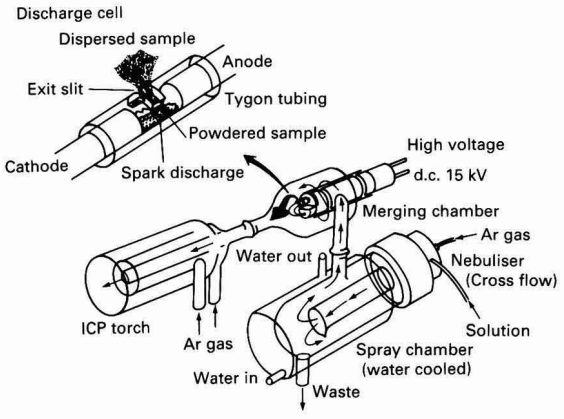

Fig. 1. Schematic diagram of apparatus for the spark dispersion - merging sample introduction system. About 1 mg of powdered sample was dispersed by the spark discharge and was carried to the ICP torch from the spray chamber with an aerosol

state; the surface of the titanium rod was rougher than that of the stainless-steel rod. Furthermore, the finely polished stainless-steel is more easily cleaned in order to eliminate any possible retention of the powdered sample.

The sample housing in the discharge cell is made from Tygon tubing with caps at both ends of the electrodes. The discharge cell is placed in the Pyrex merging chamber.

The high voltage (15 kV d.c.) required for the spark discharge was generated using an electrical circuit embedded in a commercially available electronic igniter (Model Panaspark, Matsushita Electric).

Samples

Geological standard rocks, JB-1, -2 and -3 (basalts) and JG-1 (granodiorite), prepared by the Geological Survey of Japan, were used for measurement. These sample materials have a mesh size of 150–200.

Procedure

Approximately 1 mg of powdered sample was loaded on to the discharge cell, which was then placed in the merging chamber (see Fig. 1). Immediately before the sample analysis, the parameters such as the ICP gas flow-rates, lens biases, peak shape and the resolution of the mass spectra were optimised using a standard solution containing Mg, In and Pb.

A procedure of repeating the sample loading followed by evacuation is most suited for quantitative analysis. To load a new sample, the discharge cell has to be removed from the merging chamber with the ICP power off. After loading the sample, any drift in the instrumental response can be detected by the introduction of a standard solution through nebulisation, this is another advantage of the present merging sample introduction technique. Drift in the instrumental response was approximately ±10% after the sample loading and evacuation procedure, the accuracy of the measurements being limited by the difficulties in reproducing the sample loading conditions accurately. Therefore, the use of a discharge cell, which enabled both loading and evacuation of the powdered sample with the ICP on, would be desirable to improve the accuracy of the results.

For the introduction of powder, the intermittent (8 Hz) high voltage (15 kV d.c.) was charged on both ends of the electrodes. The spark current was approximately 3 A. Any leakage of the spark noise increased the background signal count. Background count rates of 40–80 counts s^{-1} were observed when the spark discharge was on. In this study, general background count rates of 20–30 counts s^{-1}, comparable to that of the conventional nebulisation introduction, could be obtained with a shielded (earthed) cable for the high voltage output. The intermittent spark discharge (8 Hz) dispersed the sample particles, which were mixed with the aerosol in the merging chamber, and carried directly into the ICP. Operational parameters for both isotopic and multi-element analyses are listed in Table 1. The integration time for the isotopic and the multi-element analyses are 20 and 50 s per run, respectively. A practical number of runs that could be carried out on a 1-mg sample were 4 for the isotopic and 3 for the multi-element analysis. Inter-sample precision was approximately 20 and 40% for the isotopic and the multi-element analysis, respectively. The fluctuations in signal intensity may reflect an inherent instability in the dispersion rate of the powdered samples.

Results and Discussion

Signal Shape

The effect of the dispersion rate on signal intensity was investigated. The rate of sample dispersion was to a great extent dependent on the power of the spark discharge, the mesh size of the powdered sample and the size of the orifice of the discharge cell. Unfortunately, the power of the spark discharge could not be controlled, as the spark current of the high voltage generator used could not be regulated. Furthermore, it is very difficult to adjust the mesh size of the powdered sample obtained by pulverisation. Therefore, the rate of sample dispersion was controlled by adjusting the size of the orifice of the discharge cell (Fig. 2). The signal shape of ^{138}Ba in JB-1 is shown in Fig. 2. As shown in the figure, a large orifice gave a high count rate, and a small orifice gave a signal with a longer duration. Hence, although a higher sensitivity could be obtained with a large orifice, the signal was transient. On the other hand, a signal of longer duration is more favourable when scanning a wider mass region. Moreover, as shown in Fig. 3, the rate of sample dispersion affects the shape of the mass spectrum. The peak shape of a mass spectrum obtained with a slower dispersion rate, Fig. 3(*a*), is identical with that obtained with conventional nebulisation sample introduction. However, as observed in Fig. 3(*b*), for each of the mass spectra obtained with a high dispersion rate, the tops of the peaks are jagged. It is likely that the jagged shape is due to a non-homogeneous rate of sample dispersion occurring with the larger sample orifice. This is one of the possible explanations for the peak shape, another is a drift in the tuning condition of the ion optics due to the introduction of a large amount of powdered sample at the higher dispersion rate. When too many sample particles are introduced into the ICP at one time, however, there may be a matrix effect. Thus, a signal of longer duration is important for both the multi-element and/or isotopic analyses. A sample housing orifice of 1 × 2 mm was employed for the latter experiments.

The electrode spacing is another important parameter affecting signal intensity. With an electrode spacing of greater than 5 mm, the electrical noise resulting from the spark discharge can sometimes affect the background count of the mass spectrum. There were no significant changes in the mass spectrum or the shape of the signal with an electrode spacing of less than 4 mm. The electrode spacing is important in order to ensure sufficient capacity for the sample housing. In this study, the amount of powdered sample was fixed at 1 mg, so an electrode spacing of 4 mm was employed for all further work.

The isotopic ratio of U in JB-1 was observed with the present spark dispersion - merging sample introduction technique. The concentration of U is low (1.8 μg g^{-1})[14] and the isotopic abundance of ^{235}U very low (0.715%). Despite these difficulties, an isotope ratio for $^{235}U/^{238}U$ of 0.0070 ±

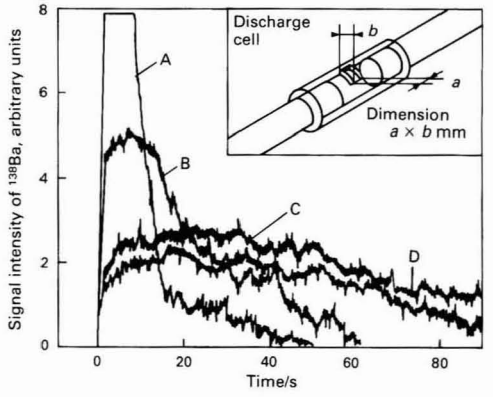

Fig. 2. Effect of size of the orifice of the discharge cell on signal shape of ^{138}Ba in JB-1. The amount of sample, JB-1, loaded on was 1 mg. The size of orifice was: A, 2 × 3; B, 1 × 3; C, 1 × 2; and D, 1 × 1 mm

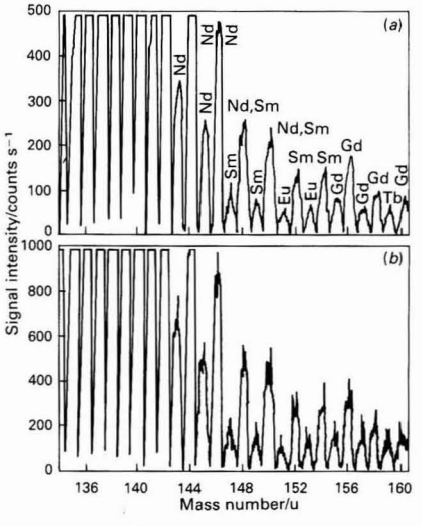

Fig. 3. Mass spectrum of light REE obtained by the spark dispersion - merging sample introduction technique for JB-1. Size of orifice: (*a*) 1 × 2; and (*b*) 2 × 3 mm

0.0013 was obtained, which is in agreement with the reported value of 0.0072.

Elemental Analysis

In order to evaluate the present spark dispersion - merging sample introduction technique for use as an effective quantitative method, four geological standard rocks, JB-1, -2 and -3 and JG-1 were analysed. In the REE determination, ^{147}Sm was used as the internal standard because its mass number is midway through the REE spectrum and it has sufficient intensity for normalisation. The abundances of the REE in the four geological standard rocks are calibrated for by assuming that all the isotopes have the same sensitivity as ^{147}Sm. The REE abundances obtained, together with literature values, are listed in Table 2. In these analyses, the deviations from the reported values are *ca.* ±20% for almost all the REEs. As can be seen in the table, the deviations from the reported values are dependent on the mass difference between the analyte ion and ^{147}Sm. As reported in an earlier paper,[15] the closer the atomic numbers the more preferable the element is for the internal standardisation, as differences in elemental sensitivity depend mostly on differences in the atomic number and chemical nature. The chemical nature of the REE was assumed to be nearly identical in this work. Thus, for the rather short mass range being used and with the precision obtained, the difference in elemental sensitivity could be corrected for using a single internal standard (^{147}Sm). Isobaric interferences from oxide ions were not corrected for because the percentages of metal oxide to parent ion (MO^+/M^+) were *ca.* 1–3%, which were comparable to those obtained with conventional nebulisation sample introduction. The correction factors for oxide interference are 4–6%; these levels are not considered to cause erroneous measurement within the precision of the method.

Table 2. Analytical results (μg g^{-1}) of JB-1, -2 and -3 and JG-1 obtained by spark dispersion - merging sample introduction. Literature values in parentheses. ^{147}Sm was used as internal standard

Element	JB-1 Found (*)	JB-2 Found (*)	JB-3 Found (*)	JG-1 Found (†)
^{139}La	30.3 (35.7)	2.25 (2.32)	7.63 (7.79)	11.6 (20.3)
^{140}Ce	86.6 (66.7)	13.2 (6.88)	36.7 (20.2)	40.3 (43.6)
^{141}Pr	8.37 (6.04)	1.28 (1.09)	4.06 (2.80)	4.49 (4.85)
^{146}Nd	30.9 (26.0)	6.72 (6.53)	16.5 (15.3)	17.6 (18.8)
^{147}Sm	5.17 (5.17)	2.39 (2.39)	4.18 (4.18)	4.36 (4.36)
^{151}Eu	1.32 (1.49)	1.10 (0.820)	1.56 (1.28)	0.62 (0.66)
^{157}Gd	4.80 (5.16)	2.07 (3.15)	3.11 (4.62)	3.62 (3.82)
^{159}Tb	0.67 (0.761)	0.63 (0.624)	0.45 (0.766)	0.71 (0.79)
^{163}Dy	3.11 (4.25)	2.57 (3.79)	2.53 (4.40)	4.10 (3.20)
^{165}Ho	0.68 (0.853)	0.48 (0.890)	0.40 (0.970)	0.60 (0.55)
^{166}Er	1.82 (2.39)	1.34 (2.60)	1.47 (2.60)	1.22 (1.68)
^{169}Tm	0.25 (0.318)	0.25 (0.399)	0.18 (0.390)	1.0 (0.49)
^{172}Yb	1.81 (2.17)	2.0 (2.61)	1.19 (2.46)	2.11 (1.63)
^{175}Lu	0.23 (0.317)	0.23 (0.386)	0.15 (0.367)	0.35 (0.53)

* See reference 15.
† See references 16 and 17.

In order to extend the versatility of the spark dispersion - merging sample introduction technique, the technique was applied to the semi-quantitative analysis of a wider mass region (^{45}Sc–^{238}U), two possible approaches were tried. Firstly, the internal standardisation method, used for the REE determination previously, was employed. In this approach ^{138}Ba was used as the internal standard, because again its mass number is midway through the scan region and ^{138}Ba has sufficient intensity for normalisation. The column C_1 in Table 3 lists the relative abundances of various isotopic elements in JB-1 and JG-1 calculated by assuming that all the isotopes have the same sensitivity as ^{138}Ba. Comparison between the C_1 values and those quoted in the literature, C_{ref}, shows that some of the lighter elements show C_1 values higher than C_{ref}. Furthermore, volatile elements such as Br, I, Tl and Bi give higher values, and refractory elements such as Ti and Zr show lower values for C_1 compared with C_{ref}. The differences between the C_1 and C_{ref} values indicate the different sensitivities for the elements.

The relative sensitivity factors (RSFs) of the elements in JB-1 and JG-1 are plotted in Fig. 4. Here the RSF refers to a sensitivity factor relative to ^{138}Ba, expressed by C_1/C_{ref}. As can be seen in the figure, the volatile elements such as Br, I, Tl and Bi have large RSFs, *i.e.*, high sensitivities. On the other hand, the RSFs for refractory elements such as Ti and Zr are low. The transmission rate of each analyte from the discharge cell to the ICP can be considered equal, as mechanical dispersion was employed for the sample introduction process. From the RSF of each of the elements, it was deduced that the most important process in determining the RSFs is volatilisation in the ICP. However, some of the refractory elements such as Mo, W and U show high RSFs. The high sensitivities of

Table 3. Abundances (μg g^{-1}) of 47 elements in two geological standard rocks. C_1, Calculated assuming equal sensitivity for every element. C_2, Calibrated using JB-1 as a standard

Element (isotope)	JB-1		JG-1			Detection limit (3σ)/ ng g^{-1}
	C_1	C_{ref}*	C_1	C_2	C_{ref}*	
^{45}Sc	19	(27)	13	18.5	(6.5)	71
^{48}Ti	1150	(8030)	690	4800	(1600)	390
^{51}V	120	(211)	29	51	(24)	61
^{55}Mn	1030	(1200)	370	430	(490)	170
^{59}Co	34	(38.4)	4.8	5.4	(4)	96
^{60}Ni	160	(139)	13	11	(6)	520
^{63}Cu	48	(56)	2.8	3.3	(1.5)	77
^{68}Zn	116	(84)	61	44	(41)	102
^{69}Ga	22	(20)	33	30	(18)	24
^{72}Ge	2.0	(1.3)	2.0	1.3	(1.3)	15
^{75}As	1.2	(2.3)	0.26	0.50	(0.3)	44
^{81}Br	11	(0.60)	0.43	0.024	(0.068)	5.1
^{85}Rb	78	(41.2)	360	190	(181)	12
^{88}Sr	150	(435)	76	220	(184)	72
^{89}Y	5.3	(25.5)	6.2	30	(30.8)	77
^{90}Zr	50	(153)	4.9	15	(111)	210
^{93}Nb	25	(31)	17	21	(15)	19
^{98}Mo	32	(34.4)	8.7	9.4	(1.5)	26
^{111}Cd	0.44	(0.103)	0.34	0.08	(0.023)	14
^{115}In	0.31	(0.055)†	0.40	0.07	(0.046)†	3.6
^{120}Sn	6.6	(1.8)	42	11	(4.1)	6.2
^{121}Sb	1.3	(0.23)	0.5	0.09	(0.1)	2.6
^{127}I	0.6	(0.029)	0.40	0.02	(0.015)	5.4
^{133}Cs	3.7	(1)	67	18	(10)	1.2
^{138}Ba‡	490	(490)	462	462	(462)	12
^{139}La	46	(36)	25	20	(22)	6.6
^{140}Ce	160	(67)	39	17	(43)	4.0
^{141}Pr	17	(8.7)	4.6	2.4	(2.3)	3.7
^{146}Nd	29	(27)	20	19	(20.6)	18
^{152}Sm	9.4	(5.16)	9.4	5.2	(4.5)	36
^{153}Eu	2.2	(1.5)	0.77	0.53	(0.69)	10
^{158}Gd	7.9	(4.8)	4.3	2.6	(3.9)	20
^{159}Tb	0.74	(0.47)	0.97	0.62	(0.63)	4.1
^{163}Dy	4.5	(4.1)	2.7	2.5	(3.2)	27
^{165}Ho	0.80	(0.7)	0.79	0.69	(0.57)	7.0
^{166}Er	2.4	(2.3)	1.3	1.2	(1.6)	22
^{169}Tm	0.35	(0.34)§	0.37	0.36	(0.49)	7.1
^{172}Yb	2.6	(2.1)	2.3	1.9	(1.5)	23
^{175}Lu	0.34	(0.3)	0.33	0.29	(0.23)	8.0
^{178}Hf	2.9	(3.4)	1.4	1.6	(3.5)	20
^{181}Ta	4.3	(4.4)	6.6	6.8	(2.9)	3.1
^{182}W	76	(19.4)	14.3	3.7	(1.3)	5.9
^{205}Tl	9.5	(0.103)†	1.1	0.18	(1.03)†	0.07
^{208}Pb	77	(7.1)	260	24	(26.2)	4.0
^{209}Bi	0.21	(0.031)	8.0	1.2	(0.52)	0.5
^{232}Th	12	(9)	12.0	9	(13.5)	4.2
^{238}U	21	(1.8)	26	2.2	(3.3)	0.4

* C_{ref}, literature data, see reference 14.
† From reference 18.
‡ ^{138}Ba was used as internal standard.
§ From reference 17.

these refractory elements were also observed in silicate rocks by the laser ablation technique.[7-9] The enhancement of the signal intensities of these refractory elements was not observed when using the laser ablation technique for standard metallic samples.[9] It is possible that this phenomenon may be attributable to the discriminative ionisation of these elements owing to the relatively high specific exposure of the surface of the microscopic grains to the high temperature plasma in the ICP. These elements may have been segregated or enriched on the surface of the microscopic grains as a secondary effect related to a recrystallisation process of the rock. However, it might be that the phenomenon observed is due to the fact that the metallic elements when in higher oxidation states tend to have a less metallic character.

The possible heterogeneity discussed here might be reduced by the introduction of a halogen or freon gas. These supplementary gases might facilitate sample decomposition and/or the formation of a volatile compound (*e.g.*, a fluoride compound) in a high-temperature plasma. If the high RSFs of the refractory elements such as Mo, W and U were caused by the possible heterogeneity or the incomplete atomisation of the analytes in the plasma, the introduction of these supplementary gases could moderate the high RSFs. However, it would be premature to offer any conclusions on this matter, as other factors such as size distribution of sample powder, sample dispersion rate or the chemical nature of the analyte, have to be taken into consideration.

It is worth noting that the RSFs of JB-1 (basalt) and of JG-1 (granodiorite) were found to be similar as shown in Fig. 4. This similarity of the RSFs between the two different samples implies that the calibration using standard rock samples, the elemental compositions of which are known, is effective in the present spark dispersion - merging sample introduction technique, even if the major chemical composition of the standard rock is very different from that of the sample analysed. This is another possible approach for the semi-quantitative analysis of elements with a wider mass region. In the column headed C_2 of Table 3, the elemental abundances of JG-1, obtained by a calibration using the RSFs of JB-1, are listed. The comparison between the results and reported values are shown in Fig. 5. As can be seen in Fig. 5(*a*), although the deviations of C_1 from C_{ref} were more than ±50%, the deviation of C_2 from C_{ref} could be reduced to below ±30% for almost all the elements [Fig. 5(*b*)]. Thus it has been shown that calibration using a standard rock is a suitable approach to the semi-quantitative analysis of powdered samples. It should be noted that JB-1 (basalt) and JG-1 (granodiorite) are different types of rocks having different matrix components. However, despite the differences in the matrices, the RSFs of the elements in JG-1 were effectively corrected by those of JB-1.

Although the calibration using a matrix-matched standard was naturally expected to improve the accuracy of a measurement, the practical limitation of the accuracy was related to the drift in sample loading rather than the difference in the

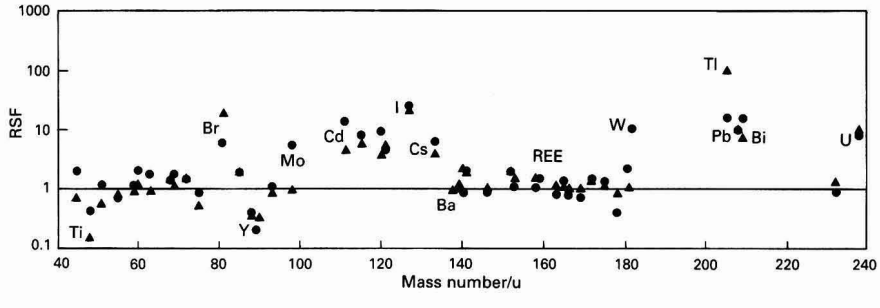

Fig. 4. Plot of value of RSF *versus* mass number. ▲, RSFs of JB-1 and ●, RSFs of JG-1

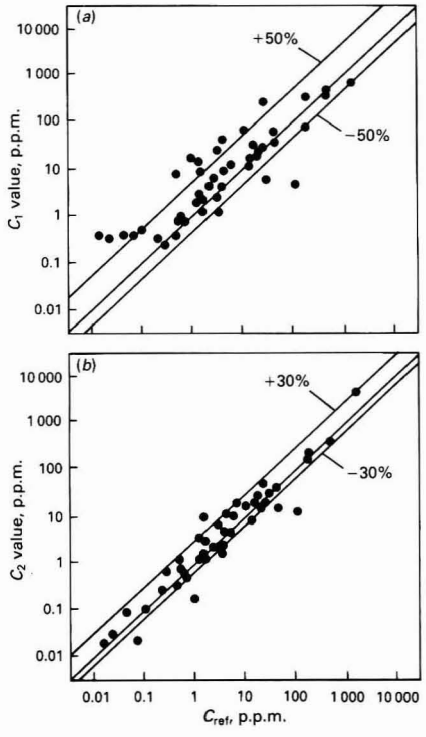

Fig. 5. Plot of analytical results of JG-1 obtained by the proposed spark dispersion - merging sample introduction technique *versus* reported values (C_{ref}): (*a*) C_1 was calculated assuming that all the isotopes have the same sensitivity as ^{138}Ba; and (*b*) C_2 was calibrated using JB-1 as a standard

matrix elements. Therefore, not only the use of a matrix matched standard for calibration, but also the control of the particle size and the adoption of a new sample loading - evacuation system as discussed earlier, would be desirable in order to improve the accuracy of the analytical results.

Calibration using a standard solution introduced by nebulisation was thought to be another effective approach for semi-quantitative analysis. However, the RSFs obtained when using a standard solution show a uniform value compared with those obtained by the direct introduction of a solid standard. Therefore, when calibrated using a standard solution, the resultant abundances of some of the volatile elements were very different from those reported previously. Although calibration using a standard solution can be a versatile technique for the semi-quantitative analysis of powdered samples, great care must be taken to avoid erroneous results for some volatile elements.

Detection Limit

The detection limits were defined as the concentration of analytes corresponding to three times the standard deviation (3σ) of the background count rates. In the calculation, the RSFs of JB-1 were used. The detection limits obtained using the proposed technique are summarised in Table 3. As shown, the elements which have larger RSFs give lower detection limits. A detection limit of better than 100 ng g^{-1} could be obtained for almost all the elements, and detection limits of better than 30 ng g^{-1} for some heavy elements. Absolute detection limits of better than 100 pg could be obtained for most elements, when the amount of sample loaded was 1 mg.

Conclusion

Rapid isotopic and elemental analyses with high sensitivity can be performed on rock samples by ICP-MS combined with spark dispersion - merging sample introduction. Calibration using a standard powdered sample is very effective for semi-quantitative analysis of over 40 elements with a relative standard deviation of less than 30%. The detection limits of most of the elements are better than 100 ng g^{-1}.

It is expected that the spark dispersion - merging sample introduction technique will promote the further progress of the wider applications of semi-quantitative and rapid multi-element analyses. Finally, the proposed technique is applicable not only to ICP-MS, but also to ICP atomic emission spectrometry (ICP-AES).

This work was supported in part by a Grant-in-Aid for Scientific Research from the Ministry of Education, Science and Culture, Japan.

References

1. Houk, R. S., Fassel, V. A., Flesch, G. D., Svec, H. J., Gray, A. L., and Taylor, C. E., *Anal. Chem.*, 1980, **52**, 2283.
2. Houk, R. S., Svec, H. J., and Fassel, V. A., *in* Price, D., and Todd, J. F. J., *Editors*, "Dynamic Mass Spectrometry," Volume 6, Heyden, London, 1981, p. 234.
3. Gray, A. L., and Date, A. R., *in* Price, D., and Todd, J. F. J., *Editors*, "Dynamic Mass Spectrometry," Volume 6, Heyden, London, 1981, p. 252.
4. Date, A. R., and Gray, A. L., *Analyst*, 1983, **108**, 1033.
5. Gray, A. L., *in* Adams, F., Gijbels, R., and Grieken, R. V., *Editors*, "Inorganic Mass Spectrometry," Wiley, New York, 1988, p. 257.
6. Gray, A. L., *Analyst*, 1985, **110**, 551.
7. Arrowsmith, P., *Anal. Chem.*, 1987, **59**, 1437.
8. Mochizuki, T., Sakashita, A., Iwata, H., Kagaya, T., Shimamura, T., and Blair, P., *Anal. Sci.*, 1988, **4**, 403.
9. Hager, J. W., *Anal. Chem.*, 1989, **61**, 1243.
10. Jiang, S.-J., and Houk, R. S., *Anal. Chem.*, 1986, **58**, 1739.
11. Jiang, S.-J., and Houk, R. S., *Spectrochim. Acta, Part B*, 1987, **42**, 93.
12. Williams, J. G., Gray, A. L., Norman, P., and Ebdon, L., *J. Anal. At. Spectrom.*, 1987, **2**, 469.
13. Hirata, T., Akagi, T., Shimizu, H., and Masuda, A., *Anal. Chem.*, 1989, **61**, 2263.
14. Govindaraju, K., *Geostand. Newsl.*, 1984, **VIII**, Special Issue.
15. Hirata, T., Shimizu, H., Akagi, T., Sawatari, H., and Masuda, A., *Anal. Sci.*, 1988, **4**, 637.
16. Toyoda, K., and Haraguchi, H., *Bull. Chem. Soc. Jpn.*, 1987, **60**, 933.
17. Potts, P. J., and Rogers, N. W., *Geostand. Newsl.*, 1986, **10**, 121.
18. Saito, T., Shimizu, H., and Masuda, A., *Geochem. J.*, 1987, **21**, 237.

Paper 0/00668H
Received February 13th, 1990
Accepted June 21st, 1990

Chemical Analysis of Impurities in Zirconia and Aluminium Nitride Ceramics by Inductively Coupled Plasma Atomic Emission Spectrometry

Charo Martínez-Lebrusant and Flora Barba
Instituto de Cerámica y Vidrio, CSIC., Arganda del Rey, 28500 Madrid, Spain

Inductively coupled plasma atomic emission spectrometry (ICP-AES) has been used for the determination of the most significant impurities (Al, Ca, Fe, Mg, P, Si and Ti) in zirconia and aluminium nitride ceramics according to the following procedure: (*i*) development of two decomposition methods for each material; (*ii*) study of spectral interferences, matrix and interelemental effects; and (*iii*) determination of the detection limits. Good precision and accuracy were attained. The procedures developed in this work can be applied to zirconia partially stabilised by the addition of CaO, MgO or Y_2O_3, tetragonal zirconia polycrystals with the addition of Y_2O_3, pure aluminium nitride or aluminium nitride with additions of alkaline earth oxides, Y_2O_3 or CeO_2.

Keywords: *Inductively coupled plasma atomic emission spectrometry; aluminium nitride ceramic; zirconia ceramic*

Few materials show as much potential as advanced ceramics. They are suitable for high-temperature engineering, electric and electronic applications.[1,2] The purity requirements for advanced ceramics are increasingly exacting owing to the dramatic effect of impurities on the physical properties of the resultant products.[3] The impurities tend to form a glassy grain boundary phase at high temperatures which results in poor mechanical performance and low creep resistance in structural ceramics. In electronic ceramics the effect of impurities is even more drastic, *e.g.*, d.c. conductivity, resistivity *versus* temperature and dielectric constant can be affected by the impurities.

For this reason, there is an increasing demand for more accurate and rapid methods of analysis. However, in the literature there is very little data available on the analysis of these materials. Flame-excited atomic absorption spectrometry was used for the analysis of zirconias,[4] however, owing to the purity of these materials this technique is not suitable. The colorimetric determination reported by Kruidhof[5] presents a lot of difficulties. A high-resolution inductively coupled plasma atomic emission spectrometric method was developed by Ishii and Satoh.[6] They only determined hafnium in high-purity zirconium oxide, the dissolution of the sample was achieved with mixtures of ammonium sulphate and concentrated sulphuric acid. This dissolution method is only appropriate for less resistant zirconia materials.

In the present work a procedure involving inductively coupled plasma atomic emission spectrometry (ICP-AES) has been developed for the determination of impurities (Al, Ca, Fe, Mg, P, Si and Ti) in the following types of advanced ceramics: (*i*) oxide ceramics (zirconia stabilised with Y_2O_3, CaO or MgO) and (*ii*) non-oxide ceramics (pure aluminium nitride or with additions of alkaline earth oxides, Y_2O_3 or CeO_2).

Experimental

Apparatus and Operating Conditions

A Jobin-Yvon Model JY-38 VHR sequential spectrometer with a high-resolution monochromator was used (Table 1). The specifications of the ICP source and operating conditions are reported in Table 2.

Table 1. Specification of the atomic emission spectrometer

Mounting	1 m crossed Czerny - Turner
Grating	3600 grooves mm^{-1}
Wavelength range	175–490 nm
Entrance slit	30 μm
Exit slit	30 μm
Photomultiplier	Hamamatsu R446

Table 2. Specification of ICP source and operating conditions

Radiofrequency generator	Durr-JY 3832
Frequency	56 MHz (+ 0.05%)
Output power	2.2 kW
Induced power	1.6 kW
Reflected power	<5 W
Pump	Peristaltic P.S. Analytical (2.1 ml min^{-1})
Nebuliser	Meinhard, TR-C2-30, pneumatic
Operating conditions—	
Outer argon flow-rate	16 l min^{-1}
Carrier argon flow-rate	0.5 l min^{-1}
Coating argon flow-rate	0.4 l min^{-1}

Chemicals

The stock standard solutions were prepared by dissolving the pure metals, oxides or salts (99.9–99.99%). The oxides Fe_2O_3, MgO, Y_2O_3, $CaCO_3$ and TiO_2 were dissolved in hydrochloric acid; Al_2O_3 was decomposed by fusion with Na_2CO_3 + $Na_2B_4O_7$ and dissolved in hydrochloric acid; SiO_2 was decomposed by fusion with Na_2CO_3 and dissolved in distilled water; and $(NH_4)_2Ce(NO_3)_6$ and $ZrOCl_2$ were dissolved in distilled water.

Samples

An oxide ceramic [zirconia stabilised with Y_2O_3 (Y-TZP)] and a non-oxide ceramic (aluminium nitride) were chosen for this work.

Sample Preparation

Two types of decomposition methods (acid attack and alkali fusion) were used to achieve complete dissolution of the samples.[7]

Method A

The sample (200.0 mg) is fused with 2.00 g of a mixture of Na_2CO_3 + $Na_2B_4O_7$ (11 + 5 moles = 53.68 + 46.32% m/m) in

a platinum crucible, and subsequently heated on a Meker burner for 15 min at 1100 °C. The cooled melt is dissolved in 50 ml of (1 + 1) hydrochloric acid and the solution diluted to 100 ml with distilled water.

Method B

This method is based on the work of Ishii and Satoh.[6] In a 100-ml beaker 200.0 mg of sample are weighed and 10 ml of concentrated H_2SO_4 and 3.5 g of $(NH_4)_2SO_4$ are added. After covering the beaker with a watchglass, the mixture is heated until SO_3 fumes appear. After cooling, the solution is diluted with distilled water in a 100-ml calibrated flask.

Method C

The sample (200.0 mg) is heated with 5 ml of concentrated HCl in a polytetrafluoroethylene (PTFE) pressure vessel[8] at 160 °C for 12 h. After cooling, the solution is diluted with distilled water and transferred carefully into a 100-ml calibrated flask.

Preparation of Standards and Calibration

Pure aqueous solutions were used for the determination of detection limits at the five wavelengths selected for each element (Table 3).

The standards used to obtain the detection limits (of the impurities in the samples) contained the reagents and the macroconstituents (ZrO_2, 2000 μg ml^{-1} or Al, 1200 μg ml^{-1}).

The calibration graphs for the analytes were obtained using a blank solution and a standard of appropriate concentration

Table 3. Spectral lines, ratio of the net signal to background signal (S/B) and detection limits in pure aqueous solutions

Oxide*	λ/nm	S/B	DL/ng ml^{-1}
Al_2O_3 (10) ..	396.152	39.1	10
	309.278	43.5	12
	394.401	21.5	21
	308.215	17.6	28
	237.324	9.9	100
CaO (0.5) ..	396.847	105.9	0.3
	393.366	208.1	0.8
	422.673	1.8	0.9
	315.887	1.9	33
	317.933	0.8	70
Fe_2O_3 (10) ..	259.940	85.8	7.4
	238.204	66.8	7.6
	239.562	48.1	12
	240.488	25.2	27
	261.187	37.2	45
MgO (1) ..	280.270	60.7	0.5
	279.553	110.1	1.8
	285.213	11.5	13
	383.826	0.8	57
	279.806	0.9	114
P_2O_5 (100) ..	213.618	38.7	97
	213.547	5.3	114
	214.914	24.1	178
	253.565	10.2	433
	255.388	4.5	745
SiO_2 (100) ..	251.611	316.1	24
	252.851	119.8	26
	251.432	104.9	26
	250.690	141.6	47
	228.158	167.2	60
TiO_2 (10) ..	334.941	499.1	0.5
	337.280	285.4	0.9
	323.452	323.6	1.2
	336.121	268.4	1.9
	368.520	206.2	1.9

* The concentration of aqueous solutions (μg ml^{-1}) is indicated in parentheses.

Table 4. Spectral interferences on the selected lines for impurities

Element	λ/nm	Interferences
Al	396.152	Interference from the Zr II 396.16-nm line and increase in emission background with Ca
	309.278	OH band
	394.401	Little interference from the Zr II 394.34-nm and Zr II 394.38-nm lines and an increase in emission background with Ca
	308.215	OH band
	237.324	Zr II 237.30-nm line interference
Fe	259.940	Increase in emission background with Zr
P	213.618	Increase in the background with Zr II 213.56 and 213.68-nm lines and Al

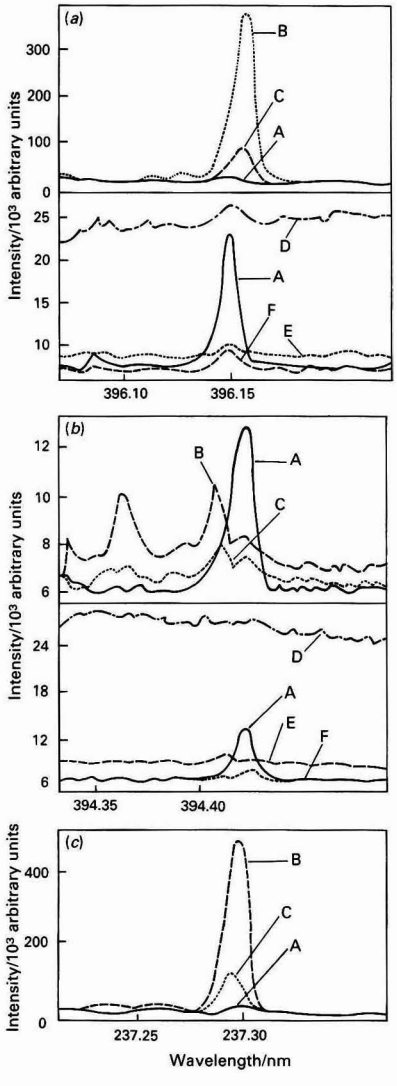

Fig. 1. Spectral scans in the vicinity of wavelengths (*a*) Al I 396.152 nm, (*b*) Al I 394.401 nm, and (*c*) Al I 237.324 nm; A, 0.2 μg ml^{-1} Al_2O_3; B, 2000 μg ml^{-1} ZrO_2; C, 200 μg ml^{-1} ZrO_2; D, 200 μg ml^{-1} CaO; E, 20 μg ml^{-1} CaO; and F, 1 μg ml^{-1} CaO

with the exception of Al_2O_3 where two standard solutions were used. These solutions were prepared matrix-matched with the decomposition reagents.

Results and Discussion

Evaluation of Sample Decomposition Methods

The fusion method with Na_2CO_3 + $Na_2B_4O_7$ is effective for both samples (zirconia and AlN).

Decomposition with $(NH_4)_2SO_4$ is useful because of its rapidity and the purity of the reagents required. Following this method, only the Y-TZP is completely dissolved.

Acid attack with HCl in a PTFE reaction vessel introduces the lowest salt content. However, this procedure can only be applied to AlN materials.

Selection of Analytical Lines

Five wavelengths were selected for each element on the basis of their sensitivity.[9,10] The ratio of net analyte intensity to background intensity and the detection limits under operating conditions, defined previously, were determined. In Table 3 the wavelengths are indicated in order of increasing detection limit. These data are very useful because this order of wavelengths does not agree with the literature.

Spectral Interferences

A study of spectral interferences was carried out. This study started on the lowest detection limit (DL) line of each analyte until one free from spectral interferences or with easily controlled interferences was found.

Spectral scans were performed in the vicinity of each wavelength with analyte solutions close to ten times the detection limits, 20 μg ml^{-1} solutions of each impurity, 200 μg ml^{-1} solutions of additive (CaO, CeO_2, MgO, HfO_2 and Y_2O_3) and 2000 μg ml^{-1} solutions of ZrO_2 and Al_2O_3. The interferences detected are given in Table 4 and in Figs. 1, 2 and 3.

It has been found that, at Al I 396.152 nm and 394.401 nm; Fe II 259.940 nm; and P I 213.618 nm, where an increase in emission background occurs, the net intensity of the analyte remains constant with and without the interferent element. The background correction was obtained at a point where the emission background remains constant in practice.

The Al I 394.401-nm line had to be used for the determination of aluminium in zirconia materials because it is subject to little spectral interference.

The inter-element correction factor for Zr on the Al I 394.401-nm line was determined. The real concentration of Al_2O_3 was obtained according to the equation

$$c_{r_{Al}} = c_{app_{Al}} - \alpha c_{Zr}$$

where $c_{r_{Al}}$ is the real concentration of alumina, $c_{App_{Al}}$ the apparent concentration of alumina, c_{Zr} the concentration of zirconia and α the inter-element correction factor.

In order to determine this factor a series of standard solutions (0, 500, 1000, 1500 and 2000 μg ml^{-1} of ZrO_2) with 0.2 μg ml^{-1} of Al_2O_3 were prepared. The concentration of $Al_2O_3(c_{app_{Al}} - c_{r_{Al}})$ *versus* the concentration of ZrO_2 is a straight line graph with slope $\alpha = 1.4 \times 10^{-5}$ (inter-element correction factor), Fig. 4.

The valid spectral lines used to perform the chemical analyses in these materials are listed in Table 5.

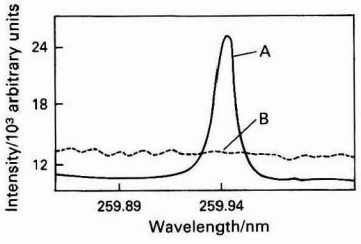

Fig. 2. Spectral scans in the vicinity of the Fe II 259.940-nm line. A, 0.2 μg ml^{-1} Fe_2O_3; and B, 2000 μg ml^{-1} ZrO_2

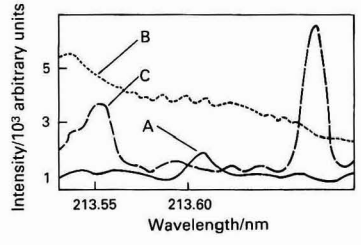

Fig. 3. Spectral scans in the vicinity of the P I 213.618-nm line. A, 1 μg ml^{-1} P_2O_5; B, 2000 μg ml^{-1} Al_2O_3; and C, 2000 μg ml^{-1} ZrO_2

Table 5. Spectral lines suitable for analysis of impurities and detection limits. Values represent concentration (μg g^{-1} and μg ml^{-1}) in the samples

	Y-TZP				AlN			
	Method A		Method B		Method A		Method C	
Impurity (wavelength)	μg g^{-1}	μg ml^{-1}	μg g^{-1}	μg ml^{-1}	μg g^{-1}	μg ml^{-1}	μg g^{-1}	μg ml^{-1}
Al_2O_3 (394.401 nm)	3	6×10^{-3}	3	6×10^{-3}	—	—	—	—
CaO (396.847 nm)	0.15	3×10^{-4}	0.04	8×10^{-5}	0.05	1×10^{-4}	0.03	7×10^{-5}
Fe_2O_3 (259.940 nm)	2	4×10^{-3}	1.5	3×10^{-3}	2	4×10^{-3}	1	2×10^{-3}
MgO (280.270 nm)	0.15	3×10^{-4}	0.2	4×10^{-4}	0.05	1×10^{-4}	0.05	1×10^{-4}
P_2O_5 (213.618)	355	71×10^{-2}	195	29×10^{-2}	310	62×10^{-2}	125	25×10^{-2}
SiO_2 (251.611 nm)	6.5	13×10^{-3}	6	12×10^{-3}	6.5	13×10^{-3}	5.5	11×10^{-3}
TiO_2 (334.941 nm)	1.9	38×10^{-4}	1.65	33×10^{-4}	0.5	10×10^{-4}	0.25	5×10^{-4}

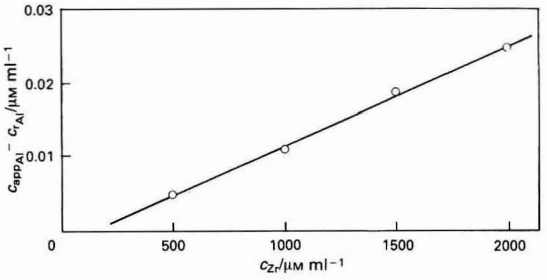

Fig. 4. Graph for the determination of the zirconium inter-element correction factor on the Al I 394.401-nm line. Slope, $\alpha = 1.4 \times 10^{-5}$

Matrix Effect

It was found that the use of hydrochloric acid in the dissolution of the aluminium nitride gives rise to a decrease in signal. This effect is more important when the mixtures $(NH_4)_2SO_4$ - H_2SO_4 or Na_2CO_3 - $Na_2B_4O_7$ are used. The effect of macroconstituents is negligible compared with the effect of decomposition reactants in the determination of trace impurities, hence the standard solutions were prepared as above.

Detection Limits

The detection limits were calculated as the concentration equivalent to 3σ of that measured on the background signal.

The results obtained by the different decomposition methods are given in Table 5.

The results obtained with the acid attack (methods B and C) are slightly lower than those obtained with the fusion method. The values for the AlN sample, decomposed with HCl (method C), are the lowest because of the reagent employed.

The results indicate that the determination of Al_2O_3, CaO, MgO, Fe_2O_3, SiO_2 and TiO_2 is feasible using ICP-AES. The detection of P_2O_5 is only possible when it is present in significant amounts.

Chemical Analysis

Five Y-TZP and AlN samples were analysed. The average of the results using the decomposition methods defined above and the standard deviation are summarised in Table 6.

There is good agreement between the results of the chemical determination obtained with the two decomposition methods for each sample.

The standard deviation values indicate good precision. Phosphorus pentoxide can not be detected in AlN material.

Accuracy

Unfortunately, standard reference materials are not available and it is difficult to compare the results obtained using different methods because of the reasons indicated in the introduction.

In this work the accuracy was obtained by adding known amounts of each element (approximately the same amount that would naturally be present) at the sample dissolution stage.

Table 6. Determination of the most significant impurities in Y-TZP and AlN. Values represent concentration (as %) and standard deviation in parentheses

	Y-TZP		AlN	
Impurity	Method A	Method B	Method A	Method C
Al_2O_3 ..	0.56 (0.01)	0.53 (0.02)	—	—
CaO	0.0012 (0.0007)	0.0010 (0.0005)	0.021 (0.003)	0.019 (0.005)
Fe_2O_3 ..	0.017 (0.001)	0.014 (0.001)	0.037 (0.007)	0.040 (0.008)
MgO	0.0021 (0.0003)	0.0017 (0.0006)	0.004 (0.006)	0.004 (0.005)
P_2O_5	0.053 (0.008)	0.052 (0.006)	ND*	ND*
SiO_2	0.12 (0.05)	0.11 (0.03)	0.052 (0.006)	0.057 (0.008)
TiO_2	0.075 (0.001)	0.075 (0.002)	0.011 (0.005)	0.013 (0.007)

* ND: not detected.

The accuracy of the results for the elements is between 95 and 105% for decomposition by Method A and between 97 and 103% for decomposition by Methods B and C., *i.e.*, the accuracy of the results obtained by the different decomposition methods for the samples is similar.

Conclusion

The results obtained in the present investigation support ICP-AES as an appropriate technique for the determination of the most important impurities (Al_2O_3, CaO, Fe_2O_3, MgO, SiO_2 and TiO_2) in zirconia and aluminium nitride ceramics. The determination of P_2O_5 is only possible when a significant concentration is present.

The procedures developed are rapid and present good precision and accuracy. Application to zirconia partially stabilised by CaO, MgO and Y_2O_3, tetragonal zirconia polycrystals with the addition of Y_2O_3 to pure aluminium nitride or to aluminium nitride with additions of alkaline earth oxides, Y_2O_3 or CeO_2 is possible

References

1. Billy, M., and Mexmain, J., *World Ceramics*, 1985, 2.
2. Clough, D. J., *Ceram. Eng. Sci. Proc.*, 1985, **6**, 1244.
3. Keler, E. K., and Andreeva, A. B., *Ogneupory*, 1958, **23**, 552.
4. Bastius, H., *Ceram. Forum. Int.*, 1984, 61, 3, 140.
5. Kruidhof, H., *Anal. Chim. Acta*, 1978, **99**, 193.
6. Ishii, H., and Satoh, K., *Talanta*, 1982, **29**, 243.
7. Fariñas, J. C., Martinez, M. R., and Barba, M. F., "Actas del II Congreso Iberoamericano de Cerámica, Vidrio y refractarios," Buenos Aires (Argentina), 1988, in the press.
8. Bernas, B., *Anal. Chem.*, 1968, **40**, 1682.
9. Boumans, P. W. J. M., *Spectrochim. Acta, Part B*, 1981, **36**, 169.
10. Brenner, I. B., Eldad, H., *ICP Inf. Newsl.*, 1984, 10, 6, 451.

Paper 0/00786B
Received February 20th, 1990
Accepted June 6th, 1990

Analysis of Organic Residues of Archaeological Origin by High-temperature Gas Chromatography and Gas Chromatography - Mass Spectrometry

Richard P. Evershed, Carl Heron and L. John Goad
Department of Biochemistry, University of Liverpool, P.O. Box 147, Liverpool L69 3BX, UK

Organic residues are extracted from materials of archaeological interest by solvent extraction and subjected directly to high-temperature gas chromatography (GC) and gas chromatography - mass spectrometry (GC - MS). The use of high-temperature GC allows intact acyl lipids, *e.g.*, triacylglycerols, diacylglycerols, monoacylglycerols and wax esters, to be analysed without prior degradation (*e.g.*, saponification) to release constituent fatty acids and alcohols. Trimethylsilylation is employed to block protic sites in free fatty acids and hydroxylated components. The data obtained from temperature programmed GC and GC - MS analyses, employing immobilised apolar (dimethyl polysiloxane type) stationary phases, provide essential compositional information that would be lost if the more conventional degradative approach to acyl lipid analysis was adopted.

Keywords: *High-temperature gas chromatography; mass spectrometry; lipid; archaeology; sherd*

There is an increasing amount of evidence to show that chemical analyses of the organic constituents from a wide variety of materials of archaeological interest can yield important information concerning past cultural and economic activities. Analysis has covered a broad spectrum of remains, including soils,[1,2] midden dumps,[3] human remains,[4–7] and other artefacts, particularly pottery containers.[8–10]

Ceramics are the major loci for the survival of residual organic matter either absorbed into the porous micro-structure of the fired clay wall or preserved in visible surface deposits. A recent investigation has shown that possible post-depositional diagenetic effects, such as contamination arising from migration of soil components, or compositional alterations through microbial activity, are minimal for lipids absorbed in potsherds.[11] Hence, these lipid residues are a direct reflection of the original contents and usage of ceramic vessels. Positive identification provides an important research area for the classification of artefact use, determined by food preparation and consumption, and by other economic, manufacturing and technological activities. The realisation of these opportunities necessitates a rapid, but informative means of study of a large number of pottery vessels.[12]

Lipids in particular are well preserved in favourable environments and have potential for use in the classification of biogenic organic matter on chemotaxonomic and biosystematic grounds. Until now, investigations of lipid constituents of archaeological materials have relied on methodologies that either do not make best use of the compositional information available, or are too time consuming to be applied to the processing of the large number of samples necessary to afford information of use to archaeologists.

We describe herein the use of high-temperature gas chromatography (GC) and gas chromatography - mass spectrometry (GC - MS) techniques in the analysis of total lipid extracts from archaeological materials. These techniques have been employed in the investigation of extracts of archaeological materials from widely varying contexts, *e.g.*, soils, peat bogs and hominid remains. However, for the purposes of this paper we will illustrate the use of these techniques in assessing the composition of lipids extracted from ceramic pot sherds.

Experimental

Materials

All solvents used were of AnalaR or HPLC grade and distilled before use. Disposable screw-topped glass vials (15 ml) were used for extractions to eliminate the possibility of cross-contamination. All other glassware was rinsed with concentrated nitric acid, de-ionised water and organic solvent before use.

Samples

Freshly excavated ceramic potsherds were obtained from the Raunds Area Project (RAP), an extensive archaeological study of a multi-period landscape in the Nene Valley, Northamptonshire, UK.[13] Sherds (5–200 g) were stored in brown paper envelopes in a deep freeze (−20 °C) until required for investigation.

Lipid Extraction

Fragments of sherd (2 g) were freed from adhering soil by scraping with a scalpel blade. The sherd was then ground to a fine powder in a de-greased pestle and mortar. Following transfer into a 15-ml glass vial and addition of a known amount of internal standard (10 or 50 μg of heptadecane), the powdered sherd was extracted by ultrasonication (2 × 15 min) with a mixture of chloroform and methanol (2 + 1; 2 × 10 ml). After each extraction, the solvent extract was freed from suspended particulate matter by centrifugation, decanted into a round-bottomed flask and reduced to a small volume by rotary evaporation. After decanting into a small, pre-weighed screw-topped vial (0.5 dram) the remaining extraction solvent was removed under a gently blown stream of dry nitrogen. The dried extracts were stored in a deep freeze (−20 °C) until required for GC and GC - MS analysis.

Trimethylsilylation

Trimethylsilyl (TMS) ether and ester derivatives were prepared by treating (60 °C, 10 min) aliquots (*ca.* 50 μg) of the total lipid extracts with an excess of *N,O*-bis(trimethylsilyl)-trifluoroacetamide.

Gas Chromatography

The GC analyses were performed on a Hewlett-Packard 5890A gas chromatograph connected to a Hewlett-Packard 3396A computing integrater/plotter. Samples were introduced by on-column injection into a 60 cm × 0.32 mm i.d. retention gap (de-activated polyimide clad fused silica, Phase Separations) connected to the analytical column via a light-weight glass-lined stainless-steel union of 0.8 mm i.d. (S.G.E.). The

analytical column was an aluminium or polyimide clad 12 m × 0.22 mm i.d. fused-silica capillary coated with BP-1 stationary phase (immobilised dimethyl polysiloxane, OV-1 equivalent 0.1 mm film thickness, S.G.E.). Helium was used as the carrier gas at a column head pressure of 20 lb in^{-2}, producing a linear flow velocity (u) of *ca.* 100 cm s^{-1}. Temperature programming was from 50 to 350 °C at 10 °C min^{-1} following a 2-min isothermal hold at 50 °C after injection. At the end of the temperature programming the GC oven was kept at 350 °C for 15 min. Flame-ionisation detection was used to monitor the column effluent.

Gas Chromatography - Mass Spectrometry

The GC - MS analyses were performed on a Pye Unicam 204 GC equipped with an S.G.E. OCI III on-column injector. The chromatograph was linked to a VG 7070H double-focusing magnetic-sector mass spectrometer. Data acquisition and processing were on a Finnigan INCOS 2300 data system. An Opus PC V personal computer equipped with Finnigan DataMaster software was linked to the INCOS to provide an additional data-processing facility. The GC - MS interface was modified to allow heating to >350 °C as described elsewhere.[14,15] The mass spectrometer was operated in the electron-ionisation mode (70 eV) while maintaining an ion source block temperature of *ca.* 300 °C. An acceleration voltage of 4 kV was used in scanning the m/z range 40–700 in a total scan cycle time of 3 s.

Results and Discussion

Lipid extracts of plant and animal tissues are complex mixtures of fatty carboxylic acids, sterols, acyl lipids, etc. In the archaeological context the composition of lipid mixtures will be altered, not only through the natural effects of decay,[16,17] but also as a result of cooking[18] and manufacturing[19] processes. Despite this, chemical analysis of organic residues has the potential to yield much useful information concerning the nature of dietary constituents and manufacturing raw materials.

Many analyses of organic residues of archaeological interest performed up to now have employed techniques, *e.g.*, thin-layer chromatography[18] and infrared spectrophotometry,[20] which lack the specificity and sensitivity necessary to characterise complex lipid mixtures effectively.[20] (For a comparison of analytical techniques applied to archaeological residues see reference 21.) Although GC has been employed previously in the study of lipid extracts of archaeological materials, the adopted approach has generally involved fractionation by adsorption chromatography (*i.e.*, column or thin-layer chromatography), then saponification to release fatty acids from complex acyl lipids. Following conversion into their methyl ester derivatives, GC has then been employed to assess the fatty acid composition (*e.g.*, reference 8).

Notable disadvantages of this above approach include: (*i*) the time-consuming nature of the overall procedure which seriously limits its usefulness in the processing of the very great numbers of samples produced from archaeological excavations; (*ii*) the destruction of the integrity of the original extract by saponification of the complex acyl lipids which removes valuable compositional information; and (*iii*) unnecessary "wet chemical" treatments of small amounts of, often irreplaceable, archaeological residues which increases the possibility of introducing contamination.

In the light of these shortcomings and in answer to the demands of our current archaeological investigations, an approach based on high-temperature GC and GC - MS has been adopted for the analysis of complex lipid extracts. By employing flexible fused-silica capillary columns coated with thin films (0.1 μm) of immobilised apolar (OV-1 type) stationary phase, it is possible to analyse complex lipid extracts, without pre-fractionation, with the only wet chemical

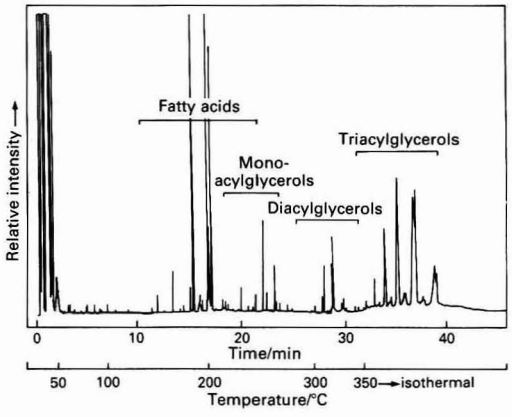

Fig. 1. High-temperature GC analysis of the total lipid extract of a sherd recovered from an Early Medieval ditch. Only the retention windows for the most prominent compound classes are marked. Peak assignments were subsequently made by high temperature GC - MS as shown in Fig. 2. See under Experimental for full details

treatment involved being trimethylsilylation of protic sites. The lack of sample clean-up obviously raises questions of contamination of the capillary GC column that would lead to loss of chromatographic performance. With this in mind a retention gap is used as a pre-column to protect the valuable analytical column. Chromatographic performance is monitored by periodic analysis of a mixture of authentic lipids. The retention gap is simply replaced when any loss of chromatographic performance is observed.

Fig. 1 shows the chromatogram obtained for the total lipid extract of an Early Medieval cooking vessel and serves to demonstrate the effectiveness of this analytical approach for the profiling of lipid extracts. The high resolution of these capillary columns means that even with such highly complex mixtures the majority of the key components are adequately resolved in a single analytical run. The high-temperature stability and thin-film thickness of the stationary phase permits the analysis of substances with Kovats' retention indices approaching 6000, thereby allowing the determination of a wide range of complex acyl lipids, including high carbon number triacylglycerols (up to at least C_{56}). As the lipid extracts commonly encountered consist of compounds of wide-ranging volatility, on-column injection is used to avoid problems of discrimination between components of high and low boiling-point.

Preliminary compound identifications are based on comparisons of GC retention times with those of authentic compounds and elution orders of homologous components. This analytical approach is similar to that described for use in the clinical profiling of total lipids from plasma.[22–24] Divergence from the clinical approach is necessary, owing to the often greater diversity and complexity of the lipid extracts encountered in this archaeological work. Most notable is the heavy reliance placed on high-temperature GC - MS to make confident peak assignments. Additionally, the lack of intact phospholipids in the archaeological extracts removes the need for the phospholipase C incubation step required in preparing clinical samples for high-temperature GC analysis.

The addition of a known amount of an internal standard during the sample work-up procedure allows quantitative assessment of the individual eluting components, based on simple comparisons of GC peak areas determined by electronic integration. The amounts of internal standard can be varied according to the demands of particular analyses. Quantitative analyses of this nature were employed recently to good effect in the comparison of the lipid content of buried sherds and adhering burial soil.[11]

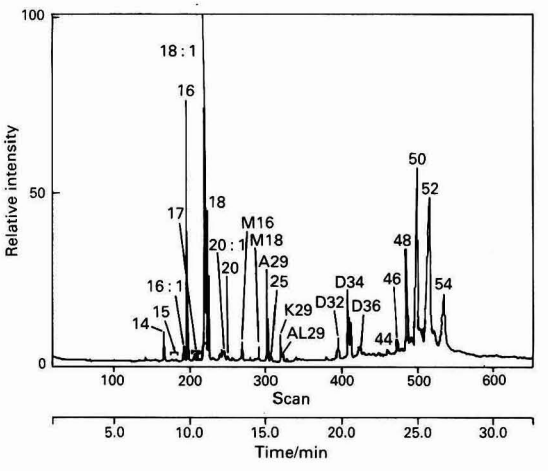

Fig. 2. Total ion current (TIC) chromatogram obtained from high-temperature GC - MS analysis of the same total lipid extract analysed by GC in Fig. 1. Peak identities: 14–18, 20 and 25, saturated fatty acids (determined as their TMS esters) containing 14–18, 20 and 25 acyl carbons, respectively; 16:1, 18:1 and 20:1, mono-unsaturated fatty acids (determined as their TMS esters) containing 16, 18 and 20 acyl carbon atoms, respectively; M16 and M18, monoacylglycerols (determined as their bis-TMS ethers) containing 16 and 18 acyl carbon atoms, respectively; D32, D34 and D36, diacylglycerols (determined as their TMS ethers) containing 32, 34 and 36 acyl carbon atoms, respectively; 44, 46, 48, 50, 52 and 54, triacylglycerols containing 44, 46, 48, 50, 52 and 54 acyl carbon atoms, respectively; A29, nonacosane; K29, nonacosan-15-one; and AL29, nonacosan-15-ol. See under Experimental for full details

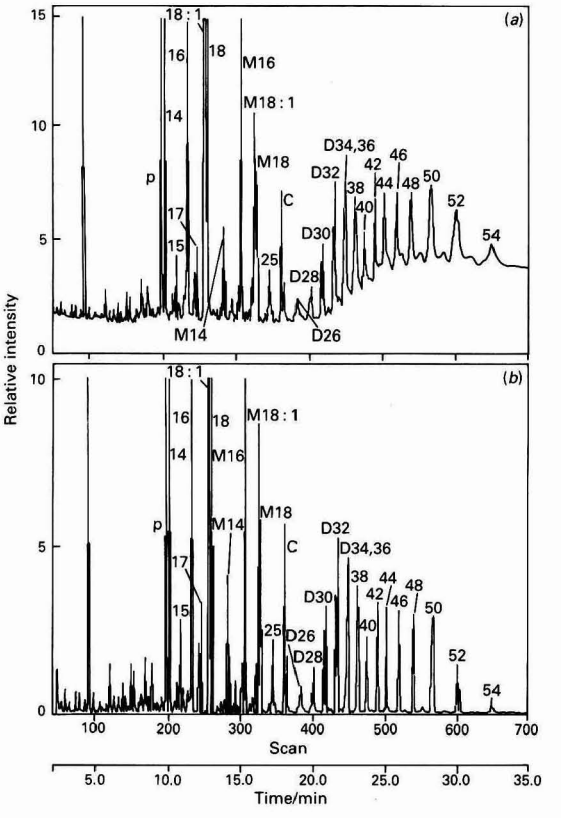

Fig. 3. (*a*) TIC chromatogram and (*b*) Biller - Biemann enhanced mass resolved TIC for the total lipid extract of a sherd recovered from a Late Saxon ditch. Peak identities: 14–18 and 25, saturated fatty acids (determined as their TMS esters) containing 14–18 and 25 acyl carbon atoms, respectively; 18:1, a mono-unsaturated fatty acid (determined as its TMS ester) containing 18 acyl carbon atoms; M14, M16 and M18, monoacylglycerols (determined as their bis-TMS ethers) containing saturated acyl moieties with 14, 16 and 18 carbon atoms, respectively; M18:1, a monoacylglycerol (determined as its bis-TMS ether) bearing a mono-unsaturated 18 carbon atom acyl moiety; D26, D28, D30, D32 and D34, diacylglycerols (determined as their TMS ethers) containing 26, 28, 30, 32 and 34 acyl carbon atoms, respectively; 36, 38, 40, 42, 44, 46, 48, 50, 52 and 54, triacylglycerols containing 36, 38, 40, 42, 44, 46, 48, 50, 52 and 54 carbon atoms, respectively; C, cholesterol (as its TMS ether derivative); and P, a phthalate plasticiser impurity probably arising from a vial cap. See under Experimental for full details

Fig. 2 shows the total ion current (TIC) chromatogram obtained by high-temperature GC - MS analysis of an aliquot of the same sample submitted to GC analysis (as in Fig. 1). The resolution of the peaks in the TIC chromatogram is largely comparable to the data obtained by GC, with flame-ionisation detection, so confirming that the performance of our modified GC - MS interface for the analysis of lipids of wide-ranging volatility is acceptable. Some loss of GC peak resolution is inevitable owing to the relatively slow scan cycle time (typically, 3 s) of our mass spectrometer. This problem would be largely eliminated if analyses were performed on a modern fast-scanning instrument. In addition to confirming identifications based on GC retention behaviour alone, GC - MS is readily able to deconvolute peaks arising from co-eluting components. The use of an automatic Biller - Biemann data enhancement routine,[25] has been found to be especially useful in this work. The enhancement routine serves not only to locate unresolved components of chromatographic peaks, but also to eliminate background column bleed ions which can be problematical, particularly in the latter stages of temperature programmed, high-temperature GC - MS analyses. Fig. 3 shows the TIC [Fig. 3(*a*)] and the Biller - Biemann enhanced mass-resolved TIC [Fig. 3(*b*)] obtained for the total lipid extract of a Late Saxon cooking vessel. As the background column bleed has been automatically subtracted, considerable time is saved during subsequent data processing. This is an important factor in this work, owing to the requirement for examining large numbers of samples for the purposes of archaeological investigation.

The identities of the various components referred to in this paper, made by GC - MS, are summarised in the respective figure captions. All the assignments have been made by the combined use of computerised library searches or through mass spectral interpretations based on established fragmentations of simple and complex lipids.[26,27]

In conclusion, we have described here the application of high-temperature GC and GC - MS to the analysis of the intact acyl lipid components of complex lipid extracts of archaeological materials for the first time. These techniques are in routine use in our laboratory, with the result that we are now able to gain insights into the origin of preserved and partially degraded lipids otherwise intractable with other currently available techniques. In addition to providing a convenient means of profiling total lipid extracts, this technique can be used as a preliminary screening method on which to base subsequent analyses targeting specific compounds or compound classes of high diagnostic potential. Final deductions concerning the origin of the organic residues extractable from artefacts constitutes a chemotaxonomic or "biological marker" problem centred on the detailed assessment of their chemical composition. This methodological approach is currently being applied to an on-going and systematic study, which envisages the sampling of many hundreds of individual

vessels. The full archaeological significance of the data referred to in this paper only becomes apparent when viewed in conjunction with conventional archaeological data, *e.g.*, contextual and environmental information.[12]

We thank the Science-Based Archaeology Committee (SBAC) of the Science and Engineering Research Council (SERC) and The Historic Buildings and Monuments Commission for England (HBMC—English Heritage) for financial support. We also thank M. C. Prescott for excellent assistance in performing the GC - MS analyses, and the RAP and V. Denham for kind provision of ceramic samples.

References

1. Knights, B. A., Dickson, C. A., Dickson, J. H., and Breeze, D. J., *J. Archaeol. Sci.*, 1983, **10**, 139.
2. Pepe, C., Dizabo, P., Scribe, P., Dagaut, J., Fillaux, J., and Saliot, A., *Rev. d'Archéom.*, 1989, **13**, 1.
3. Morgan, E. D., Titus, L., Small, R. J., and Edwards, C., *Archaeometry*, 1984, **31**, 43.
4. Evershed, R. P., and Connolly, R. C., *Naturwissenschaften*, 1988, **75**, 143.
5. Gulacar, F. O., Buchs, A., and Susini, A., *J. Chromatogr.*, 1989, **479**, 61.
6. Evershed, R. P., "Proceedings of a Conference on Archaeological Sciences," University of Bradford, 1990, in the press.
7. Evershed, R. P., *Archaeometry*, 1990, **32**, 139.
8. Condamin, J., Formenti, F., Metais, M. O., Michel, M., and Blond, P., *Archaeometry*, 1976, **18**, 195.
9. Hastdorf, C. A., and DeNiro, M. J., *Nature (London)*, 1985, **315**, 489.
10. Heron, C., Evershed, R. P., Chapman, B., and Pollard, A. M., "Proceedings of a Conference on Archaeological Sciences," University of Bradford, 1990, in the press.
11. Heron, C., Evershed, R. P., and Goad, L. J., *J. Archaeol. Sci.*, submitted for publication.
12. Heron, C., Evershed, R. P., Goad, L. J., and Denham, V., "Proceedings of a Conference on Archaeological Sciences," University of Bradford, 1990, in the press.
13. Dix, B., *Northamptonshire Arch.*, 1986/87, **21**, 3.
14. Evershed, R. P., Prescott, M. C., Goad, L. J., and Rees, H. H., *Biochem. Soc. Trans.*, 1987, **15**, 175.
15. Evershed, R. P., and Goad, L. J., *Biomed. Environ. Mass Spectrom.*, 1987, **14**, 131.
16. den Dooren De Jong, L. E., *Antonie von Leuwenhoek J. Microbiol. Serol.*, 1961, **27**, 337.
17. Thornton, M. D., Morgan, E. D., and Celoria, F., *Sci. Arch.*, 1970, **2–3**, 20.
18. Gurfinkel, D. M., and Franklin, U. M., *in* Farquahar, R. M., Hancock, R. G. V., and Pavlish, L. A., *Editors*, "Proceedings of the Twenty-sixth International Archaeometry Symposium," University of Toronto, Toronto, Canada, 1988, p. 85.
19. Mills, J. S., and White, R., "The Organic Chemistry of Museum Objects," Butterworth, London, 1987, p. 54.
20. Hill, H. E., and Evans, J., *in* Harris, D. R., and Hillman, G. C., *Editors*, "Foraging and Farming: the Evolution of Plant Exploitation," Unwin Hyman, London, 1989, p. 419.
21. Robinson, N., Evershed, R. P., Higgs, W. J., Jerman, K., and Eglinton, G., *Analyst*, 1987, **112**, 637.
22. Kuksis, A., *in* Heftmann, E., *Editor*, "Chromatography: Fundamentals and Applications of Chromatographic and Electrophoretic Methods. B. Applications," Elsevier, Amsterdam, 1983, p. B75.
23. Kuksis, A., and Myher, J. J., *J. Chromatogr.*, 1986, **379**, 57.
24. Mares, P., *in* Kuksis, A., *Editor*, "Chromatography of Lipids in Biomedical Research and Clinical Diagnosis," Elsevier, Amsterdam, 1987, p. 128.
25. Biller, J. E., and Biemann, K., *J. Mol. Evol.*, 1974, **14**, 65.
26. Odham, G., and Stenhagen, E., *in* Waller, G. R., *Editor*, "Biochemical Applications of Mass Spectrometry," Wiley, New York, 1972, Chapter 9, p. 229.
27. Budzikiewicz, H., Djerassi, C., and Williams, D. H., "Mass Spectrometry of Organic Compounds," Holden-Day, San Francisco, 1967.

Paper 0/01210F
Received March 20th, 1990
Accepted May 30th, 1990

Gas Chromatographic Separation and Determination of Chloroacetic Acids in Water by a Difluoroanilide Derivatisation Method

Hideaki Ozawa and Tadashi Tsukioka
Nagano Research Institute for Health and Pollution, 1978, Komemura, Amori, Nagano-shi, Nagano 380, Japan

A simple method for the micro-determination of chloroacetic acids in water was developed. Chloroacetic acids in a water sample were converted into the difluoroanilide derivatives by reaction with difluoroaniline and dicyclohexylcarbodiimide. The derivatives were extracted into ethyl acetate, cleaned up and determined by gas chromatography with electron-capture detection. The detection limits for monochloroacetic, dichloroacetic and trichloroacetic acids were *ca.* 2, 1 and 0.6 μg l^{-1}, respectively, in a 50-ml water sample. A pre-treatment method involving the use of an ion-exchange resin is also described, which allows determination at lower levels. The method was applied to the determination of chloroacetic acids in chlorinated water.

Keywords: *Chloroacetic acids determination; difluoroanilide derivatisation; dicyclohexylcarbodiimide; gas chromatography; chlorinated water*

Water chlorination has been accepted as one way of disinfecting potable water or wastewater from sewage-treatment plants. During chlorination, various chlorinated organic compounds are formed by the reaction of organic substances (such as humic material), in water, with chlorine. Chlorination by-products have caused much concern as hazards to health. In particular, trihalomethanes (THMs) (such as chloroform) in drinking water,[1] which are suspected of being carcinogens,[2] have received the most attention.

However, total organic halide (TOX) in chlorinated water could not be accounted for by the amount of THMs formed during chlorination.[3,4] Hence, increased attention has been paid to the non-volatile fraction of TOX. Chloroacetic acids (CAAs), such as dichloroacetic acid (DCAA) and trichloroacetic acid (TCAA), were reported to be found in relatively large amounts in chlorinated water.[5–9] Uden and Miller[10] and Norwood *et al.*[11] have surveyed municipal drinking water and detected DCAA and TCAA at μg l^{-1} or higher levels. Therefore, a simple analytical method for monitoring the concentration of CAAs in water is required from the standpoint of controlling the quality of chlorinated water, especially tap water for drinking.

A chromatographic method is often adopted for the microanalysis of CAAs, in which CAAs are generally converted into ester derivatives, *e.g.*, methyl esters, to diminish their polarity and increase their thermal stability, and these derivatives are separated and determined by chromatography. For example, trace amounts of TCAA in water have been extracted into diethyl ether, the TCAA being converted into its methyl ester with dimethyl sulphate,[12] diazomethane[13] or boron trifluoride - methanol complex,[14] and the methyl ester being separated and determined by gas chromatography with electron-capture detection (ECD),[12,14] microwave plasma emission detection,[13] or mass spectrometric detection.[9]

Previously, the authors have studied a method for converting a hydrophilic substance in aqueous media into the derivative that partitioned into an organic solvent with ease; a rodenticide (monofluoroacetate), in water, has been successfully determined by dichloroanilide derivatisation with *N,N'*-dicyclohexylcarbodiimide (DCC).[15] In the present paper, a simple method for determining trace amounts of CAAs in water by the use of anilide derivatisation is described. By reaction with 2,4-difluoroaniline (DFA) and DCC, CAAs in a sample of water were converted into difluoroanilide derivatives, which were extracted into ethyl acetate and analysed by gas chromatography with ECD.

Experimental

Reagents and Materials

Monochloroacetic acid (MCAA) and DCAA were obtained from Kanto Chemical (Tokyo, Japan). The TCAA was obtained from Tokyo Kasei Kogyo (Tokyo, Japan). Each standard solution of 1000 μg ml^{-1} was prepared in distilled water and stored. 2,4-Difluoroaniline was obtained from Tokyo Kasei Kogyo, and DCC from Kanto Chemical. Ethyl acetate solutions of DFA and DCC were prepared prior to use.

The ethyl acetate, benzene and anhydrous sodium sulphate used were of a grade suitable for pesticide residue analysis. Hydrochloric acid, sodium hydrogen carbonate and sodium chloride were of analytical-reagent grade.

Alumina (Aluminiumoxid 90; activity II–III; 70–230 mesh; Merck) was used as received, without further activation. The alumina (3 g) was packed with benzene into a glass column (10 mm i.d.). Anion-exchange resin (Dowex WGR) was treated prior to use as follows. The resin was immersed in distilled water, stirred for 30 min in 10-fold volumes (*i.e.*, 10 times the volume of the resin) of 0.5 M sodium hydroxide and washed with distilled water. Subsequently, the resin was stirred for 30 min in 10-fold volumes of 1 M hydrochloric acid, and washed with distilled water until neutral. A glass column (60 × 10 mm i.d.) packed with 5 ml of the pre-treated resin was used for each experiment.

Apparatus

A Shimadzu Model GC-3BE gas chromatograph equipped with a ^{63}Ni electron-capture detector and a Japan Electron Optics Laboratory Model JMS-D-300 gas chromatograph - mass spectrometer were used.

Procedures

Pre-treatment

The sample of water, when expected to contain high concentrations of contaminant, was pre-treated with ion-exchange resin prior to derivatisation. A 50-ml sample was passed through the ion-exchange column, and the resin was washed with 50 ml of distilled water. Subsequently, 50 ml of 1 M sodium chloride were passed through the column. The eluate (50 ml) was subjected to the following derivatisation procedure, without the addition of sodium chloride. However, when the water sample contained low concentrations of

contaminant (*e.g.*, tap water), it was not pre-treated, but directly subjected to the derivatisation procedure.

Derivatisation and extraction

A 50-ml portion of the water sample was placed in a 100-ml separating funnel, and 1 g of sodium chloride and 0.4 ml of 10 M hydrochloric acid were added. Next, 0.4 ml of 1 M DFA in ethyl acetate, 0.4 ml of 1 M DCC in ethyl acetate and 15 ml of ethyl acetate were added. The mixture was shaken for 40 min on a reciprocating shaker. After adding 5 g of sodium chloride, the aqueous layer was separated and extracted again with 5 ml of ethyl acetate. The combined organic extract was washed successively with 5 ml of 3 M hydrochloric acid, saturated sodium hydrogen carbonate solution and saturated sodium chloride solution, dried over anhydrous sodium sulphate, and evaporated to dryness.

To the residue, 2 ml of benzene were added and the mixture was evaporated to dryness. This residue was dissolved in 2 ml of benzene, and the solution was loaded on to the alumina column, together with any insoluble residue. Subsequently, benzene was passed through the column, and 20 ml of eluate were collected. The eluate was subjected to gas chromatographic analysis after appropriate dilution with benzene when necessary.

Calibration graph

Portions (50 ml) of distilled water containing 0.05–1.0-μg amounts of DCAA and of TCAA and 0.1–2.0-μg amounts of MCAA were treated as described above for the preparation of calibration standards of lower concentration. For standards of higher concentration, 0.5–5.0-μg amounts of DCAA and of TCAA and 1.0–10.0-μg amounts of MCAA were used. The calibration graph was established by peak-height measurements.

Gas Chromatographic Analysis

The difluoroanilide derivatives were separated and determined on a glass column (2.1 m × 3 mm i.d.) packed with 5% diethyleneglycol succinate (DEGS) plus 1% phosphoric acid on Chromosorb W (AW-DMCS, 60–80 mesh) and 5% Apiezon grease L plus 3% phosphoric acid on Chromosorb W (AW-DMCS; 60–80 mesh) in equal length. The former packing was in that half of the column on the injector side. The column and detector temperature was 170 °C and the injection port temperature was 190 °C. Nitrogen was used as the carrier gas (at a flow-rate of 30 ml min^{-1}).

Results and Discussion

Derivatisation

The dichloroanilide derivatisation previously developed was applicable to CAAs. However, we chose difluoroanilide derivatives of CAAs in pursuit of higher volatility. In order to determine the optimum reaction conditions for preparing difluoroanilide derivatives of CAAs by using DFA and DCC in acidic media, the effects of various amounts of hydrochloric acid, DFA and DCC were examined. The results obtained are shown in Tables 1, 2 and 3, respectively.

Maximum yields of the anilide derivatives were obtained for MCAA, DCAA and TCAA in the ranges 2–4, 1–5 and 0.5–5 mmol of hydrochloric acid, respectively. The range of the volume of hydrochloric acid that gave a constant yield was widest for TCAA and narrowest for MCAA. The optimum volume of 10 M hydrochloric acid to derivatise CAAs simultaneously at constant yields was 0.4 ml.

The yields of CAA derivatives increased with an increase in the amount of DFA, and constant yields were obtained with 0.4 mmol or more of DFA. The optimum volume of 1 M DFA was 0.4 ml in the proposed procedure.

Table 1. Effect of the amount of hydrochloric acid on the derivatisation*

Volume of 10 M HCl/ml	Relative yield,† %		
	MCAA	DCAA	TCAA
0	0	0	0
0.025	78	93	94
0.05	86	95	97
0.1	93	99	94
0.2	100	103	96
0.3	96	100	94
0.4	100	100	100
0.5	93	100	98
0.6	76	81	80

* MCAA (10 μg), DCAA (5 μg) and TCAA (5 μg) in 50 ml of water were derivatised by using 0.4 ml of 1 M DFA and 1 M DCC, with 1 g of sodium chloride.

† The relative yields obtained with 0.4 ml of 10 M hydrochloric acid were arbitrarily set at 100.

Table 2. Effect of the amount of DFA on the derivatisation*

Volume of 1 M DFA/ml	Relative yield,† %		
	MCAA	DCAA	TCAA
0.05	75	73	85
0.1	89	86	94
0.2	96	93	96
0.3	100	103	100
0.4	100	100	100
0.6	102	101	99

* MCAA (10 μg), DCAA (5 μg) and TCAA (5 μg) in 50 ml of water were derivatised by using 0.4 ml of 1 M DCC, with 0.4 ml of 10 M hydrochloric acid and 1 g of sodium chloride.

† The relative yields obtained with 0.4 ml of 1 M DFA were arbitrarily set at 100.

Table 3. Effect of the amount of DCC on the derivatisation*

Volume of 1 M DCC/ml	Relative yield,† %		
	MCAA	DCAA	TCAA
0.1	64	116	106
0.2	88	105	102
0.3	94	101	98
0.4	100	100	100
0.5	100	95	100

* MCAA (10 μg), DCAA (5 μg) and TCAA (5 μg) in 50 ml of water were derivatised by using 0.4 ml of 1 M DFA, with 0.4 ml of 10 M hydrochloric acid and 1 g of sodium chloride.

† The relative yields obtained with 0.4 ml of 1 M DCC were arbitrarily set at 100.

The yield of the MCAA derivative increased with an increase in the amount of DCC, and reached an almost constant level with 0.4 mmol of DCC. On the other hand, increasing the amount of DCC suppressed the yields of DCAA and TCAA derivatives and 0.3 mmol or more of DCC gave almost constant yields. For this reason, 0.4 ml of 1 M DCC was used in the proposed procedure although it did not afford maximum yields of all the CAAs.

The amount of sodium chloride added initially to the water sample influenced the yields of CAA derivatives. The yields of the derivatives reached a maximum with 2% m/v of sodium chloride (1 g in 50 ml), being almost constant at *ca.* 6%. Higher concentrations of sodium chloride in the sample resulted in a decrease in the yields of the derivatives.

In the derivatisation procedure, the reaction of CAAs with the reagents and extraction of the difluoroanilide derivatives formed could be achieved simultaneously by mixing the sample with derivatising reagents and extracting solvent. The effect of shaking time of the mixture on the yields of CAA

Table 4. Effect of shaking time on the derivatisation*

Shaking time/min	Relative yield,† %		
	MCAA	DCAA	TCAA
5	68	103	95
10	76	99	98
20	92	99	98
40	100	100	100
60	101	100	100
90	102	101	100
120	94	101	100

* MCAA (10 μg), DCAA (5 μg) and TCAA (5 μg) in 50 ml of water were derivatised by using 0.4 ml of 1 M DFA and 1 M DCC, with 0.4 ml of 10 M hydrochloric acid and 1 g of sodium chloride.

† The relative yields obtained after 40 min of shaking were arbitrarily set at 100.

Table 5. Separation of difluoroanilide derivatives of CAAs

	Column packing	Detection order
I	DEGS (5%) plus H_3PO_4 (1%)	TCAA (0.91),* MCAA (1.00), DCAA (1.34)
II	Apiezon grease L (5%) plus H_3PO_4 (2%)	MCAA (1.00), DCAA (1.37), TCAA (1.90)
III	I + II	MCAA (1.00), TCAA (1.17), DCAA (1.38)

* Relative retention times are given in parentheses.

derivatives was examined. The results obtained are shown in Table 4. The yields of the MCAA derivative increased with an increase in shaking time and reached a constant maximum level at 40 min. The yield of the TCAA derivative reached *ca.* 95% of the maximum level in only 5 min. The DCAA exhibited a maximum and constant derivatisation yield from 5 to 120 min. In the proposed procedure, the shaking time was set at 40 min to determine MCAA, DCAA and TCAA simultaneously. However, in the determination of DCAA and TCAA, the shaking time could be shortened to a great extent because these acids reacted rapidly.

Confirmation of the Derivatives and Conditions for Analysis

The mass spectra of MCAA, DCAA and TCAA derivatives prepared by the derivatisation procedure were measured by electron-impact ionisation (Fig. 1). The spectra showed ion peaks at *m/z* 205, 239 and 273 for MCAA, DCAA and TCAA derivatives, respectively, which corresponded to the molecular ions (M^+) of 2,4-difluoromonochloroacetanilide (MCA-DFA), 2,4-difluorodichloroacetanilide (DCA-DFA) and 2,4-difluorotrichloroacetanilide (TCA-DFA), respectively. The base peaks of 2,4-difluoroanilide derivatives of CAAs were observed at *m/z* 129, 156 and 156 for MCA-DFA, DCA-DFA and TCA-DFA, respectively.

Separation of the difluoroanilide derivatives of CAAs was investigated (Table 5). The DEGS plus phosphoric acid was inferior in durability, and separation of TCA-DFA and MCA-DFA deteriorated with successive use of this packing. The double column packed with DEGS plus phosphoric acid and Apiezon grease L plus phosphoric acid in equal lengths, gave the best result (Fig. 2). This double column was chosen as the basic analytical column. The columns packed with 5% DEGS plus 1% phosphoric acid and 5% Apiezon grease L plus 3% phosphoric acid were used as supplementary columns for confirming the identity of the derivatives.

The calibration graph was rectilinear in the ranges 1–20 and 10–100 μg l^{-1} of DCAA and TCAA, and 2–40 and 20–200 μg l^{-1} of MCAA. The MCAA was inferior to DCAA and TCAA in sensitivity to ECD. Therefore, the MCAA concentration in the standard solutions used to construct the calibration graph was twice as high as that of DCAA or TCAA. The detection limits were 2, 1 and 0.6 μg l^{-1} for MCAA, DCAA and TCAA, respectively, in 50 ml of the water sample.

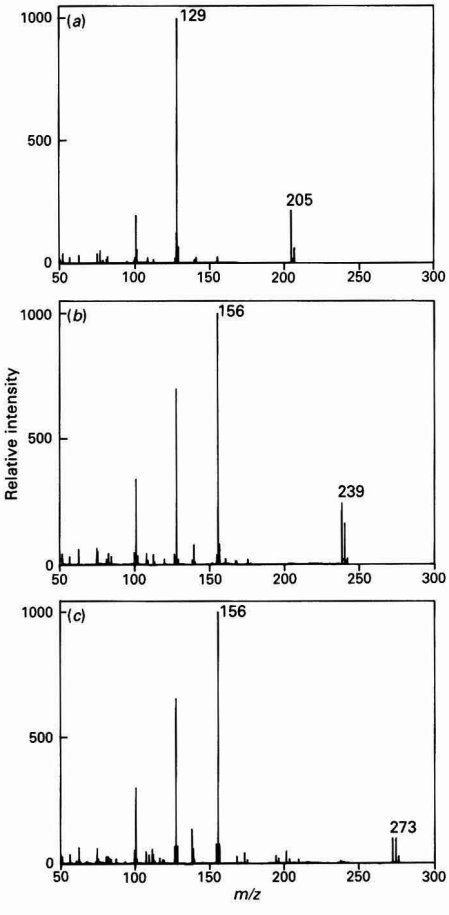

Fig. 1. Mass spectra of the difluoroanilide derivatives of chloroacetic acids. (*a*) MCA - DFA; (*b*) DCA - DFA; and (*c*) TCA - DFA. Fused-silica column (15 m × 0.53 mm i.d.) coated with OV-1701; column temperature, 160 °C; ion-source temperature, 250 °C; ionisation voltage, 70 eV; and carrier gas, He (15 ml min^{-1})

Clean-up

Pre-treatment before derivatisation

Separation and clean-up of CAAs prior to the difluoroanilide derivatisation was required for samples, such as treated wastewater, containing high concentrations of various contaminants. Previously, ion-exchange pre-treatment was successfully applied to the separation of monofluoroacetate.[16] Therefore, as a clean-up approach to the analysis of CAAs in water before derivatisation, ion-exchange chromatography was studied.

Strongly basic anion-exchange resin (Dowex 1-X8) was examined by using a sodium chloride solution as eluent. In the derivatising procedure, 50-ml portions of the sample were treated; hence the efficiency of the elution of CAAs with 50 ml of eluent was investigated (Table 6). The MCAA, DCAA and TCAA were eluted in this order, and MCAA was eluted quantitatively from the ion-exchange column with 50 ml of 1 M sodium chloride; however, DCAA and TCAA were inadequately recovered. A sodium chloride solution of higher concentration was required to elute all the CAAs simultaneously within 50 ml of the eluate. On the other hand, the

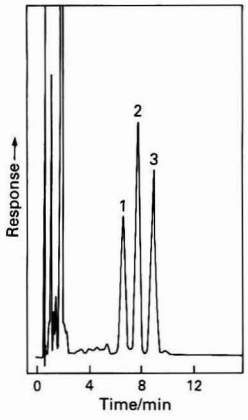

Fig. 2. Gas chromatogram of chloroacetic acid (CAA) derivatives obtained from an aqueous standard solution (MCAA, 40 μg l^{-1}; DCAA, 20 μg l^{-1}; and TCAA, 20 μg l^{-1}): 1, MCA - DFA; 2, TCA - DFA; and 3, DCA - DFA

Table 6. Elution data for CAAs* from an anion-exchange column† (I)

Eluent (NaCl) concentration/M	Recovery,‡ % MCAA	DCAA	TCAA
0.10	49	Trace	0
0.25	75	30	0
0.50	87	59	Trace
1.00	104	84	18

* MCAA, 10 μg; DCAA, 5 μg; TCAA, 5 μg.
† Dowex 1-X8; 5 ml (60 × 10 mm i.d.).
‡ Recovery from 50 ml of eluate.

Table 7. Elution data for CAAs* from an anion-exchange column† (II)

Eluent (NaCl) concentration/M	Recovery,‡ % MCAA	DCAA	TCAA
0.10	75	70	70
0.25	82	79	81
0.50	82	82	82
1.00	93	98	94
1.50	93	106	99

* MCAA, 10 μg; DCAA, 5 μg; TCAA, 5 μg.
† Dowex WGR; 5 ml (60 × 10 mm i.d.).
‡ Recovery from 50 ml of eluate.

concentration range of sodium chloride that gave a constant yield in the subsequent derivatisation step was *ca.* 2–6% m/v, and the use of sodium chloride solution at higher concentrations was, therefore, not desirable.

Weakly basic anion-exchange resin (Dowex WGR) was examined in the same way. The efficiency of elution of the CAAs was investigated with 50 ml of sodium chloride solution as eluent (Table 7). The MCAA was eluted first from the anion-exchange column, then DCAA and TCAA were eluted concurrently. Moreover, all three CAAs were recovered quantitatively within 50 ml of the eluate by using 1 M or higher concentration of sodium chloride solution.

On the basis of these results, Dowex WGR was used in the pre-treatment procedure prior to derivatisation. However, the pre-treatment procedure was not necessarily required for samples, such as tap water, containing relatively less contaminant and interfering species.

Table 8. Recovery of CAAs from "spiked" natural waters

		Concentration/ μg l^{-1}	Average recovery,* %	RSD,† %
Lake-water	MCAA	20	97	5.0
	DCAA	10	91	2.3
	TCAA	10	96	3.0
Sea-water	MCAA	20	96	2.9
	DCAA	10	100	3.4
	TCAA	10	99	1.8

* Replicates (n = 5).
† Relative standard deviation.

The pre-treatment with the anion-exchange column was also expected to be applicable to the pre-concentration of CAAs in the water sample. To 1 l of distilled water, 1 μg of MCAA, 0.5 μg of DCAA and 0.5 μg of TCAA were added, and 20-fold concentration experiments were carried out. The recoveries of MCAA, DCAA and TCAA were 64, 80 and 61%, respectively, as the average values for triplicates with a relative standard deviation of <7%.

Clean-up after derivatisation

The ethyl acetate extracts of CAA derivatives also contained derivatising reagents, side-reaction products and other contaminants. Therefore, clean-up of the ethyl acetate extracts was required.

Silica gel column chromatography for the purification of CAA derivatives in the extracts was tested. This procedure failed, however, owing to the appearance of other peaks, which interfered with the determination of the CAA derivatives.

Alumina column chromatography was also tested. Purification of the difluoroanilide derivatives of CAAs was investigated on the column (35 × 10 mm i.d.) in which 3 g of alumina were packed with benzene. Elution of the derivatives was examined with the use of various eluents, benzene giving a good result. By use of benzene as eluent, each derivative was quantitatively recovered within a 20-ml volume of the eluate, and contaminating substances could be removed to a considerable extent. However, when the eluate was concentrated into a smaller volume and subjected to gas chromatographic analysis, the determination of CAA derivatives was subject to slight interference.

When the ethyl acetate extract, obtained according to the derivatisation procedure for calibration, was adjusted to 20 ml with ethyl acetate, and 5-μl portions were directly injected on to the gas chromatographic column without clean-up, little interference was observed. A sample, such as tap water, which contained few contaminants could also be analysed without clean-up.

Recovery Experiments and Application to Authentic Samples

Recovery experiments by the standard procedure were carried out using natural waters treated with CAAs. Preliminary treatment of lake water according to the standard procedure gave no derivative peaks of CAAs. Sea water was treated without the initial addition of sodium chloride, and gave the same result. The MCAA, DCAA and TCAA were added to these samples at concentrations of 20, 10 and 10 μg l^{-1}, respectively, and subsequently determined (Table 8). In this experiment, CAAs could be determined without the clean-up procedure. The recoveries of CAAs from both samples were higher than 90% with a relative standard deviation of 5% or less. From these results, the proposed method was considered to be useful for determining CAAs at μg l^{-1} levels in water, and was applied to authentic samples.

Tap water in our laboratory and tertiary-treated wastewater from a sewage-treatment plant (*i.e.*, after the third, and final,

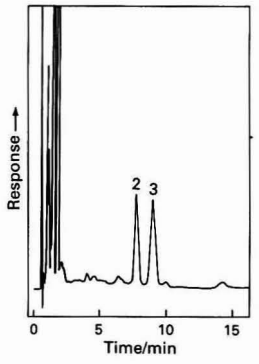

Fig. 3. Gas chromatogram of CAA derivatives for a tap water sample: 2, TCA - DFA; and 3, DCA - DFA

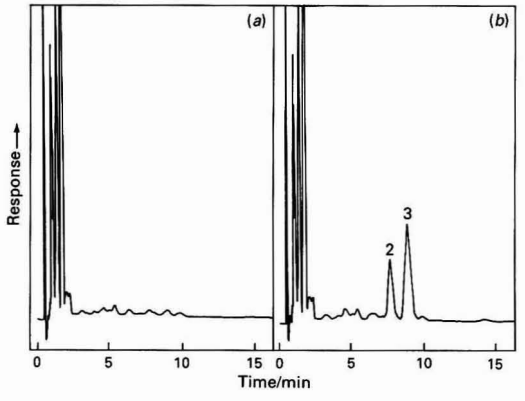

Fig. 4. Gas chromatograms for tertiary-treated wastewater: (*a*) before disinfection; and (*b*) after disinfection: 2, TCA - DFA; and 3, DCA - DFA

treatment process in this particular sewage treatment plant) were analysed. The water samples were treated with sodium sulphite, and the CAAs were determined, as soon as possible, according to the proposed method. Fig. 3 shows the gas chromatogram of CAA derivatives obtained from tap water, in which DCAA and TCAA were detected at the 14 and 10 μg l^{-1} levels, respectively. The gas chromatograms obtained for tertiary-treated wastewater are shown in Fig. 4. In the water sample after disinfection, DCAA and TCAA were detected at the 11 and 5.0 μg l^{-1} levels, respectively.

Conclusion

In this paper, a simple derivatisation procedure for determining trace amounts of CAAs in water is proposed. The CAAs are converted into those derivatives that are easily partitioned into an organic phase, which are sensitive to ECD and have good gas chromatographic properties. The proposed method is useful for the rapid determination of CAAs at μg l^{-1} levels in water.

The authors thank A. Frihata, of the Nagano Research Institute for Health and Pollution, for helpful advice.

References

1. Rook, J. J., *Water Treat. Exam.*, 1974, **23**, 234.
2. Hariss, R. H., and Breecher, E. M., *Consumer Rep.*, 1974, **39**, 436.
3. Oliver, B. G., *Can. Res.*, 1978, **11**, 21.
4. Glaze, W. H., Peyton, G. R., Saleh, F. Y., and Huang, F. Y., *Int. J. Environ. Anal. Chem.*, 1979, **7**, 143.
5. Rook, J. J., *Environ. Sci. Technol.*, 1977, **11**, 478.
6. Norwood, D. L., Johnson, J. D., Christman, R. F., Hass, J. R., and Bobenrieth, M. J., *Environ. Sci. Technol*, 1980, **14**, 187.
7. Quimby, B. D., Delaney, M. F., Uden, P. C., and Barnes, R. M., *Anal. Chem.*, 1980, **52**, 259.
8. Miller, J. W., and Uden, P. C., *Environ. Sci. Technol.*, 1983, **17**, 150.
9. Christman, R. F., Norwood, D. L., Millington, D. S., and Johnson, J. D., *Environ. Sci. Technol*, 1983, **17**, 625.
10. Uden, P. C., and Miller, J. W., *J. Am. Water Works Assoc.*, 1983, **75**, 524.
11. Norwood, D. L., Thompson, G. P., Johnson, J. D., and Christman, R. F., "Monitoring Trichloroacetic Acid in Municipal Drinking Water," US Environmental Protection Agency Report, EPA/600/D-87/150, 1985, p. 1115.
12. Chmil, V. D., *Zh. Anal. Khim.*, 1978, **33**, 2232.
13. Miller, J. W., Uden, P. C., and Barnes, R. M., *Anal. Chem.*, 1982, **54**, 485.
14. Lahl, U., Stachel, B., Schroer, W., and Zeschmar, B., *Z. Wasser Abwasser Forsch.*, 1984, **17**, 45.
15. Ozawa, H., and Tsukioka, T., *Anal. Chem.*, 1987, **59**, 2914.
16. Ozawa, H., and Tsukioka, T., *J. Chromatogr.*, 1989, **473**, 251.

Paper 0/00882F
Received February 27th, 1990
Accepted May 30th, 1990

Simultaneous Determination of Some Active Ingredients in Cough - Cold Syrups by Gas - Liquid Chromatography

Oi-Wah Lau and Yiu-Ming Cheung
Department of Chemistry, The Chinese University of Hong Kong, Shatin, N.T., Hong Kong

A simple, efficient and accurate gas - liquid chromatography (GLC) method for the simultaneous determination of eight active ingredients in cough - cold syrups has been developed. The active ingredients under study were bromhexine, chlorpheniramine, codeine, dextromethorphan, diphenhydramine, ephedrine/psuedoephedrine, guaiphenesin and papaverine. Before injection, the active ingredients were first separated, from the excipients present in the cough - cold syrups, with chloroform, from alkaline medium. They were then separated by GLC on a glass column (5 ft × 2 mm i.d.) packed with 3% of OV-25 supported on Supelcoport (80–100 mesh). The column temperature was maintained at 170 °C for 1 min, then programmed to 265 °C at a rate of 10 °C min^{-1}, and maintained at this temperature for 10 and 1 min, respectively, for samples with and without papaverine. The flow-rate of the nitrogen carrier gas was 30 ml min^{-1}. A flame-ionisation detector was used for detection, and clomipramine hydrochloride was used as the internal standard. The recoveries of the drugs ranged from 96.0 to 99.7%, and the relative standard deviations for ten replicate determinations ranged from 0.49 to 4.7%. Results are reported for nine commercially available cough - cold syrups.

Keywords: *Simultaneous determination of drugs; cough - cold syrup; gas - liquid chromatography; solvent extraction*

Bromhexine, chlorpheniramine, codeine, dextromethorphan, diphenhydramine, ephedrine, guaiphenesin, papaverine and pseudoephedrine are active ingredients commonly found in cough - cold syrups.[1,2]

High-performance liquid chromatography (HPLC)[3–6] is commonly used for the determination of the active ingredients in cough - cold mixtures. Derivative spectrophotometric methods[7–9] and gas - liquid chromatography (GLC) methods[4,5,10] have also been developed for the analysis of these drugs; however, only two or three components could be determined simultaneously by most of these methods.

This paper describes a simple and efficient GLC method for the determination of eight of the active ingredients mentioned above (ephedrine and pseudoephedrine, being stereoisomers, have similar properties and are not found together in cough - cold syrups), individually or together, in various cough - cold syrup formulations after extraction of the active ingredients into chloroform. The optimum conditions for carrying out the extraction and for the determinations were established. Nine cough - cold syrups were analysed for the contents of the active ingredients, and the results were compared with those obtained by using HPLC.[3]

Experimental

Instrumentation

Apparatus

The gas chromatograms were recorded with a Varian Model 3700 gas chromatograph, equipped with a flame-ionisation detector and attached to a Hitachi 833A data processor.

Chromatographic conditions

A glass column (5 ft × 2 mm i.d.) was packed with 3% of OV-25 on Supelcoport (80–100 mesh). The flow-rate of the nitrogen carrier gas was 30 ml min^{-1}. The flow-rates for hydrogen and air were 30 and 300 ml min^{-1}, respectively. The injection port and detector temperatures were both kept at 270 °C. The initial column temperature was kept at 170 °C for 1 min, then programmed to a final temperature of 265 °C at a heating rate of 10 °C min^{-1}, and then maintained at this temperature for 10 and 1 min, respectively, for samples with and without papaverine. The attenuation was set at 1 in the gas chromatograph and varied in the data processor (8–10, depending on the injection concentration). The chart speed of the data processor was 2.5 mm min^{-1}. The column was kept at 50 °C and at a nitrogen flow-rate of 30 ml min^{-1} when not in use. When broadening of the peaks was observed, the first few inches of the packing material near the injection port were replaced, and the column could then be used for *ca.* 6 months.

Reagents

All the drugs used were of Pharmacopoeial or equivalent purity, and were used without further purification. All other reagents were of analytical-reagent grade.

Aqueous internal standard solution

Prepared by dissolving exactly 0.0751 g of clomipramine hydrochloride in 50 ml of distilled water in a calibrated flask.

Aqueous stock solutions of the drugs

A stock solution of bromhexine hydrochloride (2.50 mg ml^{-1}) was prepared by weighing exactly 125.00 mg of the compound into 50 ml of sulphuric acid (0.1 M) in a calibrated flask.

Similarly, stock solutions of chlorpheniramine maleate (1.02 mg ml^{-1}), codeine phosphate (5.00 mg ml^{-1}), dextromethorphan hydrobromide (3.12 mg ml^{-1}), diphenhydramine hydrochloride (5.00 mg ml^{-1}), ephedrine hydrochloride (5.00 mg ml^{-1}), guaiphenesin (15.63 mg ml^{-1}), papaverine hydrochloride (1.25 mg ml^{-1}) and pseudoephedrine hydrochloride (6.24 mg ml^{-1}) were prepared by dissolving appropriate amounts of the respective drugs in 50 ml of sulphuric acid (0.1 M) in calibrated flasks.

Aqueous standard solutions

Various mixtures of drugs were prepared by mixing appropriate amounts of stock solutions of these drugs to match the active ingredients and their respective label values for each syrup. For example, for sample 4 (in Table 7), containing codeine phosphate (9.0 mg in 5 ml) and ephedrine hydrochloride (7.2 mg in 5 ml), a mixture was prepared by mixing accurately 10 ml each of the codeine phosphate and ephedrine hydrochloride stock solutions and diluting to 25 ml in a calibrated flask with 0.1 M sulphuric acid, the resulting concentrations for both drugs in this mixture being 10.0 mg in

5 ml. Other mixtures with different compositions were prepared in a similar manner.

Sample Pre-treatment

No sample pre-treatment was necessary, except for samples 7–9 (Table 7) containing high concentrations of the drugs, and they were diluted 5-fold with 0.1 M sulphuric acid.

Extraction Method

A 10-ml portion of the cough - cold syrup or aqueous standard solution was pipetted into a 100-ml separating funnel containing 10 ml of 25% v/v ammonia solution (AnalaR grade, Merck). The drugs were then extracted three times with 15-ml aliquots of chloroform. The organic layers were transferred into another separating funnel and washed with 5–6 ml of distilled water. The chloroform layer was then dried with anhydrous sodium sulphate for *ca.* 5 min, and filtered. The sodium sulphate was washed with small volumes of chloroform, and the washings were added to the filtrate, which was then diluted to 50 ml with chloroform in a calibrated flask.

Preparation of Working Internal Standard Solution

An aliquot (10 ml) of the aqueous internal standard solution was treated as for the cough - cold syrups.

Simultaneous Determination of Active Ingredients in Cough - Cold Syrup

An aliquot (5 ml) of the sample solution and several aliquots (2–10 ml) of the standard solution, after the extraction procedure described above, were evaporated to dryness under a stream of nitrogen on a water-bath at room temperature. Each residue was dissolved in 1 ml of the working internal standard solution, 3 μl of which were injected into the chromatograph with a 10-μl Hamilton syringe under the chromatographic conditions described above. The injections were performed in duplicate.

The calibration graph was obtained by plotting the peak-area ratios (drug to internal standard) against the concentrations of the drug.

The amount of each drug in the sample was deduced from the respective calibration graph.

Table 1. Peak-area ratios (individual drug to internal standard) after extraction with various solvents*

	Peak-area ratios of the drugs in the mixture†				
Extraction medium	1	2	3	4	5
Chloroform	3.405	4.332	0.4452	2.777	3.823
Dichloromethane	2.787	3.807	0.3307	2.421	3.791
Diethyl ether	2.694	1.548	0.2285	2.229	2.870
Hexane	1.005	ND‡	0.3543	2.277	0.7384
10% MeOH in $CHCl_3$	3.436	4.724	0.4308	2.850	4.234

* Chromatogaphic conditions as described under Experimental.

† The drugs in the mixture, with concentration in the organic solvent in parentheses: (1) ephedrine hydrochloride (1.54 mg ml^{-1}); (2) guaiphenesin (3.04 mg ml^{-1}); (3) chlorpheniramine maleate (0.47 mg ml^{-1}); (4) dextromethorphan hydrobromide (1.32 mg ml^{-1}); and (5) codeine phosphate (2.28 mg ml^{-1}).

‡ No guaiphenesin signal was detected.

Results and Discussion

In addition to active ingredients, most cough - cold mixtures contain dye(s), preservative(s), flavour(s) and a sweetening agent, making determination of the active ingredients difficult. Hence, HPLC has been commonly used for the analysis of cough - cold mixtures. However, it is worthwhile developing GLC methods as alternatives as gas chromatographs are common items of equipment in most laboratories and the running cost is also cheaper. The key to the success of GLC methods for the analysis of cough - cold mixtures is to develop an efficient extraction procedure capable of separating the active ingredients from the various excipients, and to choose a stationary phase that can resolve a large number of active ingredients in the mixtures.

Choice of Extraction Medium

The drugs under study are reported to be extracted by organic solvents from alkaline media.[11,12] Therefore, the aqueous solutions of the drugs were first made alkaline with 25% v/v ammonia solution before extraction. Several common organic solvents, including chloroform, dichloromethane, diethyl ether and hexane, were assessed for their suitability as the extraction medium.

A solution (10 ml) containing known amounts of chlorpheniramine maleate, codeine phosphate, dextromethorphan hydrobromide, ephedrine hydrochloride and guaiphenesin was prepared and 2-ml aliquots were extracted once with 20 ml of each solvent, and 10 ml of the organic layer were pipetted out and filtered after being dried with anhydrous sodium sulphate. The filtrate was evaporated to dryness under nitrogen, the residue was dissolved in 1 ml of the working internal standard solution, then 3.0 μl of the final solution were injected into the chromatograph. The peak-area ratios (drug to internal standard) for various organic solvents are shown in Table 1.

Table 2. Percentage extraction of each drug under study from aqueous solution (10 ml) into chloroform (3 × 15 ml). Each determination was carried out in duplicate

Drug	Concentration in aqueous solution/mg ml^{-1}	Extraction, %
Bromhexine hydrochloride	0.55	99.2
Chlorpheniramine maleate	1.03	97.4
Codeine phosphate	1.15	95.3
Dextromethorphan hydrobromide	1.03	100.1
Diphenhydramine hydrochloride	2.01	97.1
Ephedrine hydrochloride	3.00	95.1
Guaiphenesin	1.35	90.3
Papaverine hydrochloride	0.76	99.3
Pseudoephedrine hydrochloride	3.00	99.0

Table 3. Retention times and peak shapes of the drugs under study in a column (5 ft × 2 mm i.d.) packed with 3% of OV-25 on Supelcoport (80–100 mesh) under the optimised conditions

Drug	Retention time/min	Peak shape
Ephedrine hydrochloride* / Pseudoephedrine hydrochloride*	1.04	Sharp
Guaiphenesin	3.67	Sharp with tailing
Diphenhydramine hydrochloride	4.88	Sharp
Chlorpheniramine maleate	6.22	Sharp
Dextromethorphan hydrobromide	7.49	Sharp
Bromhexine hydrochloride	9.37	Sharp
Codeine phosphate	10.84	Sharp
Papaverine hydrochloride	19.14	Sharp

* Ephedrine hydrochloride and pseudoephedrine hydrochloride had the same retention time.

As the peak-area ratios so obtained were directly proportional to the amounts of drugs extracted from the aqueous into the organic phase, these ratios were used to compare the extraction capability of each solvent. The results shown in Table 1 indicate that chloroform should be the best extraction medium and hexane the poorest. The extraction capability of chloroform was enhanced by the addition of 10% v/v of methanol. Unfortunately, this mixed solvent also extracted the dyes in authentic samples. Hence, chloroform was chosen as the extraction medium for all subsequent determinations.

The percentage extraction of each drug under study from an aqueous solution into chloroform by using the procedure described under Experimental was deduced from its concentration in chloroform as determined by ultraviolet spectrophotometry. The results are shown in Table 2.

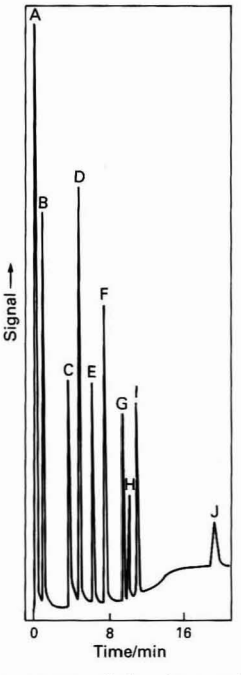

Fig. 1. Gas chromatogram of the drugs under the optimised conditions. A, Solvent; B, ephedrine hydrochloride (0.87 mg ml^{-1}); C, guaiphenesin (1.54 mg ml^{-1}); D, diphenhydramine hydrochloride (1.09 mg ml^{-1}); E, chlorpheniramine maleate (0.90 mg ml^{-1}); F, dextromethorphan hydrobromide (1.00 mg ml^{-1}); G, bromhexine hydrochloride (0.77 mg ml^{-1}); H, clomipramine hydrochloride (0.30 mg ml^{-1}); I, codeine phosphate (0.91 mg ml^{-1}); and J, papaverine hydrochloride (0.47 mg ml^{-1})

Choice of Stationary Phase

As it was intended to resolve a large number of drugs by the proposed method, the proper choice of stationary phase was also important. A number of stationary phases on Supelcoport (80–100 mesh) commonly used for the separation of non-volatile compounds, including OV-1, OV-17, OV-25 and OV-225 (3% of each), were assessed. The flow-rate of nitrogen was set at 30 ml min^{-1}, a flow-rate commonly used for the determination of drugs. The optimum temperature programming conditions for separating the drugs under study were found for each column. In terms of good peak shapes and resolution and over-all running time, the column packed with 3% of OV-25 was found to be the most satisfactory. The retention times and peak shapes of the drugs under the optimised conditions for this column are listed in Table 3, and a typical chromatogram is shown in Fig. 1. Note that ephedrine is shown, but pseudoephedrine is not, as these two compounds are stereoisomers and have the same peak shape and retention time. They have similar properties and are not found together in cough - cold mixtures.

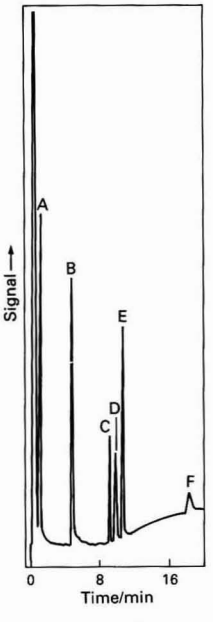

Fig. 2. Chromatogram of sample No. 1. A, Ephedrine hydrochloride; B, diphenhydramine hydrochloride; C, bromhexine hydrochloride; D, clomipramine hydrochloride; E, codeine phosphate; and F, papaverine hydrochloride

Table 4. Data for quantitative gas chromatography of the drugs under study

Drug	Working range/mg ml^{-1}	Regression equation*	Correlation coefficient	Detectable amount per injection†/μg
Bromhexine hydrochloride	0.06–0.90	$y = 2.66x - 0.03312$ ($n = 8$)	0.99992	0.18
Chlorpheniramine maleate	0.06–0.90	$y = 2.654x - 0.1076$ ($n = 8$)	0.99976	0.18
Codeine phosphate	0.10–1.54	$y = 2.810x - 0.1312$ ($n = 8$)	0.99991	0.30
Dextromethorphan hydrobromide	0.20–1.52	$y = 3.474x - 0.3337$ ($n = 7$)	0.99995	0.60
Diphenhydramine hydrochloride	0.20–1.58	$y = 4.316x - 0.3963$ ($n = 7$)	0.99997	0.60
Ephedrine hydrochloride	0.40–1.54	$y = 3.098x - 1.172$ ($n = 6$)	0.99992	1.20
Guaiphenesin	0.35–5.38	$y = 2.911x - 0.6736$ ($n = 8$)	0.99986	1.10
Papaverine hydrochloride	0.03–0.48	$y = 3.223x - 0.04843$ ($n = 8$)	0.99986	0.10
Pseudoephedrine hydrochloride	0.50–1.87	$y = 2.790x - 0.8799$ ($n = 6$)	0.99994	1.50

* y = peak-area ratio (drug to internal standard); x = concentration of drug (mg ml^{-1}); n = number of experimentally determined values of x; and each determination was carried out in duplicate.

† The lowest possible amount of drug per injection to give a detectable signal.

Quantitative GLC of the Drugs

Quantitative studies of the drugs were made as described under Experimental.

Results were calculated from the linear regression of the standards, relating the peak-area ratios (drug to internal standard) and concentrations. The working ranges, regression equations and correlation coefficients, together with the detectable amount per injection of each drug, are shown in Table 4.

Table 5. Results of the recovery tests for the drugs under study by using the proposed method. Each result was the mean of four determinations

Drug	Amount added/mg per 5 ml	Recovery,* %
Bromhexine hydrochloride	3.02	96.2 (0.6)
Chlorpheniramine maleate	3.01	97.9 (1.2)
Codeine phosphate	5.02	99.7 (1.2)
Dextromethorphan hydrobromide	5.08	96.0 (0.5)
Diphenhydramine hydrochloride	5.25	98.8 (1.1)
Ephedrine hydrochloride	5.04	97.8 (0.9)
Guaiphenesin	17.9	98.1 (1.3)
Papaverine hydrochloride	1.68	97.0 (1.6)
Pseudoephedrine hydrochloride	6.24	97.5 (1.7)

* RSD in parentheses.

Table 6. Precision of the results for the proposed method

Drug	Concentration/ mg ml^{-1}	RSD,* %
Bromhexine hydrochloride	0.77	0.73
Chlorpheniramine maleate	0.90	1.3
Codeine phosphate	0.91	2.0
Dextromethorphan hydrobromide	1.00	0.49
Diphenhydramine hydrochloride	1.09	1.3
Ephedrine hydrochloride	0.87	4.7
Guaiphenesin	1.54	3.4
Papaverine hydrochloride	0.47	3.3
Pseudoephedrine hydrochloride	1.25	1.7

* For ten replicate determinations.

Recovery Tests and Precision

Recovery tests were performed by adding a known amount of each drug to a cough - cold syrup where it was known to be absent. The mean results of four analyses ranged from 96.0 to 99.7% (Table 5), and these can be considered to be good recoveries.

The precision of the proposed method was checked by calculating the relative standard deviation (RSD) for ten replicate determinations of the drugs under study, and the results are shown in Table 6. The RSDs ranged from 0.49 to 4.7%.

Determination of Active Ingredients in Cough - Cold Syrups

The contents of the drugs under study in nine commercially available cough - cold syrups were determined in triplicate by using the proposed method. The samples contained combinations of several active ingredients, which were identified by comparing the retention time of the peaks observed with those obtained from standard solutions, containing the respective active ingredients, examined under the same conditions. The results obtained were compared with those obtained by an established HPLC method[3] and with the corresponding label values. The assay results for the samples studied are presented in Table 7. A typical chromatogram (for sample 1) is shown in Fig. 2, where no additional peaks arising from excipients are evident.

From Table 7, it can be seen that the results obtained with the proposed method were in good agreement with those obtained by using the counter-check HPLC method and with the respective label values.

Conclusion

A simple, efficient and accurate GLC method for the simultaneous determination of bromhexine, chlorpheniramine, codeine, dextromethorphan, diphenhydramine, ephedrine (or pseudoephedrine), guaiphenesin and papaverine in the cough - cold syrups has been developed. The proposed method involved a preliminary extraction with chloroform, which has been shown to be successful in

Table 7. Assay results for the determination of various active ingredients in cough - cold syrups

Sample	Ingredients	Label value/ mg per 5 ml	Percentage of label claim: Proposed method*	Percentage of label claim: HPLC method
1	Bromhexine hydrochloride	2.5	92.5 (0.2)	95.2
	Codeine phosphate	4.5	101.5 (0.1)	103.8
	Diphenhydramine hydrochloride	4.5	104.4 (0.4)	96.2
	Ephedrine hydrochloride	4.5	101.4 (1.3)	97.1
	Papaverine hydrochloride	1.25	90.9 (3.8)	90.4
2	Chlorpheniramine maleate	1.0	93.7 (2.6)	93.0
	Dextromethorphan hydrobromide	5.0	95.3 (0.3)	99.4
	Guaiphenesin	25.0	96.5 (1.5)	91.6
3	Chlorpheniramine maleate	1.0	88.3 (0.8)	93.0
	Dextromethorphan hydrobromide	5.0	95.1 (0.2)	100.6
	Guaiphenesin	25.0	98.5 (1.3)	96.4
4	Codeine phosphate	9.0	99.6 (0.3)	102.8
	Ephedrine hydrochloride	7.2	94.8 (1.0)	97.9
5	Chlorpheniramine maleate	4.0	97.0 (0.9)	100.8
6	Chlorpheniramine maleate	2.0	84.4 (0.7)	85.5
	Codeine phosphate	10.0	90.6 (3.3)	88.5
	Ephedrine hydrochloride	5.0	90.0 (3.3)	89.0
7	Guaiphenesin	100.0	103.1 (1.3)	102.5
8	Guaiphenesin	100.0	111.4 (1.7)	115.3
	Pseudoephedrine hydrochloride	30.0	107.8 (2.7)	111.9
9	Guaiphenesin	100.0	97.3 (0.5)	99.4
	Pseudoephedrine hydrochloride	30.0	102.3 (2.7)	105.6

* Mean of triplicate measurements; relative standard deviation in parentheses.

extracting the basic drugs from the sample matrices so that interference from excipients, such as dyes, flavours and preservatives, could be minimised. The time for running a chromatogram for the syrups was 10 min or less when papaverine was absent, and *ca.* 20 min when the latter drug was present. The method has been applied successfully and conveniently to the determination of the drugs mentioned above, individually or together, in nine commercial cough - cold syrups. The method is also suitable as a stability-indicating assay.

The authors thank C. S. Mok of the Government Laboratory for helpful discussions.

References

1. "The Pharmaceutical Codex," Eleventh Edition, The Pharmaceutical Press, London, 1979, pp. 112, 182, 215, 258, 299, 326, 400, 637 and 761.
2. Reynolds, J. E. F., *Editor*, "Martindale, The Extra Pharmacopoeia," Twenty-ninth Edition, The Pharmaceutical Press, London, 1989, pp. 906, 448, 1298, 908, 452, 1462, 910, 1598 and 1478.
3. Lau, O. W., Chan, K., Lau, Y. K., and Wong, W. C., *J. Pharm. Biomed. Anal.*, 1989, **7**, 725, and references cited therein.
4. Rao, E. V., Rao, G. R., Raghuveer, S., and Khadgapathi, P., *Analyst*, 1987, **112**, 871.
5. Gibbs, V., and Zaide, Z., *J. Pharm. Sci.*, 1984, **73**, 1248.
6. Carnevale, L., *J. Pharm. Sci.*, 1983, **72**, 196.
7. Leung, C.-P., and Law, C.-K., *Analyst*, 1989, **114**, 241.
8. Murtha, J. L., Julian, T. N., and Radebaugh, G. W., *J. Pharm. Sci.*, 1988, **77**, 715.
9. Hoover, J. M., Soltero, R. A., and Bansal, P. C., *J. Pharm. Sci.*, 1987, **76**, 242.
10. Bambagiotti-Alberti, M., Pinzauti, S., and Vincieri, F. F., *Pharm. Acta Helv.*, 1987, **62**, 175; *Anal. Abstr.*, 1987, **49**, 8E51.
11. Clarke, E. G. C., *Editor*, "Isolation and Identification of Drugs," Volume 1, The Pharmaceutical Press, London, 1974, pp. 255, 268, 289, 315, 327, 464 and 525.
12. Clarke, E. G. C., *Editor*, "Isolation and Identification of Drugs," Volume 2, The Pharmaceutical Press, London, 1975, p. 1011.

Paper 0/01425G
Received April 2nd, 1990
Accepted May 30th, 1990

Quantitative Analysis of Alkaloids From Cinchona Bark by High-performance Liquid Chromatography

David V. McCalley
Department of Science, Bristol Polytechnic, Frenchay, Bristol BS16 1QY, UK

A procedure has been developed for the extraction and quantitative analysis of the major alkaloids from Cinchona bark using high-performance liquid chromatography. The method uses a commercial octylsilyl-bonded column, recommended for basic compounds, in the reversed-phase mode. The method is reproducible (relative standard deviation approximately 4% for each alkaloid) and gives quantitative recovery of alkaloids added to bark samples (100–103%). A variety of different types of bark have been studied successfully in the validation scheme. The method can be extended to the analysis of some minor alkaloids which are of interest in the elucidation of the biosynthetic pathways of alkaloid production.

Keywords: *Cinchona alkaloid; high-performance liquid chromatography; basic compound*

The principal Cinchona alkaloids quinine (Qn), quinidine (Qd), cinchonine (Cn) and cinchonidine (Cd) are important compounds used in the pharmaceutical, food and drink industries. The spread of resistance to the synthetic drug chloroquine in the parasite *Plasmodium falciparum* has re-established quinine as an antimalarial drug; there is also interest in the antimalarial activity of other Cinchona alkaloids. Quinidine, a diastereoisomer of quinine, is widely used as an antiarrhythmic drug. Quinine is a major source of bitter flavouring in the food industry. Cinchona bark continues to be the source of these compounds, in the absence of a commercially viable synthetic route of production.[1] The structural formulae of some of the alkaloids found in Cinchona bark are given below.

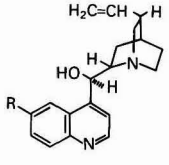

Qn, R = OCH_3
Cd, R = H

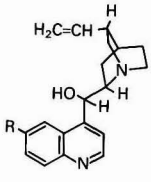

Qd, R = OCH_3
Cn, R = H

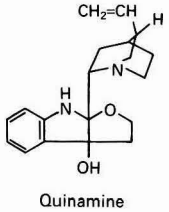

Quinamine

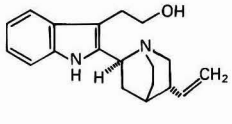

Cinchonamine

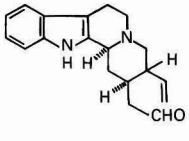

Corynantheal

The quantitative analysis of Cinchona bark has been performed for many years in order to ascertain its commercial value by the classical methods of titrimetry, gravimetry and polarimetry. More recently, the analysis of the Cinchona alkaloids has been reported using high-performance liquid chromatography (HPLC). High-performance LC procedures have been published using both normal phase systems with a silica column, and with reversed-phase systems primarily on octyl- or octadecylsilyl columns. Although normal phase systems can give excellent results,[2] reversed-phase systems are generally considered more convenient and the cost of the eluents is lower when large numbers of determinations are carried out.[3] However, reversed-phase chromatography is complicated by the high basicity of the alkaloids (pK_a value of quinine = 9.7[4]). This property can lead to severe peak tailing or even complete retention of the alkaloids, due to interaction with underivatised silanol groups that persist on the surface of these columns.[5] It is likely that ion-exchange interactions occur between protonated alkaloid and isolated highly acidic silanols, which are dissociated even at relatively low pH.[6]

In this paper further observations on the HPLC analysis of the Cinchona alkaloids using a column recommended for the analysis of basic compounds are reported. Detailed quantitative aspects of extraction and recovery of alkaloids from bark using HPLC analysis are also described; no papers appear to have dealt with this subject previously.

Experimental

The HPLC system, incorporating an Altex 100 pump, a Philips LC3 UV detector and a Rheodyne 7125 valve, was as used previously.[7] Column efficiency (N) and asymmetry factor (As) were calculated at half and 10% of peak height using a microcomputer data station. The principal column used was LiChrosorb RP-8 Select B, 5 μm, 25 × 0.4 cm i.d. (Merck, Darmstadt, FRG). Ten microlitre injections of sample were invariably used.

The phosphate eluent was prepared by dissolving 6.805 g of pure potassium dihydrogen orthophosphate in 425 cm^3 of distilled water, adjusting to pH 3.0 with concentrated phosphoric acid and mixing with 75 cm^3 of acetonitrile (HPLC grade, Fisons, Loughborough, Leicestershire, UK). This method of preparation resulted in a phosphate concentration slightly above 0.1 M although this was of no significance. The hexylamine phosphate buffer was prepared by pipetting 3.30 cm^3 of hexylamine into 460 cm^3 of distilled water, adjusting to pH 3.0 with concentrated phosphoric acid and mixing with 40 cm^3 of acetonitrile. When the solutions are prepared in this way, problems of buffer precipitation in the instrument are, to a great extent, avoided. To remove hexylamine from the column washing with distilled water followed by pure methanol until a stable baseline is obtained is recommended.

Quinine, quinidine and dihydroquinidine (HQd) were obtained from Fluka (Buchs, Switzerland), cinchonine and

cinchonidine from Sigma (Poole, Dorset, UK), dihydroquinine (HQn), dihydrocinchonine (HCn) and dihydrocinchonidine (HCd) from ACF Chemiefarma (Maarssen, The Netherlands). The Cn and Cd standards were found, by HPLC analysis, to contain significant amounts of the corresponding dihydro compounds (16 and 6%, respectively). These figures were taken into account in all quantitative work. The Qn and Qd standards contained <3% dihydro compounds and thus no correction factors were utilised.

Bark samples (ground and passed through a No. 30 BS sieve) and standards were dried in an oven at 80 °C to constant mass before use. In the general method 1 g of dried bark was ground with 0.3 g of $Ca(OH)_2$ and 3 cm^3 of 5% NaOH and left to stand for 0.5 h before extraction. Smaller masses of bark (100 mg) with proportional amounts of reagent were also used. Quantitative transfer into a Soxhlet thimble was facilitated by the use of a small volume of methanol, even if toluene was employed as the major extraction solvent. Samples were Soxhlet extracted for 7 h, using at least ten syphoning cycles per hour, with organic solvent. Small portions of extract (typically 50–100 μl) were evaporated to dryness under a stream of helium at room temperature and diluted with mobile phase (typically 0.5–1.0 cm^3).

Results and Discussion

HPLC Analysis of Alkaloids

In a previous report,[7] it was shown that the choice of reversed-phase column was critical for the analysis of Cinchona alkaloids. LiChrosorb RP-8 Select B, a column especially manufactured for the analysis of basic compounds, was shown to be amongst the few which give acceptable peak shapes in the absence of silanol masking agents incorporated in the eluent. Fig. 1(*b*) shows the good performance obtained with this column using a simple phosphate buffer. The efficiency of this 5-μm column averaged 10 000–11 000 plates with an asymmetry factor of 1.3–1.4 which represents an improvement on the equivalent 7-μm column previously tested.[7] The use of the masking agent hexylamine is obligatory for many other commercial reversed-phase columns which give severe peak tailing for basic compounds. Fig. 1(*a*) indicates that the use of hexylamine buffer with the LiChrosorb RP-8B column gives near perfect peak symmetry (*As* = 1.0–1.1) although a slight drop in efficiency was recorded (8 000–9 000 plates). Use of columns without a masking agent is recommended if possible as there is no requirement for washing after use (see under Experimental) in order to restore normal characteristics. A further advantage of the LiChrosorb RP-8B column is its good hydrolytic stability, as unusually, its performance for basic compounds seems to be unaffected by storage.[8]

Hermans-Lokkerbol *et al.*[9] suggest a modification of the original method, using the LiChrosorb RP-8B column with an eluent of 2% tetrahydrofuran (THF) added to an acetonitrile - 0.1 M potassium phosphate buffer containing 0.005 M hexylamine.[9] The THF was apparently added to improve peak shape, not to alter selectivity. However, the plate counts reported were about half those shown in the present study, indicating that the modification was unnecessary. The lower performance may be attributed, at least in part, to the use of larger injection volumes (up to 50 μl in a 100-μl loop) and flow above optimum, which can both degrade efficiency.[10]

The indole alkaloids quinamine (QAm) and cinchonamine (CnAm) are usually minor constituents of Cinchona bark and thus their analysis is rarely undertaken. However, these alkaloids are present in greater amounts in leaves, and along with the aldehyde corynantheal may be of significance in the study of the biosynthetic pathways of alkaloid production in cell cultures.[9] Both QAm and CnAm elute with an excellent peak shape in either buffer system using the LiChrosorb column. The retention of these indole alkaloids and corynantheal relative to the quinoline alkaloids is decreased by the addition of hexylamine; the amine concentration can be adjusted to give useful selectivity effects. Thus QAm (capacity factor, $k' = 4.4$) and corynantheal ($k' = 5.5$) elute between Cd ($k' = 3.4$) and Qd ($k' = 6.7$) when using 0.05 M hexylamine buffer; however, they elute after HQn in the non-hexylamine buffer thus removing the possibility of co-elution. (Values of k' for QAm, corynantheal and HQn: 9.2, 11.7 and 8.5, respectively.) With either isocratic buffer system CnAm has a long retention time ($k' > 25$; see also reference 11). A simple step-gradient analysis is recommended, increasing the acetonitrile content after the elution of HQn if the analysis of CnAm is to be performed routinely. For instance, the retention time of CnAm is only about 30 min with the simple phosphate buffer containing 20% acetonitrile. Isocratic systems in which the organic modifier concentration is high in order to reduce the retention time of CnAm (for instance by addition of the strong solvent THF) show a significant loss of resolution of the earlier eluting peaks.[9] The corynantheal peak is very broad in either buffer, with a column efficiency of <1000 plates. Caution is necessary in the analysis of compounds with carbonyl groups when using an eluent containing hexylamine owing to the possibility of the formation of a Schiff's base. It is possible that the hexylamine completely derivatises corynantheal, a theory which has been supported by mass spectral studies.

With some commercially available columns, the improvement in performance even after addition of 0.05 M hexylamine is rather limited. This would seem to indicate that some other factor contributes to the peak tailing of Cinchona alkaloids,

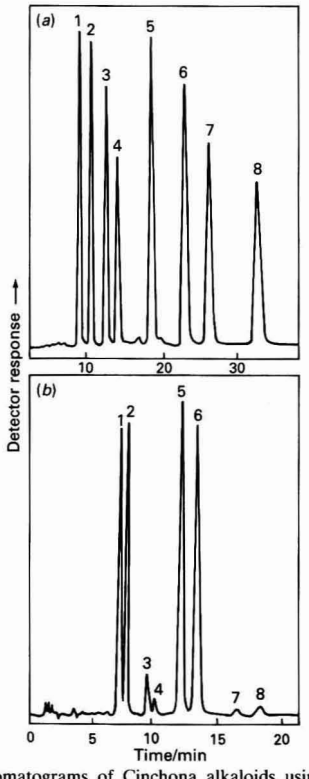

Fig. 1. Chromatograms of Cinchona alkaloids using LiChrosorb RP-8 Select B column. Peak identities: 1, Cn; 2, Cd; 3, HCn; 4, HCd; 5, Qd; 6, Qn; 7, HQd; and 8, HQn. Detection, 220 nm; sample volume, 10 μl; and flow-rate, 1 cm^3 min^{-1}. (*b*) Eluent 15% acetonitrile in 0.1 M phosphate buffer, adjusted to pH 3.0 with phosphoric acid. Approximately 250 ng of four major alkaloids showing dihydro impurities; (*a*) Eluent 8% acetonitrile in 0.05 M hexylamine adjusted to pH 3.0 with phosphoric acid. Approximately 250 ng each standard

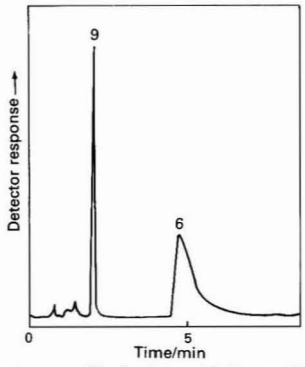

Fig. 2. Chromatogram of 9, nicotine and 6, Qn on pH stable alumina ODS column (10 cm, 3 μm). Eluent, acetonitrile - ammonia (55 + 45), pH 11.4

other than silanol group interaction. Recently, pH stable octadecylsilyl columns have become available which can be used with eluents at very high pH values at which the alkaloids are not protonated. Fig. 2 shows a chromatogram of quinine together with nicotine, another basic compound, on an alumina-ODS type column. Quinine still gives poor results; nicotine gives a much better peak shape, even though it is more basic ($pK_a = 11.0$[4]) than quinine. However, the stereochemistry of the basic group is likely to be important. It is possible that the Cinchona alkaloids might undergo detrimental interaction with metal ions in the column.[12] The study of such effects is hampered by the confidential nature of the commercial column specification and the necessity to destroy the column in order to analyse the packing.

Detection and Calibration of the System

A detection wavelength of 220 nm was generally used for the determination of the Cinchona alkaloids as this is in the region of their maximum ultraviolet absorbance. Cinchonamine and corynantheal also give strong absorbance in this region; although the maximum absorbance for QAm occurs nearer to 200 nm, it still has adequate absorbance at 220 nm. An indication of the purity of the peaks can be gained by monitoring the absorbance ratio at 220 nm and some other suitable wavelength (*e.g.*, 312 nm). The detector response *versus* concentration of solution injected was assessed over the range 0–100 mg l^{-1} for each of the principal Qn alkaloids using the hexylamine buffer system. Using peak height as a measure of detector response, the calibration graphs were linear over this range with correlation coefficients for Cn, Cd, Qd and Qn of 0.9999, 0.9999, 0.9998 and 0.9998, respectively. For peak-area measurements the correlation coefficients were 0.9999, 0.9997, 0.9999 and 0.9998, respectively. Calibration graphs for the simple phosphate buffer yielded similar values. In general, it was considered preferable to use peak-height measurements (from the data system) rather than peak area as they are less susceptible to potential interference from co-extracted material. Interference is rarely a problem with Cinchona bark extracts due to the relatively high alkaloid content (confirmed by studies using a photodiode array detector[13]) but this factor may be of significance when analysing the low levels of alkaloids typically found in cell culture samples.

Extraction of Alkaloids From Cinchona Bark

The Bruxelles standard method for pre-treatment and extraction of Cinchona bark[14] involves grinding and sieving, drying at 110 °C (at which temperature no loss of alkaloids was reported), treatment with alkali and finally Soxhlet extraction with benzene. However, this method was established for the subsequent determination of only two alkaloids (Cd and Qn)

Table 1. Evaluation of different solvents for Soxhlet extraction of Cinchona bark. (*Cinchona ledgeriana*). All results given as per cent. of bark, dry mass

Solvent	Cincho-nine	Cincho-nidine	Quinidine	Quinine
Toluene	<0.02	0.11	<0.02	0.58
TCA - methanol	0.23	1.10	0.15	6.37
$Ca(OH)_2$ - NaOH - methanol	0.21	1.09	0.15	6.34
$Ca(OH)_2$ - NaOH - toluene	0.22	1.11	0.16	6.20
Methanol	0.20	1.05	0.13	5.94

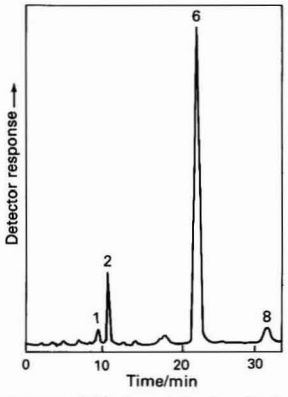

Fig. 3. Chromatogram of *Cinchona ledgeriana* bark after extraction with toluene - alkali. Peak identities and eluent as for Fig. 1(*a*)

whilst using classical methods; to our knowledge it has never been evaluated using HPLC. More recently Haznagy[15] has suggested that preliminary treatment of Cinchona bark with concentrated trichloroacetic acid (TCA) followed by ammonia solution, prior to Soxhlet extraction with benzene, gives increased recovery of alkaloids by possible partial denaturation of cellulose and by a type of ion-pair extraction mechanism. Haznagy compared a number of different extraction procedures, using classical methods to investigate the Qn content of the extracts. Table 1 shows the results obtained for the extraction of the four principal Cinchona alkaloids by using HPLC, for subsequent analysis. The bark sample extracted with toluene alone gave poor results which were attributed to the polar and basic nature of the alkaloids. However, addition of calcium hydroxide and sodium hydroxide prior to toluene extraction gave much higher results. Both methods with toluene gave pale yellow extracts indicating a low level of co-extracted material. Extraction with methanol after the addition of alkali gave similar values for alkaloid content, although extraction with methanol alone appeared to give slightly lower values. Both procedures using methanol gave deep yellow extracts although there was no evidence of interference in the chromatograms that were obtained subsequently. The pre-treatment method of Haznagy[15] followed by methanol extraction would seem an exhaustive procedure, however, alkaloid values did not appear to be higher. Furthermore, deep brown extracts were obtained, indicating the presence of large amounts of co-extractants. Reagent peaks can also produce serious interference with the analysis of Qn, thus this procedure is not recommended.

The results indicate that there is no apparent basis for modification of the traditional method of bark extraction. A typical chromatogram of bark extracted in this way is shown in Fig. 3. The use of this procedure, commercially, for the extraction of alkaloids from bark is another factor worth considering in adopting it for analytical purposes. However, other suitable solvent systems probably exist and ultrasonic

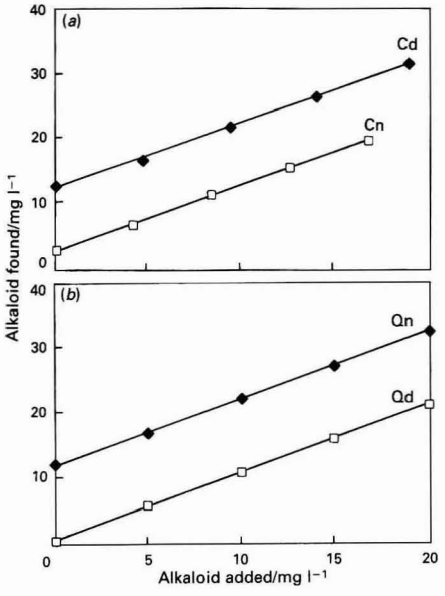

Fig. 4. Recoveries of alkaloids spiked into *Cinchona calisaya* bark. Peak identities and eluent as for Fig. 1(*b*). Recovery of (*a*) Cn and Cd; and (*b*) Qn and Qd

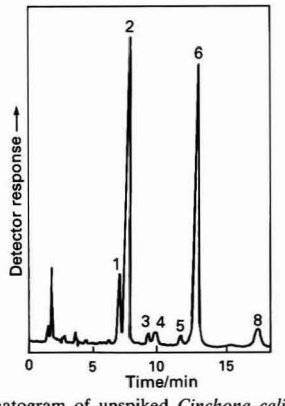

Fig. 5. Chromatogram of unspiked *Cinchona calisaya* bark after extraction with toluene - alkali. Peak identities and eluent as for Fig. 1(*b*)

extraction can provide a more rapid alternative to the Soxhlet method.[13]

Recovery Studies of Alkaloids From Bark

In order to validate further the methods used, 100-mg samples of a Cinchona bark (*Cinchona calisaya*) were spiked with amounts of Cn, Cd, Qd and Qn by the addition of a concentrated solution of the alkaloids. The solution was prepared by weighing out equal amounts of each solid and dissolving them in methanol. The presence of varying amounts of dihydro impurities in the standard compounds, resulted in a slightly different range of additions of pure standard compound. The samples were then extracted using the usual method. The endogenous levels of Cn, Cd, Qd and Qn in the original dry sample were 0.25, 1.23, 0.34 and 1.20%, respectively, with solution concentrations for HPLC analysis of 2.5, 12.3, 3.4 and 12.0 mg l^{-1}. Fig. 4 shows that the recovery of alkaloids over the range added (equivalent to 5–20 mg l^{-1} for Qn and Qd; 4.2–16.8 mg l^{-1} for Cn; and 4.7–18.8 mg l^{-1} for Cd) was linear. The mean recoveries for Cn, Cd, Qd and Qn obtained from the slopes of the lines were 101, 101, 103 and 100%, respectively, which indicates excellent performance. However, such additions can never simulate the exact occurrence of the alkaloids in bark and thus the results should be treated with some caution. Fig. 5 shows a chromatogram of the unspiked bark. Comparison with Fig. 3 shows clearly the natural variations in alkaloid content which can occur in different samples.

Table 2. Determination of the precision of bark extraction with toluene after alkali addition followed by HPLC. All results were calculated from extraction and analysis of five samples of homogenised *Cinchona succirubra* bark

Parameter	Cinchonine	Cinchonidine	Quinidine	Quinine
Mean (% of bark dry mass)	0.52	2.50	<0.03	3.73
Standard deviation, %	0.025	0.11	—	0.15
RSD, %	4.8	4.3	—	4.1

Assessment of Precision of the Analysis

In order to assess the precision of the analysis, a *Cinchona succirubra* sample was analysed repeatedly using extraction with toluene after alkali addition. The results are presented in Table 2. The precision of the entire analytical process for Cn, Cd and Qn in terms of the relative standard deviation (RSD) is about 4%. Unfortunately, it was not possible to calculate the relevant values for Qd due to the low endogenous levels of the compound in the sample. The precision of the analysis could probably be improved by the addition of an internal standard to the bark prior to extraction. Dihydroquinine has been recommended[9] but is clearly a significant constituent of the samples that were analysed in the present study. The selection of an internal standard is complicated by the large number of similar compounds present in Cinchona bark and the difficulty of simulating the occurrence of the compounds in the plant matrix.

The authors thank R. Verpoorte, University of Leiden, The Netherlands for the kind gifts of corynantheal, cinchonamine and quinamine, and ACF Chemiefarma, Maarssen, The Netherlands for gifts of the dihydroalkaloid standards. D. Millen, AFP Consultants, Reading, UK, is thanked for helpful discussions. The samples of bark were kindly provided by R. W. Walker, Fife, UK.

References

1. Verpoorte, R., Schripsema, J., and van der Leer, T., *in* Brossi, A., *Editor*, "The Alkaloids," Academic Press, San Diego, 1988, Volume 34, Chapter 6, p. 331.
2. McCalley, D. V., *J. Chromatogr.*, 1983, **260**, 184.
3. Wijnsma, R., and Verpoorte, R., *Cell Culture Somatic Cell Genetics Plants*, 1988, **5**, 335.
4. Budavari, S., *Editor*, "The Merck Index," Eleventh Edition, Merck, Rahway, NJ, 1989.
5. McCalley, D. V., *Chromatographia*, 1983, **17**, 264.
6. Cox, G. B., and Stout, R. W., *J. Chromatogr.*, 1987, **384**, 315.
7. McCalley, D. V., *J. Chromatogr.*, 1986, **357**, 221.
8. Engelhardt, H., and Jungheim, M., *Chromatographia*, 1990, **29**, 59.
9. Hermans-Lokkerbol, A., van der Leer, T., and Verpoorte, R., *J. Chromatogr.*, 1989, **479**, 39.
10. Meyer, V. R., *J. Chromatogr.*, 1985, **334**, 197.
11. Hamill, J. D., Robins, R. J., and Rhodes, M. J., *Planta Med.*, 1989, **55**, 354.
12. Ohtsu, Y., Shiojima, Y., Okumura, T., Koyama, J., Nakamura, K., Nakata, O., Kimata, K., and Tanaka, N., *J. Chromatogr.*, 1989, **481**, 147.
13. Wadley, I., and McCalley, D. V., unpublished work.
14. Lebrun, I., Warlet, M., and Schicharevitch, G., *Ind. Chim. Belge*, 1950, **15**, 328.
15. Haznagy, A., *Pharmazie*, 1976, **31**, 713.

Paper 0/00918K
Received February 28th, 1990
Accepted June 7th, 1990

Polymers With Reactive Functions as Sampling and Derivatising Agents

Part 1. Effective Sampling and Simultaneous Derivatisation of an Airborne Amine

Kazik Jedrzejczak and Virindar S. Gaind
Occupational Health Laboratory, Ontario Ministry of Labour, 101 Resources Road, Weston, Ontario M9P 3T1, Canada

A mixture of silica gel and a polymeric anhydride containing an *o*-acetylsalicyl group as the labelling moiety, was used for the collection and simultaneous derivatisation of airborne primary aliphatic amines, with *n*-butylamine as the model. The reaction product, *n*-butyl-*o*-acetylsalicylamide, was determined quantitatively by high-performance liquid chromatography using a reversed-phase column and ultraviolet detection at 220 nm. The lower limit of detection for *n*-butylamine was 1 μg and the detector response was linear between 10 and 1000 μg. The efficiency of sampling was confirmed using a Test Atmosphere Generation System.

Keywords: *High-performance liquid chromatography; sampling and simultaneous derivatisation of amines; polymeric anhydride; solid phase derivatisation*

Alkylamines have been employed extensively as corrosion inhibitors and as chemical intermediates in the production of polymers, pharmaceuticals and ion-exchange resins. The alkylamines are toxic via all routes of exposure, *i.e.*, inhalation, ingestion and through contact. The American Conference of Governmental Industrial Hygienists (ACGIH) has adopted a Threshold Limit Value-Time Weighted Average (TLV-TWA) in the range 5–10 p.p.m. for various volatile alkylamines.[1] The lower aliphatic amines have been determined quantitatively using gas chromatography (GC) or high-performance liquid chromatography (HPLC) after derivatisation.[2] However, due to their reactivity, potential for adsorption on solid surfaces, oxidation and decomposition, the collection procedures employed in the existing sampling and analytical methods for trace determination of alkylamines have been inefficient.[3]

The National Institute of Occupational Safety and Health (NIOSH) recommends silica gel for the collection of aliphatic amines in the workplace followed by quantification with GC using a flame ionisation detector.[4] Charcoal,[5] acidified silica gel[6] and Tenax[7] in sorbent sampling tubes have also been employed for the collection of airborne amines. None of these sampling methods utilised derivatisation to stabilise the amines or to enhance their sensitivity. Some unsuccessful attempts have been made to use reagent-coated solid sorbents (chemisorption).[8] These sorbents were found to be impractical because of the problems encountered in removing the excess of reagent and the instability of the coating materials towards the passage of air through the tubes.

The present workers were intrigued by the absence of positive results for lower aliphatic amines in most of the field samples collected on silica-gel tubes and analysed by GC. Also, poor and erratic recoveries of alkylamines from silica gel and other sorbents were encountered, especially after air was passed through the sampling tubes spiked with the amine standards, indicating the need for stabilising the amines during sample collection.

This paper describes the development of a solid sorbent sampler containing a polymer-bound anhydride [P-ASA, Fig. 1(*a*)] combined with silica gel. The P-ASA derivatises the amines "*in situ*" during sample collection, yielding a stable and non-volatile product which can be determined quantitatively using HPLC with UV detection. The advantages of using polymeric reagents for derivatisation are: (*i*) in contrast to unbound coating materials, polymers are non-volatile and unaffected by the passage of air; (*ii*) the stability of anhydrides is enhanced following their immobilisation on polystyrene; (*iii*) derivatisation occurs *in situ* during the collection of samples; (*iv*) reactions on a polymeric support are often more selective and give fewer side products; (*v*) the excess of reagent helps achieve a greater reaction yield; and (*vi*) the problem of removing the excess of derivatising reagent from the reaction mixture is eliminated.

The efficacy of the P-ASA + silica gel sorbent as a collecting medium and a derivatising reagent for airborne *n*-butylamine, was established by conducting tests on a Test Atmosphere Generation System (TAGS), which simulates real sampling conditions. Earlier, Chou *et al.*[9] used P-ASA for off-line derivatisation of primary and secondary amines.

Experimental

Reagents

Chloromethylated polystyrene (4.2 mequiv. g^{-1}) was obtained from Bio-Rad Labs. (Richmond, CA, USA) and trichloromethylchloroformate (diphosgene) was supplied by Fluka Chemical (Ronkonkoma, NY, USA). All aliphatic amines, acetylsalicylic acid and salicylic acid were from Aldrich Chemical (Milwaukee, WI, USA). These chemicals were of the highest purity available and were used without further purification.

All solvents were of glass-distilled quality and purchased from the Caledon Laboratory (Georgetown, Ontario, Canada). Water was doubly distilled after treatment with $KMnO_4$.

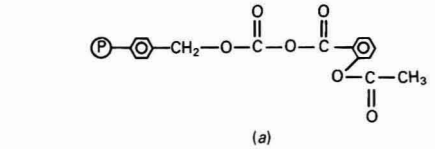

(*a*)

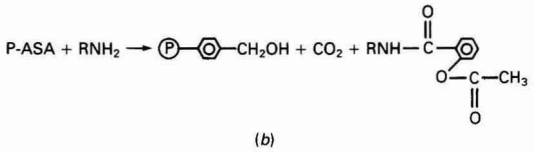

(*b*)

Fig. 1. (*a*) Structure of P-ASA; (*b*) reaction of P-ASA with the amine. Ⓟ = Polystyrene backbone

Apparatus

Bendix Model 44 air sampling pumps were used. The air sampling silica-gel tubes (Catalogue No. 226-10-06), Tenax tubes (Catalogue No. 226-35-03), XAD-2 (Catalogue No. 226-30) and XAD-7 tubes (Catalogue No. 226-30-12-07) were obtained from SKC (Eighty Four, PA, USA). The HPLC system consisted of a Spectra-Physics Model SP 8100 liquid delivery unit equipped with an auto-injector, an SP 4100 data system and an SP 8400 variable wavelength UV detector. The gas chromatograph - mass spectrometer was a Hewlett-Packard Model HP 5985 with an HP 7920 data system.

The Test Atmosphere Generation System (TAGS) was from SRI (Menlo Park, CA, USA). It can generate up to 12 uniformly loaded samples from a dynamically generated test atmosphere.

Synthesis and Characterisation of the Polymeric Anhydride P-ASA

The polymeric anhydride containing the *o*-acetylsalicyl group (P-ASA) was prepared from chloromethylpolystyrene, as previously described by Martin *et al.*,[10] with the modifications that were more easily manageable. Trichloromethylchloroformate was substituted for phosgene and the polymer was washed extensively with acetonitrile until the filtrate gave no absorbance at 220 nm.

The amount of labelling moiety in 1 g of the polymeric support was determined by saponification of the latter and quantification of the amount of salicylic acid formed using HPLC.[11] The HPLC conditions for the determination of salicylic acid were as follows: mobile phase, water - acetonitrile (50 + 50, v/v, pH 3 adjusted with 80% phosphoric acid); flow-rate, 1.0 ml min^{-1}; C_{18} reversed-phase column; and UV detector, 254 nm. The average calculated loading was 1.3 mequiv. g^{-1}, which indicated that for 1 g of the final polymeric reagent, there were 1.3 milliequiv. of the *o*-acetylsalicyl group attached.

In situ Derivatisation Reaction of Amine and P-ASA With HPLC Determination of the Derived Amide

The derivatisation reaction between the polymeric anhydride P-ASA and *n*-butylamine [Fig. 1(*b*)] collected or spiked on a sorbent was worked up by the addition of 1.0 ml of acetonitrile to the sorbent placed in a glass vial. The vial was crimp-sealed with a PTFE-lined cap and then maintained at 60 °C for 15 min. An aliquot of acetonitrile solution was withdrawn and injected into a high-performance liquid chromatograph operating under the following conditions: column, Brownlee Labs., 250 × 4.6 mm stainless-steel containing Spheri-10 RP-18, 10 μm; detector, wavelength λ = 220 nm; mobile phase, acetonitrile + water (30 + 70) at 1.0 ml min^{-1}; injection volume, 20 μl.

A typical chromatogram obtained under the above conditions is shown in Fig. 2 and represents 10 μg of *n*-butylamine [retention time (RT) = 4.3 min]. The least amount of *n*-butylamine which could be reproducibly detected after the derivatisation reaction was 1.0 μg. The linearity of the detector response and optimum amount of P-ASA required for derivatising 0.1 mg of *n*-butylamine was established under the conditions described above.

Preparation of Sample Collection Tubes

For the evaluation of P-ASA as a sample collecting sorbent, tubes were made with P-ASA mixed with silica gel, Tenax, XAD-2 and XAD-7. The mixed sorbents were prepared by blending 1 g of each sorbent with 0.1 g of P-ASA in an agate mortar.

All sampling tubes were made of glass (70 mm in length and 4 mm i.d.) and contained two sections of the sorbent. The front section of each sampling tube contained 100 mg and the back section 50 mg, of the prepared sorbent. The two sections were separated with a urethane foam plug and the ends were closed with silanised glass wool plugs.

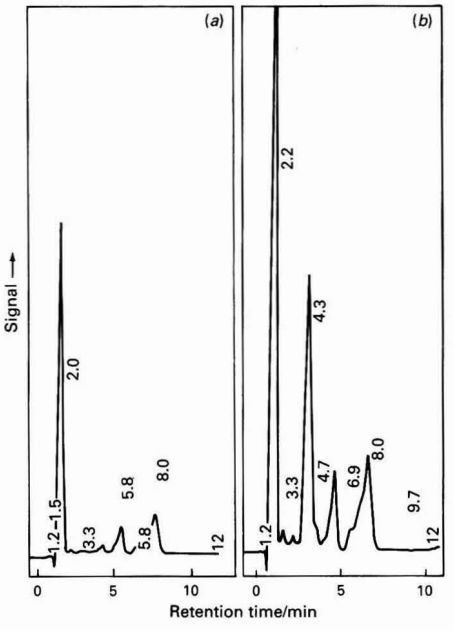

Fig. 2. Liquid chromatogram of *n*-butylamine derivative (10 μg) after collection on silica gel + P-ASA resin mixture (10 + 1). (*a*) Blank and (*b*) sample. Column, Spheri-10 RP-18, 10 μm; UV detector, wavelength λ = 220 nm; mobile phase, acetonitrile - water (30 + 70) at 1.0 ml min^{-1}

Recovery of Spiked *n*-Butylamine on Various Sorbents

For evaluation of the recovery of spiked *n*-butylamine and the effect of the passage of air through the tube, a known amount of *n*-butylamine (*i.e.*, 20 and 100 μg) was injected into the front sections of replicate sampling tubes containing silica gel and tubes prepared with the mixed sorbent, *i.e.*, (10 + 1, silica gel + P-ASA). Air (4 l at 0.2 l min^{-1}) was drawn through one of each set of tubes, while no air was drawn through the second set of spiked tubes. The amount of *n*-butylamine in both sections of each tube was determined quantitatively.

For work-up of the silica-gel tubes, 1.0 ml of acetonitrile was added to the silica gel with 10 mg of P-ASA followed by the usual work-up, before analysis. This step was omitted for sampling tubes containing silica gel + P-ASA mixture.

The amount of *n*-butylamine remaining on the sorbent after the passage of air through the tube was expressed as recovery (%).

Evaluation of Sample Collection Efficiency Through TAGS

The efficiency of sample collection under real conditions was assessed by connecting various sampling tubes to the outlets of the TAG system during operation in order to generate a uniform atmosphere of *n*-butylamine. The TAG system had 12 sampling outlets each with a sample flow-rate of 0.2 l min^{-1}. Sample was generally collected for 20 min (4 l). The sorbent in both sections of each tube was analysed for *o*-acetylsalicylamide.

Using this system, the collection efficiency of airborne *n*-butylamine on P-ASA mixed with silica gel was compared with other sorbents, *i.e.*, Tenax, XAD-2 and XAD-7. In addition, the stability of the collected amine on mixed P-ASA + silica-gel sorbent was confirmed.

Results and Discussion

Precision and Linearity of the Derivatisation Reaction

The linearity and precision of the derivatising reaction of *n*-butylamine with the mixed P-ASA + silica gel sorbent was established by reacting 10, 50, 100, 500 and 1000 μg of *n*-butylamine with an excess of P-ASA reagent and quantifying the derivative formed. The results obtained from ten replicates at each level are summarised in Table 1.

The relative standard deviation ranged between 2.83 and 6.07%, showing that the reaction is highly reproducible under the conditions used. The average peak-area data also show that the derivatising reaction was linear in the range 10–1000 μg of amine.

Mass Spectra of *n*-Butyl-*o*-salicylamide

The identity of the amide was confirmed via electron impact mass spectrometry which showed the base peak at *m/z* 121 and molecular ion at *m/z* 235. The chemical ionisation (CI) spectrum obtained with methane as the reagent gas yielded the molecular ion peak at *m/z* 236 (M + 1) as the base peak. Other characteristic peaks at *m/z* 264 (M + 29) and *m/z* 276 (M + 41) were also discernible. Selective ion monitoring (SIM) could be used to quantify 1.0 μg of the derivative.

Recovery of *n*-Butylamine Spiked on Sorbents

The results for the recovery of *n*-butylamine spiked on the front sections of tubes containing silica gel and a mixture of silica gel + P-ASA sorbent after passage of 4 l of air are given in Table 2. When spiked with 20 μg the tubes containing mixed silica gel + P-ASA showed an average recovery of 98.5% compared with 10.0% for silica-gel tubes. When spiked with 100 μg, the recovery of *n*-butylamine was 96.8% for the mixed sorbent, compared with 34.1% for silica gel, showing that *n*-butylamine collected on silica gel is not stable on exposure to air. However, when mixed with 10% P-ASA, the spiked amine was stabilised through its reaction with the latter leading to considerably improved recoveries of amine.

Optimisation of the Amount of P-ASA Resin for Derivatisation

Table 3 shows the effect of adding incremental amounts of P-ASA (2.0–50 mg) to an acetonitrile solution (1.0 ml) of *n*-butylamine (0.1 mg). After the usual work up, the peak area, due to the derivative formed, increased significantly when the amount of P-ASA was increased from 2 to 10 μg. Further increases in the amount of P-ASA used did not enhance the peak area and gave no advantage in terms of reaction yields. It was decided to use 10 mg of P-ASA to effect the derivatisation of a typical sample of amine.

Validation of Optimised P-ASA : Silica Gel Ratio Using TAGS

The minimum practical amount of sorbent needed to prepare the sampling tube was about 100 mg, for the front section. In order to confirm the optimised amount of P-ASA for use in the preparation of the sorbent sampling tubes, P-ASA was mixed with silica gel in various ratios and the mixed sorbents evaluated with respect to sample collection efficacy using TAGS.

The results in Table 4 show that the optimum ratio of P-ASA to silica gel was 10 : 100 which gave no breakthrough of the amine during sample collection. Increasing the amount of P-ASA did not improve the sample collection significantly, but gave higher background peaks.

This further confirmed that the 10 : 100 ratio for P-ASA to silica gel, optimised through spiking was effective for the collection of airborne amines.

Evaluation of Other Solid Sorbents Mixed With P-ASA

In a sampling experiment conducted using TAGS, P-ASA resin mixed with silica gel was compared with other similar mixtures containing XAD-2, XAD-7 and Tenax.

Table 5 summarises the results for *n*-butylamine collected on the front and back sections of the tubes containing different mixtures of P-ASA and also P-ASA alone. The mixture of silica gel + P-ASA resin (10 : 1) yielded maximum recovery with negligible breakthrough of the amine from the front section even when the amount of amine collected was above

Table 1. Precision and linearity of the *n*-butylamine - P-ASA reaction (n = 10)

Amount of amine/μg	Average area, arbitrary units	Relative standard deviation, %
10.0	9718	2.83
50.0	48490	3.79
100.0	96180	5.98
500.0	502230	4.65
1000.0	1006460	6.07

Table 2. Recovery of *n*-butylamine spiked on various sorbents

Sorbent	Amount of amine added/μg	Amount of amine found/μg	Average recovery, %
Silica gel + P-ASA tubes (10 + 1) . .	20.0	20.7	98.5
		20.0	
		19.3	
	100.0	93.0	96.8
		106.2	
		91.3	
Silica-gel tubes . .	20.0	3.1	10.0
		1.3	
		1.7	
	100.0	31.5	34.1
		30.5	
		40.2	

Table 3. Optimisation of the P-ASA - *n*-butylamine reaction

Amount of P-ASA added/mg	Average area, arbitrary units
2.0	2262041
5.0	2359451
10.0	3018475
20.0	3087032
30.0	3001797
50.0	3143264

Table 4. Collection of amine vapours on a mixture of silica gel + P-ASA with different ratios

Silica gel : P-ASA resin ratio/mg	Tube No.	Amount of amine	
		Front/μg	Back/μg
100 : 1	1	111.9	3.9
	2	107.0	—*
	3	133.8	7.1
100 : 5	4	121.8	1.0
	5	93.2	0.1
	6	135.5	0.1
100 : 10	7	109.5	—*
	8	137.5	—*
	9	131.5	—*
100 : 20	10	135.7	—*
	11	123.9	0.6
	12	132.5	—*

* Less than 1.0 μg.

Table 5. Collection of *n*-butylamine vapours on different sorbents mixed with P-ASA

Collection sorbent	Tube No.	Amount of amine Front/μg	Back/μg
Silica gel + P-ASA resin (10 : 1) . .	1	640.2	0.4
	2	645.0	—*
	3	616.5	—*
Tenax + P-ASA resin (10 : 1) . .	4	14.5	15.9
	5	3.3	12.6
	6	12.5	5.8
XAD-2 + P-ASA resin (10 : 1) . .	7	8.6	25.1
	8	78.2	1.7
	9	5.1	0.6
XAD-7 + P-ASA resin (10 : 1) . .	10	—*	6.1
	11	—*	—*
	12	—*	—*
P-ASA resin	13	8.4	8.2
	14	9.6	7.0
	15	10.5	7.4

* Less than 1.0 μg.

Table 6. Comparison of collection of amine vapours on mixed sorbent *versus* silica-gel tubes

Sorbent	Tube No.	Amount of amine Front/μg	Back/μg
Silica gel + P-ASA tubes (10 : 1) . .	1	143.3	—*
	2	158.6	—*
	3	196.7	—*
	4	157.0	—*
	5	152.6	—*
	6	132.3	—*
Silica-gel tubes	7	32.1	—*
	8	44.3	—*
	9	31.7	—*
	10	33.3	0.6
	11	29.5	0.2
	12	37.3	—*

* Less than 1.0 μg.

600 μg. The precision of the amine found in the front section was also good. Further work was carried out on this mixed sorbent only.

The efficiency of samples collected using tubes containing silica gel + P-ASA was compared with silica-gel tubes in a TAGS test. Six of the tubes contained silica gel only and the other six had the mixture of silica gel + P-ASA resin.

The results of the analyses in Table 6 show that the amount of *n*-butylamine collected on sampling tubes containing P-ASA + silica-gel mixture, in which the amine reacted with polymeric anhydride during collection, was consistently higher showing the superiority of P-ASA + silica gel as a collecting medium for airborne amines.

Storage Stability

The stability of the (amine + P-ASA) reaction product was assessed by spiking the mixed sorbent tubes with 20 μg of *n*-butylamine and then storing at 4 °C for various periods of time. The amide formed was quantified after storing both types of tubes for 0, 3, 7, 10 and 14 d. The amount of amine recovered is given in Table 7. It was found that the *n*-butylamine was stable on the mixed sorbent for at least 14 d with recoveries in the range 76–100%.

Table 7. Stability of *n*-butylamine spiked on mixed sorbent tubes

Day sample was analysed	Amount of amine added/μg	Amount of amine found/μg	Average recovery, %
0	20.0	20.0	
0	20.0	20.0	100.0
3	20.0	20.0	
3	20.0	20.0	100.0
7	20.0	17.9	
7	20.0	17.5	89.0
10	20.0	16.8	
10	20.0	16.5	83.0
14	20.0	15.2	
14	20.0	15.4	76.0

Conclusions

Polymeric anhydride (P-ASA) mixed with silica gel provides an efficient solid sorbent for the collection and *in situ* derivatisation of airborne amines. The proposed method of sample collection stabilises the volatile analyte and attaches a chromophore to the non UV absorbing amine, making it amenable to a sensitive and specific HPLC quantification.

Work on other polymers with reactive functions capable of simultaneous sample collection, and derivatisation of highly reactive airborne chemicals, will be reported later.

The authors thank M. A. Nazar, Chief Scientist, Occupational Health Laboratory of Ontario Ministry of Labour, for helpful suggestions during the preparation of this manuscript. G. E. Garreton provided technical assistance in the initial stages of this project.

References

1. "Threshold Limit Values and Biological Exposure Indices for 1988–89," American Conference of Governmental Industrial Hygienists, Cincinnati, OH, 1989.
2. Knapp, D. R., "Handbook of Analytical Derivatisation Reactions," Wiley-Interscience, New York, pp. 65–145.
3. Pellizzari, E. D., and Krost, J. K., *Anal. Chem.*, 1984, **56**, 1813.
4. "Manual of Analytical Methods," Volume 6, Method No. S148, and Volume 1 Method No. P & CAM 221, National Institute of Occupational Safety and Health, Cincinnati, OH, 1981.
5. Fuselli, S., Benedetti, G., and Mastrangeli, R., *Atmos. Environ.*, 1982, **16**, 2943.
6. Bouyoucos, S. A., and Melcher, R. G., *Am. Ind. Hyg. Assoc. J.*, 1983, **44**, 119.
7. Fitzpatrick, M. R., Warner, P. O., Thiel, D. P., Lubs, P. L., and Kerfoot, E. J., *Am. Ind. Hyg. Assoc. J.*, 1983, **44**, 425.
8. Andersson, K., Hallgren, C., Levin, J. O., and Nilsson, C. A., *Am. Ind. Hyg. Assoc. J.*, 1985, **46**, 225.
9. Chou, T. Y., Collagen, S. T., Kao, M. D., Krull, I. S., Dorschel, C., and Bidlingmeyer, B., *J. Chromatogr.*, 1986, **367**, 335.
10. Martin, G. E., Shambhu, B., Shakhshir, S. R., and Degenis, G. A., *J. Org. Chem.*, 1978, **43**, 4571.
11. Gao, C.-X., Chou, T.-Y., Colgan, S. T., Krull, I. S., Dorschel, C., and Bidlingmeyer, B., *J. Chromatogr. Sci.*, 1988, **26**, 449.

Paper 0/01675F
Received April 17th, 1990
Accepted June 4th, 1990

6,7-Dimethoxy-1-methyl-2(1*H*)-quinoxalinone-3-propionylcarboxylic Acid Hydrazide: A Highly Sensitive Fluorescence Derivatisation Reagent for Carboxylic Acids in High-performance Liquid Chromatography

Masatoshi Yamaguchi, Tetsuharu Iwata, Kouji Inoue, Shuuji Hara and Masaru Nakamura
Faculty of Pharmaceutical Sciences, Fukuoka University, Nanakuma, Jonan-ku, Fukuoka 814-01, Japan

6,7-Dimethoxy-1-methyl-2(1*H*)-quinoxalinone-3-propionylcarboxylic acid hydrazide was found to be a highly sensitive fluorescence derivatisation reagent for carboxylic acids in high-performance liquid chromatography. The reaction conditions were optimised for various C_5–C_{20} saturated fatty acids. The reagent readily reacted with the fatty acids in aqueous solution in the presence of pyridine and 1-ethyl-3-(3-dimethylaminopropyl)carbodiimide at room temperature to produce the corresponding fluorescent derivatives, which were separated on a reversed-phase column, Biofine RPC-SC 18 B, by gradient elution with 40–100% aqueous methanol. The derivatives were detected spectrofluorimetrically at 447 nm with excitation at 365 nm. The detection limits (signal to noise ratio = 3) for the acids were 3–6 fmol for an injection volume of 10 μl. The reagent was also applied to the derivatisation of some metabolites of arachidonic acid.

Keywords: *6,7-Dimethoxy-1-methyl-2(1-H)-quinoxalinone-3-propionylcarboxylic acid hydrazide; fluorescence detection; carboxylic acid; high-performance liquid chromatography*

Various fluorescence derivatisation reagents have been proposed for the determination of carboxylic acids by high-performance liquid chromatography (HPLC). Most of the reagents have coumarin,[1–5] phenanthrene,[6–8] anthracene,[9–11] pyrene[12,13] or dimethylaminonaphthalene moieties[14–16] as the fluorophore, and halogenomethyl and halogenoacyl,[1–3,6,9,12] amino,[7,8,16] hydrazino,[14] hydroxy[4,10,15] and diazomethyl[5,11,13] groups as the reactive group towards carboxylic acids. It has been previously reported[17] that the 6,7-dimethoxy-1-methyl-2(1*H*)-quinoxalinone (DMEQ) moiety fluoresces intensely, and hence, 3-bromomethyl-DMEQ has been proposed as a highly sensitive fluorescence derivatisation reagent for carboxylic acids in HPLC. However, these reagents generally require dried aprotic solvents, higher temperatures and prolonged heating in the derivatisation reaction. An ultraviolet derivatisation reagent, 2,4-dinitrophenylhydrazine, was developed to overcome the problems described above.[18] The reagent reacted with carboxylic acids in aqueous solution using 1-ethyl-3-(3-dimethylaminopropyl)carbodiimide (EDC) as the coupling agent to give the corresponding acid hydrazides. However, the HPLC method with this reagent has limited sensitivity.

In this paper, the synthesis of two DMEQ carboxylic acid hydrazides (reagents **III** and **VI** in Table 1) is reported and the reaction of the reagents with fatty acids was examined as part of a survey of effective fluorescence derivatisation reagents for carboxylic acids. Hence, 6,7-dimethoxy-1-methyl-2(1*H*)-quinoxalinone-3-propionylcarboxylic acid hydrazide (reagent **III**) was developed as a sensitive fluorescence derivatisation reagent for carboxylic acids. The reagent readily reacts with carboxylic acids in aqueous solution in the presence of pyridine and EDC at room temperature to produce intensely fluorescent DMEQ derivatives. The derivatisation reaction was also applied to some metabolites of arachidonic acid.

Table 1. Compound, reagent and product structures

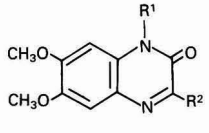

Compound, reagent and product	R^1	R^2
I	H	CH_2CH_2COOH
II	CH_3	$CH_2CH_2COOCH_3$
III	CH_3	$CH_2CH_2CONHNH_2$
IV	H	COOH
V	CH_3	$COOCH_3$
VI	CH_3	$CONHNH_2$
VII	CH_3	$CH_2CH_2CONHNHCO(CH_2)_{16}CH_3$
VIII	CH_3	$CONHNHCO(CH_2)_{16}CH_3$

Experimental

Apparatus

Uncorrected fluorescence spectra and intensities were measured with a Hitachi 650-60 spectrofluorimeter (Tokyo, Japan) in 1-cm quartz cells; spectral bandwidths of 10 nm were used in both the excitation and emission monochromators. Proton nuclear magnetic resonance (^{1}H NMR) spectra were obtained with a Hitachi R-90H spectrometer at 90 MHz using a *ca* 5% solution of *N*,*N*-dimethylformamide-d_7 and dimethyl sulphoxide-d_6 containing tetramethylsilane as an internal standard (abbreviations used: s, singlet; t, triplet; m, multiplet; and br, broad). Field desorption mass spectra (MS) were recorded on a JEOL DX-300 spectrometer (Tokyo, Japan).

Chemicals

All chemicals were of analytical-reagent grade unless stated otherwise. Distilled, de-ionised water was used. Valeric (C_5), caproic (C_6), caprylic (C_8), capric (C_{10}), lauric (C_{12}), myristic (C_{14}), palmitic (C_{16}), margaric (C_{17}), stearic (C_{18}) and arachidic (C_{20}) acids, thromboxane B_2, prostaglandin B_2 and leukotriene B_4 were purchased from Sigma (St. Louis, MO, USA). Stock solutions of the C_5–C_{20} acids (1×10^{-4} M) were prepared in *N*,*N*-dimethylformamide and diluted further with water to give the required concentrations. Thromboxane B_2, prostaglandin B_2 and leukotriene B_4, commercially supplied as solutions in ethanol, were diluted directly with water to the desired concentrations before use. 1,2-Diamino-4,5-dimethoxybenzene (DDB) was prepared as described previously[19]; it is now commercially available from Dojindo Laboratories (Kumamoto, Japan).

Synthesis of Reagents III and VI

Reagent **III**

Compound **I** (Table 1) was prepared by the reaction of α-ketoglutaric acid with DDB as described previously.[20] Compound **I** (1.5 g) dissolved in 100 ml of anhydrous methanol was treated with an ethereal diazomethane solution prepared by the established method.[21] The reaction mixture was evaporated to dryness *in vacuo*. The residue, dissolved in 30 ml of chloroform, was purified by column chromatography (25 × 3.5 cm i.d. column) on silica gel 60 (*ca.* 139 g, 70–230 mesh; Japan Merck, Tokyo, Japan) with hexane - ethyl acetate (1 + 1) as eluent to give compound **II** (0.92 g, 62%).

Compound **II** (0.9 g) was dissolved in 100 ml of aqueous 45% hydrazine hydrate and the mixture was heated at 100 °C for *ca.* 60 min. The resulting precipitate was recrystallised from ethanol to give reagent **III** (0.72 g, 80%).

Reagent **VI**

Compound **IV** was prepared by the reaction of α-ketomalonic acid with DDB as described previously.[22] Reagent **VI** was synthesised via compound **V** by treating compound **IV** (1.5 g) in the same manner as described for reagent **III**. Reagent **VI** (0.9 g, 60%) was recrystallised from ethanol.

Reagents **III** and **VI** were stable in the crystalline state for 1 year or longer even in daylight. The reagents dissolved in *N,N*-dimethylformamide could be used for at least 2 weeks.

Products of the Reaction of Stearic Acid With Reagents III and VI

Reagent **III** (or **VI**) (500 mg), stearic acid (462 mg) and EDC (314 mg) were dissolved in 100 ml of 2% pyridine in ethanol and the mixture was allowed to stand at room temperature for 3 h. The mixture was evaporated to dryness under reduced pressure. The residue, dissolved in a small amount of ethyl acetate, was chromatographed on a silica gel 60 column (25 × 2.5 cm i.d., *ca.* 75 g, 70–230 mesh) with the same solvent. The main fraction was evaporated to dryness and the residue was recrystallised from ethanol to give product **VII** (0.4 g, 42%) [or product **VIII** (0.4 g, 44%)].

Compound, Reagent and Product Characterisation

Compound **II**

Colourless needles. M.p. 178–179 °C. ^{1}H NMR (Me_2NCHO-d_7): δ (p.p.m.) 2.85 (t, J = 7 Hz, 2H), 3.13 (t, J = 7 Hz, 2H), 3.66 (s, 3H), 3.72 (s, 3H), 3.92 (s, 3H), 4.02 (s, 3H), 7.09 (s, 1H), 7.27 (s, 1H). Elemental analysis: calculated for $C_{15}H_{18}N_2O_5$: C, 58.82; H, 5.92; N, 9.15%; found: C, 58.94; H, 5.87; N, 9.19%. MS: *m/z* 306 (M^+).

Reagent **III**

Colourless needles. M.p. 205–206 °C. ^{1}H NMR (Me_2NCHO-d_7): δ (p.p.m.) 2.63 (t, J = 7 Hz, 2H), 3.12 (t, J = 7 Hz, 2H), 3.71 (s, 3H), 3.92 (s, 3H), 4.02 (s, 3H), 3.4–4.4 (br, 2H), 7.08 (s, 1H), 7.28 (s, 1H), 8.9–9.1 (br, 1H). Elemental analysis: calculated for $C_{14}H_{18}N_4O_4$: C, 54.90; H; 5.92; N, 18.29%; found: C, 55.01; H, 5.73; N, 18.27%. MS: *m/z* 306 (M^+).

Compound **V**

Pale yellow needles. M.p. 163–164 °C. ^{1}H NMR (Me_2SO-D_6): δ (p.p.m.) 3.80 (s, 3H). 3.96 (s, 3H), 4.03 (s, 3H), 4.07 (s, 3H), 6.72 (s, 1H), 7.38 (s, 1H). Elemental analysis: calculated for $C_{13}H_{14}N_2O_5$; C, 56.12; H, 5.04; N, 10.07%; found: C, 56.13; H, 5.04; N, 9.98%. MS: *m/z* 278 (M^+).

Reagent **VI**

Orange powder. M.p. 276–278 °C. ^{1}H NMR (Me_2NCHO-d_7): δ (p.p.m.) 3.7–3.9 (br, 2H), 3.75 (s, 3H), 3.97 (s, 3H), 4.09 (s, 3H), 7.47 (s, 1H), 7.90 (s, 1H), 9.0–9.2 (br, 1H). Elemental analysis: calculated for $C_{12}H_{14}N_4O_4$; C, 51.80; H, 5.05; N, 20.13%; found: C, 51.70; H, 5.15; N, 20.18%. MS: *m/z* 278 (M^+).

Product **VII**

Colourless needles. M.p. 194–196 °C. ^{1}H NMR (Me_2NCHO-d_7): δ (p.p.m.) 0.76 (t, J = 7 Hz, 3H), 1.16 (s, 28H), 1.3–1.7 (m, 2H), 2.11 (t, J = 7 Hz, 2H), 2.53 (t, J = 7 Hz, 2H), 3.01 (t, J = 7 Hz, 2H), 3.60 (s, 3H), 3.81 (s, 3H), 3.90 (s, 3H), 6.97 (s, 1H), 7.24 (s, 1H), 9.4–9.6 (br, 2H). Elemental analysis: calculated for $C_{32}H_{52}N_4O_5$: C, 67.10; H, 9.15; N, 9.78%; found: C, 67.02; H, 9.30; N, 9.73%. MS: *m/z* 572 (M^+).

Product **VIII**

Orange powder. M.p. 192–194 °C. ^{1}H NMR (Me_2NCHO-d_7): δ (p.p.m.) 0.76 (t, J = 7 Hz, 3H), 1.1–1.8 (m, 32H), 3.61 (s, 3H), 3.82 (s, 3H), 3.92 (s, 3H), 6.88 (s, 1H), 7.25 (s, 1H), 9.4–9.6 (br, 2H). Elemental analysis: calculated for $C_{30}H_{48}N_4O_5$: C, 65.38; H, 9.08; N, 10.52%; found: C, 65.28; H, 9.00; N, 10.34%. MS: *m/z* 544 (M^+).

Derivatisation Procedure

To 100 μl of a test solution of fatty acids in water were added 50 μl each of 2 M EDC and 10% pyridine (both in water) and 100 μl of 4.9 mM reagent in *N,N*-dimethylformamide. The mixture was warmed at room temperature (15–30 °C) for 15 min and then a portion (100 μl) was injected into the chromatograph. For the reagent blank, 10 μl of water in place of 100 μl of the test solution were subjected to the same procedure.

HPLC Apparatus and Conditions

A Waters 510 high-performance liquid chromatograph equipped with a U6K universal injector (10-μl loop) and a Hitachi F1000 fluorescence spectrometer equipped with a 12-μl flow cell operated at an excitation wavelength of 365 nm and an emission wavelength of 447 nm were used. The column temperature was ambient (20–27 °C). For the separation of the DMEQ derivatives of fatty acids, a gradient elution was carried out by using a Hitachi 833A solvent gradient device. A Biofine RPC-SC 18 B column (250 × 4.6 mm i.d., 5 μm; JASCO, Tokyo, Japan) and a TSK gel ODS-120T column (250 × 4.6 mm i.d., 5 μm; Tosoh, Tokyo, Japan) were used. The other chromatographic conditions are as given in the figure captions.

Results and Discussion

Products of the Reaction of Stearic Acid With Reagents III and VI and Their Fluorescence Properties

The products of the reaction of stearic acid with reagents **III** and **VI** were confirmed as the corresponding DMEQ derivatives (products **VII** and **VIII**, respectively, in Table 1) by the elemental analysis data and by the MS and ^{1}H NMR spectral data.

The fluorescence properties of products **VII** and **VIII** in methanol, acetonitrile, water and their mixtures, which have been widely used as mobile phases in reversed-phase chromatography, were examined to find a suitable mobile phase for the HPLC separation of the DMEQ derivatives of saturated C_5–C_{20} fatty acids.

The fluorescence excitation (maximum, 365 nm) and emission (maximum, 447 nm) spectra of product **VII** in methanol were almost identical with those in water and acetonitrile (Fig. 1). The maxima in aqueous methanol and acetonitrile were independent of the concentration of water. On the other hand, the fluorescence intensities in aqueous methanol were higher than those in aqueous acetonitrile at any water concentration. The fluorescence intensity was

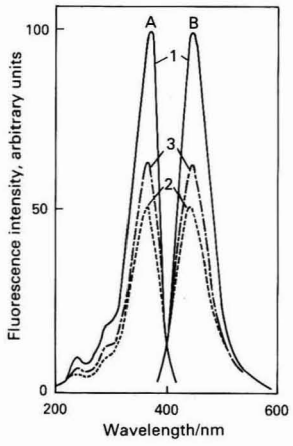

Fig. 1. A, Fluorescence excitation; and B, emission spectra of compound **VII** (1.0 mmol ml^{-1}) in 1, methanol; 2, acetonitrile; and 3 water

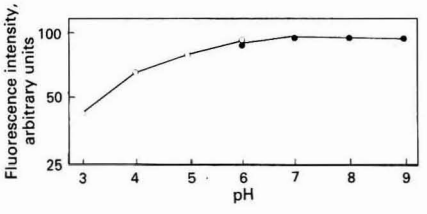

Fig. 2. Effect of pH on the fluorescence intensity of compound **VII** (1.0 nmol ml^{-1}), ○, in 0.1 M citrate; and ●, 0.1 M phosphate buffer

almost maximum at water concentrations of 0–70% in aqueous methanol, but decreased in proportion to the water concentration at ≥70%. The most intense fluorescence of product **VII** occurred in neutral and alkaline solutions (Fig. 2). These results suggest that aqueous methanol is suitable as a mobile phase in reversed-phase chromatography of the DMEQ derivatives of the fatty acids with gradient elution.

The fluorescence excitation and emission maxima (415 and 485 nm, respectively) of product **VII** in methanol, acetonitrile and water were shifted to longer wavelengths compared with those of **VII**. The fluorescence intensity of **VIII** in these solvents was much lower than that of **VII**; the intensity of **VIII** was *ca.* one hundredth of that of **VII**.

Evaluation of Reagents III and VI as Fluorescence Derivatisation Reagents

In order to compare the potential of reagents **III** and **VI** for the determination of fatty acids, their reactivities towards the fatty acids tested were examined. No differences in the reactivities (reaction time and temperature, and yield of reaction product) were found between the two reagents. However, the fluorescence intensities (peak heights) obtained with **III** were about 100 times higher than those obtained with **VI** for all the fatty acids tested; this is due to the difference in the fluorescence intensities of reaction products **VII** and **VIII** as described above. Therefore, reagent **III** was selected for further investigation in order to establish suitable reaction conditions for quantifying fatty acids.

Derivatisation Conditions

The conditions were examined using a mixture of the fatty acids (1.0 nmol ml^{-1} each).

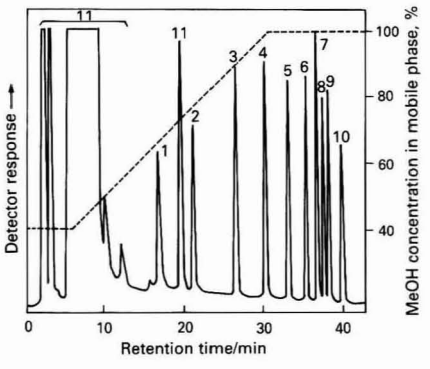

Fig. 3. Chromatogram of DMEQ derivatives of saturated fatty acids. A portion (100 µl) of a standard mixture of the acids (each 1.0 nmol ml^{-1}) was treated according to the described procedure. 1, C_5; 2, C_6; 3, C_8; 4, C_{10}; 5, C_{12}; 6, C_{14}; 7, C_{16}; 8, C_{17}; 9, C_{18}; and 10, C_{20} acids. 11, Reagent blank components. Column, Biofine RPC-SC 18 B; mobile phase, gradient elution with aqueous MeOH (0–6 min, 40%; 6–30 min, 40–100%; and 30–50 min, 100% MeOH); and flow-rate, 1.0 ml min^{-1}

Reagent **III** was found to dissolve in *N,N*-dimethylformamide, but not in water, acetonitrile or acetone; the reagent solution was therefore prepared in *N,N*-dimethylformamide. The most intense peaks were obtained at concentrations greater than *ca.* 2.0 mM of the reagent solution for all the fatty acids; 4.0 mM was used in the procedure.

1-Ethyl-3-(3-dimethylaminopropyl)carbodiimide and pyridine were used to facilitate the derivatisation of fatty acids with reagent **III**. Maximum and constant peak heights were attained at pyridine concentrations in the solution in the range 7–15%; 10% was selected as optimum. The peak heights for the acids were maximum and constant at concentrations of EDC higher than 1.0 M; 2.0 M was employed.

The derivatisation reaction of fatty acids with reagent **III** apparently occurred even at 0 °C; higher temperatures allowed the fluorescence to develop more rapidly. However, at 60 °C the peak heights decreased. At room temperature (15–30 °C), the peak heights for all the fatty acids were almost maximum after standing for 10 min. Hence, the solution was allowed to stand at room temperature for 15 min in the procedure. The DMEQ derivatives in the final mixture were stable for at least 24 h in daylight at room temperature. The yield of the fluorescent derivatives from stearic acid under the conditions employed was found to be 74.2% by comparing the value of the peak height for stearic acid with that of product **VII**.

Separation of DMEQ Derivatives of Fatty Acids

The simultaneous separation of DMEQ derivatives of C_5–C_{20} fatty acids was achieved on a reversed-phase column, Biofine RPC-18B, by gradient elution with aqueous methanol. Fig. 3 shows a typical chromatogram obtained with a gradient of methanol between 40 and 100% in the mobile phase. All the peaks were completely separated within 42 min. The change in the methanol concentration had no effect on the fluorescence excitation and emission maximum wavelengths of the DMEQ derivatives of all the fatty acids; the spectra were virtually identical with those of compound **VII**.

It appears from Fig. 3 that different fatty acids have different peak responses. This might be due to the differences in the yields of the fluorescent derivatives from fatty acids and/or the quantum yields of the derivatives.

Precision, Calibration and Detection Limit

The precision was established by repeated determinations using a standard mixture of fatty acids (1.0 nmol ml^{-1} each).

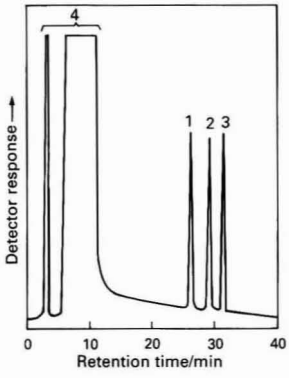

Fig. 4. Chromatogram of DMEQ derivatives of metabolites of arachidonic acid. A portion (100 μl) of a standard mixture of the metabolites (each 1.0 nmol ml^{-1}) was treated according to the described procedure. 1, Thromboxane B_2; 2, prostaglandin B_2; 3, leukotriene B_4; and 4, reagent blank components. HPLC conditions: TSK gel ODS-120T column; other conditions as in Fig. 3

The relative standard deviations did not exceed 1.2% for any of the fatty acids examined [$n = 10$ in each instance).

The relationships between the peak heights and the amounts of the individual fatty acids were linear from 30 fmol to at least 5.0 pmol per injection volume (10 μl). The linear correlation coefficients were 0.992 or better for all the fatty acids.

The detection limits for the fatty acids were 3–6 fmol at a signal to noise (S/N) ratio of 3.

Reaction of Reagent III With Compounds Other than Linear Saturated Fatty Acids

Unsaturated fatty acids (myristoleic, palmitoleic, oleic, linoleic, arachidonic and eicosapentaenoic), hydroxycarboxylic acids (lactic and malic), dicarboxylic acids (oxalic, malonic, succinic and adipic) and aromatic carboxylic acids (benzoic, salicylic and cinnamic) reacted with reagent **III** under the derivatisation conditions described to produce fluorescent derivatives. A chromatogram of the DMEQ derivatives of the metabolites of arachidonic acid is shown in Fig. 4; the detection limits (S/N ratio = 3) were about 5–10 fmol. α-Keto acids (pyruvic, α-ketoglutaric and phenylpyruvic) and 17 different α-amino acids did not fluoresce under the derivatisation conditions employed. Other substances such as alcohols, sugars, amines, aldehydes, ketones, phenols and sulphydryl compounds gave no fluorescent derivatives under these conditions. These observations suggest that the reagent is selective for carboxylic acids.

Conclusion

Reagent **III** is the first fluorogenic reagent that permits the derivatisation of carboxylic acids in aqueous solution. The derivatisation reaction proceeds rapidly even at moderate temperatures. The reagent is very sensitive and should be useful as a fluorescence derivatisation reagent for the HPLC determination of biologically important carboxylic acids, particularly thermally labile acids such as metabolites of arachidonic acid.

References

1. Dünges, W., *Anal. Chem.*, 1977, **49**, 442.
2. Farinotti, R., Siard, P., Bourson, J., Kirkiacharian, S., Valeur, B., and Mahuzier, G., *J. Chromatogr.*, 1983, **269**, 81.
3. Tuchiya, H., Hayashi, T., Naruse, H., and Takagi, N., *J. Chromatogr.*, 1982, **234**, 121.
4. Goya, S., Takadate, A., Fujino, H., and Irikura, M., *Yakugaku Zasshi*, 1980, **100**, 744.
5. Takadate, A., Tahara, T., Fujino, H., and Goya, S., *Chem. Pharm. Bull.*, 1982, **30**, 4120.
6. Watkins, W. D., and Peterson, M. B., *Anal. Biochem.*, 1982, **125**, 30.
7. Lloyd, J. B. F., *J. Chromatogr.*, 1980, **189**, 359.
8. Ikeda, M., Shimada, K., Sakaguchi, T., and Matsumoto, U., *J. Chromatogr.*, 1984, **305**, 261.
9. Korte, W. D., *J. Chromatogr.*, 1982, **243**, 153.
10. Lingeman, H., Hulshoff, A., Underberg, W. J. M., and Offermann, F. B. J. M., *J. Chromatogr.*, 1984, **290**, 215.
11. Nimura, N., and Kinoshita, T., *Anal. Lett.*, 1980, **13**, 191.
12. Kamada, S., Maeda, M., and Tsuji, A., *J. Chromatogr.*, 1983, **272**, 29.
13. Nimura, N., Kinoshita, T., Yoshida, T., Uetake, A., and Nakai, C., *Anal. Chem.*, 1988, **60**, 2067.
14. Goto, J., Goto, N., Hikichi, A., Nishimaki, T., and Nambara, T., *Anal. Chim. Acta*, 1980, **120**, 187.
15. Ryan, P. J., and Honeyman, T. W., *J. Chromatogr.*, 1984, **312**, 461.
16. Lee, Y.-M., Nakamura, H., and Nakajima, T., *Anal. Sci.*, 1989, **5**, 209.
17. Yamaguchi, M., Hara, S., Matsunaga, R., Nakamura, M., and Ohkura, Y., *J. Chromatogr.*, 1985, **346**, 227.
18. Miwa, H., Hiyama, C., and Yamamoto, M., *J. Chromatogr.*, 1985, **321**, 165.
19. Nakamura, M., Toda, M., Saito, H., and Ohkura, Y., *Anal. Chim. Acta*, 1982, **134**, 39.
20. Hara, S., Yamaguchi, M., Nakamura, M., and Ohkura, Y., *Chem. Pharm. Bull.*, 1985, **33**, 3493.
21. Schlenk, H., and Gellerman, J. L., *Anal. Chem.*, 1960, **32**, 1412.
22. Iwata, T., Yamaguchi, M., Hara, S., Nakamura, M., and Ohkura, Y., *J. Chromatogr.*, 1986, **362**, 209.

Paper 0/01779E
Received April 23rd, 1990
Accepted June 19th, 1990

Method for the Extraction Chromatographic Separation of Barium From Other Elements With Dibenzo-18-crown-6

Baburao S. Mohite, Chandrakant D. Jadage and Shridhar R. Pratap
Department of Chemistry, Shivaji University, Kolhapur-416 004, India

A method has been developed for the extraction chromatographic separation of barium from 0.01 M picric acid solution with dibenzo-18-crown-6 coated on hydrophobic silica gel as the stationary phase. Various mineral acids can be used as stripping agents. Barium was separated from other elements by selective extraction and the separation of barium from alkali and alkaline earth metals, uranium, thorium and lead was achieved. The method was applied to the determination of barium in real samples.

Keywords: *Barium separation; extraction chromatography; dibenzo-18-crown-6; standard rock sample; barite and witherite*

Barium has attracted considerable attention in recent years because it is a major constituent of fission products and is present in many industrial products. The determination of barium in environmental samples such as rocks, minerals, marine organisms and bone is important in terms of geochemistry and biochemistry. However, these environmental samples often contain large amounts of calcium and other alkaline earth metals which may cause spectral interferences. Hence it is essential to separate barium from other elements for its precise determination. Crown ethers have been found to be the most versatile extractants for alkali and alkaline earth elements.[1] Chromogenic crown ethers[2–5] and other crown ethers in the presence of murexide have been used for the spectrophotometric determination of barium. Dibenzo derivatives of crown ethers[6–9] have been used for the extraction and extractive separation of barium from other elements. The separation behaviour of alkaline earth metal ions with poly- and bis-crown ethers[10–13] has been reported. Crown ethers and cryptands attached to organic polymers[14–19] have been used as ion-exchange resins. Cryptand-222[20] has been used to remove trace amounts of radiobarium from mammals. The separation of alkaline earth metals has been carried out using extraction chromatography with dibenzo-18-crown-6[21]; however, the separation ability of the polyether column depended on pH and on the addition of ethanol to the $NaClO_4$ solution used as the eluting agent.

This paper describes a systematic investigation of the extraction chromatographic behaviour of barium, and its separation from other elements at macro and trace levels from picrate media on a silica-gel column coated with dibenzo-18-crown-6 (DB18C6).

Experimental

Apparatus

A Zeiss spectrophotometer, a digital pH meter (ELICO, Model LI-120) with glass and calomel electrodes and a Pyrex glass chromatographic column (20 × 0.8 cm i.d.) with a glass-wool plug at the bottom were used.

Reagents

A stock solution of barium (1.00 mg ml^{-1}) was prepared by dissolving 1.90 g of barium nitrate (AnalaR grade, BDH) in 1000 ml of distilled water. The solution was standardised gravimetrically.[22] Dilute solutions containing 250 μg ml^{-1} of barium were prepared by appropriate dilution.

Dibenzo-18-crown-6 (Aldrich) was used without further purification.

Picric acid solution (5×10^{-2} M) was prepared by dissolving 5.728 g of picric acid in 500 ml of distilled water. For safety reasons[23] it is advisable to keep the picric acid in a moist condition in a bottle with a cork stopper to avoid the possibility of an explosion.

Silica gel was rendered hydrophobic and coated with DB18C6 using the following procedure. Silica gel (100–200 mesh) was dried at 120 °C for 2 h. A stream of dry nitrogen was passed through a small Durant tube containing 25 ml of dimethyldichlorosilane. The dimethyldichlorosilane vapour was passed through a U-tube containing the silica gel for 2–3 h to replace the free hydroxyl groups near the surface with silyl groups. The treated silica gel was then washed with anhydrous methanol and dried at 100 °C.

A 2.5% coating of DB18C6 on hydrophobic silica gel was produced by dissolving DB18C6 in chloroform and slowly removing the chloroform from the suspension using a rotary evaporator until dry silica gel was obtained. About 3.8 g of the coated silica gel were slurried with distilled water and poured into a glass chromatographic column (20 × 0.8 cm i.d.). A 10-cm column bed was used after pre-conditioning with 0.01 M picric acid.

General Procedure

An aliquot of a solution containing 250 μg of barium was mixed with 2.0 ml of 0.05 M picric acid so that the concentration of the latter was 0.01 M in a total volume of 10 ml. The solution was then passed through the column, pre-conditioned with 0.01 M picric acid, at a flow-rate of 0.5 ml min^{-1}. The barium was extracted on the column in the form of an orange band which was then stripped from the column using various mineral acids. Fractions (5 ml) were collected and the barium content was determined spectrophotometrically with Sulfonazo-III at 640 nm.[24] The concentration of barium was calculated from a calibration graph.

Results and Discussion

Systematic studies of the extraction of barium on silica gel coated with DB18C6 were conducted by varying the picric acid concentration from 1×10^{-4} to 5×10^{-2} M. The extraction of barium was found to be quantitative from 1×10^{-2} M picric acid. Hence, subsequent extraction experiments were carried out at a picric acid concentration of 1×10^{-2} M.

To ascertain the amount of barium that could be extracted with the 10-cm column, extraction studies were performed by varying the amount of barium from 250 to 2500 μg. Extraction was found to be quantitative up to 2300 μg of barium.

After extraction, barium was stripped from the column with various mineral acids such as hydrochloric, nitric, perchloric and hydrobromic acid in the concentration range 0.01–5.0 M. It was found that the elution of barium from the column was

quantitative with all the acids studied in the concentration range 0.01–5.0 M. The total volume of mineral acid required for complete recovery of barium varied from 25 to 50 ml in the concentration range 0.5–0.01 M, respectively, whereas with 1–5 M acids the volume of mineral acid required was in the range 25–5 ml, respectively. When mineral acids of higher concentration (>5 M) were used as stripping agents there was a leaching of DB18C6 from the column.

Separation of Barium From Binary Mixtures

An aliquot of a solution containing barium and the foreign ion to be tested was taken and picric acid was added so that its concentration was 0.01 M in a total volume of 10 ml. The solution was then passed through the column at a flow-rate of 0.5 ml min^{-1}; subsequently, the column was washed with 0.01 M picric acid. Those foreign ions not extracted by DB18C6 passed through the column. Strontium and lead were co-extracted with barium, but could be stripped from the column with water. Barium was then eluted with 2 M nitric acid. Most of the elements and anions were tolerated in high ratios (Table 1).

Table 1. Separation of barium from binary mixtures. Amount of Ba taken, 250 μg

Foreign ion	Added as	Amount taken/mg	Ba found/ μg	Recovery of Ba, %
Li^+	LiCl	6.0	250	100.0
Na^+	NaCl	15.0	250	100.0
K^+	KCl	20.0	248	99.2
Rb^+	RbCl	20.0	250	100.0
Cs^+	CsCl	16.0	245	98.0
NH_4^+	NH_4Cl	4.0	246	98.4
Be^{2+}	$Be(NO_3)_2.4H_2O$	18.0	249	99.8
Mg^{2+}	$MgCl_2.6H_2O$	25.0	250	100.0
Ca^{2+}	$CaCl_2$	21.0	250	100.0
Sr^{2+}*	$Sr(NO_3)_2$	7.5	248	99.2
Co^{2+}	$CoCl_2.6H_2O$	5.5	250	100.0
Ni^{2+}	$NiCl_2.6H_2O$	25.0	250	100.0
Cu^{2+}	$CuCl_2.2H_2O$	2.0	245	98.0
Zn^{2+}	$ZnCl_2$	15.0	250	100.0
Cd^{2+}	$CdCl_2$	4.0	250	100.0
Pb^{2+}*	$Pb(NO_3)_2$	5.5	250	100.0
Al^{3+}	$Al(NO_3)_3.9H_2O$	10.0	248	99.2
Cr^{3+}	$Cr(NO_3)_3.9H_2O$	16.5	250	100.0
Fe^{3+}	$FeCl_3.6H_2O$	15.0	245	98.0
Y^{3+}	$Y(NO_3)_3$	3.0	248	99.2
La^{3+}	$La(NO_3)_3.6H_2O$	5.0	250	100.0
Ce^{3+}	$CeCl_3.6H_2O$	3.0	250	100.0
Ti^{4+}	$K_2TiO(C_2O_4)_2.2H_2O$	5.0	245	98.0
Th^{4+}	$Th(NO_3)_4$	16.0	250	100.0
V^{5+}	NH_4VO_3	8.0	250	100.0
UO_2^{2+}	$UO_2(NO_3)_2.6H_2O$	5.0	249	99.8
Mo^{6+}	$(NH_4)_6Mo_7O_{24}.4H_2O$	5.5	248	99.2
W^{6+}	$Na_2WO_4.2H_2O$	6.0	245	98.0
Cl^-	HCl	20.0	250	100.0
Br^-	HBr	22.0	250	100.0
I^-	HI	6.0	250	100.0
NO_3^-	HNO_3	30.0	248	99.8
ClO_4^-	$HClO_4$	12.5	250	100.0
SCN^-	NaSCN	1.0	245	98.0
CH_3COO^-	CH_3COOH	8.5	250	100.0
PO_4^{3-}	H_3PO_4	20.0	248	99.8
BO_3^{3-}	H_3BO_3	10.0	250	100.0
Oxalate	Oxalic acid	7.5	250	100.0
Ascorbate	Ascorbic acid	12.5	248	99.8
Tartrate	Tartaric acid	8.0	250	100.0
EDTA†	EDTA	6.5	250	100.0

* Co-extraction.
† EDTA = ethylenediaminetetraacetic acid.

Separation of Barium From Ternary Mixtures

In developing a method for the separation of barium from various elements in multi-component mixtures, various properties of barium were exploited (Table 2). Hence, when a mixture of beryllium or magnesium or calcium, strontium and barium was passed through the column with 0.01 M picric acid, beryllium or magnesium or calcium was not extracted and passed through the column. Strontium was co-extracted with barium, but was stripped from the column with water, whereas barium was stripped with 2 M nitric acid.

Similarly, for a mixture of an alkali metal, lead and barium the alkali metal was not extracted and hence passed through the column. The extracted lead was stripped with water, whereas barium was eluted with 2 M nitric acid.

For a mixture of uranium, lead and barium, the uranium passed through the column. The extracted lead was eluted with water and finally barium was stripped with 2 M nitric acid.

The separation of thorium, lead and barium was accomplished similarly.

In previous studies of solvent extraction,[8] barium was separated from other alkaline earth elements from picrate medium using different crown ethers and other extractants; however, in the present work separation of barium from lead, uranium, thorium, strontium and other elements was accomplished using only DB18C6. In the solvent extraction studies,[8] the stripping of barium was quantitative with 0.05–8.0 M solutions of the stripping agent; however, in extraction chromatography the elution of barium was quantitative even with 0.01 M solutions of mineral acids.

Application to the Determination of Barium in Real Samples

The method was applied to the determination of barium in barite and witherite minerals, a synthetic plastic stabiliser and standard rock samples. A weighed amount of barite, witherite or plastic stabiliser was dissolved in the usual manner.[8,25] The standard rock samples were brought into solution as described previously.[26] An aliquot of the sample solution was passed through the column as described above. All the other species passed through the column except strontium and lead, which were co-extracted with barium. The extracted lead or strontium was removed by washing the column with water, whereas barium was eluted with 2 M nitric acid. The results of triplicate analyses are shown in Tables 3 and 4.

Table 2. Separation of barium from multi-component mixtures

Serial No.	Metal ion	Amount taken/mg	Amount found/mg	Stripping agent	Recovery, %
I	Be/Mg/Ca	10.00	10.00	NEPC*	100.00
	Sr	7.00	6.98	H_2O	99.71
	Ba	0.25	0.25	2 M HNO_3	100.00
II	Li/Na/K/Rb/Cs	3.5	3.5	NEPC	100.00
	Pb	3.0	3.98	H_2O	99.5
	Ba	0.25	0.255	2 M HNO_3	102.00
III	U	5.0	5.0	NEPC	100.00
	Pb	3.0	3.95	H_2O	98.75
	Ba	0.25	0.25	2 M HNO_3	100.00
IV	Th	10.0	10.0	NEPC	100.00
	Pb	3.0	4.0	H_2O	100.00
	Ba	0.25	0.25	2 M HNO_3	100.00

* NEPC = No extraction passing through the column.

Table 3. Determination of barium in real samples

		Barium, %	
No.	Sample	Present	Found
1	Barite	58.80	58.82
2	Witherite	69.60	69.50
3	Plastic stabiliser	11.48	11.45

Table 4. Determination of trace levels of barium in United States Geological Survey (USGS) standard rock samples

No.	Sample	Barium, p.p.m. Certified	Found
1	USGS G-2	1850	1860
2	USGS BHVO-I	130	135
3	Syenite SY-2	460	470
4	Basaltic BR	1050	1060

Conclusion

The proposed method has several advantages. As barium is selectively extracted from a large number of metal ions, it is possible to separate barium not only from alkali and other alkaline earth metals but also from lead, uranium, thorium and fission products. Similarly, the separation of barium from halides, phosphate and other anions is possible even when these are present in higher concentrations. The method can be applied to the separation of barium at trace levels and at higher concentrations in real samples. The time required for analysis is *ca.* 2 h. The method is very simple, highly selective, rapid and reproducible. The recovery of barium in all instances from duplicate determinations is 100 ± 2%. The reproducibility of the procedure is ±2%.

We are grateful to the Honourable Vice-Chancellor, Dr. K. B. Powar, for his encouragement and for providing the United States Geological Survey rock samples and also to the Board of Research in Nuclear Sciences, Department of Atomic Energy, Government of India, for sponsoring the project, No. 37/12/88-G, and for financial assistance.

References

1. Mohite, B. S., *PhD Thesis*, Indian Institute of Technology, Bombay, 1986.
2. Loehr, H. G., and Voegtle, F., *Chem. Ber.*, 1985, **118**, 905.
3. Van, G. J., Sudhoelter Ernst, J. R., Lambeck, P. V., Popma Theo, J. A., Gerritsma, G. J., and Reinhoudt, D. N., *J. Chem. Soc., Chem. Commun.*, 1988, 693.
4. Kashanian, S., and Shamsipur, M., *Inorg. Chim. Acta*, 1989, **155**, 203.
5. Gholivand, M. B., Kashanian, S., and Shamsipur, M., *Polyhedron*, 1987, **6**, 535.
6. Takeda, Y., Oshio, K., and Segava, Y., *Chem. Lett.*, 1979, 601.
7. Rais, J., Kyrs, M., and Kadlekova, L., *Proc. Int. Solvent Extr. Conf.*, 1974, **2**, 1705.
8. Mohite, B. S., and Khopkar, S. M., *Anal. Chim. Acta*, 1988, **206**, 363.
9. Strzelbicki, J., and Bartsch, R. A., *Anal. Chem.*, 1981, **53**, 2247.
10. Maeda, T., Kimura, K., and Shono, T., *Fresenius Z. Anal. Chem.*, 1982, **313**, 407.
11. Nakajima, M., Kimura, K., and Shono, T., *Anal. Chem.*, 1983, **55**, 463.
12. Nakajima, M., Kimura, K., and Shono, T., *Bull. Chem. Soc. Jpn.*, 1983, **56**, 3052.
13. Lauth, M., and Gramain, P., *J. Liq. Chromatogr.*, 1985, **8**, 2403.
14. Blasius, E., Adrian, W., Janzen, K. P., and Klautke, G., *J. Chromatogr.*, 1974, **96**, 89.
15. Blasius, E., and Janzen, K. P., *Chem. Ing. Tech.*, 1975, **96**, 89.
16. Blasius, E., Janzen, K. P., and Neumann, W., *Mikrochim. Acta (Wien), Part II*, 1977, 279.
17. Shehori, E., and Jagur-Grodzinski, J., *J. Appl. Polym. Sci.*, 1976, **20**, 773.
18. Shehori, E., and Jagur-Grodzinski, J., *J. Appl. Polym. Sci.*, 1976, **20**, 1665.
19. Blasius, E., Janzen, K. P., Keller, M., and Lander, H., *Talanta*, 1980, **27**, 107.
20. Mueller, W. H., *Trace Elem. Metab. Man Anim., Proc. Int. Symp., 5th*, 1984, 559.
21. Lada, W. A., and Smulek, W., *Radiochem. Radioanal. Lett.*, 1978, **34**, 41.
22. Vogel, A. I., "A Text-Book of Quantitative Inorganic Analysis," Longmans, London, 1975, p. 554.
23. Sax, N. I., "Dangerous Properties of Industrial Materials," Van Nostrand Reinhold, New York, 1984, p. 2230.
24. Kemp, P. J., and Williams, M. B., *Anal. Chem.*, 1973, **45**, 124.
25. Squirrell, D. C. M., *Analyst*, 1981, **106**, 1042.
26. Mohite, B. S., and Khopkar, S. M., *Talanta*, 1985, **32**, 565.

Paper 0/00695E
Received February 14th, 1990
Accepted June 13th, 1990

Relevance of the Reaction of Aluminium With Pyrocatechol Violet to Speciation and Complexation Capacity Analysis

Gregory M. Morrison
Department of Sanitary Engineering, Chalmers University of Technology, S-412 96 Göteborg, Sweden

Pyrocatechol Violet is shown to separate uncomplexed aluminium effectively in the presence of model and natural ligands. Application to freshwater samples shows that the measurement is critically dependent on reaction time. Use of a short reaction time reflects the nature of the colloidal ligands rather than the presence of inorganic aluminium. A short reaction time with Pyrocatechol Violet and separation by equilibrium dialysis were not found to be suitable separation methods for inorganic and organic aluminium species. The results indicate the analytical difficulties in determining inorganic aluminium in natural water samples. However, it is shown that the reaction of aluminium, after 30 min, with Pyrocatechol Violet is promising for the assessment of aluminium complexation by fulvic acid.

Keywords: *Aluminium speciation; Pyrocatechol Violet; complexation; dialysis; fulvic acid*

The spectrophotometric determination of aluminium is generally not sufficiently sensitive for the speciation analysis of aluminium in natural waters. Discrimination between inorganic and organic aluminium can be achieved by spectrophotometric analysis in samples where acidification has mobilised aluminium to concentrations greater than 0.5 μM.[1,2] For the Pyrocatechol Violet and 8-hydroxy-7-iodoquinoline-5-sulphonic acid methods it has been shown that precise measurements can be made after short reaction times, despite slow colour development, to provide an indication of the content of inorganic monomeric aluminium.[1,3] Rapidly reacting species have also been analysed by reaction with 8-hydroxyquinoline[4,5] and ion-exchange resins such as Chelex-100[6,7] and Amberlite 120.[8] Separation of inorganic and organic aluminium species has been achieved by equilibrium dialysis.[9]

In this paper, the detection of inorganic aluminium and the determination of complexation capacity, by the Pyrocatechol Violet method, in the presence of model organic ligands and of organic ligands present in natural water samples, are examined. It is demonstrated that short reaction times do not indicate the presence of inorganic monomeric aluminium, but that the complete reaction can be used to indicate the aluminium bound to fulvic acid.

Experimental

Methods

Total dissolved aluminium was determined by direct injection of a filtered, acidified (0.01 M HNO_3) sample (25 ml) into an inductively coupled plasma mass spectrometer (VG PlasmaQuad). Standards were prepared in the range 0.1–5 μM.

Inorganic aluminium was determined by reaction with Pyrocatechol Violet followed by spectrophotometric detection of the coloured product at 585 nm. A 1-ml portion of Pyrocatechol Violet solution (2.5 mM) was added to filtered sample aliquots (50 ml), followed by 5 ml of 0.03 M hexamine buffer (pH 6.1). Aluminium standards were prepared in acetate buffer (10 mM) at pH 4.5, and treated in the same way. Detection of inorganic aluminium was by absorbance measurement at 585 nm after a reaction time of between 10 s and 60 min, depending on the experiment. Correction for interference by iron was made either with standard iron solutions[10] or by the presence of a mixed hydroxylammonium chloride (30 mM) and phenanthroline (0.1 mM) reagent.[11] The absorptivity was 28 l $mmol^{-1}$ cm^{-1}.

Titrations of aluminium were performed by additions of aluminium standard to sample aliquots (50 ml) adjusted to pH 4.5 by the addition of 3 M acetate buffer (0.5 ml). In most instances, dilution (from 2- to 5-fold) of water samples was required in order to achieve complete titration within the linear standard range for aluminium determination (4–11 μM). A series of standards was made for each reaction time.

Small organic ligands (defined here as dissolved) in lake water were separated *in situ* for 4 d over Spectrapor dialysis tubing (nominal relative molecular mass cut-off, 1000) into dialysis bags containing 100–200 ml of ultra-pure water (doubly distilled, then passed through a Milli-Q system). Larger organic ligands (defined here as colloidal) were retained by the same dialysis tubing in filtered samples, by extraction five times with 1 l of ultra-pure water, with the water changed every 2 h.

Reagents

Ethylenediaminetetraacetic acid (EDTA) and nitrilotriacetic acid (NTA) were obtained from Merck.

Freeze-dried H^+-saturated fulvic acid, extracted from Norwegian lake water, was donated by the Swedish Environmental Protection Agency in Stockholm.

Water Samples

Water samples (1 l) were collected from three lakes (Kullsjön, Långa Stamsjön and Bävsjön), which have all been limed and are located in the Lerum region, *ca.* 20 km east of Göteborg. A further sample was collected from Aspen, also in Lerum, which is a lake of naturally neutral pH.

The samples were filtered (<0.45 μm) and stored at 4 °C. Dialysis bags were suspended at a depth of 1 m in Långa Stamsjön by means of a buoy.

The water quality of the samples is shown in Table 1. The fluoride levels in the lakes were not high enough to affect aluminium standards in the spectrophotometric method.

Results and Discussion

Complexation titrations were found to be a useful procedure for investigating the reaction of aluminium with Pyrocatechol Violet in the presence of model and natural ligands.

Table 1. Quality of water samples with reference to possible interferents

Source	pH	F/μM	DOC*/mg l^{-1}	Fe/μM
Kullsjön	7.5	<5	4.8	0.2
Långa Stamsjön	7.3	<5	5.4	<0.2
Aspen	7.1	<5	5.3	0.4
Bävsjön	6.9	<5	5.5	2.0

* Dissolved organic carbon.

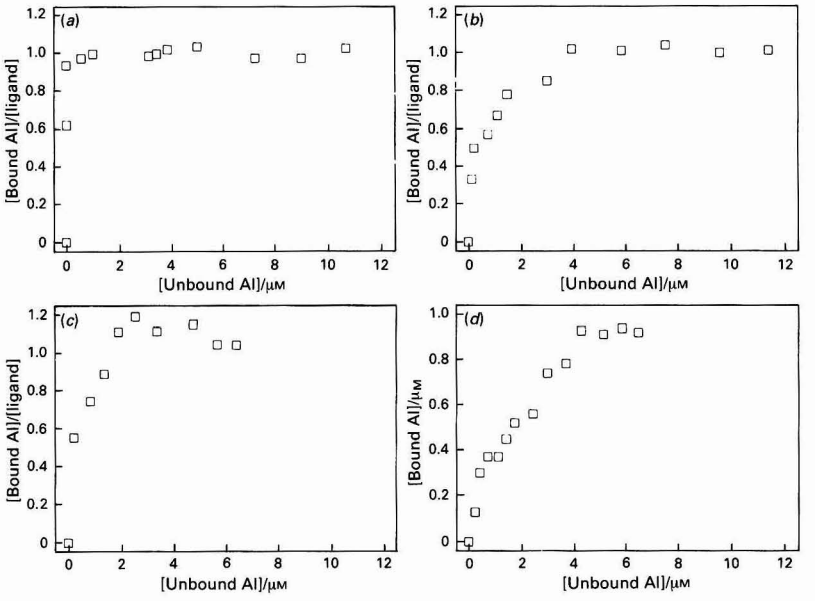

Fig. 1. Complexation profiles for aluminium with (*a*) EDTA, 5.95 μM; (*b*) NTA, 5.24 μM; (*c*) citrate, 1 μM; and (*d*) fulvic acid, 2.28 mg l^{-1}. In (*d*) the *y*-axis is expressed as [bound Al] because fulvic acid cannot be expressed as a ligand concentration with any degree of certainty

Table 2. Aluminium speciation in the water samples

Source	Pyrocatechol Violet reactive Al/μM	Total Al/μM	Complexation capacity/μM
Kullsjön	1.1	1.4	0.5
Långa Stamsjön . .	<0.5	0.3	2.0
Aspen	<0.5	0.2	3.1
Bävsjön	1.5	4.4	0.7

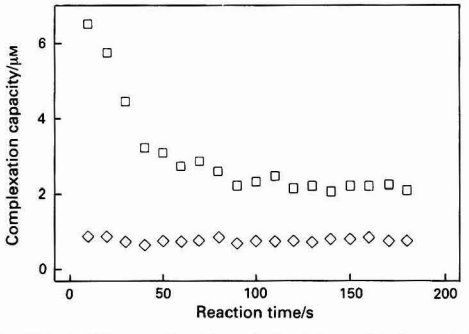

Fig. 2. Effect of the reaction time of aluminium with Pyrocatechol Violet on complexation capacity measurements of ◇, fulvic acid (1.628 mg l^{-1}); and □, water samples from Långa Stamsjön

Recent studies have shown that the commonly used copper titration, with differential-pulse anodic stripping voltammetry as metal ion detector, underestimates the binding capacity of model ligands as determined by means of an ion-selective electrode and bioassay.[12,13] Fig. 1 shows that, for EDTA and NTA, the expected 1:1 binding is found with aluminium, where the Pyrocatechol Violet reaction at 30 min indicates inorganic aluminium. The slightly elevated citrate value may be due to reagent impurity. Fulvic acid shows a similar complexation profile to that of NTA, with a binding capacity for fulvic acid of 0.41 mmol g^{-1}.

Table 3. Dissolved and colloidal complexation capacity in water samples from Långa Stamsjön

Date	Complexation capacity/μM Dissolved	Colloidal	Total
10/10/89*	—	—	1.8
18/10/89*	—	1.0	2.3
20–23/10/89† . .	1.3	—	—
23–27/10/89† . .	1.0	—	—
27/10/89*	—	0.9	2.0
27–31/10/89† . .	1.5	—	—
31/10/89*	—	0.7	1.4

* Sample.
† Sampling period.

Examination of Fig. 1 demonstrates that approximately a 5-fold excess of aluminium was required to saturate the fulvic acid fully, a result also generally found for the water samples. A complexation capacity of 0.5–1.5 μM can, therefore, be completely titrated within the linear standard range of Pyrocatechol Violet. Tannic acid was also tested, but too great an excess of aluminium was required to allow a precise determination of complete saturation. This limitation in the experimental determination of complexation by natural ligands has also been pointed out by Perdue.[14]

In Fig. 1 the plotting method proposed by Perdue,[14] with inorganic metal as the independent variable, is used. Perdue[14] has shown that both the direct titration curve method[15] and the use of bound metal as the independent variable[16,17] provide an incorrect estimate of complexation capacity for all but the strongest ligands.

Complexation capacities for the water samples, measured after a 30-min reaction time with Pyrocatecol Violet, are shown in Table 2. The values are of similar magnitude to those reported previously for freshwater samples analysed by bioassay, an ion-selective electrode and differential-pulse polarography.[13] In Kullsjön and Bävsjön there is little capacity left and it can be argued that further inputs of aluminium might be critical to fish in these lakes.

The reaction time with Pyrocatechol Violet has an important influence on complexation capacity (Fig. 2). The presence of reactive species (reaction times, 10–60 s) in the Långa Stamsjön sample could not be attributed to fulvic acid, and therefore, colloidal species must be responsible. Although Plankey and Patterson[18] obtained initial reaction rates for aluminium fluoride complexation in the presence of fulvic acid, it was not felt appropriate here to extrapolate the sample data to zero reaction time owing to the increased experimental error at shorter reaction times. Complexation capacities were constant between 180 s and 60 min.

Fig. 2 also casts some doubt on the use of short reaction times with complexing ligands as an indication of inorganic monomeric aluminium in water samples.[1,3–8] The measurement obtained is critically dependent on reaction time and reflects the nature of colloidal reactive ligands rather than that of inorganic aluminium. Hering and Morel[19] have shown that calcein reacts with the copper - humate complex, both after complete dissociation of the complex and through attack on the complex. The results presented here indicate that only the former reaction with Pyrocatechol Violet occurs when aluminium is complexed by fulvic acid. However, Pyrocatechol Violet can initiate both complex dissociation and attack on the complex for other, less well-defined organic ligands, which can complex aluminium in natural waters.

Further indication of the relative contributions of colloidal and dissolved organic ligands to aluminium complexation can be obtained by separation across a dialysis membrane (Table 3). For Långa Stamsjön, total filterable (<0.45 μm) complexation capacity was 1.4–2.3 μM during the sampling period. The proportion of dissolved and colloidal complexation capacity was approximately equal. The complexation of equal proportions of aluminium titrant by dissolved and colloidal ligands precludes the use of dialysis as a separation method for inorganic and organic aluminium species in natural waters.

Conclusion

Short reaction times with Pyrocatechol Violet and separation by dialysis were not found to be suitable separation methods for inorganic and organic aluminium species in natural waters. Short reaction times with Pyrocatechol Violet reflect the nature of colloidal reactive ligands rather than that of inorganic aluminium. However, the reaction of aluminium with Pyrocatechol Violet after 30 min was used to provide an estimate of complexation by fulvic acid in lake water.

C. Haraldsson, of the Department of Marine and Analytical Chemistry, carried out the inductively coupled plasma mass spectrometric analysis for total aluminium.

References

1. Siep, H. M., Müller, L., and Naas, A., *Water, Air, Soil Pollut.*, 1984, **23**, 81.
2. Lawrence, G. B., and Driscoll, C. T., *Environ. Sci. Technol.*, 1988, **22**, 1293.
3. Dempsey, B. A., "Aquatic Humic Substances, Influence on Fate and Treatment of Pollutants," Advances in Chemistry Series 219, American Chemical Society, Washington, DC, 1989, Chapter 25.
4. Barnes, R. B., *Chem. Geol.*, 1975, **15**, 177.
5. Lewis, T. E., Dobb, D. E., Henshaw, J. M., and Simon, S. J., *Int. J. Environ. Anal. Chem.*, 1988, **34**, 69.
6. Campbell, P. G. C., Bisson, M., Bougie, R., Tessier, A., and Villeneuve, J. P., *Anal. Chem.*, 1983, **55**, 2246.
7. Miller, J. R., and Andelman, J. B., *Water Res.*, 1987, **21**, 999.
8. Driscoll, C. T., *Int. J. Environ. Anal. Chem.*, 1984, **16**, 267.
9. Backes, C. A., and Tipping, E., *Water Res.*, 1987, **21**, 211.
10. Johnson, N. M., Driscoll, C. T., Eaton, J. S., Likens, G. E., and McDowell, W. H., *Geochim. Cosmochim. Acta*, 1981, **45**, 1421.
11. Dougan, W. K., and Wilson, A. L., *Analyst*, 1974, **99**, 413.
12. Plummer, D. H., *PhD Thesis*, University of Liverpool, 1986.
13. Morrison, G. M. P., and Florence, T. M., *Electroanalysis*, 1989, **1**, 107.
14. Perdue, E. M., "Aquatic Humic Substances, Influence on Fate and Treatment of Pollutants," Advances in Chemistry Series 219, American Chemical Society, Washington, DC, 1989, Chapter 19.
15. Chau, Y. K., Gatcher, R., and Lum-Shue-Chan, C., *J. Fish. Res. Board Can.*, 1974, **31**, 1515.
16. Ruzic, I., *Anal. Chim. Acta*, 1982, **140**, 99.
17. van den Berg, C. M. G., *Mar. Chem.*, 1984, **15**, 1.
18. Plankey, B. J., and Patterson, H. H., *Environ. Sci. Technol.*, 1988, **22**, 1454.
19. Hering, J. G., and Morel, F. M. M., *Environ. Sci. Technol.*, 1990, **24**, 242.

Paper 0/01398F
Received March 30th, 1990
Accepted June 1st, 1990

Turbidimetric Method for the Determination of Water-soluble Hydroxyethylcellulose in Dry Blended Cement

Asfaha Iob and Nureddin M. Abbas
Central Analytical and Materials Characterisation Laboratories, Research Institute, King Fahd University of Petroleum and Minerals, Dhahran, Saudi Arabia

A simple turbidimetric method for the determination of hydroxyethylcellulose (HEC) is described. The method involves the addition of liquefied phenol to an alkaline (Na_2CO_3) solution of HEC which results in the formation of a suspension. The turbidity of the suspension is then related to concentration by using a calibration graph. The technique was applied successfully to the determination of HEC (without the interference of carboxymethylcellulose) in dry blended cement. The detection limit of the method was found to be 0.02%. The precision of the method (using 53 p.p.m. standard HEC) at the 95% confidence limit was ±5.3%.

Keywords: *Hydroxyethylcellulose determination; turbidity; cement additive; carboxymethylcellulose*

Hydroxyethylcellulose (HEC) is widely used in the oil industry for many purposes such as the displacement of drilling fluid from the space between the well casing and the bore wall, secondary recovery from plural producing horizons, water-flooding in enhanced oil recovery (EOR), plugging a formation and fluid loss control in well cementing and fracturing. It is also used extensively in other industries as a corrosion inhibitor, binder, ceramic material, scale control additive in geothermal brines, etc. A review of the commercial utilisation of HEC is given in reference 1. In most of these instances HEC is used as a modifier or additive making up only a small portion of the total product, but still contributing significantly to the final properties of the product. The amount of HEC in the product should fall within a certain range in order to perform the respective job successfully. Hence analytical techniques are required to determine the amount of HEC in the system (product). Some of the techniques previously used for the analysis of such products include mass spectrometry,[2] pyrolysis gas chromatography,[3–6] enzymic reaction,[7] gel-permeation chromatography,[8,9] turbidimetric titration,[10] carbon-13 nuclear magnetic resonance spectroscopy[11,12] and the well known colorimetric techniques used for carbohydrate materials.[13] However, these techniques either require expensive instrumentation or the experimental sample preparations and treatments are laborious.

The technique described here is much simpler than those mentioned above and was specifically directed to the determination of HEC in dry blended cement samples (cement containing HEC). In such instances HEC is added to the cement to serve as a fluid loss control additive. If the correct amount is not added, then complications such as well plugging or too much or too little air entrainment might result. Hence there is the need for a rapid and simple method for determining the exact concentration of HEC in dry blended cement, if possible at the job site.

The method described involves the addition of liquefied phenol to an Na_2CO_3 solution of HEC. The absorbance of the resulting turbid material is then used for quantification purposes. The wavelength chosen is such that the colours due to other constituents or additives of the product do not interfere. The method is sufficiently simple to be used at a job site (utilising a portable turbidimeter or visible spectrophotometer).

Experimental

Apparatus

A Cary 2390 near infrared - ultraviolet - visible spectrophotometer (Varian) interfaced to an Apple IIe computer system was used. The Apple IIe computer (64K) had a video monitor and dual floppy disk drives. An Epson RX-80F/T+ printer was also interfaced to the computer. The "Master Kinetics Storage Program" (Varian) was used for studying the stability of the suspension. This program permitted the collection, display and storage of information derived from the kinetic runs on to data disks. Instrumental set-ups were also automatically stored and recalled to simplify analysis preparation.

Reagents

Liquefied phenol. About 90 g of solid phenol were weighed in a 400-ml beaker and 10 ml of de-ionised water added. The mixture was then stirred for about 1 h until a clear solution resulted. Alternatively, liquefied phenol that is commercially available (Fisher) can be used.

Sodium carbonate solutions, 0.5, 1.0 *and* 5.0%. Prepared by weighing the required amount of $Na_2CO_3.7H_2O$ (Fluka) in separate beakers and adding the necessary amount of de-ionised water.

Hydroxyethylcellulose. Initially, standards of HEC (Riedel de Häen) were prepared in 1.0% Na_2CO_3 solution. The concentrations of the standards were 10, 26, 53 and 107 p.p.m.

Other chemicals used included sucrose (BDH), L-ascorbic acid (BDH), fructose (Fluka), lactic acid (Riedel de Häen) and carboxymethylcellulose (CMC) (Aldrich).

Procedure

The standard solution (10 ml) was transferred into a vial and liquefied phenol (1 ml) was added to it. After mixing, the turbid material was immediately transferred into a cuvette and absorbance measurements were taken at 800 nm. This wavelength was chosen in order to avoid interference from some of the yellowish additives (mainly dispersants, which absorb in the 350–500 nm range) that are normally extracted together with HEC by the Na_2CO_3 solution. Preliminary experiments (for the stability and kinetics study) required that measurements be taken over a period of 30 min. Data (absorbance *versus* time) that were averaged within 30 s were stored on the kinetics data disk for later evaluation. The reference cell contained either water or the same solubilising medium (Na_2CO_3 solution).

Results and Discussion

The low relative molecular mass polyhydroxy products such as sucrose, fructose, ascorbic acid and lactic acid did not give a suspension on addition of phenol. However, HEC gave a very turbid solution. The turbidity increased with the concentration of HEC. On the other hand, CMC did not give a turbid

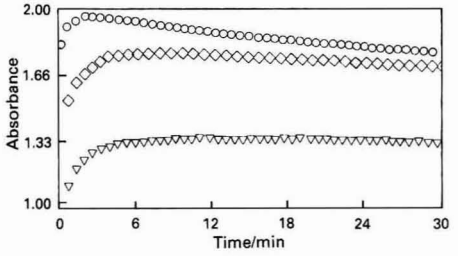

Fig. 1. Turbidity measurements (at 800 nm) of the phenol - HEC suspension as a function of time. A concentration of 200 p.p.m. of HEC was used in all instances. ○, Dissolved in 0.5% Na_2CO_3; ▽, dissolved in 1.0% Na_2CO_3; and ◇, dissolved in 5.0% Na_2CO_3

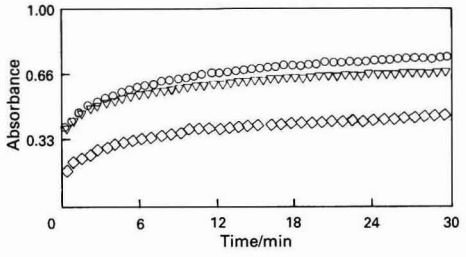

Fig. 2. Turbidity measurements (at 800 nm) of the phenol - HEC suspension as a function of time. A concentration of 53 p.p.m. of HEC was used in all instances. ○, Dissolved in 0.5% Na_2CO_3; ▽, dissolved in 1.0% Na_2CO_3; and ◇, dissolved in 5.0% Na_2CO_3

Table 1. Turbidimetric measurements (at 800 nm) of the suspension

Concentration of standard, p.p.m.	Absorbance of suspension
10	0.09
26	0.24
53	0.55
107	1.17

solution. The mechanism of suspension formation is thought to be due to the interaction of the phenolate anion with the OH group of HEC. This may explain the fact that CMC does not form a suspension. The negative phenolate anions will tend to repel the negative carboxylate anions of CMC. The stability of the suspension was studied by preparing solutions of HEC (*ca.* 200 p.p.m.) in 0.5, 1.0 and 5.0% Na_2CO_3. As can be seen in Fig. 1, in all three instances a significant and continuous increase in absorbance occurred in the first few minutes (up to about 10 min). After that time, the absorbance remained almost constant for the duration of the run with respect to the standards in 1.0 and 5.0% Na_2CO_3 solutions. However, the standard in 0.5% Na_2CO_3 solution showed a small but continuous decrease in absorbance after the initial surge. Further, the absorbance values of all three solutions were >1.2. These high absorbance values are usually beyond the normal spectrophotometric linear ranges and can give erratic results. The results found using a lower concentration of HEC (53 p.p.m.) are shown in Fig. 2. As can be seen, the absorbance values remain almost constant after about 10 min, irrespective of the Na_2CO_3 concentration. Standards in 1.0% Na_2CO_3 solution were used for preparing a working curve. Hence, for quantification purposes it was decided to take absorbance readings 15 min after mixing the reagents. The results found for the standards are shown in Table 1. The precision of the method (using 53 p.p.m. of HEC) at the 95% confidence level was found to be 5.3%.

Application

The validity of the technique was checked by using real dry blended cement. Extraction of HEC from the dry blended cement was carried out in accordance with the procedure followed for general additives, *i.e.*, using 5% Na_2CO_3 solution.[14] As the amount of HEC found in cement is normally between 0.25 and 1.0%, standards were prepared in the range of from 0.1 to 1.5%. The same type of HEC (HEC products can differ in the nature of the cross-linking or in relative molecular mass) as that found in the sample was used for preparing the standards and in the same type of cement. The type of cement, however, is not critical. Portland cement, ASTM Type 1, was used for these experiments. The Na_2CO_3 extract was filtered [through a 0.45-μm HA-type filter (Millipore)] and the filtrate treated in the same manner as the standard. As in the previous experiments, the absorbance readings were taken 15 min after mixing. An excellent correlation (r^2 = 0.999) was found for these samples (see Table 2). The calibration graph was used to evaluate two cement blend samples containing 0.25 and 0.75% HEC, respectively. Experimental results for the two samples gave values of 0.24 and 0.74%, respectively.

Table 2. Absorbance measurements of HEC standards in Portland cement Type 1 (absorbance at 800 nm)

HEC standard, % m/m	Absorbance
0.11	0.08
0.26	0.17
0.50	0.36
1.04	0.73
1.49	0.90

Hence this technique can easily be used at field sites to check the specification with regard to HEC concentration. If the specification is not met, appropriate modification could easily be carried out at this point. A portable visible spectrophotometer (or turbidimeter) such as the Bausch & Lomb Spec-20 can easily be used for such studies.

We thank the Research Institute of King Fahd University of Petroleum and Minerals for permission to publish this work.

References

1. Powell, G. M., *in* Davidson, R. L., *Editor*, "Handbook of Water-soluble Gums and Resins," McGraw-Hill, New York, 1980, 12/1–12/22.
2. Harless, H. R., and Anderson, R. L., *Text. Res. J.*, 1970, **40**, 448.
3. Ericsson, I., *Chem. Abstr.*, 1974, **81**, 121472m.
4. Diacel Chemical Industries, *Chem. Abstr.*, 1985, **102**, 80632v.
5. Hodges, K. L., Kester, W. E., Wiederrich, D. L., and Grover, J. A., *Anal. Chem.*, 1979, **51**, 2172.
6. Bartelemus, G., and Ketterer, R., *Fresenius Z. Anal. Chem.*, 1977, **286**, 161.
7. Tumanov, A. A., and Korostyleva, E. A., *Fiz-Khim. Metody. Anal.*, 1982, 111.
8. Demester, J., Bache, M., and Lauwers, A., *in* Brown, R. D., and Jurasek, L., *Editors*, "Hydrolysis of Cellulose: Mechanisms of Enzymatic and Acid Hydrolysis," *Advances in Chemistry Series, Volume* 181, American Chemical Society, Washington, DC, 1979, Chapter 5, pp. 105–116.
9. Barth, H. G., and Regnier, F. E., *J. Chromatogr.*, 1980, **192**, 275.
10. Benicka, E., Valigurova, V., and Hurt, V., *Makrotest*, 1978, **5**, 83.
11. Parfondry, A., and Perlin, A. S., *Carbohydr. Res.*, 1977, **57**, 39.
12. DeMember, J. R., Taylor, L. D., Trummer, S., Rubin, L. E., and Chilkis, C. K., *J. Appl. Polym. Sci.*, 1977, **21**, 621.
13. Davidson, E. A., "Carbohydrate Chemistry," Holt, Rinehart and Winston, New York, 1967, pp. 386–414.
14. Connolly, J. D., Hime, W. G., and Erlin, B., "Admixtures," The Concrete Society, The Construction Press, Lancaster, 1980.

Paper 0/02147D
Received May 15th, 1990
Accepted June 19th, 1990

Evaluation of a Modified Derivative Method for Spectrophotometric and Spectrofluorimetric Kinetic-based Determinations*

A. Torres, M. C. Gutierrez, S. Rubio, A. Gómez-Hens and D. Pérez-Benditot
Department of Analytical Chemistry, Faculty of Sciences, University of Córdoba, 14004 Córdoba, Spain

A selective empirical data processing method based on a modification of the conventional kinetic derivative method is reported. The method is based on parameters not directly correlated with the initial rate but which are similar to those used in derivative spectrometry such as the distance between two peaks or the value of the derivative at a single time. Two types of kinetic curves were tested, namely, curves with and without induction periods. Different order derivatives were obtained by numerical differentiation using the Savitzky - Golay method. Measured parameters were evaluated for each derivative curve in terms of linearity for the analyte of interest and selectivity with respect to an interferent, and compared with those obtained by using initial-rate measurements. The proposed method is shown to provide improved selectivity.

Keywords: *Derivative kinetic method; spectrophotometry; spectrofluorimetry; Savitzky - Golay method*

The derivative technique has found useful analytical application in kinetic analysis.[1] Several commercial instruments compute both the first and second derivative and use the second derivative to determine when the response curve has become linear and the first derivative to compute analyte concentration from data in the linear region of the response curve. As the height of the plateau in the first-derivative curve provides a direct measure of the reaction rate, the kinetic derivative method does not offer greater selectivity than the direct measurement of the initial rate.

This paper reports a more selective data processing alternative, also based on the kinetic derivative approach. It involves parameters not directly correlated with the initial rate but which are similar to those used in derivative spectrometry. Hence, the three most common parameters used were: (*a*) the value of the derivative at a single time relative to the zero-signal baseline (absorbance units time $^{-n}$, n being the derivative order); (*b*) the time interval between pre-determined points that have identical derivative signal values (time units); and (*c*) the distance between the derivative signal at two times, usually adjacent maxima and minima (absorbance units time^{-n} per time units). In order to ensure that the values obtained were commensurate, all measurements were made in units of length (cm). In choosing an appropriate measurement parameter two requirements must be fulfilled; firstly, correlation with the analyte concentration; and secondly, improvement on the selectivity of the corresponding conventional kinetic method. Various chemical systems yielding kinetic curves of various shapes were studied and their derivative curves obtained by numerical differentiation using the Savitzky-Golay method.[2] The results found show that this empirical data processing method improves on the selectivity of the determinations studied.

Experimental

Apparatus

A Pye Unicam SP6-500 ultraviolet - visible spectrophotometer and a Perkin-Elmer MPF-43A fluorescence spectrophotometer were used for spectrophotometric and spectrofluorimetric measurements, respectively. The temperature of the cell compartment was thermostated by circulating water through it; 1-cm quartz cells were used throughout. A stopped-flow module described elsewhere[3] and marketed by "Quimi-Sur Instrumentation" was fitted to the spectrophotometer in order to study the Fe^{II} - 1,10-phenanthroline system. Kinetic data were collected and manipulated by a Hewlett-Packard 98561AE computer and a 16-bit Hewlett-Packard analogue to digital converter. The computer was equipped with a dual Hewlett-Packard disk drive (9122), a Think Jet printer and a 7470 A plotter.

Reagents

All chemicals used were of analytical-reagent grade and were used without further purification. Doubly distilled water was used throughout.

Procedures for Obtaining the Kinetic Curves

Cu^{II}-catalysed hydroquinone - hydrogen peroxide system

This reaction has been described elsewhere[4] for the determination of Cu^{II} by the fixed-time method. However, the system was optimised for application of the initial-rate method. The study carried out for this purpose showed the following procedure to be the optimum: to a 10-ml calibrated flask add 0.5 ml of 2.7×10^{-3} M hydroquinone solution in 1×10^{-2} M hydrochloric acid, 2 ml of 0.2 M hydrogen peroxide, 2 ml of 1.26 M pyridine, 1 ml of 1.6 M acetic acid and an appropriate volume of Cu^{II} solution to give a final concentration between 2 and 30 μg ml^{-1}. The temperature is kept constant at 20 °C. Measurements of the variation of absorbance with time at 340 nm begin exactly 45 s after the addition of copper. The absorbance values are collected every 2 s for 800 s. The values obtained are subtracted from those given by a blank solution containing no copper.

Iodide - peroxydisulphate - thiosulphate system

After a comprehensive optimisation study of this reaction the following procedure is recommended: to a 10-ml calibrated flask add, in sequence, 1 ml of 1.75 M acetic acid - sodium acetate buffer (pH 4.0), 6 ml of 0.1 M potassium peroxydisulphate, 0.25 ml of 4×10^{-3} M sodium thiosulphate, 0.1 ml of 1% m/v starch solution and the volume of 2×10^{-2} M iodide solution required to give a final concentration between 1×10^{-3} and 5×10^{-3} M. The flask is then made up to the mark with doubly distilled water. The absorbance values are collected every 0.7 s at 578 nm at a temperature of 20 °C. Measurements are started exactly 45 s after the addition of iodide.

* Presented at the 3rd International Symposium on Kinetics in Analytical Chemistry, Dubrovnik—Cavtat, Yugoslavia, 25–28 September, 1989.

† To whom correspondence should be addressed.

Fe^{II}-induced pyridoxal-2-pyridylhydrazone - hydrogen peroxide system

The procedure followed has been described elsewhere.[5] Measurements are started exactly 1 min after the addition of Fe^{II} and the fluorescence intensity values are collected every 3 s.

Fe^{II} - 1,10-phenanthroline system

1,10-Phenanthroline is one of the most widely used reagents for the spectrophotometric determination of iron from equilibrium measurements. It was confirmed that the formation of the complex can be monitored by the stopped-flow technique and iron can be determined from initial-rate measurements. According to the study of variables affecting the reaction rate carried out, the following procedure is recommended: one of the two 10-ml reservoir syringes of the stopped-flow module is filled with a previously prepared solution containing 0.4 ml of 8.5×10^{-3} M 1,10-phenanthroline in ethanol (4 + 6) and 1 ml of 2 M acetic acid - sodium acetate buffer (pH 4.1) in a final volume of 10 ml. The other syringe is filled with a solution containing 1 ml of 2 M acetic acid - sodium acetate buffer (pH 4.1), 1 ml of 0.1 M hydroxylamine hydrochloride and different volumes of Fe^{III} standard solution to give a final concentration between 0.5 and 8 μg ml^{-1} in a final volume of 10 ml. After the two 2-ml drive syringes are filled, 0.15 ml of each solution is mixed in the mixing chamber in each run. At least three runs per sample are carried out. The absorbance changes during the reaction are monitored at 512 nm and the absorbance values are collected every 0.2 s. All measurements are carried out at 20 °C. The blank signal is negligible.

Procedure for Data Processing

Data sets of kinetic curves (absorbance - or fluorescence - time curves) were stored on floppy diskettes for processing. Data collection and processing was achieved by a suite of programs (KINDER) written by the authors (listings of KINDER are available from the authors on request). Data sets were smoothed by convolution with a 25-point quadratic - cubic least-squares function according to the Savitzky - Golay method.[2] The different derivative curves of the corresponding kinetic curves were generated by applying quadratic (first-order), quadratic - cubic (second-order), cubic - quartic (third-order) and quartic - quintic (fourth-order) Savitzky - Golay algorithms using 25 points.

Results and Discussion

In order to demonstrate the analytical possibilities of this modified derivative kinetic method, the first- to fourth-derivative curves of two kinetic profiles were obtained: (*a*) with an induction period [Cu^{II} - catalysed hydroquinone - hydrogen peroxide system, iodide - $S_2O_8^{2-}$ - $S_2O_3^{2-}$ system and Fe^{II}-induced pyridoxal-2-pyridylhydrazone (PHP) system]; and (*b*) without an induction period by using the stopped-flow technique to generate the respective kinetic curves (Fe^{II} - 1,10-phenanthroline system). In all instances, the study was based on the empirical selection of those measurement parameters that could be correlated with the analyte concentration and, in addition, improved on the selectivity of the corresponding conventional kinetic method. Hence, these parameters were not directly correlated with the reaction rate of the chemical system. It should be noted that all the *n*th-derivative curves obtained for true first-order processes are the same shape as the zero-order curve, hence no information can be drawn from those derivative curves that cannot be obtained from the original kinetic curve. In practice, an initial straight portion of the kinetic curve allows one to obtain *n*th-derivative curves with profiles other than that of the original kinetic curve, from which it is difficult to obtain parameters not directly correlated with the reaction

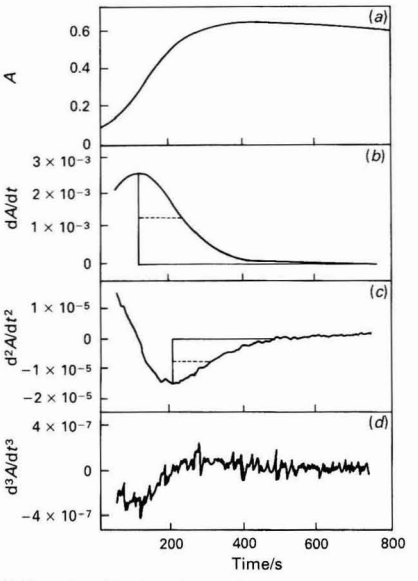

Fig. 1. Cu^{II}-catalysed hydroquinone - hydrogen peroxide system. (*a*) Absorbance - time curve; (*b*) first-; (*c*) second-; and (*d*) third-derivative curves (measurement parameters are indicated by broken lines)

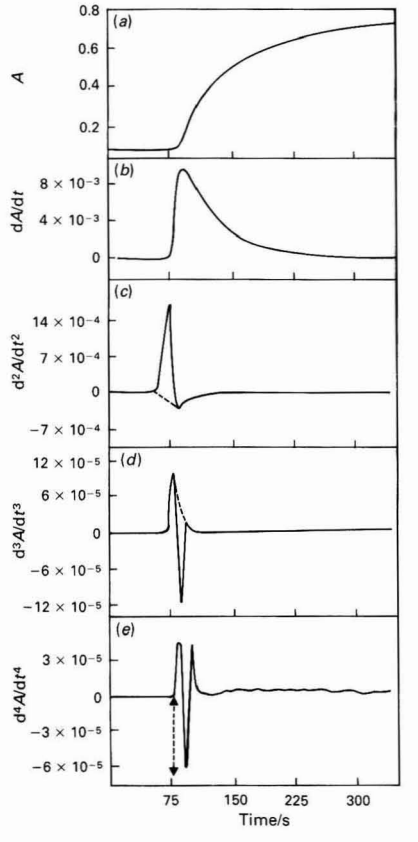

Fig. 2. Iodide - peroxydisulphate - thiosulphate system. (*a*) Absorbance - time curve; (*b*) first-; (*c*) second-; (*d*) third-; and (*e*) fourth-derivative curves (measurement parameters are indicated by broken lines)

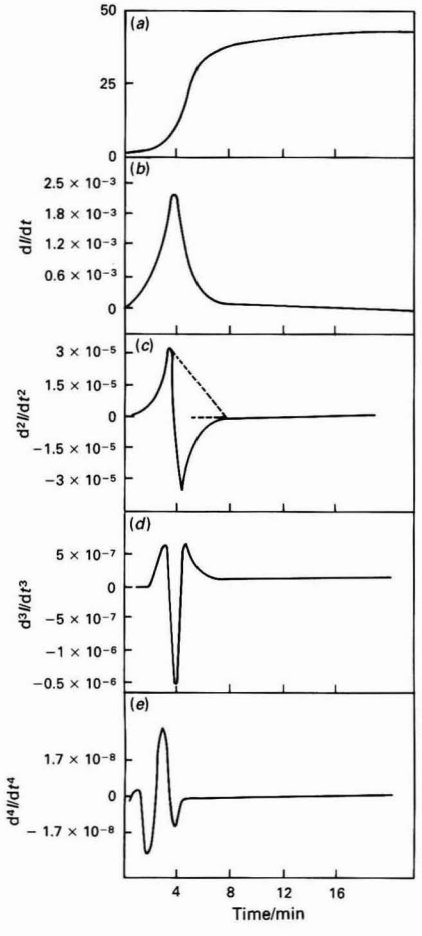

Fig. 3. Fe^{II}-induced PHP - hydrogen peroxide system. (a) Relative fluorescence intensity - time curve; (*b*) first-; (*c*) second-; (*d*) third-; and (*e*) fourth-derivative curves (measurement parameters are indicated by broken lines)

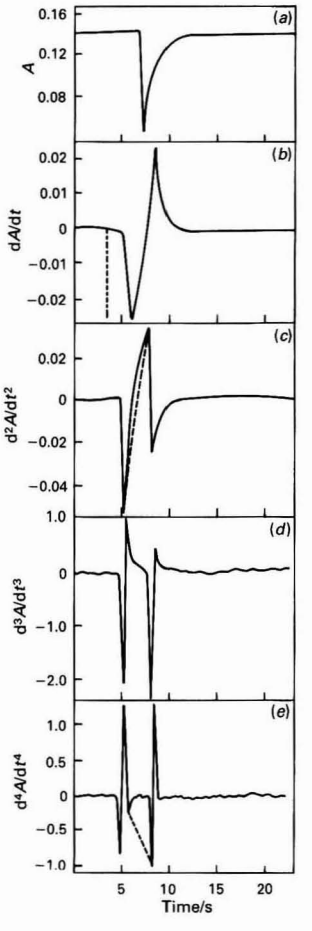

Fig. 4. Fe^{II} - 1,10-phenanthroline system. (*a*) Absorbance - time curve obtained by the stopped-flow technique; (*b*) first-; (*c*) second-; (*d*) third-; and (*e*) fourth-derivative curves (measurement parameters are indicated by broken lines)

rate. Hence, only systems yielding unconventional kinetic curves were studied. Figs. 1–4 show the kinetic curves obtained for the systems studied and the corresponding derivative curves, in which those measurement parameters that meet the two above-mentioned requirements appear as broken lines. Because the shapes of the kinetic curve and its corresponding derivative curves depend on the chemical system, it is not possible to generalise on the choice of the measurement parameter. In all instances, measurements were made in units of length (cm). The results obtained for each system studied are summarised in Tables 1 and 2 and discussed below.

Kinetic Curves With an Induction Period

Three systems yielding kinetic curves of different shape were chosen to study the analytical potential of their *n*th-derivative curves. The first system (Cu^{II}-catalysed hydroquinone - hydrogen peroxide) only showed a slight induction period; hence, from a practical point of view, it was considered to be a "quasi-first-order system." The second system (iodide - peroxydisulphate - thiosulphate) yielded a conventional Landolt-type curve, hence no variation in the signal with time was obtained until all the thiosulphate had been consumed in the reaction. Finally, the third system (Fe^{II}-induced PHP - hydrogen peroxide) was an induced reaction in which the signal obtained during the induction period changed slightly with time.

Cu^{II}-catalysed hydroquinone - hydrogen peroxide system

Fig. 1 shows the kinetic curve obtained for the Cu^{II}-catalysed oxidation of hydroquinone by hydrogen peroxide and the corresponding first-, second- and third-derivative curves obtained from it. The last derivative curve exhibits a low signal to noise (S/N) ratio, which makes it inadequate for quantification. Although the height of the first-derivative peak is directly correlated to the Cu^{II} concentration as it is a direct measure of the reaction rate, the use of this parameter did not improve on the selectivity of the determination of Cu^{II} with respect to that of Ni^{II}, which is a major interferent in the initial-rate method for Cu^{II}. However, it was found that the reciprocal of the peak half-width at half-height varied linearly with the copper concentration and resulted in enhanced tolerance to Ni^{II}. As can be seen in Table 2, whereas in the

Table 1. Features of the calibration graphs

Analyte	Reagents	Mode*	Linear range/ μg ml^{-1}	Slope (SD)/cm ml ng^{-1}	Intercept (SD)/cm	Correlation coefficient (r)	SEE
Cu^{II} ..	Hydroquinone + H_2O_2	R	5–20				
		B	2–30	9.6×10^{-5} (5.6×10^{-6})†	1.9×10^{-3} (1.0×10^{-4})†	0.994	1.2×10^{-4}
I^- ..	$S_2O_8^{2-}$ + $S_2O_3^{2-}$	R	130–630				
		F	190–460				
		C	130–500	3.7×10^{-4} (1.6×10^{-5})	0.10 (5.7×10^{-3})	0.997	5.5×10^{-3}
		D	130–250	7.9×10^{-4} (9.0×10^{-5})	0.06 (0.02)	0.994	8.1×10^{-3}
		E	130–500	1.1×10^{-3} (1.0×10^{-5})	0.02 (3.5×10^{-3})	0.999	3.4×10^{-3}
Fe^{II} ..	PHP + H_2O_2	R	0.01–0.06				
		F	0.01–0.06				
		C	0.03–0.06	116(3)	−0.5(0.16)	0.999	7.7×10^{-2}
Fe^{II} ..	1,10-Phenanthroline	R	0.5–4				
		B	0.5–8	0.86(0.01)	0.04(0.05)	0.999	0.087
		C	0.5–8	1.50(0.04)	1.2 (0.22)	0.998	0.264
		E	1–6	0.60(0.06)	1.3 (0.22)	0.990	0.231

* R = initial rate; B = first derivative; C = second derivative; D = third derivative; E = fourth derivative; and F = induction period.
† For this system, the slope and intercept are given in cm^{-1} ml μg^{-1} and cm^{-1}, respectively.

Table 2. Selectivity study

System	Analyte concentration/ μg ml^{-1}	Interference: Species	Interference: Concentration/ μg ml^{-1}	Error,* % R	F	B	C	D	E
Cu^{II} - hydroquinone - H_2O_2	5	Ni^{II}	2	4	—	a†	—	—	—
			5	25	—	a	—	—	—
			10	62	—	2	—	—	—
			15	62	—	12	—	—	—
I^- - $S_2O_8^{2-}$ - $S_2O_3^{2-}$	200	Cu^{II}	0.005	1.8	2.5	—	a	a	a
			0.01	12.5	4.5	—	a	a	a
			0.05	18.7	9.3	—	a	a	3.4
			0.10	21.9	12.5	—	a	a	5.2
			0.30	56.2	27.5	—	5.7	12.1	25.4
Fe^{II} - PHP - H_2O_2	0.03	Co^{II}	0.02	21.2	29.1	—	a	—	—
			0.03	24.1	39.2	—	a	—	—
			0.05	28.7	76.2	—	a	—	—
			0.07	41.6	127.0	—	a	—	—
			0.10	48.5	193.1	—	a	—	—
Fe^{II} - 1,10-phenanthroline	3	Co^{II}	3	23.6	—	a	1.8	—	1.7
			6	44.9	—	22.5	26.3	—	26.2

* R = initial rate; B = first derivative; C = second derivative; D = third derivative; E = fourth derivative; and F = induction period.
† a = error lower than 1%.

initial-rate method a Cu^{II} to Ni^{II} ratio of 2.5 : 1 gives an error of 4%, by using the first-derivative method, a 1 : 2 ratio results in an error of only 2%. Table 1 shows the linear range of this derivative method, which is wider than that of the corresponding initial-rate method and the features of the calibration graph. The small standard deviation (SD) of the slope and intercept and the standard error of estimate (SEE), show that the method is satisfactory. Although the second-derivative curve allows the same measurement parameter to be used for quantification purposes, the sensitivity (slope of the calibration graph) obtained is very small.

Iodide - peroxydisulphate - thiosulphate system

This system has been described elsewhere[6] for the determination of copper and iron, catalysts for this redox reaction. However, the uncatalysed reaction was chosen in order to compare the results obtained in the potential determination of iodide in the presence of copper by using initial-rate and induction-period measurements with those obtained by the methods based on the use of derivative curves of the kinetic curve. A constant amount of sodium thiosulphate was used to obtain the induction period. The broken lines shown in Fig. 2(*c–e*) correspond to the measurements that can be used to obtain the corresponding calibration graphs for iodide. As shown in Table 2, the determination of 200 μg ml^{-1} of iodide from the initial rate or induction period is interfered with by the presence of 0.01 μg ml^{-1} of copper (12.5 and 4.5% error, respectively); however, by using the data obtained from the second- and third-derivative curves, a copper concentration of up to 0.10 μg ml^{-1} was tolerated (error less than 1%). By using the fourth-derivative curve, the determination of iodide was possible in the presence of 0.05 μg ml^{-1} of copper, with an error of 3.4%. Table 1 summarises the features of the corresponding calibration graphs obtained by using this derivative approach; as can be seen, the results provided by the different parameters are satisfactory.

Fe^{II}-induced PHP - hydrogen peroxide system

The Fe^{II}-induced PHP - hydrogen peroxide reaction[5] was chosen to study the analytical application of the derivative approach to the kinetic curves obtained from a Landolt-type reaction using spectrofluorimetric detection. Fig. 3 shows the kinetic curve obtained for this system and its corresponding derivative curves. The determination of Fe^{II} from the initial rate and induction period is strongly interfered with by the presence of a Co^{II} concentration similar to that of Fe^{II} (Table 2). However, by using the measurement parameter shown in the second-derivative curve by a broken line [Fig. 3(*c*)], the determination of Fe^{II} can be carried out in the presence of a Co^{II} concentration at least three times that of Fe^{II}. Table 1 shows the features of the calibration graph obtained by this method. No quantification parameters were adequate for the

other derivative curves to increase the selectivity of the determination of Fe^{II} with respect to Co^{II}.

Kinetic Curves Without an Induction Period

Fe^{II} - 1,10-phenanthroline system

The formation of this complex was studied kinetically by using the stopped-flow technique to obtain the corresponding derivative curves shown in Fig. 4. It was found that the initial decrease preceding the rise of the kinetic curve depended on the analyte concentration when a mixture of sample and reagent was allowed to equilibrate in the flow cell before a subsequent aliquot of the same sample was processed. Hence, the rate and extent of the initial change depended on the previous and following solutions containing both aliquots of the same sample. At least three runs per sample were performed, and the data for the derivative curves were obtained from the second or subsequent runs. The different measurement parameters that were found to correlate empirically with the Fe^{II} concentration and enhance the tolerance to Co^{II} in the initial-rate method for the determination of Fe^{II} are shown by broken lines in Fig. 4. None of the parameters tested for the third-derivative curve improved on the selectivity with respect to Co^{II}. Table 1 summarises the features of the calibration graphs obtained from the first-, second- and fourth-derivative curves. In all instances, the linear range obtained was wider than that provided by the initial-rate method.

Conclusions

Although it is not possible to generalise on the advantages of this modification of the conventional derivative kinetic method owing to its empirical character and dependence on the shape of the kinetic curve obtained for the chemical system used, the results obtained for the four chemical systems studied show that the use of new measurement parameters employed in derivative kinetic methods substantially improves on the selectivity of the determinations. Regarding sensitivity, it is not possible to compare these methods with their corresponding initial-rate counterparts because the analytical parameter used in each instance is different. However, the results summarised in Table 1 show that the features of the calibration graphs obtained by this modified approach are satisfactory. In addition, the linear range of two of the systems studied was improved with respect to those provided by the corresponding initial-rate methods as a result of using this data processing method.

The authors are grateful to the CICYT (Project No. PB87-0821) for financial support.

References

1. Pardue, J. H. L., *Anal. Chim. Acta*, 1989, **216**, 69.
2. Savitzky, A., and Golay, J. E., *Anal. Chem.*, 1964, **36**, 1627.
3. Loriguillo, A., Silva, M., and Pèrez-Bendito, M., *Anal. Chim. Acta*, 1987, **199**, 29.
4. Yatsimirskii, K. B., "Kinetic Methods of Analysis," Pergamon Press, London, 1966, p. 101
5. Rubio, S., Gómez-Hens, A., and Valcárcel, M., *Anal. Chem.*, 1984, **56**, 1417.
6. Pall, A., Svehla, G., and Erdey, L., *Talanta*, 1970, **17**, 211.

Paper 9/04649F
Received October 30th, 1989
Accepted June 19th, 1990

Spectrophotometric Determination of Cysteine and Cystine in Urine

Joseph Chrastil
US Department of Agriculture, Southern Regional Research Center, New Orleans, LA 70179, USA

A spectrophotometric method for the determination of cysteine and cystine in urine is described. This method is a modification of that reported for the determination of cysteine and cystine in proteins. The determination in urine is specific and simple. The colour develops at room temperature and no pre-treatment of urine is needed. Other amino acids, urea, uric acid, ascorbic acid, bilirubin, biliverdin, carbohydrates, hormones, acetone, salicylic acid, small amounts of protein and other common components of urine do not interfere. The method is particularly suitable for the diagnosis of hepatic cystinuria and other diseases characterised by high sulphur-containing amino acids in urine.

Keywords: *Cysteine and cystine determination; spectrophotometry; urine*

Hepatic cystinuria and some other diseases are characterised by high concentrations of cystine (CSSC) and cysteine (CSH) in urine (usually >400 mg l^{-1}). Among the quantitative methods for CSSC plus CSH in urine that have been proposed are iodimetry,[1,2] polarography,[3] high-performance liquid chromatography,[4] ion-exchange chromatography,[5–8] microbiology[9–10] and colorimetry.[11–35]

Colorimetric methods are based on the reaction with nitroprusside,[11–16] phosphotungstic acid,[17–23] 1,2-naphthoquinone-4-sulphonic acid[24–32] and 2,6-dichloro-*p*-benzoquinone.[33] These colorimetric reagents react with CSH but not with CSSC and thus CSSC in urine must be reduced to CSH, which is accomplished, for example, by using Sn, Na_2SO_3, $HgCl_2$ or NaCN.

The methods suffer from high blanks, unstable colours, low specificity, high sensitivity to reaction conditions and other components present in urine and/or require laborious procedures. For example, negative results with CSSC concentrations in urine of <100 mg l^{-1} have been reported with nitroprusside,[14] lack of specificity and loss of absorption peaks with 1,2-naphthoquinone-4-sulphonic and phosphotungstic acids.[17,21,29,34,35] Additionally, phosphotungstic acid reacts with urea, ascorbic acid, tyrosine, uric acid, salicylic acid and other common components of urine. Thus, some laborious modifications of these methods have been proposed, for example, purification with charcoal[28] or precipitation with CuCl.[22,28]

It has been found that the spectrophotometric method for the determination of CSH and/or CSSC in proteins, recently published,[36] can easily be applied to urine.

Experimental

Materials

All chemicals were obtained from Aldrich and Sigma. Reagents of the highest available purity were used for the analysis.

Urine Samples

Urine was diluted 1 + 1 or more with distilled water or 0.1 M HCl. If CSSC precipitate is present, HCl must be used to dissolve it. Diluted urine was usually clear. No purification or other treatment was necessary even when the diluted urine was slightly cloudy.

Determination of Cysteine

In small test-tubes, the diluted urine sample (0.2 ml) containing 5–500 mg l^{-1} of CSH was mixed with 0.2 ml of H_2O and 0.1 ml of arsenate (5% $Na_2HAsO_4.7H_2O$ in H_2O). After 10 min, 2.3 ml of 88% HCOOH were added and mixed. Then 0.2 ml of 0.01 M OsO_4 in H_2O was added and the solution mixed on a vortex mixer. The sample was allowed to stand at room temperature for 2 h after which the absorbance was measured at 335 nm *versus* H_2O using a Shimadzu 260 double-beam spectrophotometer. For the preparation of the standard, urine was replaced by CSH (0.0025 M in 0.1 M HCl) and for the blank the standard was replaced by H_2O. The absorbance of CSH (A_{CSH}) = standard minus blank. For the urine blank, OsO_4 was replaced by H_2O and the absorbance minus the absorbance of the blank = A_1.

Determination of Cystine Plus Cysteine

In small test-tubes, a diluted urine sample (0.2 ml) containing 10–1500 mg l^{-1} of CSSC was mixed with 0.1 ml of arsenate (5% $Na_2HAsO_4.7H_2O$ in H_2O), 0.1 ml of 10 M NaOH and 0.1 ml of NaCN (10% in H_2O). After 10 min, 2.3 ml of 88% HCOOH were added and mixed on a vortex mixer. The sample was allowed to stand at room temperature for 2 h after which the absorbance was measured at 335 nm *versus* H_2O using a Shimadzu 260 double-beam spectrophotometer. For the preparation of the standard, urine was replaced by CSSC (0.0025 M in 0.1 M HCl). For the blank the standard was replaced by H_2O. The absorbance of CSSC (A_{CSSC}) = standard minus blank. For the urine blank, OsO_4 was replaced by H_2O and the absorbance minus the absorbance of the blank = A_2.

The arsenate stock solution was stable at room temperature (in a refrigerator, crystallisation may occur) and the stock solutions of cyanide, osmic acid and the standards were stable in a refrigerator for several months. Although free HCN does not evolve during the reaction because it is completely bound by arsenate and/or OsO_4 and the reagents in the test-tube are very dilute, all reagents (including concentrated HCOOH) are poisonous and must be handled cautiously.

Results and Discussion

The method described here is specific for CSH and in mixtures of CSH plus CSSC both amino acids can be determined separately by analysing two samples, one without and one with KCN. The concentration of CSH in urinary protein is usually very low but if necessary, protein may be precipitated easily by the addition of trichloroacetic acid and the supernatant used for the determination of CSH and/or CSSC. This procedure did not interfere with the colour reaction with OsO_4. Other amino acids and common components of urine (urea, uric acid, bilirubin, biliverdin, ascorbic acid, carbohydrates, hormones, acetone and/or salicylic acid) did not affect the reaction.

The diluted urine blanks (without OsO_4) had low absorb-

Table 1. Determination of CSH and CSSC in urine. All samples (except normal urine) were prepared from control urine by the addition of CSH and/or CSSC. The values are averages from duplicates

		Found/g l^{-1}		Difference, %	
CSH	CSSC	CSH	CSSC	CSH	CSSC
Normal urine I . .	—	0.050	0.020	—	—
Normal urine II	—	0.060	0.040	—	—
Control urine . .	—	0.100	0.000	—	—
0.110	0.000	0.112	0.002	+2	—
0.120	0.000	0.117	0.002	−2	—
0.150	0.000	0.151	0.000	+1	—
0.200	0.000	0.196	0.002	−2	—
0.500	0.000	0.515	0.005	+3	—
0.100	0.020	0.104	0.022	+4	+10
0.100	0.050	0.100	0.051	0	+2
0.100	0.100	0.101	0.107	+1	+7
0.100	0.200	0.104	0.204	+4	+2
0.100	0.400	0.095	0.390	−5	−2
0.100	0.600	0.102	0.608	+2	+1
0.100	0.800	0.106	0.787	+6	−2
0.100	1.000	0.096	0.991	−4	−1
0.100	1.500	0.095	1.539	−5	+3
0.150	0.400	0.148	0.422	−1	+5
0.500	0.100	0.503	0.096	+1	−4
0.400	0.800	0.408	0.791	+2	−1

ance values. The standard blank values with OsO_4 were also low and depended only on the purity of the reagents (NaCN, Na_2HAsO_4, HCOOH and OsO_4). Any reaction time between 20 min and 3 h could be used for the determination,[36] however, the sensitivity increases with time. The colour was developed at room temperature (25 ± 5 °C) for 2 h. The reproducibility was very good and the standard error of the mean from quadruplicates was less than 3%. The absorbance was linear with the concentration of CSH or CSSC in urine up to 1.0 A. Proteins and/or peptides that contained CSH or CSSC simply gave an increased absorbance value owing to their CSH and CSSC content (not shown here), however, even if protein was present in urine (normally 20–100 mg l^{-1}) its influence was very small relative to the concentrations of CSSC caused by cystinuria or other diseases.

Urine can be stored in a refrigerator for several weeks. Very small amounts of urine (0.2 ml) are needed for the analysis. The reaction rate at room temperature is only slightly influenced by temperature.[36]

Under the conditions described under Experimental, at 25 °C, both blanks had absorbance values of 0.050 and the average $A_{CSH} = A_{CSSC} = 0.802$. The equations used to calculate the concentration of CSH and/or CSSC in urine were: $A_1 \times 0.79$ = g l^{-1} CSH and $(A_2 - A_1) \times 1.57$ = g l^{-1} CSSC.

In all of the samples that were analysed (prepared from control urine by the addition of CSH and/or CSSC) a good agreement with the theoretical value was found (Table 1). The method is simple and specific, and is a useful tool for urine analysis.

References

1. Okuda, Y., *J. Biol. Chem.*, 1925, **5**, 638.
2. Virtue, R. W., and Lewis, H. B., *J. Biol. Chem.*, 1934, **104**, 415.
3. Reed, G., *J. Biol. Chem.*, 1942, **142**, 61.
4. Saetre, R., and Rabenstein, D. L., *Anal. Biochem.*, 1978, **90**, 684.
5. Westall, R. G., *Biochem. J.*, 1952, **52**, 638.
6. Stein, W. H., *J. Biol. Chem.*, 1953, **201**, 45.
7. Westall, R. G., *Biochem. J.*, 1955, **60**, 247.
8. Evered, D. F., *Biochem. J.*, 1956, **62**, 416.
9. Frankl, W., and Dunn, M. S., *Arch. Biochem.*, 1947, **13**, 93.
10. Camien, M. N., and Dunn, M. S., *J. Biol. Chem.*, 1950, **183**, 561.
11. Brand, E., Harris, M. M., and Biloon, S., *J. Biol. Chem.*, 1930, **86**, 315.
12. Lewis, H. B., *Ann. Intern. Med.*, 1932, **6**, 183.
13. Dent, C. E., and Rose, G. A., *Q. J. Med.*, 1951, **20**, 205.
14. Dent, C. E., and Wolshe, J. M., "Liver Disease," Sherlock, London, 1951, p. 22.
15. Fischl, J., Sason, I., and Segal, S., *Clin. Chem.*, 1961, **7**, 674.
16. Titaev, A. A., and Balabolkin, I. I., *Lab. Delo*, 1971, **10**, 618.
17. Looney, J. M., *J. Biol. Chem.*, 1922, **54**, 171.
18. Folin, O., and Marenzi, A. D., *J. Biol. Chem.*, 1929, **83**, 103.
19. Lugg, J. W. H., *Biochem. J.*, 1933, **26**, 2144.
20. Shinohara, K., *J. Biol. Chem.*, 1935, **110**, 263.
21. Shinohara, K., *J. Biol. Chem.*, 1935, **109**, 665.
22. Shinohara, K., and Padis, K. E., *J. Biol. Chem.*, 1936, **112**, 683.
23. Schoberl, A., and Rambacher, P., *Biochem. Z.*, 1938, **295**, 377.
24. Sullivan, M. X., *J. Biol. Chem.*, 1924, **59**, 1.
25. Sullivan, M. X., *Public Health Rep.*, 1926, **41**, 1030.
26. Lugg, J. W. H., *Biochem. J.*, 1933, **27**, 668.
27. Brand, E., Cahill, G. F., and Block, R. J., *J. Biol. Chem.*, 1935, **110**, 399.
28. Sullivan, M. X., and Hess, W. C., *J. Biol. Chem.*, 1936, **116**, 221.
29. Medes, G., and Padis, K. E., *Biochem. J.*, 1936, **30**, 941.
30. Medes, G., *Biochem. J.*, 1936, **30**, 1293.
31. Sullivan, M. X., Hess, W. C., and Howard, H. W., *J. Biol. Chem.*, 1942, **145**, 621.
32. Procos, J., *Clin. Chem.*, 1961, **7**, 97.
33. Fernandez, A. A., and Henry, R. J., *Anal. Biochem.*, 1965, **11**, 190.
34. Prunty, F. T. G., *Biochem. J.*, 1933, **27**, 387.
35. Henry, R. J., "Clinical Chemistry," Harper & Row, New York, 1964, pp. 302–308.
36. Chrastil, J., *Analyst*, 1989, **114**, 1133.

Paper 0/01952F
Received May 2nd, 1990
Accepted June 12th, 1990

Spectrophotometric Determination of Acetone Using Vanillin

Sulbha Amlathe and V. K. Gupta*
Department of Chemistry, Ravishankar University, Raipur 492 010, India

A sensitive method is described for the spectrophotometric determination of acetone in water. Acetone reacts with vanillin in alkaline medium forming a yellow - orange dye with an absorption maximum at 430 nm. Beer's law is obeyed in the range from 0.5 to 5 p.p.m. of acetone in water. Molar absorptivity and Sandell's sensitivity were found to be $11.0 \times 10^3 \pm 100$ l mol^{-1} cm^{-1} and 0.005 μg cm^{-2}, respectively. The important parameters for complete colour development were optimised and the method was used for the determination of acetone in biological samples. The method was also applied successfully to the determination of acetone in air after absorption in sodium hydrogen sulphite solution.

Keywords: *Spectrophotometry; acetone determination; water; biological sample; urine*

Acetone is a low-cost industrial solvent and chemical intermediate, which is used extensively as a solvent for oils and fats. It is used in the manufacture of smokeless powder and explosives and also in various industries, *e.g.*, in the laquer, varnishing, dyeing, leather and plastics industries.[1]

Acetone constitutes a serious fire hazard because of its high volatility. Exposure to high concentrations of acetone produces a narcotic effect and irritation of the mucous membrane. Bronchitis and gastric disturbance have also been reported. Acetone can cause dermatitis after absorption through intact skin and by inhalation.[1,2] The threshold limit value given for acetone is 1000 p.p.m.[3]

Several reagents have been used for the spectrophotometric determination of acetone, including hydroxylamine hydrochloride and bromophenol,[4] 2,4-dinitrophenylhydrazine,[5] dichromate and sulphuric acid,[6] salicylaldehyde,[4,7] diazotised *p*-aminobenzoic acid[8] and diazotised sulphanilic acid.[9] In this paper vanillin is proposed as a selective reagent for the determination of acetone in strongly alkaline medium; a yellow - orange dye is formed with an absorption maximum ($\lambda_{max.}$) at 430 nm measured against a reagent blank. The reaction conditions were optimised and the method was applied to the determination of acetone in a biological fluid. Molar absorptivity and Sandell's sensitivity were also evaluated.

Experimental

Apparatus

A Carl-Zeiss Spekol spectrophotometer with matched 1-cm cells was used for all spectral measurements. Calibrated glassware, a PIMCO rotameter (for checking air flow) and 35-ml capacity midget impingers were used.

Reagents

All chemicals used were of analytical-reagent grade, and all solutions were prepared with distilled water.

Acetone. A stock solution of 1 mg ml^{-1} (v/v) acetone was prepared in 0.5% sodium hydrogen sulphite solution. A working standard of 20 μg ml^{-1} was prepared by appropriate dilution of the stock solution.

Vanillin. Obtained from Loba Chemicals. A 2% m/v solution was prepared in 25% aqueous ethanol (*i.e.*, 25 ml of ethanol diluted to 100 ml with water).

Sodium hydroxide. A 1 M solution was used.

Sodium hydrogen sulphite. A 1% solution was prepared and a 10-ml volume was used as the absorbing solution.

Procedure

An aliquot of a solution containing 5–50 μg of acetone was placed in a 10-ml calibrated flask. To this solution 1 ml of vanillin solution followed by 1 ml of sodium hydroxide solution were added. The flask was tightly stoppered and placed in a water-bath at *ca.* 40 °C for 10 min. The flask was removed from the bath and cooled to room temperature. The absorbance of the dye was measured at 430 nm after a period of 10 min. A reagent blank was prepared in the same manner.

Results and Discussion

Spectral Characteristics

The dye formed was measured at 430 nm. The reagent blank had negligible absorbance at this wavelength.

Effect of Varying Reaction Conditions

It was found that a minimum of 1 ml of 2% vanillin solution was required for complete colour development. Larger amounts of vanillin increase the absorbance of the sample and of the reagent blank.

It was found that 1 ml of 1 M sodium hydroxide solution was sufficient to obtain maximum absorbance.

The effect of time and temperature was studied. The colour of the dye started to appear after 2 min at *ca.* 40 °C; maximum intensity was obtained after 10 min. The colour was found to be stable for *ca.* 10 h in the temperature range 15–60 °C.

Beer's Law, Sandell's Sensitivity, Molar Absorptivity and Reproducibility[10]

The colour system obeyed Beer's law in the range from 0.5 to 5 p.p.m. of acetone in a final volume of 10 ml. Molar

Table 1. Effect of foreign species. Concentration of acetone, 20 μg ml^{-1}

Compound or species	Tolerance limit,* p.p.m.
Aniline, benzene, hydroxylamine, hydrazine	2000
Ethanol, methanol	1500
Formaldehyde, *p*-chlorophenol, phenol	200
Cu^{2+}†, Fe^{3+}‡	200
Se	250
Mg^{2+}	50
Br^-, SO_3^{2-}, SO_4^{2-}	1000
Ca^{2+}†, Ba^{2+}, Sr^{2+}	300

* Causing an error of ±2% or less.
† Masked with 1 ml of 10% EDTA solution.
‡ Masked with 1 ml of 10% potassium sodium tartrate.

* To whom correspondence should be addressed.

absorptivity and Sandell's sensitivity were found to be $11.0 \times 10^3 \pm 100$ l mol^{-1} cm^{-1} and 0.005 μg cm^{-2}, respectively. The reproducibility of the method was checked by replicate analyses over a period of 7 d. Standard deviation and relative standard deviation were found to be ±0.007 A and 7%, respectively, for 30 μg of acetone in a final volume of 10 ml.

Effect of Interferents

To check the validity of the method, 20 μg of acetone in the final volume of 10 ml were determined in the presence of known amounts of foreign species commonly found with acetone. The tolerance limits for various interfering species are shown in Table 1. The tolerance limits for metal ions that formed hydroxides in alkaline medium were increased after masking with ethylenediaminetetracetic acid (EDTA) and potassium sodium tartrate solution.

Table 2. Determination of acetone in biological fluids and results of recovery studies. Amount of urine, 1 ml. A, Proposed method; B, reported method[7]

Sample	Acetone added*/μg	Total acetone found/μg		Acetone originally found/μg		Recovery, %	
		A	B	A	B	A	B
1	5	8.35	8.71	3.18	3.45	102.15	103.10
	10	13.16	13.36	3.15	3.50	100.11	98.99
	15	23.12	23.55	3.13	3.52	99.98	100.00
2	5	10.03	10.12	5.15	5.23	98.85	98.99
	10	15.20	15.19	5.21	5.19	99.99	100.00
	15	25.00	25.33	4.99	5.05	100.12	101.15
3	5	13.37	13.50	8.35	8.50	100.22	100.00
	10	18.36	18.17	8.28	8.12	101.35	100.29
	15	28.30	28.37	8.32	8.45	99.93	99.75

* Mean of three replicate analyses.

Table 3. Determination of acetone in urine samples from diabetic patients. Amount of sample taken in each instance, 1 ml. Each sample was diluted to 100 ml with distilled water. A, Proposed method; B, reported method[7]

Sample	Method A*	Method B*
1	30.13	31.00
2	32.25	33.16
3	38.17	38.35

* Mean of three replicate analyses.

Table 4. Determination of acetone in air. Samples were prepared by evaporating a few millilitres of acetone in a fume cupboard

Acetone found by proposed method*/μg	Acetone found by salicylaldehyde method*/μg
10.25	10.22
15.30	15.25
25.75	27.80
45.28	45.20
50.13	50.45

* Mean of three replicate analyses.

Application

The method was applied to the determination of acetone in a biological fluid (urine) and in air.

Urine

The determination of acetone in urine is important for patients suffering from diabetes. Acetone has been reported to be present in urine.[1] Authentic samples were deproteinated by following the method of Aldridge.[11] Synthetic samples were also prepared by adding known amounts of acetone prior to analysis. The results obtained with the proposed method and those given by a previously reported method[7] showed good agreement (Tables 2 and 3).

Air

The method was applied successfully to the determination of acetone in air using a Grab air sampling method, *i.e.*, sampling over short time periods. Owing to the fact that standard air samples containing acetone were not available, acetone vapour in air was obtained by evaporating a few millilitres of acetone in a fume cupboard. The air containing the acetone vapour was then drawn into the absorbing solution, *i.e.*, 1% sodium hydrogen sulphite solution,[4] at a flow-rate of 250 ml min^{-1} for 10 min. The absorbed acetone was determined by the reported method using salicylaldehyde.[7] The values obtained were almost identical with those obtained with the proposed method (Table 4). The proposed method is also applicable to the time weighted average (TWA) method as for the National Institute of Occupational Safety and Health, Occupational Safety and Health Act regulations.

Conclusion

The proposed one-step method is simple and sensitive. The method was compared with other spectrophotometric methods and found to be faster and of comparable or better sensitivity (Table 5). The main advantages of the proposed method over the salicylaldehyde method[7] are the shorter time required for colour development and the lower temperature of the reaction. The method is free from many interferents (Table 1) and can be used for the routine determination of acetone in water, air and urine.

We thank the Head, Department of Chemistry, Ravishankar University, for providing laboratory facilities. S. A. thanks the CSIR, New Delhi, for the award of a Senior Research Fellowship.

Table 5. Comparison with other spectrophotometric methods

No.	Reagents	$\lambda_{max.}$/nm	Determination range, p.p.m.	Remarks/reference
1	Salicylaldehyde, sodium hydroxide	535	0.52–0.99	Higher temperature, 60 °C; time, 1 h (reference 7)
2	2,4-Dinitrophenylhydrazine	530	0–50	Colour unstable; temperature, 50 °C; time, *ca.* 40 min (reference 5)
3	2-Nitrobenzaldehyde	410	10–100	Reagent unstable; time, *ca.* 30 min (reference 1)
4	Diazotised *p*-aminobenzoic acid	430	1–7	Interference from nitrite and phenol; less sensitive (reference 8)
5	Diazotised sulphanilic acid	450	0.5–8.5	Interference from nitrite and phenol; less sensitive (reference 9)
6	Vanillin, sodium hydroxide	430	0.5–5	Free from interference; time, *ca.* 20 min; more sensitive (proposed method)

References

1. Patty, F. A., "Industrial Hygiene and Toxicology," Volume II, Second Edition, Interscience, New York, 1963, pp. 1720–1731.
2. Kolthoff, I. M., Elving, P. J., and Stross, F. H., "Treatise on Analytical Chemistry," Part III, Volume 2, Wiley-Interscience, New York, 1971, p. 138.
3. Occupational and Safety Health Act, Commerce Clearing House, USA, 1984, 3825–5.
4. Ruch, W. E., "Chemical Detection of Gaseous Pollutants," Ann Arbor Science Publishers, Ann Arbor, MI, 1973, p. 29.
5. Lappin, G. R., and Clark, L. C., *Anal. Chem.*, 1951, **23**, 541.
6. Kobayashi, Y. J., *J. Chem. Soc. Jpn. Ind. Chem. Sect.*, 1953, **56**, 174; *Chem. Abstr.*, 1954, **48**, 9271.
7. Anger, V., and Ofri, S., *Fresenius Z. Anal. Chem.*, 1969, **206**, 186.
8. Bashir, W. A., and Gagop, G. W., *Microchem. J.*, 1983, **28**, 77.
9. Rahim, S. A., and Bashir, W. A., *Microchem. J.*, 1981, **26**, 329.
10. Hughes, H. K., *Anal. Chem.*, 1952, **24**, 1649.
11. Aldridge, W. N., *Analyst*, 1944, **69**, 262.

Paper 0/01147I
Received March 15th, 1990
Accepted June 11th, 1990

COMMUNICATION

Material for publication as a Communication must be on an urgent matter and be of obvious scientific importance. Rapidity of publication is enhanced if diagrams are omitted, but tables and formulae can be included. Communications receive priority and are usually published within 5–8 weeks of receipt. They are intended for brief descriptions of work that has progressed to a stage at which it is likely to be valuable to workers faced with similar problems. A fuller paper may be offered subsequently, if justified by later work.

Manuscripts are usually examined by one referee and inclusion of a Communication is at the Editor's discretion.

Preferential Distribution of Streptomycin in Pig Kidney Cortex

Pamela J. Brush, John P. M. Wood and Ian C. Shaw
Toxicology Section, Biochemistry Department, Central Veterinary Laboratory, Weybridge, Surrey KT15 3NB, UK

In 14 pig kidneys containing streptomycin, an average distribution ratio of 2.5 : 1 was found for the streptomycin between the cortex and medulla. It is suggested here that cortex alone be used, instead of mixed kidney tissue, in regulatory meat monitoring schemes.

Keywords: *Streptomycin; kidney cortex; meat monitoring*

Streptomycin is used therapeutically in veterinary medicine to combat a number of bacterial infections. It also has growth-promoting properties but is not licensed for this use.

Residues of antimicrobial drugs in animal products for human consumption are covered by an EC Directive (86/469/EEC) which requires the monitoring of drug residues in meat. Streptomycin is excreted primarily by the kidney where it is concentrated rather than in the liver: therefore, it is the kidney tissue that is analysed for streptomycin residues in statutory monitoring schemes. Previous work in this laboratory indicated that, in rats that were fed a streptomycin-containing diet for 6 d the streptomycin levels in the kidney cortex were, on average, nearly four times higher than in the medulla.[1] These investigations have now been extended to the pig. The pig is an important food-producing animal which is commonly farmed intensively and may be treated with antimicrobial drugs.

Table 1. Streptomycin concentration in pig kidneys. All results are the mean values of two determinations

Pig No.	Streptomycin concentration/mg kg^{-1}		
	Cortex (C)	Medulla (M)	C/M
1	9.97	1.53	6.52
2	5.17	3.00	1.72
3	2.01	0.89	2.26
4	12.95	7.07	1.83
5	17.13	2.63	6.51
6	13.09	4.21	3.11
7	4.42	3.77	1.17
8	7.26	5.50	1.32
9	8.57	12.17	0.70
10	76.75	19.63	3.91
11	8.22	7.47	1.10
12	1.37	1.36	1.01
13	4.83	2.02	2.39
14	3.75	2.47	1.52

Experimental

Extraction and Assay of Streptomycin

Frozen slaughterhouse kidneys were used. Fourteen pig kidneys known to contain streptomycin were dissected into cortex and medulla, which were analysed separately. Duplicate portions (0.2 g) of each tissue were homogenised in 2.0 cm^3 of phosphate buffer (0.08 M, pH 6.7, containing 0.9% m/v sodium chloride). The homogenate was centrifuged at 4 °C and 2.5 × 10^3 rev min^{-1} for 15 min. Aliquots of the supernatant were removed, diluted 10 times and 100 times with the phosphate buffer (see above), and 200-μl aliquots of these dilutions were analysed for streptomycin using an enzyme-linked immunosorbent assay (ELISA) technique developed at the Central Veterinary Laboratory.[2] This assay is linear over the range 50–200 μg kg^{-1} and the limit of detection is 50 μg kg^{-1}.

Results and Discussion

In 13 out of the 14 pig kidneys analysed, the streptomycin concentration in the cortex was higher than in the medulla. Data for individual animals are shown in Table 1. The mean cortex : medulla ratio for streptomycin concentration was 2.5. These results show a definite distribution bias for streptomycin in favour of the kidney cortex. It is, therefore, suggested that the analysis of kidney cortex rather than of mixed kidney tissue be introduced for regulatory meat monitoring schemes.

References

1. Lockyer, J. R., Bucknall, A., and Shaw, I. C., *in* Haagsma, N., Ruiter, A., and Czedik-Eysenberg, P. B., *Editors*, "Residues of Veterinary Drugs in Food," Utrecht, Rijksuniversiteit Utrecht, Faculteit der Diergeneeskunde, 1990, p. 254.
2. Jackman, R., 1989, personal communication.

Paper 0/02949A
Received July 2nd, 1990

BOOK REVIEWS

Packings and Stationary Phases in Chromatographic Techniques
Edited by Klaus K. Unger. *Chromatographic Science Series. Volume 47.* Pp. viii + 836. Marcel Dekker. 1990. Price $150.00 (USA & Canada); $180.00 (Export). ISBN 0 8247 7940 1.

Since the inception of the Marcel Dekker monograph series on Chromatographic Science, and with the publication of Calvin Giddings' excellent account of the dynamics of chromatography, over 40 volumes have appeared covering virtually all aspects of chromatography. Hitherto, the stationary phase, which is an essential component of all chromatographic systems has, largely, been neglected. Although somewhat belated this omission has now been rectified by the publication of a splendid review, written by internationally recognised experts under the editorial guidance of Klaus Unger, a scientist well known for his innovative work on liquid chromatographic packing materials.

The book provides a comprehensive review and critical analysis of the role of stationary phases and packings in gas, thin-layer and column liquid chromatography. Valuable information is given on the plethora of phases available for use by the analyst, including details of manufacture, structural properties and chromatographic behaviour, with special emphasis on factors affecting retention and selectivity. In the reviewer's opinion the book provides the essential knowledge to allow analytical chemists to select, handle and evaluate stationary phases for the solution of the full spectrum of chemical and biomedical separation problems.

The monograph consists of 13 chapters, the first of which presents a thorough historical review of the development of chromatography, essential reading for research into the origins of the technique. This is followed by an overview of packing materials which concentrates on the characterisation of the physical and chemical structural properties of stationary phases and the role of these properties in determining the efficiency and selectivity of systems in both gas and liquid chromatography.

Chapter 3 covers column packings for use in gas - solid and gas - liquid chromatography. This chapter contains a wealth of detail about the full range of commercially available sorbents, liquid phases and supports. Included is information on the manufacture, chemical structure and chromatographic properties together with guidelines for the selection of phases for a wide range of assays that should prove useful to the beginner and the established practitioner. There follows a brief account of column materials for liquid - liquid partition chromatography with solvent-generated phase systems.

Stationary phases for thin-layer chromatography are reviewed in Chapter 5. Here again much useful practical data are given about the full spectrum of sorbents for normal- and reversed-phase thin-layer chromatography. Details are given about bulk sorbents and pre-coated layers and in each instance mobile phase systems are recommended for a wide range of applications and typical separations illustrated.

A comprehensive account of column packings for liquid chromatography is given in Chapter 6. Here inorganic and organic sorbents are considered together with the full range of chemically bonded phases. Details are given of the preparation, physical and chemical characterisation together with typical analytical applications and a discussion of elution mechanisms. As with the gas chromatographic phases, discussed earlier in the text, valuable information is given on commercially available phases.

The next three chapters deal with stationary phases for size exclusion, donor - acceptor complex and ligand-exchange chromatography. These chapters not only contain useful information about the respective column materials but also helpful accounts of the theory and applications of these less familiar techniques.

A substantial account of ion-exchange chromatography is given in Chapter 10. In addition to a thorough treatment of ion exchangers, essential theoretical and practical aspects of the technique are discussed. Details are given of the majority of phases currently available, including polymer- and silica-based materials, and their analytical application is illustrated by typical examples. This chapter is followed by short yet informative accounts of phases for ion-pair, affinity and chiral-liquid chromatography.

The book is highly recommended.

M. B. Evans

Measurement Techniques for Carcinogenic Agents in Work Place Air
Commission of the European Communities. Pp. 74. Royal Society of Chemistry. 1989. Price £27.50. ISBN 0 85186 098 2.

This small book provides a useful guide to the analytical methods available for the measurement of 31 industrially used known or suspected carcinogens. The book may be seen as a companion volume to those reviews already published by the Royal Society of Chemistry dealing with the health risks associated with the occupational exposure to solvents and organochlorine solvents.[1,2]

The book is divided into chapters, one per compound, and all follow the same over-all format. Each chapter begins with the compounds' Chemical Abstracts Registry No., then synonyms, manufacture, uses, recommended method for the determination in a workshop atmosphere, other methods available and finally references. The section dealing with the recommended method is further sub-divided into sampling method, measuring method and performance characteristics of the method.

The over-all layout is easy to follow and the recommended procedures are, in most instances described in sufficient detail to allow an analytical chemist to perform them without necessarily having to refer to the source references. Most of the procedures described rely on a collection step, typically with a filter-paper or an absorbent such as silica gel or Tenax, followed by an extraction stage, and finally, either gas chromatography, high-performance liquid chromatography or atomic absorption spectrometry for quantification of the analyte. The final section dealing with "other methods" likewise provides a useful brief synopsis of alternative analytical procedures, all of which are adequately referenced.

The increasing awareness of possible health hazards associated with the prolonged industrial exposure to chemicals and the advent of the COSHH Regulations (1990) make the publication of this book particularly timely. It should also appeal to those people not directly involved in analytical chemistry, such as safety officers, chemical engineers, toxicologists and factory managers.

References

1. "Organo-Chlorine Solvents: Health Risks to Workers," The Royal Society of Chemistry, London, 1986.
2. "Solvents in Common Use: Health Risks to Workers," The Royal Society of Chemistry, London, 1988.

G. A. Mills

CUMULATIVE AUTHOR INDEX

JANUARY–OCTOBER 1990

Abad, Encarna Lorenzo, 617
Abbas, Nureddin M., 1375
Abdallah, Amin Mohamed A., 221
Abellán, Concepción, 217
Abousahl, Said, 731
Abramović, Biljana F., 79, 705, 715
Afşar, Hüseyin, 99
Ahmad, Shakeel, 287
Ahmed, Md. Jamal Uddin, 439
Akagi, Tasuku, 1329
Akama , Yoshifumi, 947
Akella, S. R. K. M., 455
Alañón, Aurelia, 1117
Albero, Maria Isabel, 989, 1257
Al-Daher, Ismail M., 645
Aleixo, Luiz M., 761
Alfassi, Zeev B., 29, 817
Allain, Pierre, 813
Alonso, J., 315
Altinoz, Sacide, 873
Alvarez, José M. Fernández, 617
Amlathe, Sulbha, 1385
Analytical Methods Committee, 459
Andres Garcia, Elena, 89
Anzano, Jesús M., 955
Aoki, Koichi, 413
Aoki, Nobumi, 435
Apak, Reşat, 99
Arent, Lori J., 899
Arima, Shoichi, 1191
Armanino, Carla, 907
Arpadjan, S. , 399
Arruda, Marco Aurélio Zezzi, 779
Ausili, Antonella, 1167
Avramides, E. J., 1037
Baeyens, Willy, 359
Baeza, J. J. Baeza, 721
Bahari, M. Shahru, 417
Baha-Uddin, Sulafa S., 1059
Balasubramanian, N., 859
Barba, Flora, 1335
Barbooti, Mahmood M., 1059
Bartle, Keith D., 125
Bartrolí, J., 315
Baty, J. D., 517, 521
Beary, Ellyn S., 911
Beaugrand, Claude, 813
Beceiro-Gonzalez, Elisa, 545
Bedair, Mona M., 449
Beksac, Sinan, 873
Belarra, Miguel A., 955
Belfiore, A., 649
Berg-Nielsen, Karen, 1265
Bermejo-Barrera, Adela, 545
Bermejo-Barrera, Pilar, 545, 549
Bermejo-Martinez, Francisco, 545, 549
Berthod, A., 933
Bhatia, Virendra K., 253
Birch, Brian J., 1277
Biziuk, Marek, 393
Blanchflower, W. John, 1323
Blanco Gomis, Domingo, 89
Blanco, Paulino Tuñón, 209, 1215
Bonilla, Milagros, 563
Bonilla Simón, Mª M., 337
Bosch Reig, F., 111
Bovara, Roberto, 889
Brainina, Khiena Z., 1301
Bralić, Marija, 737
Bramwell, Helena, 185
Braven, Jim, 189
Brennan, John D., 147
Bresadola, Silvano, 1041
Brienza, Sandra Maria Boscolo, 779
Brinkman, Jan-Henk W., 1033
Brinkman, Udo A. Th., 1033
Brooksbank, P., 507
Brossa, F., 1025
Brown, Craig J., 1197
Brown, R. Stephen, 147
Brush, Pamela J., 1389
Buldini, Pier Luigi, 1073
Burse, Virlyn W., 243
Buttery, Peter J., 1309
Bysouth, Stephen R., 571
Bystryak, Il'ya M., 839
Caballero, Manuel, 1201
Cacho, Juan, 657
Çadogan, Aodhmar, 1207
Çakar, Mira, 787
Calokerinos, Antony C., 613, 1229
Căluşaru, A., 1223
Calvo, Consuelo Pita, 549
Cámara, Carmen, 553, 563
Camoni, Ivano, 1167
Campanella, Luigi, 827
Campíns Falcó, P., 111
Canale-Gutierrez, Lucia, 1243
Cannavan, Andrew, 1323
Capitán, Fermín, 849
Capitán-Vallvey, Luis Fermín, 849
Cardone, M. J., 111
Cardwell, Terence J., 878, 1235
Carlomagno, Doralysa N., 1093
Carnero Ruiz, C., 1121
Caro, Arturo, 753
Carrascal, Isabel, 345
Carrazón, José M. Pingarrón, 869
Carrea, Giacomo, 889
Carty, Patricia, 617
Cass, Anthony E. G., 185
Castegnaro, Marcel, 129
Castillo, Juan R., 539, 955
Càstino, Mario, 907
Catterick, Timothy, 919
Cattrall, Robert W., 878, 1235
Cela, Rafael, 1201
Cella, Norberto, 341
Cerdá, Víctor, 749, 753
Chai, Fong, 143
Chakrabarti, Anil Kumar, 439
Chalk, Phillip M., 365
Chamberlain, Stephen J., 1161
Chan, Lai Kwan, 201
Chan, Wing Hong, 201, 205
Chan, Wing-Fat, 567
Chandra, Satya V., 287
Changui, Cherkaoui, 1177
Chen, Deli, 365
Chen, Le-Tian, 1019
Chen, P. Y., 29
Chen, Qing, 109
Cheung, Yiu-Ming, 1349
Chiu, Teresa P. Y., 653
Chopra, Sneh J., 253
Chrastil, Joseph, 1383
Christian, Gary D., 475
Chu, C. C., 29
Chung, Koo-soon, 965
Cipko, Edward, 593
Clark, Georgina B., 1
Clifford, Anthony A., 125
Cody, Maria K., 1
Coleman, Catherine S., 517
Conway, Brian O. B., 1
Corbisier, Veronique, 359
Cortés, Gabriel, 753
Cretella, Rubén F., 915
Criddle, W. J., 417
Crosby, Neil T., 1
Cross, Graeme J., 1235
Cudby, Michael E. A., 1313
da Silva, William José, 341
Dadgar, Darioush, 275
Dafoe, T., 507
Dakashev, Anastas Dimitrou, 1247
Dams, Richard, 17
Dart, Peter J., 13
Davidson, Alexander G., 997
Davies, Cledwyn L., 379
Dawson, George A., 1153
De Elvira Cózar, A., 337
de Gracia, Juan Pedro, 849
de Oliveira Neto, Graciliano, 761
de Ruiter, Cor, 1033
Delaporte, Thierry, 813
Di Noto, Vito, 1041
Diamond, Dermot, 1207, 1215
Díaz García, Marta Elena, 575
Díaz, José Manuel, 1201
Díaz, Victor Cabal, 209
Dommarco, Roberto, 1167
Dougé, Christophe, 813
Dowle, Chris J., 105
Duncan, Gregory, 109
Durán-Merás, Isabel, 1007
Durrani, Tariq M., 531
Ebdel-Hay, Mohamed A., 449
Ebdon, Les, 189
Economou, E. D., 765
Edmonds, Tony E., 599, 1277
Efstathiou, Constantinos E., 291
El-Gany, Nadya El-Sayed Abd, 221
Emons, Hendrik, 405, 895
Estela, J. M., 749
Evershed, Richard P., 1339
Evmiridis, Nicholaos P., 765, 771, 1103
Fadiran, Emmanuel O., 997
Fagioli, Francesco, 173
Faizullah, Azad T., 69
Farabella, Luciano, 593
Farroha, Sabri M., 57
Faruffini, G., 1025
Fattah, Fattah A., 645
Fedoroff, Michel, 731, 981
Fernandez-Alba, A. R., 329
Ferreira, José Roberto, 779
Ferreira, Vicente, 657
Ferri, Elida, 889
Fierro, Jose L. G., 345
Fleming, Paddy, 375
Flint, F. Olga, 61
Flores, Juana Rodriguez, 617
Fogg, Arnold G., 41, 305, 593, 599, 1277
Forina, Michele, 907
Forteza, R., 749
Frampton, Nicholas C., 189
Franco, Douglas Wagner, 795
Frank, Steven, 1327
Frazier, Donald O., 229
Frei, Roland W., 1033
Freney, John R., 365
Friel, James K., 269
Fudagawa, Noriko, 1185
Fumagalli, E. M., 1025
Fung, Ying-sing, 1219
Fux, Pierre, 179
Gaál, Ferenc F., 79, 715
Gaind, Virindar S., 143, 801, 925, 1359
Galceran, Mª. Teresa, 959
Galindo Riaño, M. D., 973
Gallego, Mercedes, 943
Gallorini, M., 1025
Gambetti, Luisa, 1167
Gani, David, 1313
Gao, Zhiqiang, 951
Garcia, Agustin Costa, 209, 1215
García Alvarez-Coque, M. Celia, 1125
García, Angel J. Reviejo, 869
García, Maria C., 345
García, Maria Soledad, 989, 1257
García Sánchez, F., 1003, 1121
García-Vargas, M., 973
Gardner, M. J., 371
Garrels, Rick L., 155
Gaskin, James E., 507
Gazy, Azza A., 449
Georgiou, Constantinos A., 309
Ghini, Severino, 889
Ghosh, Alpana, 969
Gibbs, Phillip N. B., 185
Gill, R., 371
Girotti, Stefano, 889
Glennon, Jeremy D., 627
Goad, L. John, 1339
Godbeer, William C., 865
Godinho, Oswaldo E. S., 761
Gómez, M., 553
Gómez-Hens, A., 1377
Gong, Cheng, 49
Gonzalo, Pedro, 345
Gramlich, John W., 1019
Grassi, Marco T., 761
Green, Monika J., 185
Greenfield, Stanley, 531
Greenway, Gillian M., 1297
Grekas, Nikos, 613
Grey, Peter, 159
Grigolo, Brunella, 889
Groce, Donald F., 243
Grzeskowiak, Roman, 1063
Guarneri, Mario, 929
Gunasingham, Hari, 35
Gupta, Anita, 421
Gupta, V. K., 1385
Gutierrez, M. C., 1377
Habboush, Albertine E., 57
Hafez, Medhat Abd El-Hamied, 221
Halvatzis, Stergios A., 1229
Hamada, Marawan A., 623
Hamano, Takashi, 435
Hamid, Junainah Abdul, 1289
Hanna, George M., 1157
Hara, Hirokazu, 1077
Hara, Shuuji, 1363
Harris, Stephen J., 1207
Hart, Barry T., 878
Hasdemir, Erdoğan, 297
Hase, Tapio A., 263
Hasebe, Kiyoshi, 413
Hassan, Eman B., 1059
Hassan, Saad S. M., 623
Haswell, Stephen J., 1063
Haustein, Catherine Hinga, 155
Head, Susan L., 243
Héberger, Károly, 725
Hehn, Karen E., 1019
Heineman, William R., 405, 895
Henderson, Gillian E., 1063
Hendra, Patrick J., 1313
Heredia Bayona, A., 1121
Hernández Córdoba, Manuel 757
Hernández López, M., 1003, 1121
Heron, Carl, 1339
Hikima, Satoshi, 413
Hirata, Takafumi, 1329
Holten, C. L. M., 1211
Hon, Ping-Kay, 567

Hosein, Sherina, 147
Hoshika, Takeshi, 535
Hoshino, Hitoshi, 133
Hou, Weiying, 139
Hougham, Bruce D., 147
Huang, Lolita, 925
Idei, Masae, 1109
Iketani, Shin-ichi, 1251
Ilcheva, Liliana Ilieva, 319, 1247
Imakita, Tsuyoshi, 1185
Imasaka, Totaro, 73
Inoue, Kouji, 1363
Iob, Asfaha, 1375
Ishibashi, Nobuhiko, 73
Ishida, Ryoei, 23
Ishikawa, Keiko, 425
Ito, Yoshio, 435
Iwashimizu, Tsuyoushi, 413
Iwata, Tetsuharu, 1363
Jackson, Simon E., 269
Jadage, Chandrakant D., 1367
Janardanan, C., 85
Janjić, Tomislav J., 383
Jaunault, Laurent, 813
Jedrzejczak, Kazik, 925, 1359
Jeng, Ingming, 109
Jiang, Mian, 49
Jinno, Tsunenobu, 535
Johnson, Brian J., 1153
Jones, Sheila J., 501
Jun, Zou, 389
Kakizaki, Teiji, 413
Kanai, Yutaka, 809
Kapoor, Vidya B., 253
Karayannis, Miltiades I., 741, 977, 1103
Katayama, Masatoki, 9
Kateman, Gerrit, 487
Kaya, Satilmis, 531
Kelly, W. Robert, 1019
Kemp, Anthony J., 1197
Kennedy, Colin D., 1067
Kennedy, D. Glen, 1323
Khanina, Rosa M., 1301
Khier, A. Aboul, 1181
Kimura, Keiichi, 1251
Kintz, Pascal, 1269
Kithinji, Jacob P., 125
Klemm, Nancy, 109
Koch, Klaus R., 823
Koh, Tomozo, 1133
Komers, Karel, 467
Korany, Mohamed A., 449
Korver, Margaret P., 243
Kotel'nikov, Aleksander I., 839
Koupparis, Michael A., 309
Kozuka, Shoji, 431
Krivokapić, Jasmina, 745
Krull, Ulrich J., 147, 883
Kubota, Hiroki, 1109
Kubota, Masaaki, 283, 939, 1185
Kuldvere, Arnold, 559
Kumar, B. S. M., 859
Kumar, T., 1319
Kura, Genichiro, 843
Kuroda, Rokuro, 431
Kurunczi, Éva K., 715
Lahsen, Joaquín, 409
Lamant, Jean-Michel, 1269
Landi, Silvio, 173
Lapeze, Jr., Chester R., 243
Lau, Oi-Wah, 653, 1349
Lau-Cam, Cesar A., 1157
Lavi, N., 817
Lee, Albert Wai Ming, 201, 205
Lee, Geum-hee, 965
Lemus, José M., 1117
Lentza-Rizos, Ch., 1037
León-González, M. Eugenia, 609
Lewis, Daniel M., 1029
Likhtenshtein, Gerts I., 839
Lima, Carlos A. S., 341
Lin, Betty, 359
Lingeman, Henk, 1033
Liu, Hai-lan, 835
Liu, Jianhua, 1089
Liu, Keshun, 1143
Liu, Kuai-zhi, 835
Locatelli, Clinio, 173
Longerich, Henry P., 269
Loos-Neskovic, Christiane, 731, 981
Lovrić, Milivoj, 45
Lowes, Stephen, 511
Luk, Shiu-fai, 653, 1219
Lukaszew, Rosa A., 915
Luque de Castro, M. D., 699
Maccà, Carlo, 631
McCalley, David V., 13, 1355
McClure, Patricia C., 243
Machado, Adélio A. S. C., 195
McKelvie, Ian D., 878
McKervey, M. Anthony, 1207
McLaughlin, Kieran, 275
McMaster, Dorothy, 275
Maddams, William F., 1313
Madrid, Yolanda, 563
Maeno, Isao, 73
Makkar, Harinder Paul S., 1309
Malcolme-Lawes, David J., 65
Malinowska, Elżbieta, 1085
Malyan, Andrew P., 105
Mangin, Patrice, 1269
Manzoori, Jamshid L., 1055
Maquieira, Angel, 1243
Marinković, Mitar M., 79
Mark, Jr., Harry B., 667
Markakis, Pericles, 1143
Marques, Edmar Pereira, 795
Márquez Gómez, J. C., 1003, 1121
Marquezini, Maria Valéria, 341
Marrero, Julieta G., 915
Martinez Calatayud, J., 855
Martínez-Lebrusant, Charo, 1335
Martinez-Lozano, M. Carmen, 217, 783
Martinez-Vidal, J. L., 329
Maru, Girish, 129
Maru, Vibuthi, 129
Marwah, Ashok K., 445
Marwah, Padma, 445
Masuda, Akimasa, 1329
Masuda, Yoshitaka , 1089
Matheson, Alasdair M., 105
Matuška, Radek, 1271
Mauras, Yves, 813
Mecherri, Mohamed O., 981
Medina Hernández, Mariá José, 1125
Meenakumari, K., 465
Mendez, Rita, 213
Menegatti, Enea, 929
Meng, Fanchang, 49
Mestres, Joan S., 1097
Metcalf, Richard C., 899
Midgley, Derek, 1283
Milovanović, Gordana A., 787, 791
Minobe, Masao, 535
Minorikawa, Masea, 23
Mishra, R. K., 969
Mitsuhashi, Yukimasa, 435
Miura, Jun'ichiro, 1191
Miura, Yasuyuki, 1133
Miyazaki, Akira, 1055
Mizuno, Takayuki, 279
Mlakar, Marina, 45
Mohite, Barburao S., 1367
Molina, R. Valero, 721
Monfort Cuenca, Enrique, 1125
Monreal, Francisco, 539
Montero, Rosa, 943
Moody, G. J., 1289
Morales, Alfonso, 409
Moreira, Josino C., 41
Mori, Shigetsugu, 1077
Moro, Antonino Lo, 641, 649
Morrison, Gregory M., 1371
Motomizu, Shoji, 389, 1109
Motta, Roberto, 889
Mottola, Horacio A., 679
Mrzljak, Robert I., 1235
Muccio, Alfonso Di, 1167
Muk, Aurora, 745
Mukai, Yoshio, 9
Mukunda Rao, S. R., 1129
Munõz de la Peña, Arsenio, 1007
Muñoz Leyva, J. A., 973
Muñoz, M., 315
Murillo, José A., 1117
Murthy, Ramesh C., 287
Nagy, Vitalii Yu., 839
Nair, S. Madhavankutty, 85
Najm, Kassim A., 645
Nakamuara, Masaru, 1363
Nakamura, Susumu, 283, 939
Nakano, Kouji, 133
Nakata, Ryuji, 425
Navalón, Alberto, 849
Nawata, Sawako, 843
Needham, Larry L., 243
Ng, Alice Chui Wah, 205
Nikolelis, Dimitrios P., 291, 883
Nitta, Akihiko, 425
Noutary, Clemente J., 915
Nukatsuka, Isoshi, 23
Oguma, Koichi, 431
Ohta, Kiyohisa, 279
Ohzeki, Kunio, 23
Ojanperä, Ilkka, 263
Oji, Yoshikiyo, 435
O'Kennedy, Richard J., 617, 1145
Olenchock, Stephen A., 1029
Ongomo, Peter, 1297
Ordieres, Arturo J. Miranda, 1215
Oshima, Mitsuko, 389
Otto, Matthias, 685
Ozawa, Hideaki, 1343
Ozsoz, Mehmet, 831
Pal, Bijoli Kanti, 439
Palacios, M. A., 553
Pambid, Ernesto R., 301
Panciatici, G., 649
Papadopoulos, Constantine G., 323
Parida, F. C., 1129
Parthasarathy, T. N., 455
Passingham, Catherine, 1313
Patel, Bharti, 1063
Patel, K. S., 969
Patterson, Ronald L. S., 501
Pazouki, Sima, 517
Peck, David V., 899
Pereiro García, Maria Rosario, 575
Pérez-Bendito, Dolores, 689, 1261, 1377
Pérez-Bustamante, Juan Antonio, 1201
Pérez-Ruiz, Tomás, 217, 783
Petersen, Martin, 1029
Petilino, Roberto, 889
Petrukhin, Oleg M., 839
Pfendt, Lidija B., 383
Pietra, R., 1025
Pillai, Vadasseril N. Sivasankara, 213
Piracci, Antonio, 907
Pla, F. Pérez, 721
Polizello, Ana Cristina M., 1093
Polkowska, Zaneta, 393
Polo Díez, Luis Maria, 337, 609, 869
Popović, Gordana V., 383
Pratap, Shridhar R., 1367
Preisler, Ladislav, 1271
Prioli, Alberto José, 341
Puchades, Rosa, 1243
Quintero, Maria del Carmen, 1261
Radić, Njegomir, 737
Raimundo, Jr., Ivo M., 761
Rajadel, Pilar, 1097
Raju, K. Ramakrishnam, 455
Rakanovic, Mila, 801
Raman, B., 93
Ramos, G. Ramis, 721
Randles, Mark A., 379
Rao, Ganti Shankar, 445
Rapaumbya, Guy-Roland, 637
Raspi, Giorgio, 641, 649
Rauret, Gemma, 959, 1097
Ravenscroft, J. E., 371
Rawle, N. W., 521
Raynor, Mark W., 125
Reading, Christopher L., 1145
Ribera, Mercè, 1097
Richards, Michael E., 797
Richter, Pablo, 409
Riise, Edel, 1265
Riley, Kenneth W., 865
Roda, Aldo, 889
Rodríguez, I., 553
Rodríguez, José R. Barreira, 209
Rodriguez, Juana, 1117
Roe, J. N., 353
Rose, Malcolm E., 511
Royaud, Isabelle A. M., 1313
Rubio, Roser, 959
Rubio, S., 1377
Rücker, G., 1181
Ruiz-Lopez, Maria-Dolores, 129
Růžička, Jaromir, 475
Sabbioni, E., 1025
Sabharwal, Sunil, 1305
Saccon, Mauro, 1041
Sadek, M. El, 1181
Sadiris, Nicholaos C., 1103
Saez, Andres, 1257
Sahoo , P., 1129
Saito, Kenichi, 431
Sakamoto, Hidefumi, 1251
Salinas, Francisco, 329, 1007
Sammartino, Maria Pia, 827
Sampedro, A. Sanchez, 855
Sánchez-Pedreño, Concepcion, 757, 989, 1257
Sanghi, Sunil K., 333
Santha, Kolla, 465
Santilio, Angela, 1167
Santos-Delgado, M. Jesús, 609
Sanz-Medel, Alfredo, 575
Sarantonis, E. G., 977
Saraswathi, Kanneganti, 465
Sarrion, S. Navasquillo, 855
Satake, Masatada, 1191
Sauvage, Jean-Paul , 637
Saxena, Praveen, 1073
Saxena, Vibha, 1073
Scalia, Santo, 929
Scollary, Geoffrey R., 1235
Scullion, S. Paul, 599, 1277
Sekido, Eiichi, 1089
Seligman, Peter F., 1327
Serra, Dinah B., 341
Seward, Eileen M., 1207
Shakir, Issam M. A., 69
Shanawany, A. El, 1181
Shaw, Ian C., 1389
Sheng, Liangquan, 951
Shinde, V. M., 93
Shono, Toshiyuki, 1251
Si, Zhi-Kun, 1139
Siegel, Paul D., 1029
Silva, Edson C., 341
Silva, Manuel, 993, 1261
Singh, Raj P., 301
Singh, Sunil Kumar, 421
Sithole, B. Bruce, 237
Sivasubramanian, K., 1129
Skinner, Craig S., 269
Sladić, Dušan M., 383
Smrek, Ann L., 243
Smyth, Malcolm R., 275, 617, 1207, 1215
Soledad Durán, Maria, 1007
Somer, Güler, 297
Spadaro, Augusto César C., 1093
Spinetti, Maria, 641
Srijaranai, Supalax, 627
Srivastava, Ashutosh, 421
Stallard, Martha O., 1327
Stang, Peter M., 1327
Stein, H. N., 1211
Stockwell, Peter B., 571

Stone, William E. E., 1177
Stoyanoff, Robert E., 801
Sugiyama, Takehiko, 279
Suzuki, Harumi, 167
Svehla, Gyula, 1207
Szklar, Roman S., 801
Szoka, F. C., 353
Szpunar-Łobińska, Joanna, 319
Tadros, Shawky H., 229
Takaki, Toshihiro, 1133
Takeda, Kikuo, 535
Tan, Chin-Huat, 35
Tanaka, S., 947
Taniguchi, Hirokazu, 9
Tao, Hiroaki, 1055
Taylor, Robert B., 797
Teien, Gerd, 259
Telting-Diaz, Martin, 1215
Temizer, Aytekin, 873
Terashita, Minoru, 425
Teresa, M., 195
Thomas, J. D. R., 417, 1289
Timotheou-Potamia, Meropi M., 1229
Tipton, Keith, 617
Toda, Shozo, 167
Tomás, Virginia, 217, 783
Tomassetti, Mauro, 827
Tong, A., 947
Toponi, Alessandro, 1073
Tor, Isset, 99
Torres, A., 1377
Townshend, Alan, 495
Trojanowicz, Marek, 319
Tsuji, Sumiko, 435
Tsukioka, Tadashi, 1343
Tyson, Julian F., 305, 531, 571, 587, 593
Ubigli, Mario, 907
Uchida, H., 933
Uden, Peter C., 525
Ulsaker, Gunnar A., 259
Utley, David, 1239
Valcárcel, Miguel, 699, 943, 993
Valente, Antonio Luiz Pires, 525
Valiente, M., 315
Valkirs, Aldis O., 1327
van Rensburg, Ancel, 605, 1049
van Staden, Jacobus F., 581, 605, 1049
van Zoonen, Piet, 1033
Vandecasteele, Carlo, 17
Vandenberg, Elaine T., 147
Vargas, Helion, 341
Vasconcelos, S. D., 195
Vasić, Vesna, 745
Vassileva, E., 399
Vecchietti, Roberto, 173
Velasco, Antonio, 993
Veltsistas, Panayotis G., 741
Verchère, Jean-François, 637
Vergori, Fabio, 1167
Vergori, Luciano, 1167
Verkman, A. S., 353
Verma, Archana, 333
Verma, Krishna K., 333
Vermeiren, Koen, 17
Vidal, Juan C., 539
Vielvoye, Léon, 1177
Vilchez, José Luis, 849
Vilchinskaya, Elena A., 1301
Villanueva Camañas, Rosa M., 1125
Viñas, Pilar, 757
Vlessidis, Athanasios G., 771
Vohra, Kay, 925
Volodarskii, Leonid B., 839
Vučić, Nevenka, 791
Wähälä, Kristiina, 263
Wallace, Heather M., 517
Wang, Erkang, 139
Wang, Jirong, 53
Wang, Joseph, 831
Wang, Xiang-wen, 305
Werner, Gerhard, 405
White, Peter C., 919
Willis, Harry A., 1313
Willis, R. G., 521
Winefordner, J. D., 933
Wong, Koon Hung, 65
Wood, John P. M., 1389
Wu, Qing-guo, 835
Wu, Weh S., 801
Xing, D. Kai-lo, 797
Yagüe, Encarna, 783
Yako, Tadaaki, 535
Yamaguchi, Masatoshi, 1363
Yamamoto, Susumu, 435
Yamamuro, Norihito, 1133
Yamazaki, Sunao, 167
Yang, Mo H., 29
Yee, K. F., 225
Ying-Kai, Xiao, 911
Yokota, Fumihiko, 23
Yoshimura, Etsuro, 167
Yoshimura, Kazuhisa, 843
Yotsuyanagi, Takao, 133
Zagatto, Elias Ayres Guidetti, 779
Zaki, Nabila S., 1059
Zannetti, Roberto, 1041
Zhao, Zaofan, 49, 951
Zhu, Gui-Yun, 1139
Zhu, Wen-Jing, 1139
Zichy, Veronica, 1313
Zolotov, Yurii A., 839
Zotou, Anastasia Ch., 323
Zoulis, Nikolaos E., 291
Zurmühl, Torsten, 1171

000805

Moving?

ADDRESS

TOWN COUNTY/STATE

POSTAL CODE COUNTRY

PLEASE PRINT YOUR NEW ADDRESS ABOVE AND RETURN THIS COMPLETED SHEET INCLUDING ADDRESS LABEL TO:

THE DISTRIBUTION CENTRE
BLACKHORSE ROAD
LETCHWORTH
HERTS SG6 1HN ENGLAND

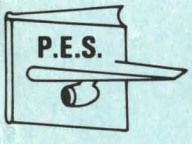

Via Publications Expediting Inc.
Elmont, N.Y. 11003

PORT BETAALD
PORT PAYÉ
AMSTERDAM

Imprimé permis numéro Asd 2

9100032654 16/06
AN

0016809
DIRECTOR,
DIVISION OF SCIENTIFIC AND TECH-
NOLOGICAL INFORMATION,
DEPARTMENT OF SCIENCE SERVICE,
RAMA V1 STREET, BANGKOK 10400,
THAILAND

BY AIR

ROYAL SOCIETY OF
CHEMISTRY

Non-delivery, return to:
Publications Expediting Inc.
P.O. Box 10020
2130 CA Hoofdorf. Holland.

1 AIR

BY-AIR

The XXVII Colloquium Spectroscopicum Internationale

XXVII CSI

1991
NORWAY

will be held in

Grieg Hall, Bergen, Norway
June 9–14 1991

IUPAC

This traditional biennial conference in analytical spectroscopy will once again provide a forum for atomic, nuclear and molecular spectroscopists worldwide to encourage personal contact and the exchange of experience.

Participants are invited to submit papers for presentation at the XXVII CSI, dealing with the following topics:

Basic theory and instrumentation of—

- Atomic spectroscopy (emission, absorption, fluorescence)
- Molecular spectroscopy (UV, VIS and IR)
- X-ray spectroscopy
- Gamma spectroscopy
- Mass spectrometry (inorganic and organic)
- Electron spectroscopy
- Raman spectroscopy
- Mössbauer spectroscopy
- Nuclear magnetic resonance spectrometry
- Methods of surface analysis and depth profiling
- Photoacoustic spectroscopy

Application of spectroscopy in the analysis of—

- Metals and alloys
- Geological materials
- Industrial products
- Biological samples
- Food and agricultural products

Special emphasis will be given to trace analysis, environmental pollutants and standard reference materials.
The scientific programme will consist of both plenary lectures and parallel sessions of oral presentation. Specific times will be reserved for poster sessions.

PRE- AND POST-SYMPOSIA

In connection with the XXVII CSI the following symposia will be organised:

Pre-symposia—

I. GRAPHITE ATOMISER TECHNIQUES IN ANALYTICAL SPECTROSCOPY
June 6–8, 1991, Hotel Ullensvang, Lofthus, Norway.

II. CHARACTERISATION OF OIL COMPONENTS USING SPECTROSCOPIC METHODS
June 6–8, 1991, Hotel Hardangerfjord, Øystese, Norway.

III. MEASUREMENT OF RADIO-NUCLIDES AFTER THE CHERNOBYL ACCIDENT
June 6–8, 1991, Hotel Solstrand, Bergen, Norway.

Post-symposium—

IV. SPECIATION OF ELEMENTS IN ENVIRONMENTAL AND BIOLOGICAL SCIENCES
June 17–19, 1991, Hotel Alexandra, Loen, Norway.

For further information contact:

THE SECRETARIAT
XXVII CSI
HSD Congress-Conference
P.O. Box 1721 Nordnes
N-5024 Bergen, Norway.
Tel. 47-5-318414, Telex 42607 hsd n, Telefax 47-5-324555

FIRST FOLD HERE

THE ANALYST READER ENQUIRY SERVICE
For further information about any of the products featured in the advertisements in this issue, write the appropriate number on the postcard, detach and post.

FOLD HERE

THE ANALYST READER ENQUIRY SERVICE

OCT'90

For further information about any of the products featured in the advertisements in this issue, please write the appropriate number in one of the boxes below.
Postage paid if posted in the British Isles but overseas readers must affix a stamp.

PLEASE USE BLOCK CAPITALS LEAVING A SPACE BETWEEN WORDS *Valid 12 months*

1 NAME

2 COMPANY

PLEASE GIVE YOUR BUSINESS ADDRESS IF POSSIBLE. IF NOT, PLEASE TICK HERE ☐

3 STREET

4 TOWN

5 COUNTY
POST CODE

6 COUNTRY

7 DEPARTMENT
DIVISION

8 YOUR JOB TITLE
POSITION

9 TELEPHONE NO

OFFICE USE ONLY REC'D PROC'D

FOLD HERE

Postage will be paid by Licensee

Do not affix Postage Stamps if posted in Gt. Britain, Channel Islands, N. Ireland or the Isle of Man

2

BUSINESS REPLY SERVICE
Licence No. WD 106

Reader Enquiry Service
The Analyst
The Royal Society of Chemistry
Burlington House, Piccadilly
LONDON
W1E 6WF
England

VERSION 3.0 NOW AVAILABLE

The PC Version of the NIST/EPA/MSDC Mass Spectral Database

National Institute of Standards and Technology, USA
Environment Protection Agency, USA
Mass Spectrometry Data Centre, UK

This unique database features:

- The mass spectra of 53,994 compounds
- retrieval in seconds
- both tabular and graphic display
- fully interactive searching by:
  - individual peaks
  - abundances of 10 major peaks
  - molecular weight
  - molecular formula
  - compound name
  - CAS Registry Number
  - identification number

  plus a complete sequential search of the entire database
- chemical structure displays for more than 96% of compounds
- a facility to create your own database alongside the NIST/EPA/MSDC Database – can search each individually or both together
- and much more . . .

". . . an excellent and inexpensive source of mass spectral data and search software for the scientific community."

Stephen R. Heller
Journal of the American Chemical Society

★ A free demonstration disk is available on request ★

SEND FOR FURTHER DETAILS NOW!

Please contact:
The Mass Spectrometry Data Centre
Royal Society of Chemistry
Thomas Graham House
Science Park, Milton Road
Cambridge CB4 4WF
United Kingdom

Telephone: (International) +44 (0)223 420066
Fax: (International) +44 (0)223 423623
Telex: 818293 ROYAL

ROYAL SOCIETY OF CHEMISTRY
Information Services

NEW

DO YOU HAVE AT YOUR FINGERTIPS EVERY MONTH AROUND 1000 NEW LITERATURE REFERENCES ON MASS SPECTROMETRY?

NOW YOU CAN WITH...

Mass Spectrometry Bulletin *PC Version*

The **Mass Spectrometry Bulletin** is now available on personal computer, providing easy access to the world's most recently published literature. It saves mass spectrometrists much invaluable time and effort, fulfilling current awareness needs efficiently and allowing complex searches to be completed in seconds. Runs on IBM pc compatible machines.

MSB pc Features:

- fast, flexible and inexpensive – there are no online charges
- provides comprehensive and varied searching
- updated monthly into a single searchable file
- convenient access in your lab or library
- includes an established software package
- easy to use

★ A free demonstration disk is available on request ★

Also available in hardcopy

Subscription prices for 1990

UK	USA	Rest of World
Mass Spectrometry Bulletin PC Version		
£430.00 (plus VAT)	$750.00	£450.00
Hard Copy and PC Version Package		
£555.00 (plus £40.50 VAT)	$995.00	£595.00
PC Version for Current Hard Copy Subscribers		
£270.00 (plus VAT)	$365.00	£280.00
Mass Spectrometry Bulletin Hard Copy		
£285.00	$630.00	£315.00

Access/Visa/Mastercard/Eurocard accepted

Order **NOW** or send for further information

Please contact:
The Mass Spectrometry Data Centre
Royal Society of Chemistry
Thomas Graham House
Science Park, Milton Road
Cambridge CB4 4WF
United Kingdom

Telephone: (International) +44 (0)223 420066
Fax: (International) +44 (0)223 423623
Telex: 818293 ROYAL

ROYAL SOCIETY OF CHEMISTRY
Information Services

Circle 006 for further information

ANALAO 115(10) 1277–1396 (1990) October 1990

The Analyst

The Analytical Journal of The Royal Society of Chemistry

CONTENTS

1277 **Adaptation of On-line Reactions Developed for Use With Flow Injection With Amperometric Detection for Use in Disposable Sensor Devices: Reductive Determination of Phosphate as Pre-formed 12-Molybdophosphate in a Capillary-fill Device**—Arnold G. Fogg, S. Paul Scullion, Tony E. Edmonds, Brian J. Birch

1283 **Glass pH Electrodes With improved Temperature Characteristics: Use of Low-impedance pH Sensor as the Inner Reference Electrode**—Derek Midgley

1289 **Multi-enzyme Electrodes for the Determination of Starch by Flow Injection**—Junainah Abdul Hamid, G. J. Moody, J. D. R. Thomas

1297 **Determination of L-Ascorbic Acid in Fruit and Vegetable Juices by Flow Injection With Immobilised Ascorbate Oxidase**—Gillian M. Greenway, Peter Ongomo

1301 **Influence of the Redox Potential of the Medium on Stripping Voltammetric Measurement Results**—Khiena Z. Brainina, Elena A. Vilchinskaya, Rosa M. Khanina

1305 **Determination of Nitrite Ion by Differential-pulse Polarography Using *N*-(1-Naphthyl)ethylenediamine**—Sunil Sabharwal

1309 **Method for the Determination of Radioactivity in the C-2 Carbon of Glycine**—Harinder Paul S. Makkar, Peter J. Buttery

1313 **Fourier Transform Raman Spectroscopy in the Analysis of Polypeptides**—David Gani, Patrick J. Hendra, William F. Maddams, Catherine Passingham, Isabelle A. M. Royaud, Harry A. Willis, Veronica Zichy, Michael E. A. Cudby

1319 **Fourier Transform Infrared Spectrometric Determination of Stearic Acid in Styrenic Polymers**—T. Kumar

1323 **Determination of Trace Amounts of Cobalt in Feed Grains and Forages by Solvent Extraction and Graphite Furnace Atomic Absorption Spectrometry**—W. John Blanchflower, Andrew Cannavan, D. Glen Kennedy

1327 **Assessment of Frozen Storage of Tributyltin in Sea-water Samples Using Hydride Derivatisation**—Aldis O. Valkirs, Martha O. Stallard, Peter M. Stang, Steven Frank, Peter F. Seligman

1329 **Direct Introduction of Powdered Samples into an Inductively Coupled Plasma Spectrometer Using a Spark Dispersion - Merging Sample Introduction Technique**—Takafumi Hirata, Tasuku Akagi, Akimasa Masuda

1335 **Chemical Analysis of Impurities in Zirconia and Aluminium Nitride Ceramics by Inductively Coupled Plasma Atomic Emission Spectrometry**—Charo Martínez-Lebrusant, Flora Barba

1339 **Analysis of Organic Residues of Archaeological Origin by high-temperature Gas Chromatography and Gas Chromatography - Mass Spectrometry**—Richard P. Evershed, Carl Heron, L. John Goad

1343 **Gas Chromatographic Separation and Determination of Chloroacetic Acids in Water by a Difluoroanilide Derivatisation Method**—Hideaki Ozawa, Tadashi Tsukioka

1349 **Simultaneous Determination of Some Active Ingredients in Cough - Cold Syrups by Gas - Liquid Chromatography**—Oi-Wah Lau, Yiu-Ming Cheung

1355 **Quantitative Analysis of Alkaloids From Chinchona Bark by High-performance Liquid Chromatography**—David V. McCalley

1359 **Polymers With Reactive Functions as Sampling and Derivatising Agents. Part 1. Effective Sampling and Simultaneous Derivatisation of an Airborne Amine**—Kazik Jedrzejczak, Virindar S. Gaind

1363 **6,7-Dimethoxy-1-methyl-2(1*H*)-quinoxalinone-3-propionyl-carboxylic Acid Hydrazide: A Highly Sensitive Fluorescence Derivatisation Reagent for Carboxylic Acids in High-performance Liquid Chromatography**—Masatoshi Yamaguchi, Tetsuharu Iwata, Kouji Inoue, Shuuji Hara, Masaru Nakamura

1367 **Method for the Extraction Chromatographic Separation of Barium From Other Elements With Dibenzo-18-crown-6**—Barburao S. Mohite, Chandrakant D. Jadage, Shridhar R. Pratap

1371 **Relevance of the Reaction of Aluminium With Pyrocatechol Violet to Speciation and Complexation Capacity Analysis**—Gregory M. Morrison

1375 **Turbidimetric Method for the Determination of Water-soluble hydroxyethylcellulose in Dry Blended Cement**—Asfaha Iob, Nureddin M. Abbas

1377 **Evaluation of a Modified Derivative Method for Spectrophotometric and Spectrofluorimetric Kinetic-based Determination**—A. Torres, M. C. Gutierrez, S. Rubio, A. Gómez-Hens, D. Pérez-Bendito

1383 **Spectrophotometric Determination of Cysteine and Cystine in Urine**—Joseph Chrastil

1385 **Spectrophotometric Determination of Acetone Using Vanillin**—Sulbha Amlathe, V. K. Gupta

COMMUNICATION

1389 **Preferential Distribution of Streptomycin in Pig Kidney Cortex**—Pamela J. Brush, John P. M. Wood, Ian C. Shaw

1391 **BOOK REVIEWS**

1393 **CUMULATIVE AUTHOR INDEX**

Typeset and printed by Black Bear Press Limited, Cambridge, England